A. Terry Bahill

The Science of Baseball

Batting, Bats, Bat-Ball Collisions, and the Flight of the Ball

Second Edition

Springer

The Science of Baseball

A. Terry Bahill

The Science of Baseball

Batting, Bats, Bat-Ball Collisions, and the Flight of the Ball

Second Edition

Springer

A. Terry Bahill
Systems and Industrial Engineering
University of Arizona
Tucson, AZ, USA

ISBN 978-3-030-03031-5 ISBN 978-3-030-03032-2 (eBook)
https://doi.org/10.1007/978-3-030-03032-2

Library of Congress Control Number: 2018958952

This Springer imprint is published by the registered company Springer Nature Switzerland AG
The registered company address is: Gewerbestrasse 11, 6330 Cham, Switzerland

Dedicated to my always smiling,
always laughing Karen

Foreword by Greg Rybarczyk

I first "met" Dr. Terry Bahill in 2005 while researching aerodynamic characteristics of batted baseballs as part of a personal project which would become the ESPN Home Run Tracker. I didn't speak to him at the time (that would come later) but rather downloaded and read many of the papers which he had posted on his website. Dr. Bahill's explanations and calculations were a great help to me at a time when my career in baseball analytics was just beginning, but as we've corresponded over the years, my admiration for his work, particularly his gift for communicating ideas, has only increased. His latest publication, *The Science of Baseball: Batting, Bats, Bat-Ball Collisions, and the Flight of the Ball* is a worthy contribution to his prodigious body of baseball research, compiled over four decades and presented with extraordinary clarity. It will serve as a valuable reference for scholarly fans, as well as baseball analysts who aspire to compete at the highest level.

Major League Baseball clubs are, as of 2018, in the midst of a revolution. The ranks of analysts employed by Major League Baseball clubs have swelled in recent years, as teams try to at least keep pace, and hopefully realize competitive advantages through the creative use of the data which is being generated and presented to teams at an unprecedented rate. Every MLB front office now employs people who scrutinize not only traditional statistics such as batting averages and home run totals, but also play-level summary metrics like pitch speed or batted-ball exit speed. The most analytically enthusiastic clubs study ball- and player-tracking data collected at rates as high as 100 data points per second, and disseminated by commercial vendors such as Baseball Info Solutions, Sport vision, Trackman, MLB Advanced Media and others. MLB's demand for new forms of baseball analysis has inspired a large and rapidly growing pool of independent analysts who conduct research via publicly available sources, hoping to earn the opportunity to offer their services as consultants to or employees of Major League front offices. More people and companies are doing more baseball-related analytical work than ever before.

Throughout my dozen years of baseball-related work, both as an individual and in my current role as an analyst with the Boston Red Sox, I've found that the best research originated with people who possessed not only thorough baseball knowledge but also a solid understanding and a proper deference to the other governing principles of the situation under study. For contract and compensation issues, these principles are those of economics; for discretionary tactical moves such as stolen base or bunt attempts, or for pitch type selection, these principles are those of game theory; for issues related to the movement of the baseball, these principles are those of physics.

Unfortunately, too often these days we see analytical work that neglects, or even runs counter to, the underlying principles, because the analyst's mastery of the relevant principles is faulty or incomplete. For some, analysis of baseball data consists of arranging it in columns and performing statistical tests on it until something "pops." I was once offered a detailed analysis that rated elite closer Koji Uehara as the 16th best pitcher on the Red Sox roster, and further opined that his devastating splitter was among the weaker individual pitches on the entire team. After I stopped laughing, I asked a few questions and learned that these dubious results could be traced to a faulty premise about the value of pitch locations. It was, essentially, a lack of understanding of one of the most important elements of pitching analysis: how to judge the results of a pitch.

More knowledgeable analysts who are familiar with the applicable principles can better detect and avoid bad data, more efficiently set up and perform the most promising statistical tests, and can more reliably interpret the results. Dr. Bahill's expert dissection of the bat–ball collision (Chaps. 1–5) and the flight of pitched and batted baseballs through the air (Chap. 7) should be read by all who wish to enhance their expertise at analysis of ball-tracking data by first understanding why the baseball moves the way it does. Complete derivations have been provided for those who wish to delve deeply into the equations, but they need not present a persistent barrier to those readers who prefer to skim the line-by-line mathematics and skip ahead to the conclusions. A prime example is the sensitivity analysis presented in Chap. 7, which describes the change in batted-ball range which follows a given change in various inputs such as batted-ball speed, batted-ball spin or air density.

Baseball analysts past, present and future are indebted to Dr. Bahill for the efforts he has made to make understanding of the complex underlying physics of baseball accessible to all at each person's chosen level of detail. His precise yet eminently accessible explanations of the physics of the bat–ball collision and the flight of the ball are more useful than ever in an era when MLBAM's Statcast system tells 30 and 100 times per second **what** has happened but leaves to the observer the task of figuring out **why** it happened (which is, of course, the key to predicting what will happen in the future, the ultimate objective of all analysts). If you wish not only to understand the game of baseball better but to contribute to the body of knowledge of the game of baseball, read this book carefully, and then read it again. For the moment, knowledge of baseball physics can still differentiate an analyst from his or her peers but in the field of baseball analytics, no competitive advantage persists for long.

Southborough, MA, USA

Greg Rybarczyk
Senior Analyst, Baseball R&D
Boston Red Sox
Creator of ESPN HR Tracker

P. O. BOX 481
ISLAMORADA, FLORIDA KEYS
33036

January 23, 1984

Prof. A. Terry Bahill
Electrical & Computer Engineering
Carnegie-Mellon University
Schenley Park
Pittsburgh, PA 15213

Dear Mr. Bahill:

Received your letter and have also had a chance to read your research, and I fully agree with your findings.

I always said I couldn't see a ball hit the bat except on very, very rare occasions and that was a slow pitch that I swung on at shoulder height. I cam very close to seeing the ball hit the bat on those occasions.

As to participating in your other experiments; at this time, I can't tell you that I can comply with your request.

Regarding the current theories of some of the present batting coaches (with which I absolutely disagree) to watch the ball go into the catcher's mitt - by doing that, you don't give yourself a chance to swing and open up properly. Try it yourself - look down at the plate and try to make a full swing. I hope you don't throw your back out of joint!

In any event, good luck with your projects.

Sincerely,

Ted Williams

Ted Williams

TW/shg

Preface

Collisions between baseballs, softballs and bats are complex and therefore their models are complex. The first purpose of this book is to show how complex these collisions can be, while still being modeled using only Newton's axioms and the conservation laws of physics. This book presents models for the speed and spin of balls and bats. These models and equations for bat–ball collisions are intended for use by high school and college physics students, engineering students, the baseball analytics community and most importantly nonprofessional students of the science of baseball. Unlike models in previous books and papers, these models use only simple Newtonian axioms and the conservation laws to explain simple bat–ball collision configurations. It is hoped that this book will help readers develop an understanding of the modeling of bat–ball collisions. The second purpose of this book is to help batters select or create baseball or softball bats that would be optimal for them. The third purpose is to show what affects air density and how air density affects the flight of the ball.

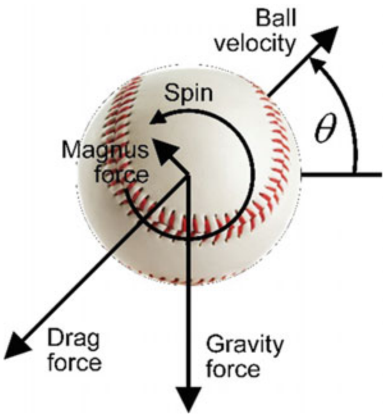

Chapter 1 lays the groundwork for analyzing bat–ball collisions and previews the theme that alternative models help you understand the system.

Chapter 2 introduces nine basic configurations of bat–ball collisions using words and figures.

Chapter 3 starts developing the equations for these configurations. It starts with the simple configurations having the ball collide with the center of mass of the bat. Then it moves on to configurations that are more complex using the same equations and development. The notation developed here will be used throughout the book.

Chapter 4 is the pinnacle of this book. It contains our most comprehensive model, which is a collision at the sweet spot of the bat with spin on the pitch. It shows which parameters are the most and least important. It also has advice for selecting and modifying each person's optimal bat. Such a bat does not have its barrel end cupped out. This chapter is unique in the science of baseball literature. It is also self-contained. You need not read previous chapters to understand it. In other words, a teacher could use this chapter in a physics or engineering course and the students would only have to buy this one chapter. The BaConLaws model presented in this chapter also describes the motion of the *bat* after the collision. Many models describe the motion of the ball after the collision but few (if any) describe the motion of the bat. When you see a batter hit a ball, do you see the recoil of the bat? Can you describe it? Well, these equations do.

Chapter 5 contains four alternative models for bat–ball collisions. Their purposes are different and are they based on different fundamental principles. The Effective Mass model was created by physicists independent of the author of this book. Therefore, comparisons to it are important for validating the model of Chap. 4. The second and third models are data-based, not theory-based. They use a different approach and they use a different *type* of data. The fourth model considers friction during the collision. It is shown that this type of collision cannot be modeled thoroughly using only the conservation laws. Our modeling technique could not handle the Collision with Friction model because our technique is only good for a point in time before the collision and a point after the collision: it cannot handle behavior during the collision. Chapter 4 fulfilled part of the first purpose of this book. It showed a complex configuration for which our technique did work. Chapter 5 completed the fulfillment of this purpose by showing a configuration for which our technique was too simple.

Nothing in Chaps. 1–5 is controversial. There are no unstated assumptions. Important equations have been derived with at least two techniques. In Chaps. 2–5, the equation numbers are the same. In other words, Eq. (2.3) is the same as Eq. (3.3) is the same as Eq. (4.3) and is the same Eq. (5.3). The equations in Chaps. 2–5 were derived using only Newton's axioms and the conservation laws of physics. The equations in Chap. 7 for the drag and Magnus forces are original and are based on more than Newton's' axioms.

Chapter 6 summarizes Chaps. 1–5. Chapters 1–6 deal with bat–ball collisions. They solve equations in closed form. There are no approximations. Chapter 7 deals with messy real systems. It uses experimental data and gives approximations.

Chapter 7 contains derivations for equations governing the flight of the ball. It shows what affects air density and how air density affects the flight of the ball. It shows that a home run ball might go 26 feet farther in Denver than in San Francisco. It also answers the question, "Which can be thrown farther a baseball or a tennis ball?" This chapter can be read independently from the rest of the book.

Chapter 8 discusses the accuracy of baseball simulations. When the television announcer says, for example, that home run went 431.1 feet. You, our reader, will know that he should have said, that the *true* range of that home run was 430 plus or minus 30 feet.

Chapter 9 presents the vertical sweetness gradient of the baseball bat. It shows that the sweet spot of the bat is one-fifth of an inch high.

Chapter 10 tackles the differences between right-handed batters and left-handed batters. It shows that neither is better than the other. Finally, it explains that cross-dominant batters *do* have an advantage on some pitches. Because for non-cross-dominant batters, the blind spot of their dominate eye can obscure the bat–ball collision.

Chapter 11 summarizes the insights and wisdom of the book. Chapter 12 presents our modeling philosophy.

We need people who can explain this book to baseball managers and general managers.

Teachers might challenge their students to try finding mistakes in this book. The author will give $25 to the first person/group to find a logical, algebraic, physics or engineering mistake in this book. Spelling, punctuation, grammar, fuzzy inconsistencies, typographical errors and broken links do not count. Send discoveries to Terry Bahill, 1622 W. Montenegro, Tucson AZ, USA 85704-1622.

Tucson, AZ, USA A. Terry Bahill

Acknowledgements

I am indebted to Al Nathan for preventing me from publishing a book with mistakes in it. Ferenc Szidarovszky ensured that the equations had no mistakes. I thank Bob Watts, Rod Cross, Bruce Gissing and Jim Close for helpful comments on the manuscript. This book is written in the first-person plural. Plural because my graduate students did all the work. Major contributions were made by Tom La Ritz, Bill Karnavas, Miguel Morna Freitas and J. Venkateswaran. Extra special thanks go to Dave Baldwin (17-year MLB pitcher with a 3.08 ERA) for inspiring my science of baseball papers.

Conflict of Interest

In the 1990s, Terry Bahill received research grants from Worth Sports Co. and Easton Sports Inc. for research on human–bat relationships. Since then he has received no money, renumeration, speaking fees, consulting contracts or research grants from any sources concerning the Science of Baseball. Bahill has no conflicts of interest regarding the content of this book.

Bahill had no preconceived notions of which models might be most appropriate for the Science of Baseball. He let the data, experiments and knowledge drive the development of this book.

Note on the Mathematics Used in This Book

Most of the mathematics in this book is simple high school algebra. If the reader prefers to just skip the equations, then my advice is to simply do so. Just read the text and you will still get a robust description of the dynamic physical interaction at work in hitting a baseball. The mathematics is there to illustrate the quantitative aspects of the phenomena described in this book.

Here is an example of a simple algebraic equation.

$$y = mx + b$$

This is the equation of a straight line. It has two variables and two constants. It says that the output variable, y, (plotted on the vertical axis in Fig. 1) is equal to the input variable, x, (plotted on the horizontal axis) multiplied by the slope, m, plus the intercept, b. A different way of writing this equation is

$$f(x) = mx + b$$

Fig. 1 Graph of a straight line

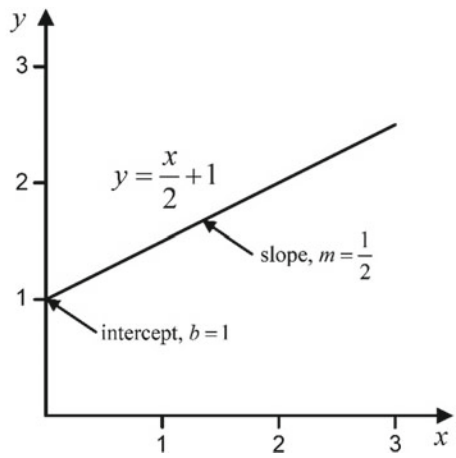

Here we have replaced y with $f(x)$, because we want to emphasize that the equation is a function of x. The naming is that the value of the dependent variable, y, depends on the value of the independent variable, x. Sometimes there can be two independent variables, like this:

$$x = w_y y + w_z z$$

This equation states that the variable x equals some weight w_y times y plus w_z times z. To emphasize the functionality, we could write it like this:

$$f(y, z) = w_y y + w_z z.$$

Variables and constants in equations are set in an *Italic font*.

OK, here is a big hairy equation. But it isn't scary.

$$v_{\text{ball-after}} = v_{\text{ball-before}} - \frac{(v_{\text{ball-before}} - v_{\text{bat-cm-before}})(1 + CoR_{1a})m_{\text{bat}}}{m_{\text{ball}} + m_{\text{bat}}}$$

It states that the velocity of the ball after its collision with the bat is equal to the velocity of the ball before its collision plus some other stuff. That other stuff includes the difference in velocities of the bat and ball before the collision times a bunch of constants. Now, that wasn't so scary, was it?

The next step up in mathematics is calculus and differential equations. However, whenever I used such equations, I 'hid them' from the reader—except for the partial differentials that were used in sensitivity functions.

Sometimes we want to know what change in the output would result from a small change in the input. For example, we want to know, if we change the input by a small amount, say Δx, what will be the change in the output, Δy. The Greek Delta, Δ, indicates change in a quantity expressed by a variable. Using simple rules that

Fig. 2 Graph of a parabola

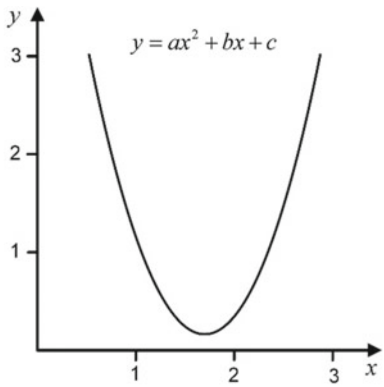

we look up in a table of derivatives on the Internet, we find that for this equation $y = mx + b$, $\frac{\Delta y}{\Delta x} = m$, the slope of the line. For small changes, we write $\frac{\Delta y}{\Delta x} = \frac{dy}{dx} = m$.

For a more complicated equation, let us consider the parabola

$$y = ax^2 + bx + c$$

shown in Fig. 2.

Once again, using rules that we look up in a table of derivatives, we find that

$$\frac{\mathrm{d}y}{\mathrm{d}x} = 2ax + b.$$

In some parts of this book, we use statistics. The following example will show the most common statistics that we use. Consider the following two sets of numbers: Set-1 = {3, 4, 5, 6 and 7} and Set-2 = {1, 3, 5, 7 and 9}.

	Set 1	Set 2
		1
	3	3
	4	
	5	5
	6	
	7	7
		9
Mean	5	5
Standard deviation	1.6	3.2

Both sets of numbers have the same mean or average. Set-1 is clustered, whereas Set-2 is spread out: it has more variation. A statistic that we use to model variation is the standard deviation. We put the numbers for Set-1 and Set-2 into a calculator and it produces the standard deviations in the above table. The standard deviation (or variance) is a measure of the spread or variation in the data. It is also used to prove that two distributions are statistically different.

We will now show an example of the most complicated mathematics that appears in this book. We will start with the equation for the ball velocity after the collision, v_{1a}, Eq. (4.8).

$$v_{1a} = v_{1b} - \frac{(v_{1b} - v_{2b} - \omega_{2b} d)(1 + CoR_{2b}) m_2 I_2}{m_1 I_2 + m_2 I_2 + m_1 m_2 d^2}$$

The subscript **b** is for *before* the bat–ball collision and **a** is for *after* the collision. The subscript 1 is for the ball and 2 is for the bat. To do a sensitivity analysis, we need the partial derivatives of v_{1a} with respect to the variables v_{1b} and v_{2b}.

To simplify let $K = \left(m_1 I_2 + m_2 I_2 + m_1 m_2 d^2\right)$
and $C = (1 + CoR_{2b}) m_2 I_2$
Therefore,

$$v_{1a} = v_{1b} - \frac{(v_{1b} - v_{2b} - \omega_{2b} d)C}{K}$$

The following partial derivatives of the function v_{1a} with respect to the variables v_{1b} and v_{2b} are easy to derive using a table of differentials. Substituting numerical values gives

$$\frac{\partial v_{1a}}{\partial v_{1b}} = 1 - \frac{C}{K} = 1 - 1.2 = -0.2$$
$$\frac{\partial v_{1a}}{\partial v_{2b}} = \frac{C}{K} = 1.2$$

This means that the velocity of the ball after the collision is influenced more by bat velocity before the collision than it is by ball velocity. That is the most complicated mathematics that we do in this book.

Just remember, the mathematics is there merely to prove that the text is correct. If you don't care about the proofs, then skip the equations. I wrote this book so that you can skip the equations and still understand the phenomena at hand using only the narrative description.

Contents

About the Author

A. Terry Bahill is an Emeritus Professor of Systems Engineering and of Biomedical Engineering at the University of Arizona in Tucson. He served as a Lieutenant in the United States Navy. He received his Ph.D. in electrical engineering and computer science from the University of California, Berkeley. He is the author of eight engineering books and over two hundred and fifty papers, over one hundred of them in peer-reviewed scientific journals. Bahill has worked with dozens of high-tech companies presenting seminars on Systems Engineering, working on system development teams and helping them to describe their Systems Engineering processes. He holds a U.S. patent for the Bat Chooser™, a system that computes the Ideal Bat Weight™ for individual baseball and softball batters. He was elected to the Omega Alpha Association, the systems engineering honor society. He received the Sandia National Laboratories Gold President's Quality Award. He is a Fellow of the Institute of Electrical and Electronics Engineers (IEEE), of Raytheon Missile Systems, of the International Council on Systems Engineering (INCOSE) and of the American Association for the Advancement of Science (AAAS). He is the Founding Chair Emeritus of the INCOSE Fellows Committee. His picture is in the Baseball Hall of Fame's exhibition "Baseball as America." You can view this picture at http://sysengr.engr.arizona.edu/.

Acronyms

BA	Batting Average
BaConLaws	Baseball Conservation Laws
CoAM	Conservation of Angular Momentum
CoE	Conservation of Energy
CoM	Conservation of Momentum
CoR	Coefficient of Restitution
KE	Kinetic Energy
LHP	Left-Handed Pitcher
MLB	Major League Baseball
NCAA	National Collegiate Athletic Association
OPS	On-base Plus Slugging
RHP	Right-Handed Pitcher
SaD	Angle between Spin axis and Direction of motion
SaD Sid	Spin axis $\times$ Direction = Spin-induced deflection
VaSa	Angle between Vertical axis and Spin axis

List of Figures

Chapter 1
Types of Bat–Ball Collisions

1.1 Introduction

Purpose: This book has four primary purposes: first, to create models for bat–ball collisions using only fundamental principles of Newtonian mechanics, second, to help a batter select or create an optimal baseball or softball bat, third, to show what affects air density and how air density affects the flight of the ball, and finally, to explain the modeling process.

1.2 Newton's Axioms

Even though Newton formulated his axioms of over 300 years ago, they still provide the best explanations for collisions between baseballs and baseball bats. Although they are presented as equations in this book, math-phobic readers can just skip the equations and read the words without loss of continuity. Newton's axioms of motion can be written as follows.

I. *Inertia or uniform motion*. Every object either remains at rest or continues to move at a constant velocity, unless acted upon by an external force.

$$\sum F = 0 \quad \Rightarrow \quad dv/dt = 0$$

Note that force, velocity, acceleration, impulse and momentum are all vector quantities, although we do not specifically mark them as such. We do not treat speed and velocity as synonyms.

A. T. Bahill, *The Science of Baseball*,
https://doi.org/10.1007/978-3-030-03032-2_1

II. *Impulse and Momentum.*

Applying a force changes the momentum, p, of a body. Momentum equals mass times velocity. The *rate* of change of momentum is directly proportional to the force applied and is in the direction of the applied force.

$$F = \frac{dp}{dt} = \frac{d(mv)}{dt} \Rightarrow F = ma$$

Stated differently, the *amount* of change in momentum of a body is proportional to the impulse applied to the body and is in the direction of the impulse. An impulse J occurs when a force F acts over an interval of time Δt, and it is given by $J = \int_{\Delta t} F dt$. Since force is the time derivative of momentum, p, it follows that $J = \Delta p = m\Delta v$. Finally, for rotational systems, applying an impulsive torque changes the angular momentum about the torque axis.

III. *Action/reaction*. For every action, there is an equal and opposite reaction.
IV. *Restitution*. The coefficient of restitution (*CoR*) is defined as the ratio of the relative speeds of two objects after and before a collision. This holds whether one object or the other is initially at rest or the objects are initially approaching each other. The *CoR* models the energy lost in a collision.

$$CoR = \frac{\text{relative speed after the collision}}{\text{relative speed before the collision}}$$

In this book, we will use these four axioms of Newton. But more importantly, we will also use the overarching conservation laws that state: *energy, linear momentum and angular momentum cannot be created or destroyed*. These laws are more general than the axioms and apply in all circumstances. Because our model is based on these Conservation Laws of physics applied to baseball, we call it the BaConLaws model for bat–ball collisions (Table 1.1).

1.2.1 Variables and Parameters

The terms variable and parameter are often used interchangeably. Nevertheless, in this book, we will try to distinguish between the terms. Our variables have equations that give them values. Our variables contain parameters that will produce different sets of equations. In this book, we will treat the following as *variables*: the inputs $v_{\text{ball-before}}$, $\omega_{\text{ball-before}}$, $v_{\text{bat-cm-before}}$, $\omega_{\text{bat-before}}$ and CoR, the outputs $\mathrm{v}_{\text{ball-after}}$, $\omega_{\text{ball-after}}$, $v_{\text{bat-cm-after}}$, $\omega_{\text{bat-after}}$ and KE_{lost}, the forces on the ball, launch velocity, launch angle and launch spin rate. The following are *parameters* of our equations: the dimensions, mass and moment of inertia of the bat and ball, the air

Table 1.1 List of variables and parameters and their abbreviations

Symbol: This table is arranged alphabetically by the symbol	Abbreviation ball = 1 bat = 2 before = b after = a	Description, if specific, then for configuration 2b unless otherwise noted	Typical values for a C243 pro stock wooden bat and a professional major league baseball player	
			SI[b] units	Baseball units
$\beta_{\text{bat-knob}}$	β	Angular velocity of a bat about the knob in configuration 2c	rad/s	rpm
CoE		Conservation of Energy	Joules	
CoM		Conservation of Momentum	kg · m/s	
CoAM		Conservation of Angular Momentum	$\text{kg} \cdot \text{m}^2/\text{s}$	
CoR		Coefficient of Restitution of a high-speed bat–ball collision	0.466	0.466
d_{bat}		Length of a bat	0.863 m	34 inch
$d_{\text{bat-cm-cop}}$	$d_{\text{cm-cop}}$	Distance from the center of mass (cm) of the bat to the sweet spot, which we define as the Center of Percussion (cop)	0.119 m	4.7 in
$d_{\text{bat-knob-cm}}$	$d_{\text{k-cm}}$	Distance from the center of the knob of the bat to the center of mass	0.568 m	22.4 in
$d_{\text{bat-knob-cop}}$	$d_{\text{k-cop}}$	Distance from the center of the knob of the bat to the center of percussion	0.687 m	27.0 in
$d_{\text{spine-cm}}$		Distance from the batter's spine to the center of mass of a bat, an experimentally measured value	1.05 m	41 in
$d_{\text{bat-cm-end}}$		Distance from the center of mass to the barrel end of a bat	0.281 m	11.1 in
$d_{\text{bat-cop-end}}$		Distance from the center of percussion to the barrel end of a bat	0.162 m	6.4 in
g		Earth's gravitational constant (at the University of Arizona)	$9.718\ \text{m/s}^2$	
I_{ball}	I_1	Moment of inertia of a baseball with respect to its center of mass	0.000079 kg m^2	$4.3\ \text{oz in}^2$

(continued)

Table 1.1 (continued)

Symbol: This table is arranged alphabetically by the symbol	Abbreviation ball = 1 bat = 2 before = b after = a	Description, if specific, then for configuration 2b unless otherwise noted	Typical values for a C243 pro stock wooden bat and a professional major league baseball player	
			SI[b] units	Baseball units
$I_{\text{bat-cm}}$	$I_2 = I_{\text{cm}}$	Moment of inertia of a bat with respect to rotations about its center of mass	0.0511 kg m^2	2792 oz in^2
$I_{\text{bat-knob}}$	I_{k}	Moment of inertia of a bat with respect to rotations about the knob	0.335 kg m^2	18,315 oz in^2
KE_{before}		Kinetic energy of a bat and a ball before the collision	370 J	
KE_{after}		Kinetic energy of a bat and a ball after the collision	175 J	
KE_{lost}		kinetic energy lost or transformed in the collision	195 J	
m_{ball}	m_1	Mass of a baseball	0.145 kg	5.125 oz
m_{bat}	m_2	Mass of a baseball bat	0.88 kg	31 oz
$\bar{m}$		$\bar{m} = \frac{m_{\text{ball}} m_{\text{bat}}}{m_{\text{ball}} + m_{\text{bat}}}$	0.124 kg	4.4 oz
M_{eff}		Mass of a portion of the bat in the effective mass model	0.707 kg	25 oz
μ_f		Dynamic coefficient of friction for a baseball sliding on a wooden bat	0.5	
r_{ball}	r_1	Radius of a baseball	0.037 m	1.45 in
r_{bat}	r_2	Radius of a baseball bat at the impact point	0.031 m	1.3 in
Pitch speed		speed of a ball at the pitcher's release point	−41 m/s	−92[a] mph
$v_{\text{ball-before}}$	v_{1b}	Linear velocity of a ball immediately before the collision, 90% of the pitch speed	−37 m/s	−83[a] mph
$v_{\text{ball-after}}$	v_{1a}	Linear velocity of a ball after the collision, often called the launch velocity or the batted-ball speed	42 m/s	93 mph

(continued)

Table 1.1 (continued)

Symbol: This table is arranged alphabetically by the symbol	Abbreviation ball = 1 bat = 2 before = b after = a	Description, if specific, then for configuration 2b unless otherwise noted	Typical values for a C243 pro stock wooden bat and a professional major league baseball player	
			SI[b] units	Baseball units
v_{bat}	v_2	Linear velocity of a bat. If a specific place or time is intended then the subscript may contain cm (center of mass), ip (impact point), before (b) or after (a)		
$v_{\text{bat-cm-before}}$	$v_{2\text{cmb}}$	Linear velocity of the center of mass of a bat before the bat–ball collision	23 m/s	51 mph
$v_{\text{bat-cm-after}}$	$v_{2\text{cma}}$	Linear velocity of the center of mass of a bat after the collision	11 m/s	25 mph
$vt_{\text{bat-ip-before}}$	$v_{2\text{ipb}}$	Total velocity of the impact point of a bat before the collision	27 m/s	60[a] mph
$vt_{\text{bat-ip-after}}$	$v_{2\text{ipa}}$	Total velocity of the impact point of a bat after the collision	11 m/s	25 mph
$\omega_{\text{ball-before}}$	$\omega_{1\text{b}}$	Angular velocity of a ball about its center of mass before the collision. This spin rate depends on the particular type of pitch	±209 rad/s	±2000 rpm
$\omega_{\text{ball-after}}$	$\omega_{1\text{a}}$	Angular velocity of a ball about its center of mass after the collision	±209 rad/s	±2000 rpm
$\omega_{\text{bat-before}}$	$\omega_{2\text{b}}$	Angular velocity of a bat about its center of mass before the collision	32 rad/s	309 rpm
$\omega_{\text{bat-after}}$	$\omega_{2\text{a}}$	Angular velocity of a bat about its center of mass after the collision	6 rad/s	56 rpm
$\omega_{\text{spine-before}}$		Angular velocity of the batter's arms about the spine	21 rad/s	201 rpm

[a]The equations of this book concern parameters right before and right after the collision, not at other times. For example, a pitcher could release a fastball with a speed of 92 mph, by the time it got to the collision zone it would have slowed down by 10% to 83 mph. Therefore, in our simulations, we used 83 mph for $v_{\text{ball-before}}$

[b]SI stands for Système International, the International System of Units

density, the drag coefficient, the Magnus coefficient, the Reynolds number and collision speed. For each invocation of an equation, they will have a fixed value. Sometimes, we will refer to variables and parameters together as properties of the model. The following are *constants* that always have the same values: π , e, $\sqrt{2}$ and the natural numbers.

1.3 Models for the Swing of a Bat

This book is about modeling and simulation of bat–ball collisions and the flight of the ball. A *model* is a simplified representation of some aspect of a real system. A *simulation* is an implementation of a model, often on a digital computer. Models are ephemeral: they are created, they explain a phenomenon, they stimulate discussion, they foment alternatives and then they are replaced by new models. In this section, we present many alternative models for the swing of a bat that we have used in this book. The purpose of developing these models was to better understand the game of baseball. Having alternative models helps ensure that you understand the physical system. No model is more correct than another. They just investigate alternative viewpoints of the physical system.

In the top panel of Fig. 1.1, the batter swings the bat with translational and rotational motions. In the middle panel, the bat motion has two rotational components, one about the batter's spine ω_{body} and another about the pivot point between the hands, ω_{wrists}. In the bottom panel, the movement of the bat before the collision is modeled as the sum of a linear translation of the center of mass of the bat before the collision, $v_{\text{bat-cm-before}}$, and the effect of an angular rotation about the a pivot point between the hands, $\omega_{\text{bat-pivot}}$. This straight-line velocity was measured in our experiments and it is called the total bat speed before the collision. These alternative models are simplifications that emphasize different aspects of the swing of the bat.

Next, we introduce the fundamental principle of a *free-end collision*. Consider this: if you toss a bat into the air, it will have linear motion and it will rotate about its center of mass. No one will be holding onto this bat; hence its ends will be free to move. Next, imagine the stationary bat of Fig. 1.2 laying on a sheet of slick ice. You are looking down on top of it. Then a baseball slams into this bat at 80 mph. This collision produces a translation and a rotation of the bat about its center of mass. The bat acts as if no one is holding onto its knob and there are no other forces acting on the bat. Hence, this collision behaves like a free-end collision. Assuming a free-end collision makes the model simpler. We need not search for other forces on the bat, because there are none.

Now, to add complexity to this model, we will allow the bat to also be moving at the beginning of the collision, as shown in Fig. 1.3. In this figure, we have shown the velocity of the bat after the collision to be less than its velocity before the

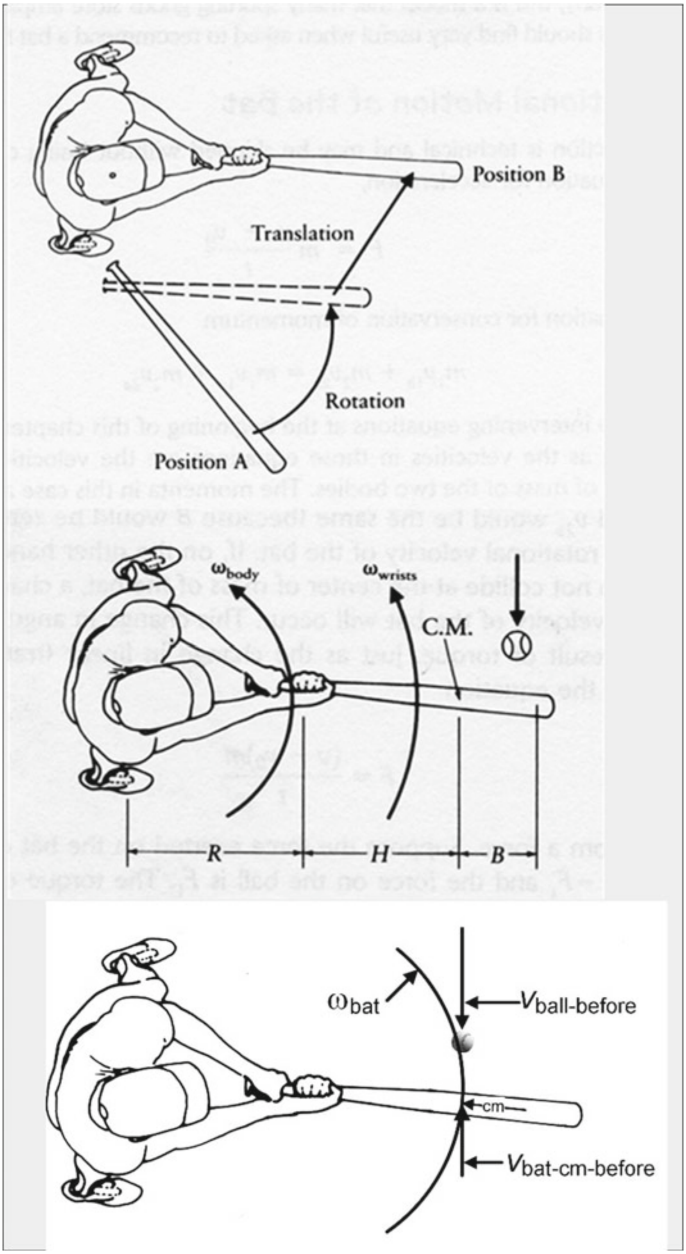

Fig. 1.1 Three models for the swing of the bat. The center of mass of the bat is represented with *cm*. The words *before* and *after* stand for before and after the bat–ball collision

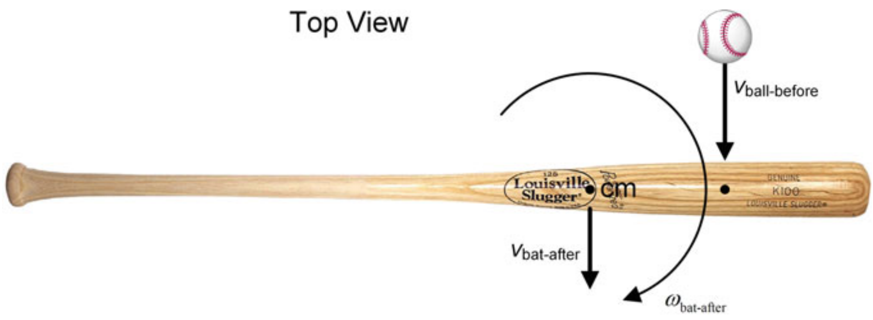

Fig. 1.2 A stationary bat involved in a free-end collision with a ball

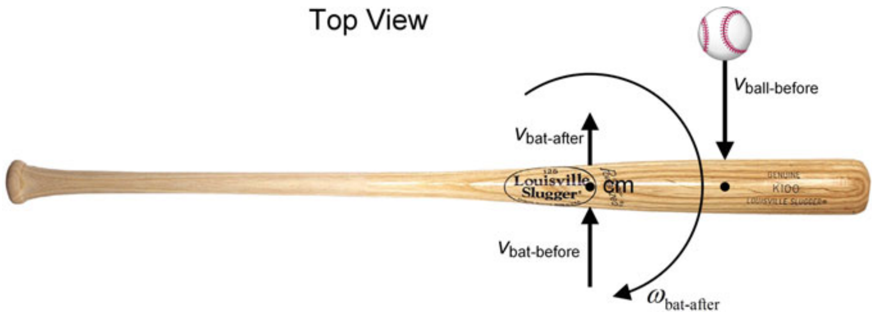

Fig. 1.3 A moving bat involved in a free-end collision with a ball

collision (its arrow is shorter). But this relationship has many possible variations depending on the relative velocities and masses of the bat and ball.

Our next model, shown in Fig. 1.4, can be used to derive equations for the speed and spin of the bat and ball after the collision in terms of those same four variables before the collision. It applies simple Newtonian axioms and the **Con**servation **Law**s of physics to **Ba**seball: therefore we call it the BaConLaws model for bat–ball collisions. It is the workhorse of this book. Its fundamental principle is that of a free-end collision. Assuming a free-end collision makes the equations of motion solvable. Most models that use Newton's axioms and the Conservation Laws to explain the motion of the bat assume free-end collisions. This model is used extensively in Chaps. 3 and 4.

This paragraph introduces the bat Effective Mass model, which is the most popular *physics*-of-baseball model for bat–ball collisions. It also assumes a free-end collision. In this model, the ball does not collide with the whole bat, it only collides with a segment of the bat, as shown in Fig. 1.5. The equations for this model are simpler than those of the BaConLaws model, yet the model is just as accurate. However, for non-physicists, it is not as intuitive.

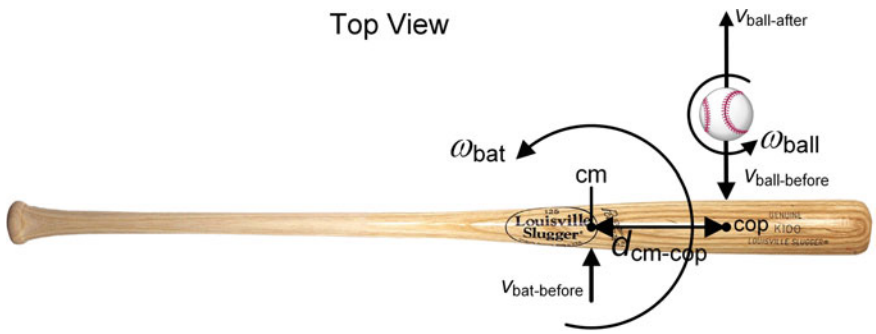

Fig. 1.4 The BaConLaws model for a bat and a ball involved in a free-end collision. The abbreviation cop stands for the center of percussion, the sweet spot of the bat

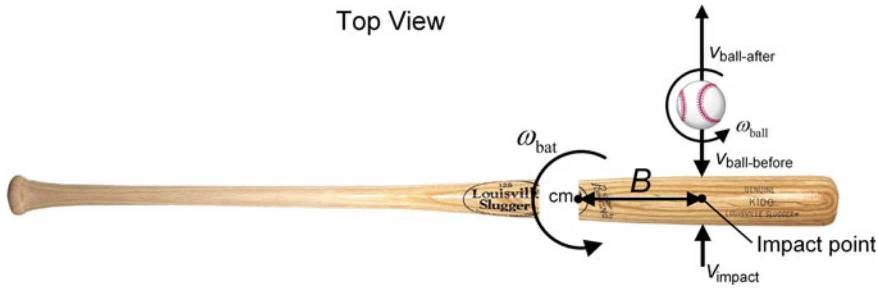

Fig. 1.5 The Effective Mass model

Recent studies of bat and ball motions have used multiple video cameras and commercial prepackaged software to measure and compute bat speed. These are similar to the computer-camera systems that are used to overlay pitch trajectories on MLB television replays. However, instead of computing the speed and rotation of the bat and ball, as in the free-end collision models, these modelers measure only the motion of the center of mass of the bat as shown in Fig. 1.6. This model gives an equation for the path of the bat, but there is no equation for the ball. During the collision, the batter is exerting a force on the bat. Therefore, it is not a free-end collision.

The Sliding Pin model of Fig. 1.7 (whose name will be explained in Chap. 5) models a new type of data; data derived from computer-video-camera systems similar to those installed in MLB stadiums. In the free-end collision models, the input data were the translational and rotational velocities at the *center of mass* of the bat. In contrast, the Sliding Pin model uses the translational and rotational velocities at the *knob* of the bat. The batter is holding the knob end. Therefore, this is not a free-end collision. We do not have equations for the forces produced by the batter, therefore we cannot create equations for the flight of the ball. This model is

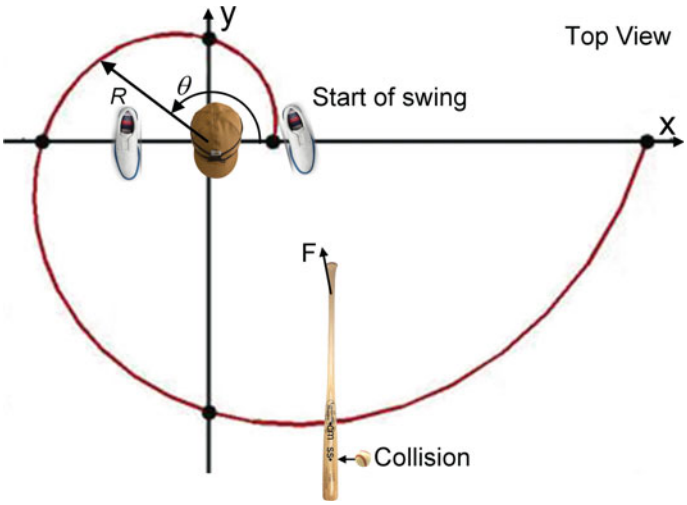

Fig. 1.6 The Spiral Center of Mass model. Top view showing the batter's cap and shoes. The red spiral is the path of the center of mass of the bat

Fig. 1.7 The sliding pin model for the swing of the bat

attractive because this is what the spectator sees, a big sweeping motion about the knob.

Finally, when friction is important, more forces must be added to the model, as shown in Fig. 1.8. The free-end collision models are valid for points in time before and after the collision. They are not valid during the collision. This Collision with Friction model represents the behavior of the ball *during* the collision. Although its equations are consistent, this model was not fully developed because the ball behavior during the collision is too complicated. See Fig. 5.7.

These ten alternative models use different inputs and produce different outputs. They are used for different purposes. Each models a different aspect of the swing of the bat. None models all aspects of the swing. However, studied as a whole, they should provide a good understanding of the swing of a baseball bat.

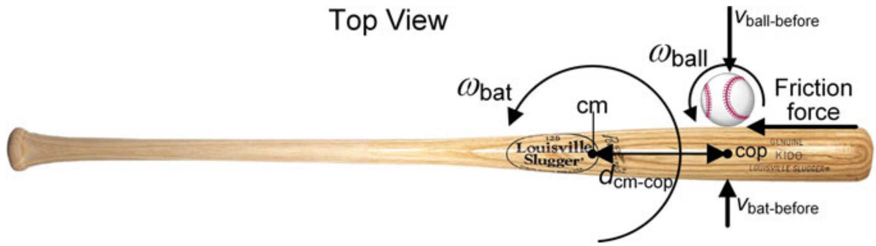

Fig. 1.8 Collision with friction model

Modeling philosophy note. Having several alternative models helps ensure that you understand the physical system. No model is more correct than another. They just emphasize different views of the physical system.

1.4 Summary

This chapter presented Newton's laws of motion, our table of abbreviations and nomenclature for describing collisions. It also gave ten simple models for a person swinging a bat.

Chapter 2
Configurations of Bat–Ball Collisions

2.1 Introduction

Purpose: The purpose of this chapter is to present alternative configurations of bat–ball collisions. Then to explain the configurations that we can model and those that we cannot.

This chapter presents nine alternative configurations of bat–ball collisions. For each of these configurations, we model the state of the bat and the ball at a point in time just before the collision and at another point just after the collision. We are not modeling the behavior (1) during the collision, (2) long before the collision (the pitched ball) or (3) long after the collision (the batted ball). The flight of the pitch and the batted ball are modeled in Chap. 7. First, we will give some definitions that will be helpful in describing collisions in general.

2.2 Characterizing Bat–Ball Collisions

A collision can be *elastic* or *inelastic*. In an elastic collision (such as a steel ball or a superball bouncing off a large steel plate), there is practically no energy lost or transformed. Whereas in an inelastic collision (such as a bat–ball collision), energy is transformed. Most authors call this the energy *lost*, but it is not lost: it is merely transformed into a different form, such as heat in the ball, vibrations in the bat, acoustic energy in the "crack of the bat," friction and permanent deformations of the bat and ball. This book considers only inelastic collisions where kinetic energy is lost.

A. T. Bahill, *The Science of Baseball*,
https://doi.org/10.1007/978-3-030-03032-2_2

2.2.1 Collision Taxonomy

There are many kinds of collisions between two rigid bodies. One kind, where the duration of the collision is short and the area of the collision is small, is called an *impact*. Bat–ball impacts are described with the following three characteristics: dimension, location and direction. The following definitions, involving these characteristics, hold before and after the collision.

2.2.1.1 Dimension

If the equations of motion can be described in a two-dimensional (2D) plane, then the impact is *planar*. For example, the game of billiards is, for the most part, planar. Otherwise, if the equations of motion require description in three-dimensional (3D) space, then the impact is *nonplanar*.

2.2.1.2 Line of Impact

For an impact between two objects, there is a common tangent plane that is perpendicular to the radius of curvature of each object at the point of contact. The line that is perpendicular to this plane at this point is called the *line of impact*.

2.2.1.3 Location

An impact is *central* if the centers of mass of both bodies are on the line of impact, otherwise the impact is *eccentric*.

2.2.1.4 Direction

An impact is *direct* if the directions of motion of both the bodies are on the line of impact; it is *parallel* if the direction of the center of mass one body is on the line of impact and the other is on a parallel line, otherwise the impact is *oblique*.

These terms are useful because they predict the complexity of the equations of motion. Planar-central-direct impacts are the simplest because all motions are along the same axis and there are no impulsive torques. Nonplanar-eccentric-oblique impacts have the most complicated equations. These terms also help a person to determine the type of analysis that will be necessary to study a certain collision configuration. If you are going to simulate a collision, then your first decisions will involve choosing values for these characteristics (Table 2.1).

Table 2.1 Top-level decisions for simulating bat–ball collisions

Characteristic	Allowable set of values {legal values}
Dimension of analysis	{Planar, nonplanar}
Location of collision	{Central, eccentric}
Direction of motion	{Direct, parallel, oblique}
Point of contact	{Center of mass, sweet spot, impact point}

2.3 Collisions at the Center of Mass

2.3.1 Configuration 1a

Configuration 1a is a head-on collision at the center of mass of the bat, as shown in Fig. 2.1. Spin on the ball and bat are not considered. This simple type of analysis was done by Bahill and Karnavas (1989). It uses Conservation of Linear Momentum (CoM) and the Coefficient of Restitution (*CoR*).

Configurations 1a and 1b are planar, central, direct impacts.

The impact is planar because the governing equations are in the *x-y* plane. This collision can be drawn on a flat piece of paper.

The impact is central because the line of impact passes through the centers of mass of both the ball and the bat.

The impact is direct because the centers of mass of both the bat and the ball are moving along the line of impact. This means that the initial tangential (*y*-axis and *z*-axis) velocity components are zero.

In this model, the bat does not rotate.

This type of collision would produce a line drive back to the pitcher.

2.3.2 Configuration 1b

Configuration 1b is the same as configuration 1a, except that it adds KE_{lost} and Conservation of Energy as checks on the derivations. Planar, central, direct collisions (like configurations 1a and 1b) are called *head-on* collisions.

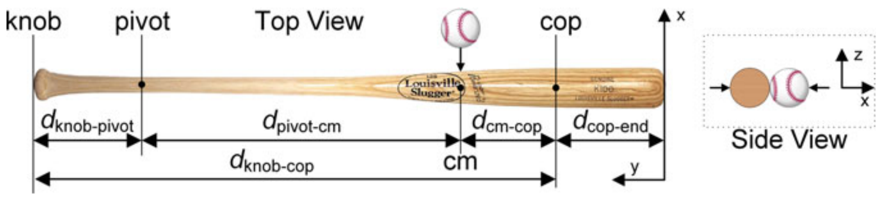

Fig. 2.1 Configurations 1a and 1b are head-on collisions at the center of mass (cm) of the bat. All figures in this book are for right-handed batters

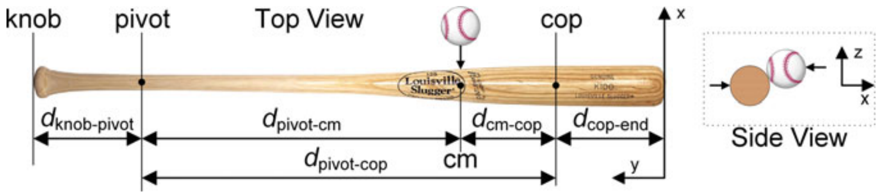

Fig. 2.2 Configuration 1c is a collision at the center of mass (cm) of the bat, but vertically it is above the long axis of the bat

2.3.3 *Configuration 1c*

Configuration 1c is a collision at the center of mass of the bat along the *y*-axis, but vertically it is above or below the long axis of the bat, as shown in Fig. 2.2. This is the same as configuration 1a, except that there is a vertical offset between the directions of motion of the bat and ball at the collision (the bat hits the bottom part of the ball) and the equations allow spin on the ball. Nathan et al. (2012) have presented experimental data for the spin on the ball after such a collision.

Configuration 1c is a planar, central, oblique impact.

The impact is planar because the impact is in the *x*-*z* plane: the bat and ball will both have *x*- and *z*-axis motion after the impact but no motion in the y direction.
The impact is central because the line of impact passes through the centers of mass of both the ball and the bat.
The impact is oblique because in the *x*-*z* plane, the motion of the bat and ball are not parallel to the line of impact.

This type of collision would typically produce a fly ball to center field, or maybe a pop-up. The equations for this type of impact will be considered in a future paper. Configuration 1c will not be mentioned again in this book.

2.4 Collisions at the Sweet Spot

The term *sweet spot* is a layman's term for a general area of the bat about two inches wide and one-fifth of an inch high centered about six inches away from the barrel end of the bat, as shown in Fig. 2.3. Section 3.3.1.1 gives nine possible definitions for the sweet spot of the bat. When we are writing about a general area of the bat, or when we are reporting on papers that used the term, we will use the term sweet spot. However, in our figures, we need to be more specific. Hence, we adopt the first definition in Sect. 3.3.1.1 of the sweet spot, namely the center of percussion (cop). In our simulations, we need to specify a particular point on the bat

Fig. 2.3 The sweet spot of the bat is centered about six inches away from the barrel end of the bat. The abbreviation cm stands for center of mass and cop is the center of percussion

for the collision: therefore, we also use the center of percussion in our simulations. Finally, in our equations, we do not restrict the collision to be at any particular point on the bat: Therefore, in equations, we state that the collision occurs at the impact point (ip).

Configurations 2 are head-on collisions at the sweet spot of the bat, which we define to be the center of percussion (Bahill 2004). This type of analysis was done by Watts and Bahill (1990). Compared to Configurations 1, they move the collision from the center of mass of the bat to the sweet spot of the bat.

2.4.1 Configurations 2a and 2b

Configuration 2a is a head-on collision at the sweet spot {center of percussion (cop)} of the bat. Compared to Configuration 1a, it adds an equation based on Newton's second axioms and it adds rotation of the bat about its center of mass.

Configuration 2a is a planar, eccentric, parallel impact.

The impact is planar because the equations are in the *x*-*y* plane. This collision can be drawn on a flat piece of paper.

The impact is eccentric because the line of impact does not pass through the center of mass of the bat in the x-y plane. It could be noted that the line of impact passes through the center of mass of the bat in the *x*-*z* plane. But that is irrelevant. Once the line of impact misses the center of mass in any plane, the impact is eccentric.

The impact is parallel because the line of impact is parallel to the *x*-axis, the ball is moving along the *x*-axis and the bat's center of mass is moving parallel to the *x*-axis

Configuration 2a would produce a line drive back to the pitcher.

Configuration 2b is a collision at the sweet spot of the bat. It is similar to configuration 2a, except that it adds Conservation of Energy as a consistency check, Conservation of Angular Momentum, spin on the ball and kinetic energy lost. Configuration 2b is the pinnacle of this book.

For configurations 2, planar, eccentric, parallel collisions are called *head-on*.

For collisions 2a and 2b, which are described with Fig. 2.4, there is no torque on the ball. Therefore, there will be no change in angular velocity of the ball. For these head-on collisions, the angular velocity of the ball before the collision is the same as the angular velocity of the ball after the collision.

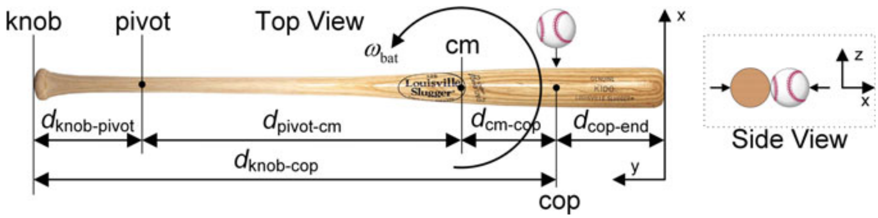

Fig. 2.4 Configurations 2 are collisions at the sweet spot {center of percussion (cop)} of the bat

2.4.2 Configuration 2c

Configuration 2c is a collision at the sweet spot of the bat with spin on the pitch. Conservation of Angular Momentum about the *z*-axis was successfully used. It replaces rotation about the center of mass with rotation about the knob of the bat, identified with β_{bat}. This is the Sliding Pin model of Chap. 5.

2.4.3 Configuration 2d

Configuration 2d is a collision at the sweet spot of the bat with spin on the pitch and friction between the bat and ball, as will be shown later in Fig. 5.2. As an obvious example of what spin can do, consider a tennis player putting sidespin on a tennis ball, the ball certainly will move sideways when it hits the ground Cross (2011). Likewise, when a spinning baseball collides with a bat, there will be a friction force that changes the rate of spin of the ball. This configuration uses the conservation of momentum and Newton's second axiom. It adds friction at the contact point and a momentum moment.

2.4.4 Configuration 3

Configuration 3 is a collision at the sweet spot of the bat, but above or below the long axis of the bat as shown in Fig. 2.5. This is the same as configuration 2b, except it adds offset to the bat–ball collision and bat twist. Nathan et al. (2012) and Kensrud et al. (2017) gave experimental data for the spin of a baseball after collisions in this type of an impact and Sawicki et al. (2003) gave simulation results.

Configuration 3 is a nonplanar, eccentric, oblique impact.

If spin on the ball causes motion in the *y*-axis direction, then the impact is nonplanar because the bat and ball will both have *x*-, *y*- and *z*-axis motion after the impact.

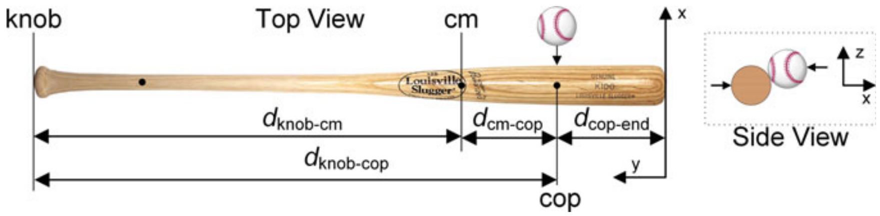

Fig. 2.5 Configuration 3 is a collision at the sweet spot (cop) of the bat, but above the horizontal axis of the bat

The impact is eccentric because the line of impact misses the center of mass of the bat in the *x*-*y* plane.

The impact is oblique because in the *x*-*z* plane, the motion of the bat and ball are not parallel to the line of impact.

This type of collision would typically produce a fly ball to center field. Configuration 3 will not be mentioned again until Chap. 9.

2.4.5 Configuration 4

Configuration 4 is an oblique collision at the sweet spot but above or below the horizontal (long) axis of the bat as shown in Fig. 2.6. This is the same as configuration 3, except that it adds the bat being rotated short of (or beyond) a line parallel to the *y*-axis at the time of the collision.

Configuration 4 is a nonplanar, eccentric, oblique impact.

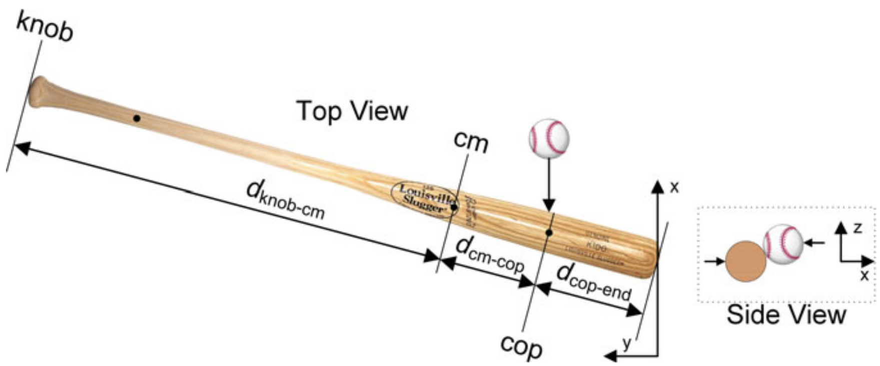

Fig. 2.6 Configuration 4 is an oblique collision at the sweet spot (cop) and above the horizontal axis of the bat

This impact is nonplanar because the bat and ball will both have *x*-, *y*- and *z*-axis motion after the impact.
The impact is eccentric because the line of impact misses the center of mass of the bat in the *x*-*y* plane.
The impact is oblique because the bat is not moving along the *x*-axis at the time of impact. This means that there will be tangential (*y*-axis) velocity components.

This type of collision would typically produce a fly ball to right (or left) field. Configuration 4 will not be mentioned again in this book.

2.5 Summary

Abbreviations used in Table 2.2.

Abbreviation	Name
CoE	Conservation of energy
CoM	Conservation of momentum
CoAM	Conservation of angular momentum
CoR	Coefficient of restitution
cm	Center of mass
KE_{lost}	The kinetic energy lost or transformed during the collision
μ_f	Coefficient of friction
e_m	Coefficient of moment restitution
ip	Impact point
ω_{ball}	Angular velocity of the ball
β_{bat}	Angular velocity of the bat about the knob

Table 2.2 shows the history of the development of the nine configurations mentioned in this book. It also shows how the details of the models differ. In configurations 1ab and 2abc, spin is allowed but it is not included in the equations because in Chap. 4, we show that spin has no effect in head-on collisions.

Table 2.3 shows the equations and constraints that were used in each model. For example, configuration 2b for a collision at the sweet spot used equations for Conservation of Linear Momentum, Coefficient of Restitution, Newton's second axiom, Conservation of Energy, Kinetic energy lost and Conservation of Angular Momentum. It used five equations and had five outputs (unknowns). It used principles of physiology, spin on the ball and rotation of the bat about its center of mass.

Modeling philosophy note. This chapter presented alternative models. They emphasize different aspects of the physical system. In this chapter, they got more and more complicated as they tried to cover more and larger aspects of the real system. This chapter sets the structure for the rest of the book. In Chap. 3, we will follow this structure except that we will add equations. But once again, we will start with baby steps and then get more complicated.

Table 2.2 Comparison of the collision configurations

Characteristic	Configuration								
	1a	1b	1c	2a	2b	2c	2d	3	4
Dimension	Planar	Planar	Planar	Planar	Planar	Planar	Planar	Nonplanar	Nonplanar
Location	Central	Central	Central	Eccentric	Eccentric	Eccentric	Eccentric	Eccentric	Eccentric
Direction	Direct	Direct	Oblique	Parallel	Parallel	Parallel	Parallel	Oblique	Oblique
Spin on the pitch	No	No	Yes	No	Yes	Yes	Yes	Yes	Yes
Rotation of bat	No	No	No	Yes	Yes	Yes	Yes	Yes	Yes
Point of contact	cm	cm	cm	ip	ip	ip	ip	ip	ip
Difference from previous configuration	Uses CoM and *CoR*, adds physiology	Adds CoE & KE_{lost}	Adds vertical offset at collision point	Moves collision to ip, adds Newton's second & ω_{bat}	Adds CoE, CoAM, ω_{ball} & KE_{lost}	Adds β_{bat} about knob	Adds μ_f friction	Adds vertical offset and twist (or roll) of the bat	Adds bat not parallel to y-axis
Developed by	Bahill and Karnavas (1989)	Chapter 3		Watts and Bahill (1990)	Chapter 4	Chapter 5	Chapter 5	Chapter 9	
Variables and parameters used to model losses	*CoR*	*CoR*	*CoR*, μ_f and e_m	*CoR*	*CoR*	*CoR*	*CoR*, and μ_f	*CoR*, μ_f and e_m	*CoR*, μ_f and e_m

Table 2.3 Equations and constraints for some of the configurations

Characteristic	Configuration					
	1a	1b	2a	2b	2c	2d
Location						
Is the collision at the center of mass (cm) or the impact point (ip)?	cm	cm	ip	ip	ip	ip
Equations						
Conservation of linear momentum	yes	yes	yes	yes	yes	
Coefficient of restitution	yes	yes	yes	yes	yes	
Newton's second axiom			yes	yes	yes	yes
Conservation of energy		yes		yes		
Kinetic energy lost		yes		yes		
Conservation of angular momentum				yes	yes	yes
Number of equations used	2	3	3	5	4	2
Number of unknowns (outputs)	2	2	1	5	3	1
Constraints						
Principles of physiology	yes	yes	yes	yes	yes	yes
Is ω_{ball} used?				yes	yes	yes
Is ω_{bat} used?			yes	yes		
Is β_{bat} used?					yes	
Is friction used?						yes

References

Bahill, A. T. (2004). The ideal moment of inertia for a baseball or softball bat. *IEEE Transactions on Systems, Man, and Cybernetics Part A: Systems and Humans*, *34*(2), 197–204.

Bahill, A. T., & Karnavas, W. J. (1989). Determining ideal baseball bat weights using muscle force-velocity relationships. *Biological Cybernetics, 62,* 89–97.

Cross, R. (2011). *Physics of baseball and softball*. Berlin: Springer.

Kensrud, J. R., Nathan, A. M., & Smith, L. V. (2017). Oblique collisions of baseballs and softballs with a bat. *American Journal of Physics, 85,* 503–509. https://doi.org/10.1119/1.4982793.

Nathan, A. M., Cantakos, J., Kesman, R., Mathew, B., & Lukash, W. (2012). Spin of a batted baseball. In: *9th Conference of the International Sports Engineering Association (ISEA), Procedia Engineering* (Vol. 34, pp. 182–187). https://doi.org/10.1016/j.proeng.2012.04.032.

Sawicki, G. S., Hubbard, M., & Stronge, W. J. (2003). How to hit home runs: Optimum baseball bat swing parameters for maximum range trajectories. *American Journal of Physics*, *71*(11), 1152–1162.

Watts, R. G., & Bahill, A. T. *Keep your eye on the ball: Curveballs, knuckleballs, and fallacies of baseball* (1st ed. 1990, 2nd ed. 2000). New York: W. H. Freeman and Co.

Chapter 3
Equations for Bat–Ball Collisions

3.1 Introduction

Purpose: The purpose of this chapter is to start presenting the incipient equations that we will use to model selected configurations of Chap. 2. We will allow the reader to progress slowly through the equations: take baby steps first.

Each of the next six sections in this chapter starts with a table that describes the inputs, outputs and equations that will be used in that section.

3.2 Collisions at the Center of Mass

For configurations 1a, 1b and 1c, the model for bat motion is a linear translation of the bat.

3.2.1 Configuration 1a

Configuration 1a is a head-on collision at the center of mass of the bat, as shown in Fig. 1.1 (bottom) and Fig. 2.1. This section uses linear velocities (meaning there is no ω_{bat} or ω_{ball}) with two equations in two unknowns (Bahill and Karnavas 1989, 1991), which are given in Table 3.1.

We will now derive the equations for a head-on (planar, central, direct) collision at the center of mass (cm) of the bat. The abbreviations used in the following equations are described in Table 1.1. Many authors, for example (Bahill and Karnavas 1989, 1991; Watts and Bahill 1990/2000; Brach 2007), have previously studied collisions using the Newtonian concepts of Conservation of Momentum

A. T. Bahill, *The Science of Baseball*,
https://doi.org/10.1007/978-3-030-03032-2_3

Table 3.1 Equations for configuration 1a, two equations and two unknowns

Inputs	$v_{\text{ball-before}}, v_{\text{bat-cm-before}}$
Outputs (unknowns)	$v_{\text{ball-after}}, v_{\text{bat-cm-after}}$
Equations	
Conservation of linear momentum	$m_{\text{ball}} v_{\text{ball-before}} + m_{\text{bat}} v_{\text{bat-cm-before}} = m_{\text{ball}} v_{\text{ball-after}} + m_{\text{bat}} v_{\text{bat-cm-after}}$
Definition of *CoR*	$CoR_{1a} = -\frac{v_{\text{ball-after}} - v_{\text{bat-cm-after}}}{v_{\text{ball-before}} - v_{\text{bat-cm-before}}}$

$$m_{\text{ball}} v_{\text{ball-before}} + m_{\text{bat}} v_{\text{bat-cm-before}} = m_{\text{ball}} v_{\text{ball-after}} + m_{\text{bat}} v_{\text{bat-cm-after}}$$

and the Kinematic Coefficient of Restitution (*CoR*)

$$CoR_{1a} = -\frac{v_{\text{ball-after}} - v_{\text{bat-cm-after}}}{v_{\text{ball-before}} - v_{\text{bat-cm-before}}}$$

to derive the following equations for the velocities of the ball and bat after the collision, which were presented in Bahill and Karnavas (1989):

$$v_{\text{ball-after}} = \frac{v_{\text{ball-before}}(m_{\text{ball}} - CoR_{1a} m_{\text{bat}}) + v_{\text{bat-cm-before}} m_{\text{bat}}(1 + CoR_{1a})}{m_{\text{ball}} + m_{\text{bat}}}$$

$$v_{\text{bat-cm-after}} = \frac{v_{\text{ball-before}} m_{\text{ball}}(1 + CoR_{1a}) + v_{\text{bat-cm-before}}(m_{\text{bat}} - m_{\text{ball}} CoR_{1a})}{m_{\text{ball}} + m_{\text{bat}}}$$

After rearranging, we have the canonical form

$$v_{\text{ball-after}} = v_{\text{ball-before}} + \frac{(v_{\text{bat-cm-before}} - v_{\text{ball-before}}) m_{\text{bat}}(1 + CoR_{1a})}{m_{\text{ball}} + m_{\text{bat}}}$$

$$v_{\text{bat-cm-after}} = v_{\text{bat-cm-before}} - \frac{(v_{\text{bat-cm-before}} - v_{\text{ball-before}}) m_{\text{ball}}(1 + CoR_{1a})}{m_{\text{ball}} + m_{\text{bat}}}$$

Historically, these derivations started with the two-rotation model for the swing of a baseball or a softball bat (Fig. 1.1, middle) and linearized the model by finding tangents to the circular motion (Fig. 1.1, bottom). Bahill and Karnavas (1989) expanded this model by measuring the speed of the swing for a few hundred baseball and softball players and used this experimental data and model, to derive equations for the batted-ball speed for each individual person.

This derivation used the following assumptions:

1. Neglect permanent deformation of the bat and ball.
2. Assume a head-on (planar, direct, central) collision at the center of mass of the bat.
3. Ignore the change in the rotational kinetic energy of the ball: the energy stored in the spin of the ball is less than one percent of the translational energy (Bahill

and Baldwin 2008). For a pitch hitting the sweet spot of the bat, the initial kinetic energy stored in the bat and the ball is 375 J, of which 1.7 J is stored in the spin of the ball: so neglecting it seems reasonable. In the section for configuration 2b, we show that for a head-on collision (without considering friction) there will be no change in the ball's angular rotation.
4. Assume that there are no tangential forces during the collision.
5. Neglect the moment of inertia of the batter's arms.
6. We assumed a free-end collision. The velocity of the bat reaches its peak at or before the collision. This means that the batter's hands and arms are no longer applying acceleration forces. Hence, we neglected forces from the batter's hands during the collision.

The reason for considering collisions at the center of mass is to allow the reader to progress slowly through the derivations. Take baby steps first. Configuration 1a in Chap. 3 takes two pages of easy equations. The BaConLaws model of Chap. 4 takes 40 pages of detailed equations.

This is the end of the Bahill and Karnavas (1989, 1991) model derivation.

3.2.1.1 Alternative Bat Effective Mass Model

The bat effective mass bat–ball collision modeling community, established by Nathan (2003), derives the batted-ball speed equation as follows. Figure 2.1 and the equation for conservation of linear momentum give us

$$m_{\text{ball}} v_{\text{ball-before}} + m_{\text{bat}} v_{\text{bat-cm-before}} = m_{\text{ball}} v_{\text{ball-after}} + m_{\text{bat}} v_{\text{bat-cm-after}}$$

We can solve this for $v_{\text{bat-cm-after}}$

$$v_{\text{bat-cm-after}} = \left\{ v_{\text{bat-cm-before}} + \frac{m_{\text{ball}} v_{\text{ball-before}} - m_{\text{ball}} v_{\text{ball-after}}}{m_{\text{bat}}} \right\}$$

and substitute this into the equation for the coefficient of restitution.

$$e = -\frac{v_{\text{ball-after}} - v_{\text{bat-cm-after}}}{v_{\text{ball-before}} - v_{\text{bat-cm-before}}}$$

$$e = -\frac{v_{\text{ball-after}} - \left\{ v_{\text{bat-cm-before}} + \frac{m_{\text{ball}} v_{\text{ball-before}} - m_{\text{ball}} v_{\text{ball-after}}}{m_{\text{bat}}} \right\}}{v_{\text{ball-before}} - v_{\text{bat-cm-before}}}$$

$$e(v_{\text{ball-before}} - v_{\text{bat-cm-before}}) = -v_{\text{ball-after}} - v_{\text{bat-cm-before}} + \frac{m_{\text{ball}}(v_{\text{ball-before}} - v_{\text{ball-after}})}{m_{\text{bat}}}$$

collecting the $v_{\text{ball-after}}$ terms on the left side yields

$$v_{\text{ball-after}} + \frac{m_{\text{ball}} v_{\text{ball-after}}}{m_{\text{bat}}} = -v_{\text{bat-cm-before}} + \frac{m_{\text{ball}} v_{\text{ball-before}}}{m_{\text{bat}}} - e(v_{\text{ball-before}} - v_{\text{bat-cm-before}})$$

grouping the terms on the right

$$v_{\text{ball-after}} + \frac{m_{\text{ball}} v_{\text{ball-after}}}{m_{\text{bat}}} = -v_{\text{bat-cm-before}} + e v_{\text{bat-cm-before}} + \frac{m_{\text{ball}} v_{\text{ball-before}}}{m_{\text{bat}}} - e v_{\text{ball-before}}$$

$$v_{\text{ball-after}} = +v_{\text{ball-before}}\left(\frac{\frac{m_{\text{ball}}}{m_{\text{bat}}} - e}{1 + \frac{m_{\text{ball}}}{m_{\text{bat}}}}\right) - v_{\text{bat-cm-before}}\frac{1-e}{1+\frac{m_{\text{ball}}}{m_{\text{bat}}}}$$

Multiply top and bottom by m_{bat} and we get the Bahill and Karnavas equation presented above and repeated here.

$$v_{\text{ball-after}} = \frac{v_{\text{ball-before}}(m_{\text{ball}} - m_{\text{bat}}CoR_{1\text{a}}) - v_{\text{bat-cm-before}}m_{\text{bat}}(1 - CoR_{1\text{a}})}{m_{\text{ball}} + m_{\text{bat}}}$$

In Sect. 5.2, we define $q = \left(\frac{e - \frac{m_{ball}}{M_{eff}}}{1 + \frac{m_{ball}}{M_{eff}}}\right)$ and then $v_{\text{ball-after}} = qv_{\text{ball-before}} + (1+q)vt_{\text{bat-before}}$.

The purpose of presenting this model here is to emphasize that it is important to consider alternative models. If their main results agree, then that validates both models. We will return to this bat Effective Mass model in Sect. 5.2.

3.2.2 Configuration 1b

Configuration 1b is a head-on collision at the center of mass of the bat, as shown in Fig. 2.1. Spin on the ball and bat are not considered. This is the same as configuration 1a, but it adds Conservation of Energy. It has three equations and two unknowns as shown in Table 3.2.

Although an additional equation is not needed, we will now present the Conservation of Energy equation as a consistency check. There is nothing in the system that will release energy during the collision (loaded springs or explosives). The bat swing is level so there will be no change in potential energy.

Before the collision, there is kinetic energy in the ball and the bat.

$$KE_{\text{before}} = \frac{1}{2}m_{\text{ball}}v^2_{\text{ball-before}} + \frac{1}{2}m_{\text{bat}}v^2_{\text{bat-cm-before}}$$

We modeled the bat velocity as a linear term comprising a translation and two rotations (See Fig. 1.1). This linear velocity is what we measured in our experiments.

$$KE_{\text{after}} = \frac{1}{2}m_{\text{ball}}v^2_{\text{ball-after}} + \frac{1}{2}m_{\text{bat}}v^2_{\text{bat-cm-after}}$$

$$KE_{\text{before}} = KE_{\text{after}} + KE_{lost} \tag{3.1}$$

Kinetic energy will be transformed to heat in the ball, vibrations in the bat and deformations of the bat and ball. The Coefficient of Restitution (CoR) models the energy that is transformed in a frictionless head-on collision between two objects.

Table 3.2 Equations for configuration 1b, which adds Conservation of Energy (CoE). It has three equations and two unknowns

Inputs	$v_{\text{ball-before}}, v_{\text{bat-cm-before}}$
Outputs	$v_{\text{ball-after}}, v_{\text{bat-cm-after}}$
Equations	
Conservation of energy	$\frac{1}{2} m_{\text{ball}} v_{\text{ball-before}}^2 + \frac{1}{2} m_{\text{bat}} v_{\text{bat-cm-before}}^2 - \frac{\bar{m}}{2}(v_{\text{ball-before}} - v_{\text{bat-cm-before}})^2 (1 - CoR_{1b}^2) = +\frac{1}{2} m_{\text{ball}} v_{\text{ball-after}}^2 + \frac{1}{2} m_{\text{bat}} v_{\text{bat-cm-after}}^2$
Conservation of linear momentum	$m_{\text{ball}} v_{\text{ball-before}} + m_{\text{bat}} v_{\text{bat-cm-before}} = m_{\text{ball}} v_{\text{ball-after}} + m_{\text{bat}} v_{\text{bat-cm-after}}$
Definition of *CoR*	$CoR_{1b} = -\frac{v_{\text{ball-after}} - v_{\text{bat-cm-after}}}{v_{\text{ball-before}} - v_{\text{bat-cm-before}}}$

Such a collision will have no tangential velocity components. The equation for the kinetic energy lost in a bat–ball collision of configuration 1b (Dadouriam 1913, Eq. (XI), p. 248; Ferreira da Silva 2007, Eq. 23; Brach 2007, Eq. 3.7) is

$$KE_{\text{lost}} = \frac{\bar{m}}{2} (\text{collision velocity})^2 (1 - CoR_{1b}^2)$$

where $\bar{m} = \frac{m_{\text{ball}} m_{\text{bat}}}{m_{\text{ball}} + m_{\text{bat}}}$.

$$KE_{\text{lost}} = \frac{\bar{m}}{2} (v_{\text{ball-before}} - v_{\text{bat-cm-before}})^2 (1 - CoR_{1b}^2) \tag{3.2}$$

This equation will be derived in the configuration 2b section. Combining these three equations (KE_{before}, KE_{after} and KE_{lost}) yields the equation for Conservation of Energy for configuration 1b

$$\begin{aligned}\frac{1}{2} m_{\text{ball}} v_{\text{ball-before}}^2 + \frac{1}{2} m_{\text{bat}} v_{\text{bat-cm-before}}^2 - \frac{\bar{m}}{2}(v_{\text{ball-before}} - v_{\text{bat-cm-before}})^2 (1 - CoR_{1b}^2) \\ = +\frac{1}{2} m_{\text{ball}} v_{\text{ball-after}}^2 + \frac{1}{2} m_{\text{bat}} v_{\text{bat-cm-after}}^2\end{aligned} \tag{3.3}$$

This assumes that there is no spin on the ball or the bat, meaning that we have ignored angular momentum. Using the numbers in Table 1.1 produces the results shown in Table 3.3.

Table 3.3 Simulation values for bat–ball collisions at the center of mass, configuration 1b

	SI units	Baseball units
Inputs		
$v_{\text{ball-before}}$	−37 m/s	−83 mph
$v_{\text{bat-cm-before}}$	23 m/s	52 mph
CollisionSpeed		135 mph
CoR_{1b}	0.475	0.475
Outputs		
$v_{\text{ball-after}}$	40 m/s	89 mph
$v_{\text{bat-cm-after}}$	11 m/s	25 mph

3.2.3 Simulation Results

Table 3.4 shows the kinetic energies for the same simulation.

A batted-ball velocity, $v_{\text{ball-after}}$, of 89 mph is reasonable. The fact that $KE_{before} = KE_{\text{after}} + KE_{lost} = 346\,\text{J}$ shows that this set of equations is consistent. As a reality check, we note that the average kinetic energy in the swings of 28 members of the San Francisco Giants baseball team was 292 J (Bahill and Karnavas 1991). Given human variability and the different circumstances for the experiments, these numbers are compatible.

Let us now consider the consequences of neglecting the spin of the ball. A typical spin rate for a curveball is 2000 rpm. So, the rotational kinetic energy in the ball will be about $0.5 I_{\text{ball}} \omega^2_{\text{ball-before}} = 1.7\,\text{J}$. This is small compared to the translational kinetic energies.

This is the end of the equations for configuration 1b. In the rest of this book, we will use Newtonian mechanics, to derive equations for the velocity of the bat and the ball after their collision, for collisions that do *not* occur at the center of mass of the bat.

3.2.4 The Coefficient of Restitution

The Coefficient of Restitution (CoR) models the energy lost in a collision between two objects. It is commonly defined as the ratio of the relative speed between the

Table 3.4 Configuration 1b kinetic energies, J

KE ball linear velocity before =	100
KE bat linear velocity before =	246
KE before total =	346
KE ball linear velocity after =	114
KE bat linear velocity after =	55
KE after =	169
KE lost =	177
KE after + KE lost =	346

two objects after a collision to the relative speed before the collision. Here are the CoR definitions for some of our configuration types. The subscripts refer to the collision type given in Chap. 2.

$$CoR_{1a,} = CoR_{1b} = -\frac{v_{\text{ball-after}} - v_{\text{bat-cm-after}}}{v_{\text{ball-before}} - v_{\text{bat-cm-before}}}$$

$$CoR_{2a} = CoR_{2b} = -\frac{v_{\text{ball-after}} - v_{\text{batcm-after}} - d_{\text{cm-ip}}\omega_{\text{bat-after}}}{v_{\text{ball-before}} - v_{\text{bat-cm-before}} - d_{\text{cm-ip}}\omega_{\text{bat-before}}}$$

$$CoR_{2c} = -\frac{v_{\text{ball-after}} - v_{\text{knob-after}} - d_{\text{knob-ip}}\beta_{\text{after}}}{v_{\text{ball-before}} - v_{\text{knob-before}} - d_{\text{knob-ip}}\beta_{\text{before}}}$$

These equations will be explained later when they are used.

The *CoR* is used to model the energy lost during a bat–ball collision. If the *CoR* were 1.0, then all the original energy would be recovered in the motion of the system after impact. However, if there were losses due to energy dissipation or energy storage, then the *CoR* would be between 0 and 1.0 (Cross 2000). In a bat–ball collision, there is energy dissipation: both the bat and the ball increase in temperature. Also both the bat and the ball store energy in vibrations. This energy is not available to be transferred to the ball, and therefore the ball velocity is smaller.

The *CoR* depends on the speed of the collision. Our simulations use the following equation for a wooden bat and a baseball $CoR = 0.61 - 0.001$ *CollisionSpeed*, where *CollisionSpeed* (the sum of the ball speed and the bat speed) is in mph. This equation came from unpublished data provided by Jess Heald of Worth Sports Co. and they assume a collision at the sweet spot of the bat. Table 3.5 gives CoRs measured in seven experimental studies.

Most of the data points for 60 mph collisions against flat walls show that baseballs are in conformance with the rules of major league baseball. However, for high speeds and wooden bats, there is a lot of variation in the data. Some studies say that the CoR of a collision between a ball and flat wooden wall is higher than the CoR of a collision between a ball and a wooden bat, and some say that it is lower. The *CoR* depends on the shape of the object that the ball is colliding with. When a baseball is shot out of an air cannon onto a flat wooden wall, most of the ball's deformation is restricted to the outer layers: the cowhide cover and the four yarn shells. However, in a high-speed collision between a baseball and a cylindrical bat, the deformation penetrates into the cushioned cork center. This allows more energy to be stored and released in the ball and the *CoR* might be higher.

The CoR also depends on where the ball hits the bat, the speed of the collision, the relative humidity, the temperature, the deformation of the objects, the surface texture and the configuration of the collision.

Figure 3.1 shows that the CoR for baseballs is a function of the collision speed, the temperature and the relative humidity. The experiments reported in Table 3.5 did not state the temperature or humidity in which their experiments were performed. Therefore, the data in Table 3.5 must be taken with a grain of salt. The data

Table 3.5 Experimental CoR values for colliding baseballs

Source	Baseball collides with	Equation	CoR value at 60 mph	CoR value at 120 mph
Jess Heald President of Worth Sports Co. 1986, reported in Watts and Bahill (1990)	Flat wooden wall	$CoR = 0.61 - 0.001\ CollisionSpeed$	0.550	0.490
Crisco 1997, NCAA report	Wooden bat	$CoR = 0.67 - 0.0015\ CollisionSpeed$	0.580	0.490
Fallon and Sherwood (2000)	Flat wooden wall		0.548	
Fallon and Sherwood (2000)	Wooden bat			0.504 at 140 mph
Drane et al. (2008)	Flat wooden wall		0.546	
Drane et al. (2008)	Wooden bat		0.537	0.503 at 90 mph
Major League Baseball rules	Flat wooden wall		0.514 to 0.568 at 58 mph	
Nathan et al. (2011)	Flat steel plate	$CoR = 0.64 - 0.0014\ CollisionSpeed$	0.556	0.472
Cross (2011), Fig. 8.5	Flat wooden wall	$CoR = 0.67 - 0.0021\ CollisionSpeed$	0.544	0.418

point at 140 mph, from Fallon and Sherwood (2000), was based on 140 valid collisions with major league baseballs: so it is probably accurate. It is given to emphasize the fact that we do not know what the CoR is for high-speed collisions. Meaning that we cannot extrapolate the Nathan et al. (2011) curve to speeds above 120 mph.

Therefore, for the simulations of this book, we will use the following equation from Worth Sports Co.

$$CoR = 0.61 - 0.001\ CollisionSpeed$$

and we will be cautious about using its values for collision speeds above 120 mph. Using this equation means that we are ignoring the effects of where the ball hits the bat (we assume that it is at the center of mass or at the sweet spot), the relative humidity, the temperature, the shape of the objects, the deformation of the objects and the surface texture (seams). We only consider major league baseballs.

The CoR is a constraint on the relationship between $v_{\text{ball-after}}$, $v_{\text{bat-cm-after}}$, $d_{\text{cm-ip}}\omega_{\text{bat-after}}$, $v_{\text{ball-before}}$, $v_{\text{bat-cm-before}}$ and $d_{\text{cm-ip}}\omega_{\text{bat-before}}$. Its numerical value is a constant that is fixed at the beginning of each evaluation.

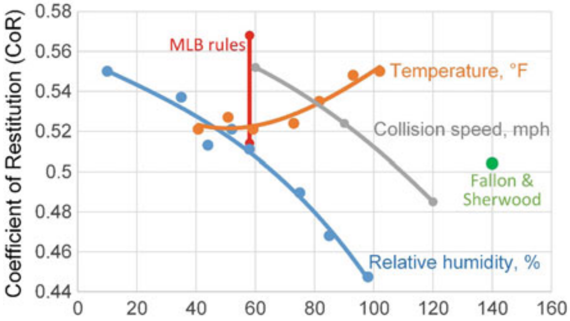

Fig. 3.1 Coefficients of Restitution (CoR) for major league baseballs as functions of temperature, collision speed and relative humidity. Data are from Nathan et al. (2011). The point at 140 mph is from Fallon and Sherwood (2000). The red line shows the major league baseball rule for a collision at 58 mph

Modeling philosophy note. George Box wrote, "All models are wrong, but some are useful (Box 1981)." In this section, we wrote that the coefficient of restitution for collisions is between zero and one, $0 \leq CoR \leq 1$. But these are not theoretical limits. For example, a baseball thrown through a window screen will have a negative CoR, whereas a ball that releases energy on every bounce, for example, one that is coated with an explosive or one that contains a spring and an escapement like a watch, can have a CoR greater than one. A model is a simplified representation of a particular view or aspect of a real system. No model can represent all views.

3.3 Collisions at the Sweet Spot

3.3.1 Configuration 2a

Configuration 2a is a head-on (planar, parallel) collision at the sweet spot of the bat, which we define to be the Center of Percussion (CoP). Watts and Bahill (1990) expanded the Bahill and Karnavas (1989) model to create configuration 2a. They introduced a third unknown, the rotation of the bat, ω_{bat}, after the collision and a third equation, which was based on Newton's second axiom. Therefore, this section has three equations, shown in Table 3.6, but we only solved for one unknown. The model for bat movement is that of a translation and a rotation about its center of mass.

Table 3.6 Equations for configuration 2a, three equations and three unknowns

Inputs	$v_{\text{ball-before}}, v_{\text{bat-cm-before}}, \omega_{\text{bat-before}}$ and COR
Outputs	$v_{\text{ball-after}}$
Equations	
Conservation of linear momentum, Eq. (3.4)	$m_{\text{ball}} v_{\text{ball-before}} + m_{\text{bat}} v_{\text{bat-cm-before}} = m_{\text{ball}} v_{\text{ball-after}} + m_{\text{bat}} v_{\text{bat-cm-after}}$
Definition of *CoR*, Eq. (3.5)	$CoR_{2a} = -\frac{v_{\text{ball-after}} - v_{\text{bat-cm-after}} - d_{\text{cm-ip}} \omega_{\text{bat-after}}}{v_{\text{ball-before}} - v_{\text{bat-cm-before}} - d_{\text{cm-ip}} \omega_{\text{bat-before}}}$
Newton's second axiom, Eq. (3.6)	$d_{\text{cm-ip}} m_{\text{ball}} (v_{\text{ball-after}} - v_{\text{ball-before}}) = -I_{\text{bat}} (\omega_{\text{bat-after}} - \omega_{\text{bat-before}})$

This section considers collisions for Impact Point (ip) that are not at the center of mass of the bat. Our objective was to derive an equation for the velocity of the ball after its collision with the bat. We expanded the previous linear model to the combined rotation plus translation model with the bat–ball impact point off of the center of mass, perhaps at the sweet spot (see Fig. 2.3). There are about a dozen definitions for the sweet spot of the bat (Bahill 2004). We will use the symbols defined in Table 1.1. Figure 2.3 is appropriate for these collisions. In the Coefficient of Restitution (*CoR*) equation, the bat speed is a combination of the bat translation before the collision and the rotation about the center of mass caused by rotations about the batter's spine and wrists. This velocity is what we measured in our experiments.

3.3.1.1 Definition of the Sweet Spot

For skilled batters, we assume that most bat–ball collisions occur near the sweet spot of the bat, which is, however, difficult to define precisely. We give nine alternative definitions for the horizontal sweet spot of the bat: the center of percussion, the node of the fundamental vibrational mode, the antinode of the hoop mode, the maximum energy transfer area, the maximum-batted-ball speed area, the maximum coefficient of restitution area, the minimum energy loss area, the minimum sensation area and the joy spot. Let us now examine each of these alternative definitions. This section is based on Bahill and Baldwin (2008).

(1) **Center of Percussion**. For most collision points, when the ball hits the bat, it produces a translation of the bat and a rotation of the bat. However, if the ball hits the bat at the center of mass, there will be a translation but no rotation, whereas, if the bat is fixed at a pivot point and the ball hits the bat at the Center of Percussion (*CoP*) for that pivot point, then there will be a rotation about that pivot point but no translation (and therefore no sting on the hands). The pivot point and the *CoP* for that pivot point are conjugate points, because if instead the bat is fixed at the *CoP* and the ball hits the pivot point then there will be a pure rotation about the *CoP*. The *CoP* and its pivot point are related by the following equation derived by Sears, Zemansky and Young (1976), where the parameters are defined in Fig. 3.1:

$$d_{\text{pivot-cop}} = \frac{I_{\text{pivot}}}{m_{\text{bat}} d_{\text{pivot-cm}}}$$

The *CoP* is not one fixed point on the bat. There is a different *CoP* for every pivot point. If the batter chokes up on the bat, the pivot point (and consequently the *CoP*) will change. In fact, the pivot point might even change during an individual swing. In this section, we assume that the pivot point is six inches (15 cm) from the knob, because that is where the batter's hands are. We could assume that the pivot point is at the end of the knob (Milanovich and Nesbit 2014). This produces a different CoP.

There are three common experimental methods for determining the *CoP* of a bat. (Method 1) *Pendular motion*: Hang a bat at a point six inches (15 cm) from the knob with 2 or 3 feet (1 m) of string. Hit the bat with an impact hammer. Hitting it off the *CoP* will make it flop like a fish out of water, because there is a translational force and a rotational force at the pivot point. Hitting it near the *CoP* will make it swing like a pendulum. (Method 2) *Toothpick pivot*: Alternatively, you can pivot the bat on a toothpick through a hole at the pivot point and strike the bat at various places. When struck near the *CoP* for that pivot point, the toothpick will not break. At other places, the translational forces will break the toothpick. (Method 3) *Equivalent pendulum*: A third method for measuring the distance between the pivot point and the *CoP* is to make a pendulum by putting a small object with a mass equal to the bat's mass on a string and adjusting its length until the pendulum's period and the bat's period are the same. This method has the smallest variability.

(2) **Node of the fundamental mode**. The node of the fundamental bending vibrational mode is the area where this vibrational mode (roughly between 150 and 200 Hz for a wooden bat) of the bat has a null point. To find this node, with your fingers and thumb, grip a bat about six inches from the knob. Lightly tap the barrel at various points with an impact hammer. The area where you feel no vibration and hear almost nothing (except the secondary vibrational crack or ping at 500–800 Hz) is the node. A rubber mallet could be used in place of an impact hammer: the point is, the hammer itself should not produce any noise. The antinode of the third bending vibrational mode may also be important.

(3) **Antinode of the hoop mode**. For hollow metal and composite baseball and softball bats, there is another type of vibration, called a hoop vibration. The walls of a hollow bat deform during a bat–ball collision. The walls are crushed in and then bounce back out. This vibration can be modeled as a hoop or a ring around the bat; this ring deforms like the vertical cross-sectional area of a water drop falling from a faucet; first, the water drop is tall and skinny, in free fall it is round and when it hits the ground it becomes short and fat. The location of the antinode of the first hoop mode is another definition of the sweet spot.

(4) **Maximum-batted-ball speed point**. There is a point on the bat that produces the maximum-batted-ball speed. Section 4.11.4 shows this point to be 9.2 cm (3.6 inches) from the center of mass, or 25.4 cm (10 inches) from the end of the barrel. This point can be computed theoretically as follows. Start with an equations for $v_{\text{ball-after}}$, such as Eq. (4.8). Take the derivative with respect to d. Set this equal to zero and solve for d. This value will depend on $v_{\text{ball-before}}$ which you obtain from, for example, Table 4.2.

(5) **Maximum coefficient of restitution area**. The Coefficient of Restitution (*CoR*) is commonly defined as the ratio of the relative speed after a collision to the relative speed before the collision. In our studies, the *CoR* is used to model the energy transferred to the ball in a collision with a bat. If the *CoR* were 1.0, then all the original energy would be recovered in the motion of the system after impact. But if there were losses due to energy dissipation or energy storage, then the *CoR* would be less than 1.0. For example, in a bat–ball collision, there

is energy dissipation: both the bat and the ball increase slightly in temperature. In one experiment, one hundred bat–ball collisions in rapid succession raised the temperature of a softball by 10 °F (Duris and Smith 2004). Also both the bat and the ball store energy in vibrations. Not all of this energy will be transferred to the ball. (For now, we ignore the kinetic energy stored in the ball's spin.) The maximum coefficient of restitution area is the area that produces the maximum *CoR* for a bat–ball collision. This area can be computed theoretically using Eq. (4.5) as described in sweet spot definition (4) above.

(6) **Maximum energy transfer area.** A collision at the maximum energy transfer area transfers the most energy to the ball. This definition says that the best contact area on the bat is that which loses the least amount of energy to bat translation, rotation, vibration, etc. This area can be computed theoretically using Eq. (4.11) as described in definition (4).

(7) **Minimum energy loss area.** There is an area that minimizes the total (translation plus rotation plus vibration) energy lost in the bat. This area depends on the fundamental bending mode, the second mode and the center of percussion. This area can be approximated theoretically using Eq. (4.11) as described in definition (4).

(8) **Minimum sensation area**. For most humans, the sense of touch is most sensitive to vibrations between 200 and 400 Hz. For each person, there is a collision area on the bat that would minimize these sensations in the hands.

(9) **Joy spot**. Finally, Williams and Underwood (1982) stated that hitting the ball at the joy spot makes you the happiest. His joy spot was centered five inches (13 cm) from the end of the barrel.

These nine areas are different, but they are close together. We group them together and refer to this *region* as the sweet spot. We measured a large number of bats (youth, adult, wood, aluminum, ceramic, titanium, etc.) and found that the sweet spot was 15–20% of the bat length from the barrel end of the bat. In our Ideal Bat Weight experiments (Bahill and Karnavas 1989, 1991) and our variable moment of inertia experiments (Bahill 2004) for adult bats, the center of the sweet spot was defined to be five inches (13 cm) from the barrel end of the bat.

It does not make sense to try getting greater precision in the definition of the sweet spot, because the concept of a sweet spot is a human concept, and it probably changes from human to human. For one example, in calculating the center of percussion, the pivot point of the bat must be known and this changes from batter to batter, and it may even change during the swing of an individual batter (Milanovich and Nesbit 2014).

Table 3.7 shows general properties for a standard Hillerich and Bradbury Louisville Slugger wooden C243 pro stock 34-inch (86 cm) bat with the barrel end cupped out to reduce weight. This is a different bat than that described in Table 1.1. These modern scientific methods of calculating the center of the sweet spot of the bat are all only a few centimeters above the true value given by Ted Williams four decades ago.

Table 3.7 Parameters for a C243 wooden bat, assuming a pivot point 6 inches from knob

	SI units	Baseball units
Length	0.863	34
Mass	0.880	31
Period (sec)	1.65	1.65
I_{knob} (kg m^2)	0.335	
I_{cm} (kg m^2)	0.0511	
Measured $d_{\text{knob-cm}}$	0.57	22.4
Measured $d_{\text{knob-cop}}$	0.69	27.2
Calculated $d_{\text{knob-cop}}$	0.69	27.2
Measured $d_{\text{pivot-cop}}$	0.55	21.7
Calculated $d_{\text{pivot-cop}}$	0.54	21.3
Calculated $d_{\text{pivot-cm}}$	0.42	16.5
Measured $d_{\text{knob-firstNode}}$	0.67	26.4
Calculated $d_{\text{knob-}cop}$ for a pivot point in the knob (cm)	0.66	26.0
Distance from the center of percussion to the end of the bat	0.162	6.38

There is no sweet spot of the bat: however, there is a sweet area and for a 34-inch wooden bat, it is five to seven inches (13–18 cm) from the barrel end of the bat. We presented nine definitions for the sweet spot of the bat. Some of these definitions had a small range of experimentally measured values (e.g., one cm for the node of the fundamental vibration mode), whereas others had a large range of experimentally measured values (e.g., 10 cm for the maximum-batted-ball speed area). But of course, none of these definitions has square sides. They are all bowl-shaped. So the width depends on how far you allow the parameter to decline before you say that you are out of the sweet area. In general, the sweet area is about two inches wide. Our survey of retired major league batters confirmed that the sweet spot of the bat is about two inches (5 cm) wide. Therefore, most of the sweet-spot definitions of this chapter fall within this region. In summary, recent scientific analyses have validated Ted William's statement that the sweet spot of the bat is an area five to seven inches from the end of the barrel.

For completeness, we note that the vertical component of the sweet spot is one-fifth of an inch high (Baldwin and Bahill 2004). See Fig. 9.6.

3.3.1.2 Coordinate System

We will use a right-handed coordinate system with the x-axis pointing from home plate to the pitching rubber, the y-axis points from first base to third base and the z-axis points straight up. A torque rotating from the x-axis to the y-axis would be positive upward. Previously, in other papers describing only the pitch, we defined the x-axis as pointing from the pitching rubber to home plate and then the y-axis went from third to first base (Bahill and Baldwin 2007). Over the plate, the ball comes downward at a ten-degree angle and the bat usually moves upward at about ten degrees, so later the z-axis will be rotated back ten degrees.

3.3.1.3 Assumptions

A1. The swing of the bat is as modeled in Fig. 3.1.
A2. Collisions at the Center of Percussion will produce a rotation about the center of mass, but no translation of the bat.
A3. For configurations 1a, 1b and 2a, we will not include the kinetic energy stored in the rotation of the baseball. That is, we assume that the pitch is a knuckleball with no spin. In later sections, we will consider a fastball and a curveball.
A5. The collision duration is short, for example, one millisecond.
A6. Because the collision duration is short and the swing is level, we can ignore the effects of gravity *during* the collision.
A7. We neglect permanent deformations of the bat and ball.
A8. The Coefficient of Restitution (*CoR*) for a baseball wooden-bat collision at major league speeds starts at about 0.55 and decreases with collision speed.
A9. For configuration 2d, Coulomb friction is a good model for a bat–ball collision. When colliding objects slide relative to each other, a friction force is generated, whose direction is tangential to the surface of contact and whose magnitude is proportional to the normal force at the point of contact. We assume that during impact the ball slides and does not roll on the bat, but the sliding halts before separation. The dynamic coefficient of friction, μ_f, is used to model these losses. This is called a Coulomb model. In contrast, a Coulomb model would not be appropriate for a pool cue hitting a ball of clay: a more complex model would be needed. A Coulomb model will be used in configuration 2d.
A10. The dynamic coefficient of friction has been measured by Bahill at $\mu_f = 0.5$.
A11. We write about kinetic energy losses during a collision: that is the way it is described in the literature. However, we should call these transformations, because, for example, kinetic energy is not lost during a collision. It might be transformed into heat in the ball, vibrations in the bat, acoustic energy in the "crack of the bat" or deformations of the bat or ball.
A12. In this book, we do not model the moment of inertia of the batter's arms.
A13. Pictures of bats in this book are for wooden bats. However, the equations and conclusions are the same for wooden and aluminum bats. The differences would be in the mass, moment of inertia and dimensions.
A14. We do not differentiate between day games and night games. We know that when the shadow of the stadium is between the pitcher and the batter, the batter's performance is reduced. We ignore this effect.

A15. Assume free-end collisions. For impacts at the sweet spot of the bat, the momentum transfer to the ball is complete by the time the elastic wave arrives at the handle. Therefore, any action by the hands will affect the bat at the impact point only after the ball and bat have separated, Nathan (2000). This is the most restrictive assumption that we make. It assumes that the collision is short and occurs at a point.

3.3.1.4 Conservation of Linear Momentum

The law of Conservation of Linear Momentum states that linear momentum will be conserved in a collision if there are no external forces. We will approximate the bat's motion before the collision with the tangent to the curve of its arc. For a collision anywhere on the bat, every point on the bat has the same angular velocity, but the linear velocities will be different, which means that $vt_{\text{bat-before}}$ is a combination of translations and rotations unique for each point on the bat. Conservation of momentum in the direction of the x-axis states that the momentum before plus the external impulse will equal the momentum after the collision. There are no external impulses during the ball–bat collision: therefore, this is the equation for Conservation of Linear Momentum

$$m_{\text{ball}} v_{\text{ball-before}} + m_{\text{bat}} v_{\text{bat-cm-before}} = m_{\text{ball}} v_{\text{ball-after}} + m_{\text{bat}} v_{\text{bat-cm-after}} \tag{3.4}$$

3.3.1.5 Definition of the Coefficient of Restitution

The kinematic Coefficient of Restitution (*CoR*) was defined by Sir Isaac Newton as the ratio of the relative velocity of the two objects after the collision to the relative velocity before the collision at the point of impact.

In our models, for a collision at any Impact Point (ip), we have

$$CoR_{2a} = -\frac{v_{\text{ball-after}} - v_{\text{bat-cm-after}} - d_{\text{cm-ip}} \omega_{\text{bat-after}}}{v_{\text{ball-before}} - v_{\text{bat-cm-before}} - d_{\text{cm-ip}} \omega_{\text{bat-before}}} \tag{3.5}$$

These variables and parameters are illustrated in Fig. 3.2. A note on notation: ω_{bat} is the angular velocity of the bat *about its center of mass*, $v_{\text{bat-cm}}$ is the linear velocity *of the center of mass* of the bat in the x-direction and $d_{\text{cm-ip}}$ is the distance between the center of mass and the point of impact. We measured $v_{\text{bat-cm-before}} + d_{\text{cm-ip}} \omega_{\text{bat-before}}$, which is experimental data that depends on our model formulation (Fig. 3.2) and the kinematics of the person swinging the bat.

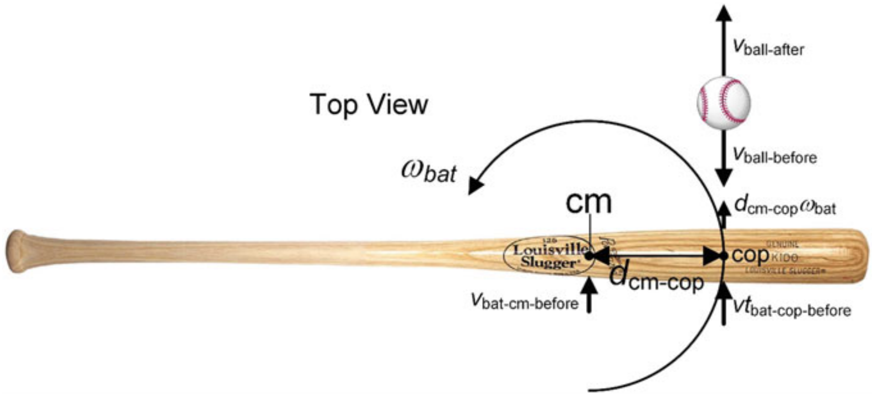

Fig. 3.2 This figure shows $v_{\text{ball-before}}$, $v_{\text{bat-cm-before}}$, $v_{\text{ball-after}}$ and $d_{\text{cm-ip}}\omega_{\text{bat}}$, which are used to define the Coefficient of Restitution for configuration 2

3.3.1.6 Newton's Second Axiom

Watts and Bahill (1990) derived the following equation from Newton's second axiom that states that a force acting on an object produces acceleration in accordance with the equation $F = ma$. If an object is accelerating, then its velocity and momentum are increasing. This axiom is often stated as applying an impulsive force to an object will change its momentum. According to Newton's third axiom, when a ball hits a bat at the impact point there will be a force on the bat in the direction of the negative x-axis, let us call this $-F_1$, and an equal but opposite force on the ball, called F_1. This force will be applied during the duration of the collision, called t_c. When a force is applied for a short period of time, it is called an impulse. According to Newton's second axiom, an impulse will change momentum. The force on the bat will create a torque of $-d_{\text{cm-ip}}F_1$ around the center of mass of the bat. An impulsive torque will produce a change in angular momentum of the *bat*.

$$-d_{\text{cm-ip}}F_1 t_c = I_{\text{bat}}(\omega_{\text{bat-after}} - \omega_{\text{bat-before}})$$

Now this impulse will also change the linear momentum of the *ball*.

$$F_1 t_c = m_{\text{ball}}(v_{\text{ball-after}} - v_{\text{ball-before}})$$

Multiply both sides of this equation by $d_{\text{cm-ip}}$ and add these two equations to get the equation for Newton's second axiom.

$$d_{\text{cm-ip}} m_{\text{ball}}(v_{\text{ball-after}} - v_{\text{ball-before}}) = -I_{\text{bat}}(\omega_{\text{bat-after}} - \omega_{\text{bat-before}}) \tag{3.6}$$

These equations were derived for the bat–ball system. Therefore, there were no external impulses. (If the collision is at the sweet spot, then the batter's arms do not

Table 3.8 Simulation values for bat–ball collisions at the sweet spot, configuration 2a

	SI units (m/s, rad/s)	Baseball units (mph, rpm)
Inputs		
$v_{\text{ball-before}}$	−37	−83
$v_{\text{bat-cm-before}}$	23	52
$\omega_{\text{bat-before}}$	32	309
$vt_{\text{bat-cop-before}}$	28	62
CoR_{2a}	0.465	
Output		
$v_{\text{ball-after}}$	41	92

apply an impulse.) Equations (3.4), (3.5) and (3.6) produce the following equation for the batted-ball velocity (Watts and Bahill 1990/2000). Its derivation will be given in the next chapter.

$$v_{\text{ball-after}} = \frac{v_{\text{ball-before}}\left(m_{\text{ball}}I_{\text{bat}} - m_{\text{bat}}I_{\text{bat}}CoR_{2a} + m_{\text{ball}}m_{\text{bat}}d^2_{\text{cm-ip}}\right) + v_{\text{bat-cm-before}}m_{\text{bat}}I_{\text{bat}}(1 + CoR_{2a}) + m_{\text{bat}}d_{\text{cm-ip}}\omega_{\text{bat-before}}I_{\text{bat}}}{m_{\text{ball}}I_{\text{bat}} + m_{\text{bat}}I_{\text{bat}} + m_{\text{ball}}m_{\text{bat}}d^2_{\text{cm-ip}}}$$

or

$$v_{\text{ball-after}} = v_{\text{ball-before}} - \frac{(v_{\text{ball-before}} - v_{\text{bat-cm-before}})m_{\text{bat}}I_{\text{bat}}(1 + CoR_{2a}) + m_{\text{bat}}d_{\text{cm-ip}}\omega_{\text{bat-before}}I_{\text{bat}}}{m_{\text{ball}}I_{\text{bat}} + m_{\text{bat}}I_{\text{bat}} + m_{\text{ball}}m_{\text{bat}}d^2_{\text{cm-ip}}}$$

The output for the above equation, for typical inputs, is given in Table 3.8. Equations for $v_{\text{bat-cm-after}}$ and $\omega_{\text{bat-after}}$ were not derived by Watts and Bahill (1990/2000). They will be derived in the next chapter.

3.3.1.7 Simulation Values Configuration 2a

Figure 1.1 (bottom) is appropriate for configurations 1a and 1b, if the bat translation and rotation are measured and modeled with one vector, $v_{\text{bat-cm}}$. With a change from the center of mass to the sweet spot, again Fig. 1.1 (bottom) is appropriate for configurations 2a and 2b, if the bat translation and rotation are measured and modeled with two vectors, $v_{\text{bat-cm}}$ and ω_{bat}. Later, it will be shown that Fig. 1.1 (bottom) is also appropriate for configuration 2c, if the bat translation and rotation are measured and modeled with two vectors, $v_{\text{knob-trans}}$ and β_{bat}.

This is the end of the Watts and Bahill (1990/2000) derivation, called configuration 2a. This chapter gave background, a literature review and the overarching organization of bat–ball collision configurations. The next chapter will drill into configuration 2b.

In our simulation for configuration 2a, whose results are given in Table 3.8, we used an impact point speed of 62 mph (28 m/s). Where did that number come from? Table 3.9 shows the results of several studies performed over the last few decades that have measured the speed of the baseball bat. These studies are listed in chronological order. For now, we only give the results for male collegiate and professional baseball players. This table gives the average speed of the sweet spot, which was usually defined as the center of percussion. This is the total speed of the sweet spot meaning the translational plus rotational velocities.

Table 3.9 gives average sweet-spot speeds for seven studies of male college and professional batters. When multiple bats were used, we chose the bat closest to that described in Table 1.1. In our simulations, we used 62 mph for the total bat speed, which we defined to be the linear plus rotational speed of the sweet spot of the bat.

Some studies in the literature filtered their data and only included selected batters, usually the fastest. Internet sites that are trying to sell their equipment and services typically cite bat speeds between 70 and 90 mph (31–40 m/s). We think that these numbers are bogus. The big websites such as mlb.com, espn.com/mlb/ and hittrackeronline.com give the leaders in many categories, meaning that they have selected, for example, the 20 fastest players out of 750. This would be misleading if the reader thought that these numbers were *representative* of major league batters. In Table 3.9, we give average values for sweet-spot speeds.

Table 3.9 Average total sweet-spot speed before a collision

Average speed of the sweet spot (m/s)	Average speed of the sweet spot (mph)	Subjects, only males	References
26	58	28 San Francisco Giants	Database of Bahill and Karnavas (1989)
31	69	7 selected professional baseball players	Welch et al. (1995)
30	68	19 baseball players	Crisco et al. (2002)
27	60	16 college baseball players	Fleisig et al. (2002)
26	58	7 college baseball players	Koenig et al. (2004)
27	60	10 collegiate baseball players	Higuchi et al. (2016)
28	62	700 swings of major league baseball players where the outcome was a hit	Willman[a] (2017)
27	60	All MLB batters 2015–17	Chamberlain[a] (2017)

[a]These sources did not state whether these swing speeds were at the center of mass, the sweet spot or the impact point, but we assumed the impact point

Chamberlain (2017) used Statcast data and their “estimated swing speed” function for all swings by MLB batters for 2015–2017 and produced the swing speed information in Table 3.10. Unfortunately, after that publication, Statcast removed that function.

Next, we wanted to know how these laboratory measurements compare major league batters in actual games. Figure 3.3 shows the batted-ball speed as a function of the total bat speed before the collision. Using the data of Willman (2017) for the year 2016, we found that for 15,000 base hits in major league baseball the average batted-ball speed was 91 mph. This figure shows that, given physiological variation, the average major league batter has a high enough bat speed to occasionally hit a home run, when the batted ball has the ideal spin and launch angle. However, most major league batters seldom hit home runs. Indeed, of the 2200 active players listed by MLB.com, half of them have never hit a home run in their major league careers. The simulation summarized in Table 3.8 shows that a typical ball velocity before the collision, $v_{\text{ball-before}}$, of 83 mph (37 m/s) and an average bat speed, $vt_{\text{bat-cop-before}}$, of 62 mph (28 m/s) would produce an average batted-ball speed, $v_{\text{bat-after}}$, of 92 mph (41 m/s), which would not be enough for a home run in any major league stadium. Our rule of thumb is that it takes a batted-ball speed of 100 mph (45 m/s), under optimal conditions, to produce a home run.

Most *recent* studies of bat speed have used multiple video cameras and commercial prepackaged software to measure and compute bat speed (Willman 2017). Unfortunately, these systems have no calibration tests. On television, the batted-ball speed is often called the exit speed, the exit velocity or the launch speed.

The studies of Fleisig et al. (2001, 2002), Cross (2009), Milanovich and Nesbit (2014) and King et al. (2012) decomposed the center of percussion speed into two components: the linear translation velocity and the angular rotation velocity, $vt_{\text{bat-cop-before}} = v_{\text{cm}} + d_{\text{cm-cop}}\omega_{\text{cm-before}}$. A consensus of these four databases produced

$$vt_{\text{bat-cop-before}} = 23 + 0.134 \times 32 = 28\,\text{m/s} = 62\,\text{mph}$$

which we used in our simulations.

Table 3.10 Estimated swing speed (mph) for MLB batters

Year	Minimum	Average	Maximum	Standard deviation
2015	52.4	59.7	66.5	2.26
2016	51.6	59.8	65.5	2.26
2017	51.3	59.3	66.1	2.21
Overall	51.3	59.6	66.5	2.25

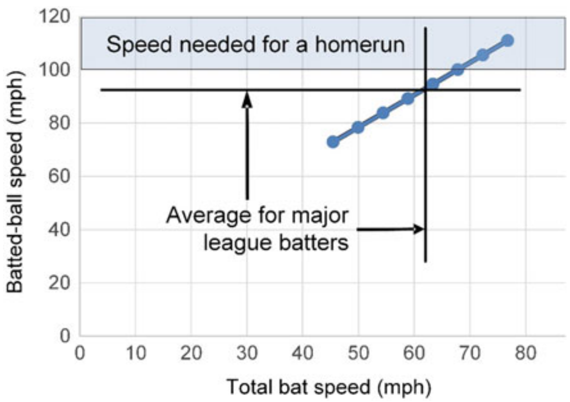

Fig. 3.3 Batted-ball speed as a function of total bat speed

If the average bat speed is only 62 mph and, according to Fig. 3.3, a bat speed of 68 mph is needed for a home run, then how can anyone ever hit a home run? The answer is that 62 mph is an average for a particular batter. All of his swings are not at that speed: some of his swings will be faster and some will be slower. The distribution of the individual swing speeds will follow a curve as in Fig. 3.4. This curve shows that this batter's average bat speed is 62 mph. 34.1% of his swings will be between 62 and 64 mph. 13.6% will be between 64 and 66 mph. 2.2% will be between 66 and 68 mph. Finally, the group we want, 0.1% will be faster than 68 mph, the speed needed for a home run. Thus, for this batter, 0.1% or one in a thousand of his swings would be fast enough to produce a home run, if he launched the ball at an optimal angle of 30° with backspin of 2000 rpm.

A similar analysis could be done for all batters in a group instead of just one batter. The analysis would be the same except that the standard deviation would be larger, as shown in Table 5.1.

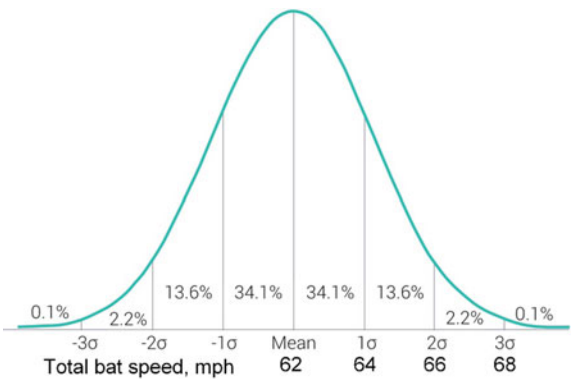

Fig. 3.4 Distribution of bat speeds for an individual batter. The standard deviation was estimated from Watts and Bahill (1990/2000) Fig. 43, Bahill (2004) and unpublished data

3.4 Spin on the Ball

The motion of the ball is characterized by its two vectors: velocity and spin. Because they are vectors, they have two components: a magnitude and a direction. The velocity v_{ball} has a magnitude, called speed, and a direction, as shown in Fig. 3.5. The spin ω_{ball} has a magnitude, called the spin rate, and an axis of rotation.

In this section, we will prove that in head-on collisions without friction (e.g., configurations 1a, 1b, 2a, 2b and 2c), for a pitch of any spin, there will be no change in the spin of the ball. First, for such collisions, simple inspection of the figures shows that there are no torques on the ball. Therefore, there should be no changes in the momenta.

Next, let us use the law of Conservation of Angular Momentum about the center of mass of the bat. When the ball contacts the bat, as shown in Fig. 3.6, the ball has linear momentum of $m_{\text{ball}}v_{\text{ball-before}}$. However, the ball does not know if it is translating or if it is tied on a string and rotating about the center of mass of the bat. Therefore, following conventional practice in physics for Conservation of Angular Momentum analyses, we will model the ball as also rotating about the bat's center of mass at a distance $d = d_{\text{cm-ip}}$. In effect, the ball has an initial angular momentum of $m_{\text{ball}}d_{\text{cm-ip}}v_{\text{ball-before}}$ about an axis through the bat's center of mass. In addition, it is possible to throw a curveball so that it spins about the vertical, z-axis, as also shown in Fig. 3.6. We call this a purely horizontal curveball (although it will still drop more due to gravity, than it will curve horizontally). The curveball will have angular momentum of $I_{\text{ball}}\omega_{\text{ball-before}}$ about an axis parallel to the z-axis. However, this is its momentum about *its* center of mass and we want the momentum about the axis through the center of mass of the *bat*. Therefore, we use the parallel axis theorem, producing $(I_{\text{ball}} + m_{ball}d^2)\omega_{\text{ball-before}}$.

Now, the bat has an initial angular momentum of $I_{\text{bat}}\omega_{\text{bat-before}}$. It also has an angular momentum about the bat's center of mass due to the bat translational momentum $m_{\text{bat}}dv_{\text{bat-before}}$, however, in this case $d = 0$ because the center of mass

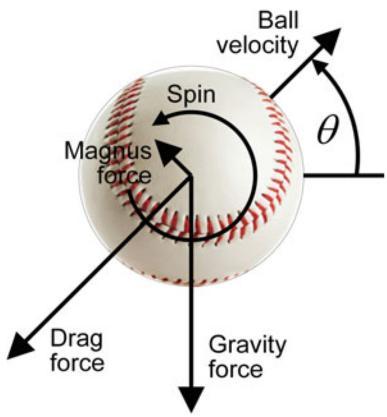

Fig. 3.5 Velocity and spin of the baseball

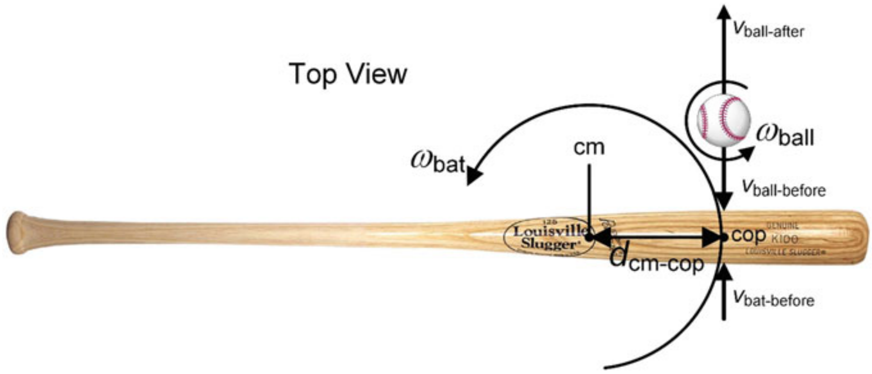

Fig. 3.6 The variables and parameters $v_{\text{ball-}before}$, $v_{\text{bat-}before}$, ω_{ball}, $d_{\text{cm-}ip}$ and ω_{bat} that are used in the Conservation of Angular Momentum equation for a bat–ball collision system

of the bat is passing through its center of mass. L is the symbol used for angular momentum. I guess all the cool letters (like F, m, a, v, I, ω, d, etc.) were already taken, so gray-bearded physicists were stuck with the blah symbol L. Therefore, the initial angular momentum about an axis through the center of mass of the bat is

$$L_{\text{initial}} = m_{\text{ball}} v_{\text{ball-before}} d + \left(I_{\text{ball}} + m_{\text{ball}} d^2\right) \omega_{\text{ball-before}} + I_{\text{bat}} \omega_{\text{bat-before}}$$

All of these momenta are positive, pointing out of the page.

For the angular momentum after the collision, we will treat the ball, as before, as an object rotating around the axis of the center of mass of the bat with angular momentum, $m_{\text{ball}} v_{\text{ball-after}} d_{\text{cm-ip}}$. Now we could treat the bat as a long slender rod with a moment of inertia of $m_{\text{bat}} d_{\text{bat}}^2/12$, where d_{bat} is the bat length. However, this is only an approximation and we have actual experimental data for the bat moment of inertia. Therefore, the bat angular momentum is $I_{\text{bat}} \omega_{\text{bat-after}}$. Thus, our final angular momentum about an axis through the center of mass of the bat is

$$L_{final} = m_{\text{ball}} v_{\text{ball-after}} d + \left(I_{\text{ball}} + m_{\text{ball}} d^2\right) \omega_{\text{ball-after}} + I_{\text{bat}} \omega_{\text{bat-after}}$$

The law of Conservation of Angular Momentum states that when no external torque acts on an object the initial angular momentum about some axis equals the final angular momentum about that axis.

$$L_{\text{initial}} = L_{\text{final}}$$
$$m_{\text{ball}} v_{\text{ball-before}} d + \left(I_{\text{ball}} + m_{\text{ball}} d^2\right) \omega_{\text{ball-before}} + I_{\text{bat}} \omega_{\text{bat-before}}$$
$$= m_{\text{ball}} v_{\text{ball-after}} d + \left(I_{\text{ball}} + m_{\text{ball}} d^2\right) \omega_{\text{ball-after}} + I_{\text{bat}} \omega_{\text{bat-after}}$$

Newton's second law states that applying an impulsive torque changes the angular momentum about the torque axis. Here, the impulsive torque is caused by the change in linear momenta. Therefore,

$$dm_{\text{ball}}(v_{\text{ball-after}} - v_{\text{ball-before}}) = -I_{\text{bat}}(\omega_{\text{bat-after}} - \omega_{\text{bat-before}})$$

$$\omega_{\text{bat-after}} = \left\{ \omega_{\text{bat-before}} - \frac{dm_{\text{ball}}}{I_{\text{bat}}}(v_{\text{ball-after}} - v_{\text{ball-before}}) \right\}$$

Let us substitute this $\omega_{\text{bat-after}}$ into our Conservation of Angular Momentum equation above.

$$\begin{aligned} &m_{\text{ball}} v_{\text{ball-before}} d + (I_{\text{ball}} + m_{\text{ball}} d^2)\omega_{\text{ball-before}} + I_{\text{bat}}\omega_{\text{bat-before}} \\ &= m_{\text{ball}} v_{\text{ball-after}} d + (I_{\text{ball}} + m_{\text{ball}} d^2)\omega_{\text{ball-after}} + I_{\text{bat}} \left\{ \omega_{\text{bat-before}} - \frac{dm_{\text{ball}}}{I_{\text{bat}}}(v_{\text{ball-after}} - v_{\text{ball-before}}) \right\} \end{aligned}$$

We want to solve this for the angular velocity of the ball after the collision, $\omega_{\text{ball-after}}$

$$\begin{aligned} &(I_{\text{ball}} + m_{\text{ball}} d^2)\omega_{\text{ball-after}} = \\ &+m_{\text{ball}} v_{\text{ball-before}} d + (I_{\text{ball}} + m_{\text{ball}} d^2)\omega_{\text{ball-before}} + I_{\text{bat}}\omega_{\text{bat-before}} \\ &-m_{\text{ball}} v_{\text{ball-after}} d - I_{\text{bat}}\omega_{\text{bat-before}} + dm_{\text{ball}}(v_{\text{ball-after}} - v_{\text{ball-before}}) \end{aligned}$$

Cancel the terms in color and we get

$$\begin{aligned} &(I_{\text{ball}} + m_{\text{ball}} d^2)\omega_{\text{ball-after}} = (I_{\text{ball}} + m_{\text{ball}} d^2)\omega_{\text{ball-before}} \\ &\omega_{\text{ball-after}} = \omega_{\text{ball-before}} \end{aligned}$$

We have now proven that for head-on collisions, for a pitch with any spin about the z-axis, the spin of the ball before and after is the same. What about a pitch that has spin about the z-axis and also about the y-axis, like most pitches? The collision will not change ball rotation. As shown above, it will not change the spin about the z-axis. We could write another set of equations for angular momentum about the y-axis. However, the bat has no angular momentum about the y-axis, so there is nothing to affect the ball spin about the y-axis. In conclusion, a head-on collision between a bat and a ball will not change the spin on the ball. Some papers have shown a relationship between the ball spin before and the ball spin after, but they were using oblique collisions as in configuration 3 (Nathan et al. 2012; Kensrud et al. 2016). We have not considered friction in this section. It will not be covered until Sect. 5.5.

3.5 Summary

This chapter presented the equations for a collision at the center of mass of the bat and for a simple collision at the sweet spot. For configurations 1a and 1b, it gave the velocity of the bat and the ball after the collision. For configuration 1b, it also gave the equation for the kinetic energy lost in the collision. It showed how the definition of the coefficient of restitution would change, as our models got more complex. It gave nine alternative definitions of the sweet spot of the bat. It stated general assumptions that we will use throughout this book. It gave an equation for the velocity of the ball after the collision. Finally, it proved that for head-on collisions without friction $\omega_{\text{ball-after}} = \omega_{\text{ball-before}}$.

References

Bahill, A. T. (2004). The ideal moment of inertia for a baseball or softball bat. *IEEE Transactions on Systems, Man, and Cybernetics Part A: Systems and Humans, 34*(2), 197–204.

Bahill, A. T., & Baldwin, D. G. (2007). Describing baseball pitch movement with right-hand rules. *Computers in Biology and Medicine, 37,* 1001–1008.

Bahill, A. T., & Baldwin, D. G. (2008). Mechanics of baseball pitching and batting. In: *Applied biomedical engineering mechanics* (Chap. 16, pp. 445–488). Dhanjoo Ghista, CRC Press and Taylor & Francis Asia Pacific.

Bahill, A. T., & Karnavas, W. J. (1989). Determining ideal baseball bat weights using muscle force-velocity relationships. *Biological Cybernetics, 62,* 89–97.

Bahill, A. T., & Karnavas, W. J. (1991, April). The ideal baseball bat. *New Scientist, 130*(1763), 26–31.

Baldwin, D. G., & Bahill, A. T. (2004). A model of the bat's vertical sweetness gradient. In: M. Hubbard, R. D. Mehta, & J. M. Pallis (Eds.), *The engineering of sport 5* (Vol. 2) *Proceedings of the 5th International Engineering of Sport Conference* (pp. 305–311), September 13–16, 2004, Davis, CA, International Sports Engineering Association (ISEA), Sheffield, UK.

Box, J. F. (1981). Gosset, fisher, and the t distribution. *The American Statistician, 35*(2), 61–66.

Brach, R. M. (2007). *Mechanical impact dynamics: Rigid body collisions*. New York: Wiley.

Chamberlain, A. Exploring statcast's estimated swing speed, August 11, 2017. https://www.fangraphs.com/fantasy/exploring-statcasts-estimated-swing-speed/. Last accessed June 2018.

Crisco, J. J., Greenwald, R. M., Blume, J. D., & Penna, L. H. (2002). Batting performance of wood and metal baseball bats. *Medicine & Science in Sports & Exercise, 34*, 1675–1684. https://doi.org/10.1249/01.mss.0000031320.62025.57.

Cross, R. (2000, November). The coefficient of restitution for collisions of happy balls, unhappy balls, and tennis balls. *American Journal of Physics, 68*(11), 1025–1031.

Cross, R. (2009). Mechanics of swinging a bat. *American Journal of Physics, 77*(1), 36–43.

Cross, R. (2011). *Physics of baseball and softball*. Berlin: Springer.

Dadouriam, H. M. (1913). *Analytic Mechanics for students of physics and engineering* (p. 248). New York: D. Van Nostrand Co.

Drane, P. J., Sherwood, J.A., Jones, J.W., & Connelly, T.P. (2008). The effect of baseball construction on the game of baseball (P275). In: *The engineering of sport* (Vol. 7, pp. 681–688). Paris: Springer.

Duris, J., & Smith, L. (2004). Evaluation test methods used to characterize softballs. In: M. Hubbard, R. D. Mehta & J. M. Pallis (Eds.), *Proceedings of the 5th Conference of Engineering of Sport* (Vol. 2, pp. 80–86). International Sports Engineering Association (ISEA), ISBN 0-9547861-1-4.

Fallon, L. P., & James A., Sherwood, J. A. (2000). *Performance comparison of the 1999 and 2000 major league baseballs.* University of Massachusetts Lowell, June 27, 2000. http://baseball.physics.illinois.edu/UML2000.pdf.

Ferreira da Silva, M. F. (2007). Meaning and usefulness of the coefficient of restitution. *European Journal of Physics, 28,* 1219–1232. https://doi.org/10.1088/0143-0807/28/6/019.

Fleisig, G. S., Zheng, N., Stodden, D. F., & Andrews, J. R. Relationship between bat mass properties and bat velocity. *Biomechanics Symposia 2001,* University of San Francisco.

Fleisig, G. S., Zheng, N., Stodden, D. F., & Andrews, J. R. (2002). Relationship between bat mass properties and bat velocity. *Sports Engineering, 5,* 1–8. https://doi.org/10.1046/j.1460-2687.2002.00096.x.

Higuchi, T., Nagami, T., Nakata, H., Watanabe, M., Isaka, T., & Kanosue, K. (2016). Contribution of visual information about ball trajectory to baseball hitting accuracy. *PLOS One*, Published: February 5, 2016, http://dx.doi.org/10.1371/journal.pone.0148498.

Kensrud, J. R., Nathan, A. M., & Smith, L. V. (2016, October). Oblique collisions of baseballs and softballs with a bat. *American Journal of Physics*.

King, K., Hough, J., & McGinnis, R. (2012). A new technology for resolving the dynamics of a swinging bat. *Sports Engineering, 15,* 41–52.

Koenig, K., Mitchell, N. D., Hannigan, T. E., & Cluter, J. K. (2004). The influence of moment of inertia on baseball/softball bat swing speed. *Sports Engineering, 7*, 105–117.

Milanovich M., & Nesbit S. M. (2014, January). A three-dimensional kinematic and kinetic study of the college-level female softball swing. *Journal of Sports Science & Medicine, 13*(1), 180–191 (PMCID: PMC3918556).

Nathan, A. M. (2000). Dynamics of the baseball-bat collision. *American Journal of Physics*, *68* (11), 979-990.

Nathan, A. M. (2003). Characterizing the performance of baseball bats. *American Journal of Physics, 71,* 134–143.

Nathan, A. M., Smith, L. V., Faber, W. L., & Russell, D. A. (2011). Corked bats, juiced balls, and humidors: The physics of cheating in baseball. *American Journal of Physics, 79*(6), 575–580.

Nathan, A. M., Cantakos, J., Kesman, R., Mathew, B., & Lukash, W. (2012). Spin of a batted baseball. *Procedia Engineering, 34*, 182–187. https://doi.org/10.1016/j.proeng.2012.04.032 (9th Conference of the International Sports Engineering Association (ISEA)).

Sears, F. W., Zemansky, M. W., & Young, H. D. (1976). *University physics*. Reading, MA: Addison-Wesley.

Watts, R. G., & Bahill, A. T. *Keep your eye on the ball: Curveballs, knuckleballs, and fallacies of baseball* (1st edn, 1990, 2nd edn 2000). New York: W. H. Freeman and Co.

Welch, C. M., Banks, S. A., Cook, F. F. & Draovitch, P. (1995). Hitting a baseball: A biomechanical description. *J. Orthopaedic and Sports Physical Therapy*, *22*, 193-201.

Willman, D. (2017). BaseballSavant, https://baseballsavant.mlb.com/statcast_search. Last accessed August 2018.

Williams, T., & Underwood, J. (1982). *The science of hitting*. New York: Simon and Schuster.

Chapter 4
The BaConLaws Model for Bat–Ball Collisions

4.1 Introduction

Purpose: The purpose of this chapter is to explain bat–ball collisions with a complete, precise, correct set of equations, without jargon. The BaConLaws model describes head-on bat–ball collisions at the sweet spot of the bat. This model gives equations for the speed and spin of the bat and ball after the collision in terms of these same variables before the collision. It also gives advice for selecting or creating an optimal bat.

Configuration 2b is our most comprehensive model. It models a collision at the sweet spot of the bat with spin on the pitch. The model for the movement of the bat is a translation and a rotation about its center of mass. To configuration 2a, it adds Conservation of Energy, Conservation of Angular Momentum, KE_{lost} and ball spin. It has five equations and five unknowns, which are shown in Table 4.1. It is named the BaConLaws model because it is based on the conservation laws of physics applied to baseball. This chapter is unique in the science of baseball literature, because no one before has derived the post-collision equations for ball speed, bat speed and bat angular velocity from basic Newtonian axioms. It is also unusual in the field of mathematical modeling, because in derivations all of the intermediary steps are given. This was done to increase replicability.

One of the assumptions for this model is that the bat–ball collision is a free-end collision. That means that the bat acts as if no one is holding onto its knob. To visualize this, imagine that the bat is laying on a sheet of ice and you are looking down on top of it, as in Fig. 4.1. Then a baseball slams into the bat at 80 mph. This collision produces a translation and a rotation of the bat about its center of mass.

A note on notation. Nothing in this chapter requires the collision be at the sweet spot of the bat. Therefore, in our equations, we use the general symbol "ip" to indicate the impact point as in $d_{\text{cm-ip}}$ to denote the distance between the center of mass and the impact point. However, in our simulations, we require numerical values for a particular bat. Therefore, when presenting the results of our simulations, we use "cop"

A. T. Bahill, *The Science of Baseball*,
https://doi.org/10.1007/978-3-030-03032-2_4

Table 4.1 Equations for the BaConLaws model, five equations and five unknowns

Inputs	$v_{\text{ball-before}},\ \omega_{\text{ball-before}},\ v_{\text{bat-cm-before}},\ \omega_{\text{bat-before}}$ and CoR
Outputs (unknowns)	$v_{\text{ball-after}},\ \omega_{\text{ball-after}},\ v_{\text{bat-cm-after}},\ \omega_{\text{bat-after}},$ and KE_{lost}
Equations	
Conservation of Energy, Eq. (4.3)	$\frac{1}{2}m_{\text{ball}}v^2_{\text{ball-before}} + \frac{1}{2}I_{\text{ball}}\omega^2_{\text{ball-before}} + \frac{1}{2}m_{\text{bat}}v^2_{\text{bat-cm-before}} + \frac{1}{2}I_{\text{bat}}\omega^2_{\text{bat-before}}$ $= \frac{1}{2}m_{\text{ball}}v^2_{\text{ball-after}} + \frac{1}{2}I_{\text{ball}}\omega^2_{\text{ball-after}} + \frac{1}{2}m_{\text{bat}}v^2_{\text{bat-cm-after}} + \frac{1}{2}I_{\text{bat}}\omega^2_{\text{bat-after}} + KE_{\text{lost}}$
Conservation of Linear Momentum, Eq. (4.4)	$m_{\text{ball}}v_{\text{ball-before}} + m_{\text{bat}}v_{\text{bat-cm-before}} = m_{\text{ball}}v_{\text{ball-after}} + m_{\text{bat}}v_{\text{bat-cm-after}}$
Definition of CoR, Eq. (4.5)	$CoR_{2\text{b}} = -\frac{v_{\text{ball-after}} - v_{\text{bat-cm-after}} - d_{\text{cm-ip}}\omega_{\text{bat-after}}}{v_{\text{ball-before}} - v_{\text{bat-cm-before}} - d_{\text{cm-ip}}\omega_{\text{bat-before}}}$
Newton's Second Law, Eq. (4.6)	$d_{\text{cm-ss}}m_{\text{ball}}(v_{\text{ball-after}} - v_{\text{ball-before}}) = -I_{\text{bat}}(\omega_{\text{bat-after}} - \omega_{\text{bat-before}})$
Conservation of Angular Momentum, Eq. (4.7s)	$L_{\text{ball-before}} + L_{\text{bat-before}} = L_{\text{ball-after}} + L_{\text{bat-after}} m_{\text{ball}}v_{\text{ball-before}}d$ $+ (I_{\text{ball}} + m_{\text{ball}}d^2)\omega_{\text{ball-before}} + I_{\text{bat}}\omega_{\text{bat-before}}$ $= m_{\text{ball}}v_{\text{ball-after}}d + (I_{\text{ball}} + m_{\text{ball}}d^2)\omega_{\text{ball-after}} + I_{\text{bat}}\omega_{\text{bat-after}}$

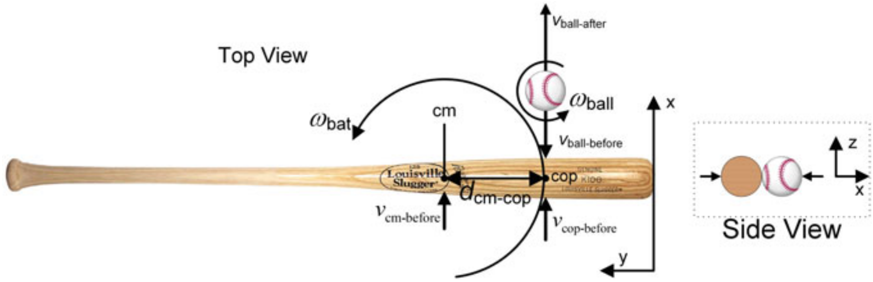

Fig. 4.1 A drawing of configuration 2b for the BaConLaws model

to denote the center of percussion. For example, the symbol $d_{\text{cm-cop}}$ indicates the distance between the center of mass and the center of percussion.

The BaConLaws model comprises a translation and a rotation of the bat about its center of mass. If you toss a bat into the air, it will have linear motion and it will rotate about its center of mass. Because the bat is a rigid object, all points on the bat must have the same angular velocity. If there is no rotation just a translation, then all points on the bat will have the same linear velocity. If there is a rotation about the center of mass and a translation, then each point on the bat will have a total velocity that is equal to the linear velocity of the center of mass plus the angular velocity of the center of mass times its distance from the center of mass. For example, the total velocity of impact point is

$vt_{\text{bat-ip}} = v_{\text{bat-cm}} + d_{\text{cm-ip}}\omega_{\text{cm}}$

The velocity of the sweet spot is given the symbol $vt_{\text{bat-ss}}$ to emphasize that it is the *total* velocity of the sweet spot meaning the vector sum of the linear translational velocity and the angular rotational velocity. If we had measured the velocity of a bat at a particular point and that bat was being swung by a human, then we measured the total of linear velocity and angular rotational velocity. Hence, we measured vt_{cop} or vt_{cm}. In our *equations,* we use the linear components, v_{cop} and v_{cm}, but in our *experiments* we actually measure the total velocities, vt_{cop} and vt_{cm}.

The first physics of baseball paper that derived an equation for the batted-ball velocity in terms of the bat and ball velocities and angular rotations about the center of mass of the bat was that of Kirkpatrick (1963). He assumed a free-end collision by assuming that the collision was so short that the linear and angular impulses applied by the bat were negligible. If his Eq. (5) is tailored for a short-duration head-on collision, like configuration 2b in Fig. 4.1, by setting $\theta = \varphi = K = \Omega = 0$, then we get our Eq. (4.8).

4.2 Definition of Variables and Parameters

Inputs $v_{\text{ball-before}}$, $\omega_{\text{ball-before}}$, $v_{\text{bat-cm-before}}$, $\omega_{\text{bat-before}}$ and CoR

$v_{\text{ball-before}}$ is the linear velocity of the *ball* in the x-direction (from home plate to the pitcher's rubber) before the collision.

$\omega_{\text{ball-before}}$ is the angular velocity of the *ball about its center of mass* before the collision.

$v_{\text{bat-cm-before}}$ is the linear velocity of the *center of mass of the bat* in the x-direction before the collision.

$\omega_{\text{bat-before}}$ is the angular velocity of the *bat about its center of mass* before the collision.

$CoR_{2\text{b}}$ is the coefficient of restitution for configuration 2b.

Outputs $v_{\text{ball-after}}$, $\omega_{\text{ball-after}}$, $v_{\text{bat-cm-after}}$, $\omega_{\text{bat-after}}$ and KE_{lost}

$v_{\text{ball-after}}$ is the linear velocity *of the ball* in the x-direction after the collision.

$\omega_{\text{ball-after}}$ is the angular velocity of the *ball about its center of mass* after the collision.

$v_{\text{bat-cm-after}}$ is the linear velocity *of the center of mass* of the bat in the x-direction after the collision.

$\omega_{\text{bat-after}}$ is the angular velocity of the bat *about its center of mass* after the collision.

KE_{lost} is the kinetic energy lost or transformed in the collision.

We want to solve our equations for the outputs $v_{\text{ball-after}}$, $\omega_{\text{ball-after}}$, $v_{\text{bat-cm-after}}$, $\omega_{\text{bat-after}}$ and KE_{lost}.

We will use the following fundamental equations of physics: Conservation of Energy, Conservation of Linear Momentum, the Definition of Kinematic *CoR*, Newton's second axiom and the Conservation of Angular Momentum.

4.2.1 Condensing the Notation for the Equations

First, we want to simplify the notation by making the following substitutions. These abbreviations are contained in Table 1.1, but by repeating them here, it makes this chapter independent from the rest of the book.

$$
\begin{aligned}
&d_{\text{cm-ip}} = d\\
&I_{\text{bat}} = I_2 = I_{\text{cm}}\\
&m_{\text{ball}} = m_1\\
&m_{\text{bat}} = m_2\\
&v_{\text{ball-before}} = v_{1\text{b}}\\
&v_{\text{ball-after}} = v_{1\text{a}}\\
&v_{\text{bat-cm-before}} = v_{2\text{b}}\\
&v_{\text{bat-cm-after}} = v_{2\text{a}}\\
&\omega_{\text{bat-before}} = \omega_{2\text{b}}\\
&\omega_{\text{bat-after}} = \omega_{2\text{a}}
\end{aligned}
$$

These substitutions produce the following equations:

Conservation of Energy

$$
\begin{aligned}
&\frac{1}{2}m_{\text{ball}}v^2_{\text{ball-before}} + \frac{1}{2}I_{\text{ball}}\omega^2_{\text{ball-before}} + \frac{1}{2}m_{\text{bat}}v^2_{\text{bat-cm-before}} + \frac{1}{2}I_{\text{bat}}\omega^2_{\text{bat-before}}\\
&= \frac{1}{2}m_{\text{ball}}v^2_{\text{ball-after}} + \frac{1}{2}I_{\text{ball}}\omega^2_{\text{ball-after}} + \frac{1}{2}m_{\text{bat}}v^2_{\text{bat-cm-after}} + \frac{1}{2}I_{\text{bat}}\omega^2_{\text{bat-after}} + KE_{\text{lost}}
\end{aligned}
\tag{4.3}
$$

$$
m_1v^2_{1\text{b}} + m_2v^2_{2\text{b}} + I_2\omega^2_{2\text{b}} = +m_1v^2_{1\text{a}} + m_2v^2_{2\text{a}} + I_2\omega^2_{2\text{a}} + 2\,KE_{\text{lost}} \tag{4.3s}
$$

In the label (4.3s), "s" stands for short.

Conservation of Linear Momentum

Assume that the bat and ball are point masses with all of their mass concentrated at the center of mass.

$$
m_{\text{ball}}v_{\text{ball-before}} + m_{\text{bat}}v_{\text{bat-cm-before}} = m_{\text{ball}}v_{\text{ball-after}} + m_{\text{bat}}v_{\text{bat-cm-after}} \tag{4.4}
$$

$$
m_1v_{1\text{b}} + m_2v_{2\text{b}} = m_1v_{1\text{a}} + m_2v_{2\text{a}} \tag{4.4s}
$$

Definition of the Coefficient of Restitution (*CoR*)

$$CoR_{2b} = -\frac{v_{\text{ball-after}} - v_{\text{bat-cm-after}} - d_{\text{cm-ip}}\omega_{\text{bat-after}}}{v_{\text{ball-before}} - v_{\text{bat-cm-before}} - d_{\text{cm-ip}}\omega_{\text{bat-before}}} \tag{4.5}$$

$$CoR_{2b} = -\frac{v_{1a} - v_{2a} - d\omega_{2a}}{v_{1b} - v_{2b} - d\omega_{2b}} \tag{4.5s}$$

Newton's second axiom states that applying an impulsive torque changes the angular momentum about the torque axis. Therefore,

$$d_{\text{cm-ip}} m_{\text{ball}}\left(v_{\text{ball-after}} - v_{\text{ball-before}}\right) = -I_{\text{bat}}\left(\omega_{\text{bat-after}} - \omega_{\text{bat-before}}\right) \tag{4.6}$$

$$dm_1(v_{1a} - v_{1b}) = -I_2(\omega_{2a} - \omega_{2b}) \tag{4.6s}$$

We have ignored the angular velocity of the ball because in Sect. 3.4 we proved that for head-on collisions without friction $\omega_{\text{ball-after}} = \omega_{\text{ball-before}}$.

Conservation of Angular Momentum

The initial and final angular momenta comprise ball translation, ball rotation, bat translation and bat rotation about its center of mass.

$$L_{\text{initial}} = L_{\text{final}}$$

$$\begin{aligned} &m_1 v_{1b} d + \left(I_1 + m_1 d^2\right)\omega_{1b} + I_2\omega_{2b} \\ &= +m_1 v_{1a} d + \left(I_1 + m_1 d^2\right)\omega_{1a} + I_2\omega_{2a} \end{aligned} \tag{4.7s}$$

Summary of simplifications, with units

$$\begin{array}{ll} A = \frac{(v_{1b} - v_{2b} - d\omega_{2b})(1 + CoR_{2b})}{m_1 I_2 + m_2 I_2 + m_1 m_2 d^2} & \frac{1}{\text{kg}^2\text{m s}} \\ B = (v_{1b} - v_{2b} - d\omega_{2b})(1 + CoR_{2b}) & \text{m/s} \\ C = v_{1b} - v_{2b} - d\omega_{2b} & \text{m/s} \end{array}$$

$$D = \frac{m_1 d^2}{I_2} \quad \text{unitless}$$

$$G = v_{2b} m_2 I_2(1 + CoR_{2b}) + \omega_{2b} m_2 d I_2(1 + CoR_{2b}) \quad \text{kg}^2\text{m}^3/\text{s}$$

$$G = (v_{2b} + \omega_{2b} d)(1 + CoR_{2b}) m_2 I_2 \quad \text{kg}^2\text{m}^3/\text{s}$$

$$K = (m_1 I_2 + m_2 I_2 + m_1 m_2 d^2) \quad \text{kg}^2\text{m}^2$$

$$\bar{m} = \frac{m_1 m_2}{m_1 + m_2} \quad \text{kg}$$

Note that none of these simplifications contains the outputs $v_{\text{ball-after}}$, $\omega_{\text{ball-after}}$, $v_{\text{bat-cm-after}}$, $\omega_{\text{bat-after}}$ and KE_{lost}. The most useful simplifications are the ones that are constants, independent of velocities after the collision. Using these simplifications allows us to print these long equations in a book. These simplifications are only used during the derivations. They are removed from the output equations. We will now use the Newtonian axioms in Eqs. (4.4), (4.5) and (4.6) to find $v_{\text{ball}-\text{after}}$, $v_{\text{bat}-\text{cm}-\text{after}}$ and $\omega_{\text{bat}-\text{after}}$.

4.3 Finding Ball Velocity After the Collision

First, we will solve for the velocity of the ball after the collision, $v_{\text{ball-after}}$. This section follows the development of Watts and Bahill (1990/2000).

Start with Eq. (4.6) and solve for the angular velocity of the bat after the collision, ω_{2a}

$$dm_1(v_{1a} - v_{1b}) = -I_2(\omega_{2a} - \omega_{2b})$$

$$\boxed{\omega_{2a} = \omega_{2b} - \tfrac{dm_1}{I_2}(v_{1a} - v_{1b})}$$

This equation was derived from Eq. (4.6). We will use it repeatedly. Next, we use Eq. (4.5) and solve for the velocity of the bat after the collision, v_{2a}

$$CoR_{2b} = -\frac{v_{1a} - v_{2a} - d\omega_{2a}}{v_{1b} - v_{2b} - d\omega_{2b}}$$

$$CoR_{2b}(v_{1b} - v_{2b} - d\omega_{2b}) = -v_{1a} + v_{2a} + d\omega_{2a}$$

$$v_{2a} = v_{1a} + CoR_{2b}(v_{1b} - v_{2b} - d\omega_{2b}) - d\omega_{2a}$$

This equation was derived from Eq. (4.5). We will use this expression repeatedly. Next, substitute ω_{2a} into this v_{2a} equation. We put the substitution in squiggly braces {} to make it obvious what has been inserted.

$$v_{2a} = v_{1a} + CoR_{2b}\ (v_{1b} - v_{2b} - d\omega_{2b}) - d\left\{\omega_{2b} - \frac{dm_1}{I_2}(v_{1a} - v_{1b})\right\}$$

Let $D = \frac{m_1 d^2}{I_2}$ and $C = \{v_{1b} - v_{2b} - d\omega_{2b}\}$

$$v_{2a} = v_{1a} + \{D\}(v_{1a} - v_{1b}) + CoR_{2b}\{C\} - d\omega_{2b}$$

$$v_{2a} = v_{1a}(1 + D) - v_{1b}D + CoR_{2b}C - d\omega_{2b}$$

Prepare to substitute this v_{2a} into Eq. (4.4) by multiplying by the mass of the bat, m_2

$$m_2v_{2a} = \{m_2v_{1a}(1 + D) - m_2Dv_{1b} + m_2CoR_{2b}\ C - m_2d\omega_{2b}\}$$

Now substitute this m_2v_{2a} into Eq. (4.4)

$$m_1 v_{1b} + m_2 v_{2b} = m_1 v_{1a} + m_2 v_{2a} \tag{4.4}$$

$$m_1 v_{1b} + m_2 v_{2b} = m_1 v_{1a} + \{m_2 v_{1a}(1 + D) - m_2 D v_{1b} + m_2 CoR_{2b}\ C - m_2 d\omega_{2b}\}$$

Put all v_{1a} terms on the left.

$$m_1 v_{1a} + m_2 v_{1a}(1 + D) = m_1 v_{1b} + m_2 v_{2b} + m_2 D v_{1b} - m_2 CoR_{2b}\ C + m_2 d\omega_{2b}$$

Replace the dummy variables C and D and we get

$$m_1 v_{1a} + m_2 v_{1a}\left\{1 + \frac{m_1 d^2}{I_2}\right\} = m_1 v_{1b} + m_2 v_{2b} + m_2\left\{\frac{m_1 d^2}{I_2}\right\} v_{1b} - m_2 CoR_{2b}$$
$$\{v_{1b} - v_{2b} - d\omega_{2b}\} + m_2 d\omega_{2b}$$

grouping with respect to $v_{1a},\ v_{1b},\ v_{2b}$ and ω_{2b} yields

$$v_{1a}\left[m_1 + m_2 + \frac{m_1 m_2 d^2}{I_2}\right] = v_{1b}\left[m_1 + \frac{m_1 m_2 d^2}{I_2} - m_2 CoR_{2b}\right]$$
$$+ v_{2b} m_2 (1 + CoR_{2b})\ + \omega_{2b} m_2 d(1 + CoR_{2b})$$

Multiply by the moment of inertia of the bat, I_2.

$$v_{1a}\left[m_1 I_2 + m_2 I_2 + m_1 m_2 d^2\right] = v_{1b}\left[m_1 I_2 + m_1 m_2 d^2 - m_2 CoR_{2b} I_2\right]$$
$$+ v_{2b} m_2 I_2 (1 + CoR_{2b}) + \omega_{2b} m_2 d I_2 (1 + CoR_{2b})$$

Rearrange

$$\boxed{v_{1a} = \frac{v_{1b}\left(m_1 I_2 - m_2 I_2\ CoR_{2b} + m_1 m_2 d^2\right) + v_{2b} m_2 I_2 (1 + CoR_{2b}) + d\omega_{2b} m_2 I_2 (1 + CoR_{2b})}{m_1 I_2 + m_2 I_2 + m_1 m_2 d^2}}$$

Expanding the abbreviations gives

$$\begin{aligned} v_{\text{ball-after}} = v_{\text{ball-before}} & \frac{(m_{\text{ball}} I_{\text{bat}} - m_{\text{bat}} I_{\text{bat}}\ CoR_{2b} + m_{\text{ball}} m_{\text{bat}} d^2)}{m_{\text{ball}} I_{\text{bat}} + m_{\text{bat}} I_{\text{bat}} + m_{\text{ball}} m_{\text{bat}} d^2} \\ + v_{\text{bat-cm-before}} & \frac{m_{\text{bat}} I_{\text{bat}} (1 + CoR_{2b})}{m_{\text{ball}} I_{\text{bat}} + m_{\text{bat}} I_{\text{bat}} + m_{\text{ball}} m_{\text{bat}} d^2} \\ + d\omega_{\text{bat-before}} & \frac{m_{bat} I_{bat} (1 + CoR_{2b})}{m_{\text{ball}} I_{\text{bat}} + m_{\text{bat}} I_{\text{bat}} + m_{\text{ball}} m_{\text{bat}} d^2} \end{aligned} \tag{4.8}$$

This equation was derived from Eqs. (4.4), (4.5) and (4.6).

Now we want to rearrange this normal form equation into its canonical form.

Let $K = \left(m_1 I_2 + m_2 I_2 + m_1 m_2 d^2\right)$

$$G = v_{2b} m_2 I_2 (1 + CoR_{2b}) + \omega_{2b} m_2 d I_2 (1 + CoR_{2b})$$

$$v_{1a} = \frac{v_{1b}(m_1 I_2 - m_2 I_2 CoR_{2b} + m_1 m_2 d^2)}{K} + \frac{G}{K}$$

add $\left(v_{1b} - \frac{v_{1b} K}{K}\right)$ to the right side

$$v_{1a} = \{v_{1b}\} + \frac{v_{1b}(m_1 I_2 - m_2 I_2 CoR_{2b} + m_1 m_2 d^2)\{-v_{1b}(m_1 I_2 + m_2 I_2 + m_1 m_2 d^2)\}}{K} + \frac{G}{K}$$

Simplify

$$v_{1a} = v_{1b} + \frac{v_{1b}(m_1 I_2 - m_2 I_2 CoR_{2b} + m_1 m_2 d^2 - m_1 I_2 - m_2 I_2 - m_1 m_2 d^2)}{K} + \frac{G}{K}$$

$$v_{1a} = v_{1b} + \frac{v_{1b}(-m_2 I_2 - m_2 I CoR_{2b})}{K} + \frac{G}{K}$$

$$v_{1a} = v_{1b} + \frac{-v_{1b} m_2 I_2 (1 + CoR_{2b}) + G}{K}$$

$$v_{1a} = v_{1b} + \frac{-v_{1b} m_2 I_2 (1 + CoR_{2b}) + v_{2b} m_2 I_2 (1 + CoR_{2b}) + \omega_{2b} m_2 d I_2 (1 + CoR_{2b})}{K}$$

Finally, we get the canonical form for the linear velocity of the ball after the collision:

$$\boxed{v_{1a} = v_{1b} - \frac{(v_{1b} - v_{2b} - d\omega_{2b})(1 + CoR_{2b}) m_2 I_2}{m_1 I_2 + m_2 I_2 + m_1 m_2 d^2}} \tag{4.8c}$$

This equation was derived from Eqs. (4.4), (4.5) and (4.6). Expanding the abbreviations gives

$$v_{\text{ball-after}} = v_{\text{ball-before}} - \frac{(v_{\text{ball-before}} - v_{\text{bat-cm-before}} - \omega_{\text{bat-before}} d)(1 + CoR_{2b}) m_{\text{bat}} I_{\text{bat}}}{m_{\text{ball}} I_{\text{bat}} + m_{\text{bat}} I_{\text{bat}} + m_{\text{ball}} m_{\text{bat}} d^2}$$

Please note that nothing in this section required the collision to be at the sweet spot of the bat. In these equations, $d_{\text{cm-ip}}$ could be replaced with any positive distance to the point of impact. That is why we usually used the letter d without a subscript.

If the collision is at the center of mass of the bat instead of at the sweet spot, then $d = d_{\text{cm-ip}} = 0$. Now we replace CoR_{2b} with CoR_{1a} and the above equation reduces to

$$v_{1a} = v_{1b} + \frac{(v_{2b} - v_{1b})(1 + CoR_{1a})m_2 I_2}{m_1 I_2 + m_2 I_2}$$

cancelling I_2 yields

$$v_{1a} = v_{1b} + \frac{(v_{2b} - v_{1b})(1 + CoR_{1a})m_2}{m_1 + m_2}$$

$$v_{\text{ball-after}} = v_{\text{ball-before}} - \frac{(v_{\text{ball-before}} - v_{\text{bat-cm-before}})(1 + CoR_{1a})m_{\text{bat}}}{m_{\text{ball}} + m_{\text{bat}}}$$

We derived this equation previously in the section entitled "Collisions at the center of mass, Configuration 1a." The subscripts of CoR refer to the collision configuration names not to the ball and bat before and after.

4.4 Finding Bat Velocity After the Collision

As before, we start with Eq. (4.6) and solve for the angular velocity of the bat after the collision, ω_{2a}

$$dm_1(v_{1a} - v_{1b}) = -I_2(\omega_{2a} - \omega_{2b})$$

$$\omega_{2a} = \omega_{2b} - \frac{dm_1}{I_2}(v_{1a} - v_{1b})$$

We will use this expression repeatedly. Next use Eq. (4.5) and solve for the velocity of the bat after the collision, v_{2a}

$$CoR_{2b} = -\frac{v_{1a} - v_{2a} - d\omega_{2a}}{v_{1b} - v_{2b} - d\omega_{2b}}$$

$$CoR_{2b}(v_{1b} - v_{2b} - d\omega_{2b}) = -v_{1a} + v_{2a} + d\omega_{2a}$$

$$v_{2a} = v_{1a} + CoR_{2b}(v_{1b} - v_{2b} - d\omega_{2b}) - d\omega_{2a}$$

Substitute ω_{2a} into this v_{2a} equation. I put the substitution in squiggly braces { } to make it obvious what has been inserted.

$$v_{2a} = v_{1a} + CoR_{2b}\ (v_{1b} - v_{2b} - d\omega_{2b}) - d\left\{\omega_{2b} - \frac{dm_1}{I_2}(v_{1a} - v_{1b})\right\}$$

So far, this derivation is identical to that in the previous section.

Now, let $C = v_{1b} - v_{2b} - d\omega_{2b}$

$$v_{2a} = v_{1a} + \frac{m_1 d^2}{I_2}(v_{1a} - v_{1b}) + CoR_{2b}\{C\} - \omega_{2b} d$$

Equation (4.8) derived in the previous section is

$$v_{1a} = v_{1b} - \frac{(v_{1b} - v_{2b} - d\omega_{2b})(1 + CoR_{2b})m_2 I_2}{m_1 I_2 + m_2 I_2 + m_1 m_2 d^2}$$

As before, let $K = (m_1 I_2 + m_2 I_2 + m_1 m_2 d^2)$

$$v_{1a} = v_{1b} - \frac{(v_{1b} - v_{2b} - d\omega_{2b})(1 + CoR_{2b})m_2 I_2}{K}$$

$$\text{Let B} = (v_{1b} - v_{2b} - d\omega_{2b})(1 + CoR_{2b})$$

$$v_{1a} = \left\{ v_{1b} - \frac{Bm_2 I_2}{K} \right\}$$

Put this into both places for v_{1a} in the v_{2a} equation above.

$$v_{2a} = \left\{ v_{1b} - \frac{Bm_2 I_2}{K} \right\} + \frac{m_1 d^2}{I_2}\left(\left\{ v_{1b} - \frac{Bm_2 I_2}{K} \right\} - v_{1b} \right) + CoR_{2b}\ C - \omega_{2b} d$$

Now multiply by K

$$v_{2a}K = \left\{ v_{1b}K - \frac{Bm_2 I_2}{K}K \right\} + \frac{m_1 d^2}{I_2}\left[v_{1b}K - K\frac{Bm_2 I_2}{K} - v_{1b}K \right] + CoR_{2b}\ CK - \omega_{2b} dK$$

$$v_{2a}K = v_{1b}K - Bm_2 I_2 + \frac{m_1 d^2}{I_2}\left[v_{1b}K - Bm_2 I_2 - v_{1b}K \right] + CoR_{2b}\ CK - \omega_{2b} dK$$

Cancel the terms in color

$$v_{2a}K = v_{1b}K - Bm_2 I_2 + \frac{m_1 d^2}{I_2}\left[-Bm_2 I_2 \right] + CCoR_{2b}\ K - \omega_{2b} dK$$

$$\text{Substitute B} = (v_{1b} - v_{2b} - d\omega_{2b})(1 + CoR_{2b})$$

$$v_{2a}K = v_{1b}K - \{(v_{1b} - v_{2b} - d\omega_{2b})(1 + CoR_{2b})\}m_2 I_2 - \frac{m_1 d^2}{I_2}[\{(v_{1b} - v_{2b} - d\omega_{2b})(1 + CoR_{2b})\}m_2 I_2] + CCoR_{2b}\ K - \omega_{2b} dK$$

Let us write this as three variables v_{1b}, v_{2b} and $d\omega_{2b}$ with their associated coefficients.

$$
\begin{aligned}
v_{2a}K = {} & v_{1b}K - v_{1b}m_2I_2(1+CoR_{2b}) + v_{2b}m_2I_2(1+CoR_{2b}) + \omega_{2b}m_2dI_2(1+CoR_{2b}) \\
& - v_{1b}m_1m_2d^2(1+CoR_{2b}) + v_{2b}m_1m_2d^2(1+CoR_{2b}) + \omega_{2b}m_1m_2d^3(1+CoR_{2b}) \\
& + v_{1b}CoR_{2b}\ K - v_{2b}CoR_{2b}\ K - \omega_{2b}dK(1+CoR)
\end{aligned}
$$

Rearrange

$$
\begin{aligned}
v_{2a}K = {} & v_{1b}K - v_{1b}m_2I_2(1+CoR_{2b}) - v_{1b}m_1m_2d^2(1+CoR_{2b}) + v_{1b}CoR_{2b}\ K \\
& + v_{2b}m_2I_2(1+CoR_{2b}) + v_{2b}m_1m_2d^2(1+CoR_{2b}) - v_{2b}CoR_{2b}\ K \\
& + \omega_{2b}m_2dI_2(1+CoR_{2b}) + \omega_{2b}m_1m_2d^3(1+CoR_{2b}) - \omega_{2b}dK(1+CoR)
\end{aligned}
$$

Now let us break up the $(1+CoR_{2b})$ terms.

$$
\begin{aligned}
v_{2a}K = {} & v_{1b}K - v_{1b}m_2I_2 - v_{1b}m_2I_2CoR_{2b} - v_{1b}m_1m_2d^2 \\
& - v_{1b}m_1m_2d^2CoR_{2b} + v_{1b}CoR_{2b}\ K + v_{2b}m_2I_2 \\
& + v_{2b}m_2ICoR_{2b} + v_{2b}m_1m_2d^2 + v_{2b}m_1m_2d^2CoR_{2b} \\
& - v_{2b}CoR_{2b}K + \omega_{2b}m_2dI_2 + \omega_{2b}m_2dI_2CoR_{2b} \\
& + \omega_{2b}m_1m_2d^3 + \omega_{2b}m_1m_2d^3CoR_{2b} - \omega_{2b}dK \\
& - \omega_{2b}dKCoR_{2b}
\end{aligned}
$$

Are any of these terms the same? No. OK, now let's substitute

$$
K = \left(m_1I_2 + m_2I_2 + m_1m_2d^2\right)
$$

and hope for cancellations.

$$
\begin{aligned}
v_{2a}K = {} & v_{1b}\left(m_1I_2 + m_2I_2 + m_1m_2d^2\right) - v_{1b}m_2I_2 - v_{1b}m_2I_2CoR_{2b} \\
& - v_{1b}m_1m_2d^2 - v_{1b}m_1m_2d^2CoR_{2b} + v_{1b}CoR_{2b}\left(m_1I_2 + m_2I_2 + m_1m_2d^2\right) \\
& + v_{2b}m_2I_2 + v_{2b}m_2I_2CoR_{2b} + v_{2b}m_1m_2d^2 + v_{2b}m_1m_2d^2CoR_{2b} \\
& - v_{2b}CoR_{2b}\left(m_1I_2 + m_2I_2 + m_1m_2d^2\right) \\
& + \omega_{2b}m_2dI_2 + \omega_{2b}m_2dI_2CoR_{2b} + \omega_{2b}m_1m_2d^3 + \omega_{2b}m_1m_2d^3CoR_{2b} - \omega_{2b}\left(m_1dI_2 + m_2dI_2 + m_1m_2d^3\right) \\
& - \omega_{2b}\left(m_1dI_2 + m_2dI_2 + m_1m_2d^3\right)CoR_{2b}
\end{aligned}
$$

The terms in color cancel, leaving

$$
\begin{aligned}
& v_{2a}K = v_{1b}m_1I_2(1+CoR_{2b}\ ) \\
& + v_{2b}(-m_1I_2CoR_{2b}\ + m_2I_2 + m_1m_2d^2) \\
& - \omega_{2b}m_1dI_2(1+CoR_{2b})
\end{aligned}
$$

Continuing this simplification,

distribute the second term and add $-v_{2b}m_1I_2 + v_{2b}m_1I_2$

$$\begin{aligned}
v_{2a}K &= +v_{1b}m_1I_2(1+CoR_{2b}) - v_{2b}m_1I_2CoR_{2b}\{-v_{2b}m_1I_2 + v_{2b}m_1I_2\} + v_{2b}m_2I_2 + v_{2b}m_1m_2d^2 - \omega_{2b}m_1dI_2(1+CoR_{2b})\\
&= (v_{1b} - v_{2b})m_1I_2(1+CoR_{2b}) + v_{2b}m_1I_2 + v_{2b}m_2I_2 + v_{2b}m_1m_2d^2 - \omega_{2b}m_1dI_2(1+CoR_{2b})\\
&= (v_{1b} - v_{2b})m_1I_2(1+CoR_{2b}) + v_{2b}K - \omega_{2b}m_1dI_2(1+CoR_{2b})\\
&= v_{2b}K + (v_{1b} - v_{2b})m_1I_2(1+CoR_{2b}) - \omega_{2b}m_1dI_2(1+CoR_{2b})
\end{aligned}$$

Finally, divide by K to get the velocity of the bat after the collision in canonical form.

$$\boxed{v_{2a} = v_{2b} + \frac{(v_{1b} - v_{2b} - d\omega_{2b})(1+CoR_{2b})m_1I_2}{(m_1I_2 + m_2I_2 + m_1m_2d^2)}}$$

This equation was derived from Eqs. (4.4), (4.5), (4.6) and (4.8). Expanding our abbreviations, we get

$$v_{\text{bat-cm-after}} = v_{\text{bat-cm-before}} + \frac{(v_{\text{ball-before}} - v_{\text{bat-cm-before}} - \omega_{\text{bat-before}}d)(1+CoR_{2b})m_{\text{ball}}I_{\text{bat}}}{m_{\text{ball}}I_{\text{bat}} + m_{\text{bat}}I_{\text{bat}} + m_{\text{ball}}m_{\text{bat}}d^2} \tag{4.9}$$

We can change this into our normal form by first combining the two terms over one common denominator.

$$\begin{aligned}
v_{2a} &= v_{2b}\frac{(m_1I_2 + m_2I_2 + m_1m_2d^2)}{(m_1I_2 + m_2I_2 + m_1m_2d^2)} + \frac{(v_{1b} - v_{2b} - d\omega_{2b})(1+CoR_{2b})m_1I_2}{(m_1I_2 + m_2I_2 + m_1m_2d^2)}\\
&= \frac{v_{2b}(m_1I_2 + m_2I_2 + m_1m_2d^2) + (v_{1b} - v_{2b} - d\omega_{2b})(1+CoR_{2b})m_1I_2}{(m_1I_2 + m_2I_2 + m_1m_2d^2)}
\end{aligned}$$

and then simplifying

$$\boxed{v_{2a} = \frac{v_{2b}\left(-m_1I_2CoR_{2b} + m_2I_2 + m_1m_2d^2\right) + v_{1b}m_1I_2(1+CoR_{2b}) - \omega_{2b}m_1dI_2(1+CoR_{2b})}{(m_1I_2 + m_2I_2 + m_1m_2d^2)}}$$

Expanding our abbreviations, we get

$$\begin{aligned}
v_{\text{bat-cm-after}} = v_{\text{ball-before}}&\frac{m_{\text{ball}}I_{\text{bat}}(1+CoR_{2b})}{m_{\text{ball}}I_{\text{bat}} + m_{\text{bat}}I_{\text{bat}} + m_{\text{ball}}m_{\text{bat}}d^2}\\
&+ v_{\text{bat-cm-before}}\frac{(-m_{\text{ball}}I_{\text{bat}}CoR_{2b} + m_{\text{bat}}I_{\text{bat}} + m_{\text{ball}}m_{\text{bat}}d^2)}{m_{\text{ball}}I_{\text{bat}} + m_{\text{bat}}I_{\text{bat}} + m_{\text{ball}}m_{\text{bat}}d^2}\\
&- d\omega_{\text{bat-before}}\frac{m_{\text{ball}}I_{\text{bat}}(1+CoR_{2b})}{m_{\text{ball}}I_{\text{bat}} + m_{\text{bat}}I_{\text{bat}} + m_{\text{ball}}m_{\text{bat}}d^2}
\end{aligned}$$

4.5 Alternative Derivation of Bat Velocity After the Collision

This time, let us start with the normal form for Eq. (4.8).

$v_{1a} = \frac{v_{1b}\left(m_1 I_2 - m_2 I_2\ CoR_{2b} + m_1 m_2 d^2\right) + v_{2b} m_2 I_2 (1 + CoR_{2b}) + \omega_{2b} m_2 d I_2 (1 + CoR_{2b})}{m_1 I_2 + m_2 I_2 + m_1 m_2 d^2}$
Let
$C = (v_{1b} - v_{2b} - d\omega_{2b})$
$D = \frac{m_1 d^2}{I_2}$
$K = (m_1 I_2 + m_2 I_2 + m_1 m_2 d^2)$
$Q = (m_1 I_2 - m_2 I_2\ CoR_{2b} + m_1 m_2 d^2)$
$R = m_2 I_2 (1 + CoR_{2b})$
$S = m_2 d I_2 (1 + CoR_{2b})$
making these substitutions yields
$v_{1a} = \frac{v_{1b} Q + v_{2b} R + \omega_{2b} S}{K}$

In the previous section, we used Eq. (4.5) and solved for the velocity of the bat after the collision, v_{2a}

$$v_{2a} = v_{1a} + CoR_{2b}(v_{1b} - v_{2b} - d\omega_{2b}) - d\omega_{2a}$$

Now we need to get rid of anything with a subscript of *after*, like ω_{2a}. Therefore, take Eq. (4.6) and solve for the angular velocity of the bat after the collision, ω_{2a}.

$$\omega_{2a} = \left\{ \omega_{2b} - \frac{dm_1}{I_2}(v_{1a} - v_{1b}) \right\}$$

Now, substitute this into the above v_{2a} equation to get

$$v_{2a} = v_{1a} + CoR_{2b}(v_{1b} - v_{2b} - d\omega_{2b}) - d\left\{ \omega_{2b} - \frac{dm_1}{I_2}(v_{1a} - v_{1b}) \right\}$$

$$v_{2a} = v_{1a}(1 + D) - Dv_{1b} + CoR_{2b}\ (v_{1b} - v_{2b} - d\omega_{2b}) - d\omega_{2b}$$

Substitute v_{1a} into this v_{2a} equation

$$v_{2a} = \left\{ \frac{v_{1b} Q + v_{2b} R + \omega_{2b} S}{K} \right\}(1 + D) - Dv_{1b} + CoR_{2b}\ (v_{1b} - v_{2b} - d\omega_{2b}) - \omega_{2b} d$$

$$v_{2a} = \frac{v_{1b}Q + v_{2b}R + \omega_{2b}S}{K} + \frac{v_{1b}QD + v_{2b}RD + \omega_{2b}SD}{K}$$
$$- Dv_{1b} + CoR_{2b}(v_{1b} - v_{2b} - d\omega_{2b}) - \omega_{2b}d$$
$$v_{2a}K = v_{1b}Q + v_{2b}R + \omega_{2b}S + v_{1b}QD + v_{2b}RD + \omega_{2b}SD$$
$$- Dv_{1b}K + v_{1b}CoR_{2b}K - v_{2b}CoR_{2b}K - \omega_{2b}dK(1 + CoR_{2b})$$

Collect similar terms.

$$\begin{aligned} v_{2a}K = {} & v_{1b}Q + v_{1b}QD - Dv_{1b}K + v_{1b}CoR_{2b}\ K + v_{2b}R + v_{2b}RD \\ & - v_{2b}CoR_{2b}\ K + \omega_{2b}S + \omega_{2b}SD - \omega_{2b}dK(1 + CoR_{2b}) \end{aligned}$$

Now replace D, K and Q in the v_{1b} term.

$$\begin{aligned} v_{2a}K = {} & +v_{1b}\left[\begin{array}{l} +\left(m_1I_2 - m_2I_2\ CoR_{2b} + m_1m_2d^2\right) \\ +\dfrac{m_1d^2}{I_2}\left(m_1I_2 - m_2I_2\ CoR_{2b} + m_1m_2d^2\right) \\ -\dfrac{m_1d^2}{I_2}\ \left(m_1I_2 + m_2I_2 + m_1m_2d^2\right) \\ +CoR_{2b}\ \left(m_1I_2 + m_2I_2 + m_1m_2d^2\right) \end{array}\right] \\ & + v_{2b}[R + RD - CoR_{2b}\ K] + \omega_{2b}\{S + SD - dK(1 + CoR_{2b})\} \end{aligned}$$

Simplify

$$\begin{aligned} v_{2a}K = {} & +v_{1b}m_1I_2(1 + CoR_{2b}) \\ & + v_{2b}[R + RD - CoR_{2b}\ K] \\ & + \omega_{2b}(S + SD - dK(1 + CoR_{2b})\ ) \end{aligned}$$

Now replace D, K, R and S.

$$\begin{aligned} v_{2a}K = {} & +v_{1b}m_1I_2(1 + CoR_{2b}) \\ & +v_{2b}\left[+m_2I_2(1 + CoR_{2b}) + m_2I_2(1 + CoR_{2b})\frac{m_1d^2}{I_2} - CoR_{2b}(m_1I_2 + m_2I_2 + m_1m_2d^2)\right] \\ & +\omega_{2b}\left(m_2dI_2(1 + CoR_{2b}) + m_2dI_2(1 + CoR_{2b})\frac{m_1d^2}{I_2} - (m_1dI_2 + m_2dI_2 + m_1m_2d^3)(1 + CoR_{2b})\right) \end{aligned}$$

The terms in color cancel.

$$\begin{aligned} v_{2a}K = &+v_{1b}[m_1 I_2(1+CoR_{2b})] \\ &+v_{2b}\left[+m_2 I_2 + m_1 m_2 d^2 + m_1 m_2 d^2 CoR_{2b} - CoR_{2b}(m_1 I_2 + m_1 m_2 d^2)\right] \\ &+\omega_{2b}(1+CoR_{2b})\left(m_2 d I_2 + m_2 d I_2 \frac{m_1 d^2}{I_2} - (m_1 d I_2 + m_2 d I_2 + m_1 m_2 d^3)\right) \end{aligned}$$

And now these terms in color cancel.

$$\begin{aligned} v_{2a}K = &+v_{1b}[m_1 I_2(1+CoR_{2b})] \\ &+v_{2b}\left[+m_2 I_2 + m_1 m_2 d^2 - m_1 I_2 CoR_{2b}\right] \\ &-\omega_{2b} m_1 d I_2(1+CoR_{2b}) \end{aligned}$$

Simplify

$$\boxed{\begin{aligned} v_{2a}K = &+v_{2b}\left[-m_1 I_2 CoR_{2b} + m_2 I_2 + m_1 m_2 d^2\right] \\ &+ v_{1b} m_1 I_2(1+CoR_{2b}) \\ &- \omega_{2b} m_1 d I_2(1+CoR) \end{aligned}}$$

Expanding our abbreviations gives

$$\begin{aligned} v_{\text{bat-cm-after}} = &\, v_{\text{ball-before}} \frac{m_{\text{ball}} I_{\text{bat}}(1+CoR_{2b})}{m_{\text{ball}} I_{\text{bat}} + m_{\text{bat}} I_{\text{bat}} + m_{\text{ball}} m_{\text{bat}} d^2} \\ &+ v_{\text{bat-cm-before}} \frac{(-m_{\text{ball}} I_{\text{bat}} CoR_{2b} + m_{\text{bat}} I_{\text{bat}} + m_{\text{ball}} m_{\text{bat}} d^2)}{m_{\text{ball}} I_{\text{bat}} + m_{\text{bat}} I_{\text{bat}} + m_{\text{ball}} m_{\text{bat}} d^2} \\ &- d\omega_{\text{bat-before}} \frac{m_{\text{ball}} I_{\text{bat}}(1+CoR_{2b})}{m_{\text{ball}} I_{\text{bat}} + m_{\text{bat}} I_{\text{bat}} + m_{\text{ball}} m_{\text{bat}} d^2} \end{aligned}$$

This is the same equation that we derived before.

4.6 Finding Bat Angular Velocity After the Collision

Now we want to find ω_{2a}(the angular velocity of the bat after the collision) in terms of the input variables and parameters. The following equation gives the velocity of the ball after the collision, v_{1a} from the canonical form of Eq. 4.8.

$$v_{1a} = \left\{ v_{1b} - \frac{(v_{1b} - v_{2b} - d\omega_{2b})(1+CoR_{2b}) m_1 I_2}{m_1 I_2 + m_2 I_2 + m_1 m_2 d^2} \right\}$$

From Eq. (4.6) we solve for the angular velocity of the bat after the collision, ω_{2a}

$$\omega_{2a} = \omega_{2b} - \frac{m_1 d}{I_2}(v_{1a} - v_{1b})$$

Substitute v_{1a} into this ω_{2a} equation

$$\omega_{2a} = \omega_{2b} - \frac{m_1 d}{I_2}\left\{ v_{1b} - \frac{(v_{1b} - v_{2b} - d\omega_{2b})(1 + CoR_{2b})m_1 I_2}{m_1 I_2 + m_2 I_2 + m_1 m_2 d^2} \right\} + \frac{m_1 d}{I_2} v_{1b}$$

cancel the terms in red

$$\omega_{2a} = \omega_{2b} + \frac{m_1 d}{I_2}\left[\frac{(v_{1b} - v_{2b} - d\omega_{2b})(1 + CoR_{2b})m_1 I_2}{m_1 I_2 + m_2 I_2 + m_1 m_2 d^2} \right]$$

and finally we get

$$\boxed{\omega_{2a} = \omega_{2b} + \frac{(v_{1b} - v_{2b} - d\omega_{2b})(1 + CoR_{2b})m_1 I_2}{m_1 I_2 + m_2 I_2 + m_1 m_2 d^2}} \tag{4.10}$$

This equation was derived from Eqs. (4.6) and (4.8). We can change this into our normal form by first combining the two terms over one common denominator.

$$\omega_{2a} = \omega_{2b} \frac{m_1 I_2 + m_2 I_2 + m_1 m_2 d^2}{m_1 I_2 + m_2 I_2 + m_1 m_2 d^2} + \frac{(v_{1b} - v_{2b} - d\omega_{2b})(1 + CoR_{2b})m_1 I_2}{m_1 I_2 + m_2 I_2 + m_1 m_2 d^2}$$

$$= \frac{\omega_{2b}(m_1 I_2 + m_2 I_2 + m_1 m_2 d^2) + (v_{1b} - v_{2b}) m_1 m_2 d (1 + CoR) - m_1 m_2 d^2 \omega_{2b}(1 + CoR_{2b})}{m_1 I_2 + m_2 I_2 + m_1 m_2 d^2}$$

Cancel duplicate terms and we get the normal form

$$\boxed{\omega_{2a} = \frac{\omega_{2b}\left(m_1 I_2 + m_2 I_2 - m_1 m_2 d^2 CoR_{2b}\right) + (v_{1b} - v_{2b}) m_1 m_2 d (1 + CoR_{2b})}{m_1 I_2 + m_2 I_2 + m_1 m_2 d^2}}$$

4.7 Three Output Equations in Three Formats

We will now summarize by giving equations for $v_{\text{ball-after}}$, $v_{\text{bat-cm-after}}$ and $\omega_{\text{bat-after}}$ in all three formats. First, we give the equation for the velocity of the ball after the collision in normal form

$$\begin{aligned}
v_{\text{ball-after}} = v_{\text{ball-before}} & \frac{(m_{\text{ball}} I_{\text{bat}} - m_{\text{bat}} I_{\text{bat}}\ CoR_{2b} + m_{\text{ball}} m_{\text{bat}} d^2)}{m_{\text{ball}} I_{\text{bat}} + m_{\text{bat}} I_{\text{bat}} + m_{\text{ball}} m_{\text{bat}} d^2} \\
& + v_{\text{bat-cm-before}} \frac{m_{\text{bat}} I_{\text{bat}} (1 + CoR_{2b})}{m_{\text{ball}} I_{\text{bat}} + m_{\text{bat}} I_{\text{bat}} + m_{\text{ball}} m_{\text{bat}} d^2} \\
& + d\omega_{\text{bat-before}} \frac{m_{bat} I_{bat} (1 + CoR_{2b})}{m_{\text{ball}} I_{\text{bat}} + m_{\text{bat}} I_{\text{bat}} + m_{\text{ball}} m_{\text{bat}} d^2}
\end{aligned}$$

in canonical form

$$v_{\text{ball-after}} = v_{\text{ball-before}} - \frac{(v_{\text{ball-before}} - v_{\text{bat-cm-before}} - d\omega_{\text{bat-before}})(1 + CoR_{2b})m_{\text{bat}}I_{\text{bat}}}{m_{\text{ball}}I_{\text{bat}} + m_{\text{bat}}I_{\text{bat}} + m_{\text{ball}}m_{\text{bat}}d^2}$$

and in reduced canonical form

$$\text{Let}\, A = \frac{(v_{\text{ball-before}} - v_{\text{bat-cm-before}} - d\omega_{\text{bat-before}})(1 + CoR_{2b})}{m_{\text{ball}}I_{\text{bat}} + m_{\text{bat}}I_{\text{bat}} + m_{\text{ball}}m_{\text{bat}}d^2}$$
$$v_{\text{ball-after}} = v_{\text{ball-before}} - Am_{\text{bat}}I_{\text{bat}}$$

Now, we give the equation for the linear velocity of the bat after the collision in normal form

$$\begin{aligned} v_{\text{bat-after}} = v_{\text{ball-before}} & \frac{m_{\text{ball}}I_{\text{bat}}(1 + CoR_{2b})}{m_{\text{ball}}I_{\text{bat}} + m_{\text{bat}}I_{\text{bat}} + m_{\text{ball}}m_{\text{bat}}d^2} \\ & + v_{\text{bat-cm-before}} \frac{(-m_{\text{ball}}I_{\text{bat}}CoR_{2b} + m_{\text{bat}}I_{\text{bat}} \ + m_{\text{ball}}m_{\text{bat}}d^2)}{m_{\text{ball}}I_{\text{bat}} + m_{\text{bat}}I_{\text{bat}} + m_{\text{ball}}m_{\text{bat}}d^2} \\ & - d\omega_{\text{bat-before}} \frac{m_{\text{ball}}I_{\text{bat}}(1 + CoR_{2b})}{m_{\text{ball}}I_{\text{bat}} + m_{\text{bat}}I_{\text{bat}} + m_{\text{ball}}m_{\text{bat}}d^2} \end{aligned}$$

in canonical form

$$v_{\text{bat-after}} = v_{\text{bat-before}} + \frac{(v_{\text{ball-before}} - v_{\text{bat-cm-before}} - d\omega_{\text{bat-before}})(1 + CoR_{2b})m_{\text{ball}}I_{\text{bat}}}{m_{\text{ball}}I_{\text{bat}} + m_{\text{bat}}I_{\text{bat}} + m_{\text{ball}}m_{\text{bat}}d^2}$$

and in reduced canonical form

$$v_{\text{bat-after}} = v_{\text{bat-before}} + Am_{\text{ball}}I_{\text{bat}}$$

Finally, we give the equation for the angular velocity of the bat after the collision in normal form

$$\begin{aligned} \omega_{\text{bat-after}} = v_{\text{ball-before}} & \frac{m_{\text{ball}}m_{\text{bat}}d(1 + CoR_{2b})}{m_{\text{ball}}I_{\text{bat}} + m_{\text{bat}}I_{\text{bat}} + m_{\text{ball}}m_{\text{bat}}d^2} \\ & - v_{\text{bat-cm-before}} \frac{m_{\text{ball}}m_{\text{bat}}d(1 + CoR_{2b})}{m_{\text{ball}}I_{\text{bat}} + m_{\text{bat}}I_{\text{bat}} + m_{\text{ball}}m_{\text{bat}}d^2} \\ & + \omega_{\text{bat-before}} \frac{(m_{\text{ball}}I_{\text{bat}} + m_{\text{bat}}I_{\text{bat}} \ - m_{\text{ball}}m_{\text{bat}}d^2CoR_{2b})}{m_{\text{ball}}I_{\text{bat}} + m_{\text{bat}}I_{\text{bat}} + m_{\text{ball}}m_{\text{bat}}d^2} \end{aligned}$$

in canonical form

$$\omega_{\text{bat-after}} = \omega_{\text{bat-before}} + \frac{(v_{\text{ball-before}} - v_{\text{bat-cm-before}} - d\omega_{\text{bat-before}})(1 + CoR_{2b})m_{\text{ball}}m_{\text{bat}}d}{m_{\text{ball}}I_{\text{bat}} + m_{\text{bat}}I_{\text{bat}} + m_{\text{ball}}m_{\text{bat}}d^2}$$

and in reduced canonical form

$$\omega_{\text{bat-after}} = \omega_{\text{bat-before}} + Am_{\text{ball}}m_{\text{bat}}d$$

We now want to add the equation for Conservation of Energy, Eq. (4.3).

4.8 Adding Conservation of Energy and Finding KE_{lost}

This approach, of adding Conservation of Energy to the set of bat–ball collision equations, is unique in the science of baseball literature. From configuration 1b, we had that before the collision there is kinetic energy in the ball and kinetic energy in the bat.

$$KE_{\text{before}} = \frac{1}{2}m_{\text{ball}}v^2_{\text{ball-before}} + \frac{1}{2}m_{\text{bat}}v^2_{\text{bat-cm-before}}$$

And after the collision, there is also kinetic energy in the ball and bat system.

$$KE_{\text{after}} = \frac{1}{2}m_{\text{ball}}v^2_{\text{ball-after}} + \frac{1}{2}m_{\text{bat}}v^2_{\text{bat-cm-after}}$$

However, they are not equal. In bat–ball collisions, some kinetic energy is transformed into heat, vibrations and deformations. This is called the kinetic energy lost or transformed. It is modeled with the CoR.

$$KE_{\text{lost}} = KE_{\text{before}} - KE_{\text{after}}$$

In the configuration 1b section, we stated that

$$KE_{\text{lost-config-1b}} = \frac{\bar{m}}{2}(\text{collision velocity})^2\left(1 - CoR^2_{1b}\right)$$

where $\bar{m} = \frac{m_{\text{ball}}m_{\text{bat}}}{m_{\text{ball}} + m_{\text{bat}}}$.

$$KE_{\text{lost-config-1b}} = \frac{\bar{m}}{2}\left(v_{\text{ball-before}} - v_{\text{bat-cm-before}}\right)^2\left(1 - CoR^2_{1b}\right)$$

This is Eq. (3.2).

However, this equation for kinetic energy lost is not valid for the BaConLaws model because we now also have angular kinetic energy in the rotation of the bat. There are no springs in the system and the bat swing is level; therefore, there is no change in potential energy. Before the collision, there is kinetic energy in the bat created by rotation of the batter's body and arms plus the translational kinetic energy of the ball.

$$KE_{\text{before}} = \frac{1}{2} m_{\text{ball}} v_{\text{ball-before}}^2 + \frac{1}{2} m_{\text{bat}} v_{\text{bat-cm-before}}^2 + \frac{1}{2} I_{\text{ball}} \omega_{\text{ball-before}}^2 + \frac{1}{2} I_{\text{bat}} \omega_{\text{bat-before}}^2$$

As always, ω means rotation about the center of mass of the object. The collision will make the bat spin about its center of mass. If the collision is at the Center of Percussion for the pivot point, then it will produce a rotation about the center of mass, but no translation.

$$KE_{\text{after}} = \frac{1}{2} m_{\text{ball}} v_{\text{ball-after}}^2 + \frac{1}{2} m_{\text{bat}} v_{\text{bat-cm-after}}^2 + \frac{1}{2} I_{\text{ball}} \omega_{\text{ball-after}}^2 + \frac{1}{2} I_{\text{bat}} \omega_{\text{bat-after}}^2$$

$$\begin{aligned} KE_{\text{before}} = KE_{\text{after}} + KE_{\text{lost}} \frac{1}{2} m_{\text{ball}} v_{\text{ball-before}}^2 & \\ + \frac{1}{2} m_{\text{bat}} v_{\text{bat-cm-before}}^2 + \frac{1}{2} I_{\text{ball}} \omega_{\text{ball-before}}^2 + \frac{1}{2} I_{\text{bat}} \omega_{\text{bat-before}}^2 & \\ = \frac{1}{2} m_{\text{ball}} v_{\text{ball-after}}^2 + \frac{1}{2} m_{\text{bat}} v_{\text{bat-cm-after}}^2 + \frac{1}{2} I_{\text{ball}} \omega_{\text{ball-after}}^2 + \frac{1}{2} I_{\text{bat}} \omega_{\text{bat-after}}^2 + KE_{lost} & \end{aligned}$$

In our reduced notation

$$\frac{1}{2} m_1 v_{1b}^2 + \frac{1}{2} m_2 v_{2b}^2 + \frac{1}{2} I_1 \omega_{1b}^2 + \frac{1}{2} I_2 \omega_{2b}^2 = \frac{1}{2} m_1 v_{1a}^2 + \frac{1}{2} m_2 v_{2a}^2 + \frac{1}{2} I_1 \omega_{1a}^2 + \frac{1}{2} I_2 \omega_{2a}^2 + KE_{\text{lost}}$$

The KE_{before} and the KE_{after} are easy to find. It is the KE_{lost} that is hard to find.

In Sect. 3.4, we proved that for head-on collisions without friction $\omega_{\text{ball-before}} = \omega_{\text{ball-after}}$. Therefore, the ball spin terms in these Conservation of Energy equations cancel resulting in

$$0 = m_1 v_{1b}^2 + m_2 v_{2b}^2 + I_2 \omega_{2b}^2 - m_1 v_{1a}^2 - m_2 v_{2a}^2 - I_2 \omega_{2a}^2 - 2KE_{\text{lost}}$$

From before, we have

$$\begin{aligned} A &= \frac{(v_{1b} - v_{2b} - d\omega_{2b})(1 + CoR_{2b})}{m_1 I_2 + m_2 I_2 + m_1 m_2 d^2} \\ v_{1a} &= v_{1b} - A m_2 I_2 \\ v_{2a} &= v_{2b} + A m_1 I_2 \\ \omega_{2a} &= \omega_{2b} + A m_1 m_2 d \\ \omega_{1a} &= \omega_{1b} \end{aligned}$$

Substituting A, the linear velocity of the ball after the collision, v_{1a}, the linear velocity of the bat after the collision, v_{2a} and the angular velocity of the bat after the collision, ω_{2a} into the new Conservation of Energy equation yields

$$2KE_{\text{lost}} = \begin{cases} m_1 v_{1b}^2 + m_2 v_{2b}^2 + I_2 \omega_{2b}^2 - m_1 (v_{1b} - Am_2 I_2)^2 \\ -m_2 (v_{2b} + Am_1 I_2)^2 - I_2 (\omega_{2b} + Am_1 m_2 d)^2 \end{cases}$$

Now we want to put this into the form that we had for Eq. (3.2) in the section for configuration 1b. The following derivation is original. First, we expand the squared terms.

$$2KE_{\text{lost}} = m_1 v_{1b}^2 + m_2 v_{2b}^2 + I_2 \omega_{2b}^2 - m_1 (v_{1b}^2 - 2v_{1b} Am_2 I_2 + A^2 m_2^2 I_2^2)$$
$$-m_2 (v_{2b}^2 + 2v_{2b} Am_1 I_2 + A^2 m_1^2 I_2^2) - I_2 (\omega_{2b}^2 + 2\omega_{2b} Am_1 m_2 d + A^2 m_1^2 m_2^2 d^2)$$

cancel terms in the same color

$$2KE_{\text{lost}} = -m_1 (-2v_{1b} Am_2 I_2 + A^2 m_2^2 I_2^2)$$
$$-m_2 (+2v_{2b} Am_1 I_2 + A^2 m_1^2 I_2^2) - I_2 (2\omega_{2b} Am_1 m_2 d + A^2 m_1^2 m_2^2 d^2)$$

distribute the leading terms

$$2KE_{\text{lost}} = 2v_{1b} Am_1 m_2 I_2 - A^2 m_1 m_2^2 I_2^2$$
$$-2v_{2b} Am_1 m_2 I_2 - A^2 m_1^2 m_2 I_2^2 - 2\omega_{2b} Am_1 m_2 d I_2 - A^2 m_1^2 m_2^2 d^2 I_2{}^2$$

Rearrange

$$2KE_{\text{lost}} = 2v_{1b} Am_1 m_2 I_2 - 2v_{2b} Am_1 m_2 I_2 - A^2 m_1^2 m_2 I_2^2 - A^2 m_1 m_2^2 I_2^2 - 2\omega_{2b} Am_1 m_2 d I_2$$
$$- A^2 m_1^2 m_2^2 d^2 I_2$$

factor

$$2KE_{\text{lost}} = Am_1 m_2 I_2 2(v_{1b} - v_{2b}) - A^2 m_1 m_2 I_2 (m_1 I_2 + m_2 I_2 + m_1 m_2 d^2) - 2\omega_{2b} Am_1 m_2 d I_2$$

factor out $Am_1 m_2 I_2$

$$2KE_{\text{lost}} = Am_1 m_2 I_2 \left[2(v_{1b} - v_{2b}) - A(m_1 I_2 + m_2 I_2 + m_1 m_2 d^2) - 2\omega_{2b} d\right]$$

Substitute for A

$$2KE_{\text{lost}} = Am_1 m_2 I_2 \left[2(v_{1b} - v_{2b}) - \left\{\frac{(v_{1b} - v_{2b} - d\omega_{2b})(1 + CoR_{2b})}{m_1 I_2 + m_2 I_2 + m_1 m_2 d^2}\right\}(m_1 I_2 + m_2 I_2 + m_1 m_2 d^2)\right.$$
$$\left. -2\omega_{2b} d\right]$$

$$2KE_{\text{lost}} = Am_1 m_2 I_2 [2(v_{1b} - v_{2b}) - (v_{1b} - v_{2b})(1 + CoR_{2b}) + d\omega_{2b}(1 + CoR_{2b}) - 2\omega_{2b} d]$$

factor $(v_{1b} - v_{2b})$ out of the first two terms and combine the last two terms

$$2KE_{\text{lost}} = Am_1 m_2 I_2 [(v_{1b} - v_{2b})(1 - CoR_{2b}) - d\omega_{2b}(1 - CoR_{2b})]$$

factor $(1 - CoR_{2b})$

$$2KE_{\text{lost}} = Am_1 m_2 I_2 (1 - CoR_{2b})(v_{1b} - v_{2b} - d\omega_{2b})$$

substitute for A

$$2KE_{\text{lost}} = \left\{ \frac{(v_{1b} - v_{2b} - d\omega_{2b})(1 + CoR_{2b})}{m_1 I_2 + m_2 I_2 + m_1 m_2 d^2} \right\} m_1 m_2 I_2 (1 - CoR_{2b})$$
$$(v_{1b} - v_{2b} - d\omega_{2b})$$

$$2KE_{\text{lost}} = \frac{m_1 m_2 I_2}{m_1 I_2 + m_2 I_2 + m_1 m_2 d^2} (v_{1b} - v_{2b} - d\omega_{2b})$$
$$(1 + CoR_{2b})(1 - CoR_{2b})(v_{1b} - v_{2b} - d\omega_{2b})$$

Finally, we get

$$\boxed{KE_{\text{lost}} = \frac{1}{2} \frac{m_1 m_2 I_2}{m_1 I_2 + m_2 I_2 + m_1 m_2 d^2} (v_{1b} - v_{2b} - d\omega_{2b})^2 \left(1 - CoR_{2b}^2\right)}$$

or

$$KE_{\text{lost}} = \frac{1}{2} \frac{m_{\text{ball}} m_{\text{bat}} I_{\text{bat}} \left(v_{\text{ball-before}} - v_{\text{bat-cm-before}} - \omega_{\text{bat-before}} d\right)^2 \left(1 - CoR_{2b}^2\right)}{m_{\text{ball}} I_{\text{bat}} + m_{\text{bat}} I_{\text{bat}} + m_{\text{ball}} m_{\text{bat}} d^2} \tag{4.11}$$

This is a general result for the BaConLaws model. It is original and unique.

Now for a collision at the center of mass of the bat, like configurations 1a and 1b, d = 0. Therefore,

$$KE_{\text{lost}} = \frac{1}{2} \frac{m_1 m_2}{m_1 + m_2} (v_{1b} - v_{2b})^2 (1 - CoR_{1b}^2)$$

When we substitute $\bar{m} = \frac{m_1 m_2}{m_1 + m_2}$, we get

$$KE_{\text{lost}} = \frac{\bar{m}}{2} (v_{1b} - v_{2b})^2 (1 - CoR_{1b}^2)$$

This is the same as Eq. (3.2) that we gave in Sect. 3.2.2 for configuration 1b where we mentioned that this is an old, well-known equation that is hard to derive.

$$KE_{\text{lost}} = \frac{\bar{m}}{2} (v_{\text{ball-before}} - v_{\text{bat-cm-before}})^2 (1 - CoR_{1b}^2)$$

Likewise, if the spin of the bat about its center of mass is zero before the collision $\omega_{2b} = 0$, then our KE_{lost} equation Eq. (4.11) also reduces to that given for configuration 1b, Eq. (3.2).

In this section, we derived a general equation and showed that if the collision were at the center of mass ($d = 0$) *or* the bat had no spin $\omega_{2b} = 0$, then the general equation reduced to the simple equation of configuration 1b. We conclude that adding an equation for Conservation of Energy to the model proved the consistency of our set of equations.

4.9 Adding Conservation of Angular Momentum

In this section, which is almost the same as Sect. 3.5, we will prove that for a head-on collision, without friction, for a pitch of any spin there will be no change in the spin of the ball. To do this, we will use the law of Conservation of Angular Momentum about the center of mass of the bat. When the ball contacts the bat, as shown in Fig. 4.2, the ball has linear momentum of $m_{\text{ball}} v_{\text{ball-before}}$. However, the ball does not know if it is translating or if it is tied on a string and rotating about the center of mass of the bat. Following conventional practice in physics, we will model the ball as rotating about the bat's center of mass at a distance $d = d_{\text{cm-ip}}$. Therefore, the ball has an initial angular momentum of $m_{\text{ball}} d_{\text{cm-ip}} v_{\text{ball-before}}$ about an axis through the bat's center of mass. In addition, it is possible to throw a curveball so that it spins about the vertical, z-axis, as also shown in Fig. 4.2. We call this a purely horizontal curveball (although it will still drop more due to gravity, than it will curve horizontally). The curveball will have angular momentum of $I_{\text{ball}} \omega_{\text{ball-before}}$ about an axis parallel to the z-axis. However, this is its momentum about *its* center of mass and we want the momentum about the axis through the center of mass of the *bat*. Therefore, we use the parallel axis theorem producing $(I_{\text{ball}} + m_{ball} d^2) \omega_{\text{ball-before}}$.

The bat has an initial angular momentum of $I_{\text{bat}} \omega_{\text{bat-before}}$. It also has an angular momentum about the bat's center of mass due to the bat translation momentum $m_{\text{bat}} v_{\text{bat-before}}$; however, in this case $d = 0$ because the center of mass of the bat is passing through its center of mass. L is the symbol used for angular momentum. I guess all the cool letters (like F, m, a, v, I, ω, d, etc.) were already taken, so old-time physicists were stuck with the blah symbol L. Therefore, the initial angular momentum about the center of mass of the bat is

$$L_{\text{initial}} = m_1 v_{1\text{b}} d + \left(I_1 + m_1 d^2\right) \omega_{1b} + I_2 \omega_{2\text{b}}$$

All of these momenta are positive, pointing out of the page (Fig. 4.2). (Remember that $v_{1\text{b}}$ is a negative number.)

For the final angular momentum, we will treat the ball, as before, as an object rotating around the axis of the center of mass of the bat with angular momentum, $m_{\text{ball}} v_{\text{ball-after}} d_{\text{cm-ip}}$. Now we could treat the bat as a long slender rod with a moment of inertia of $m_{\text{bat}} d_{\text{bat}}^2 / 12$, where d_{bat} is the bat length. However, this is only an approximation and we have actual experimental data for the bat moment of inertia. Therefore, the bat angular momentum is $I_{\text{bat}} \omega_{\text{bat-after}}$. Thus, our final angular momentum about the center of mass of the bat is

$$L_{\text{final}} = m_1 v_{1\text{a}} d + \left(I_1 + m_1 d^2\right) \omega_{1\text{a}} + I_2 \omega_{2\text{a}}$$

The law of Conservation of Angular Momentum states that when no external torque acts on an object the initial angular momentum about some axis equals the final angular momentum about that axis.

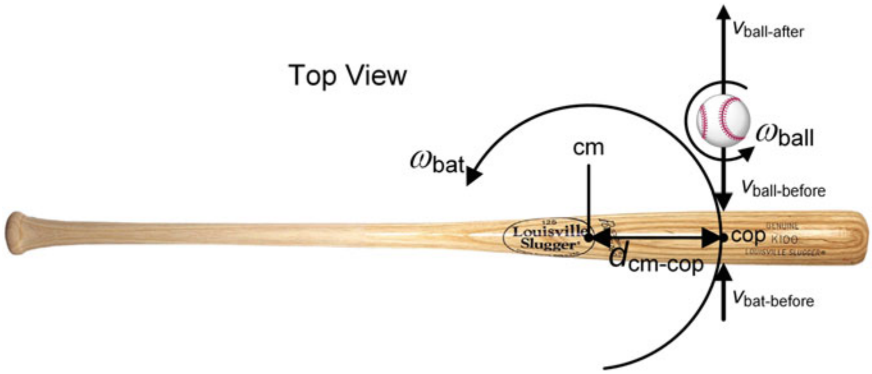

Fig. 4.2 This figure shows $v_{\text{ball-before}}$, $v_{\text{ball-after}}$, ω_{ball}, $d_{\text{cm-ip}}$ and ω_{bat}, which are used in the Conservation of Angular Momentum equation for the BaConLaws model

$$\boxed{\begin{array}{l} L_{\text{initial}} = L_{\text{final}} \\ m_1 v_{1b} d + (I_1 + m_1 d^2)\omega_{1b} + I_2\omega_{2b} = m_1 v_{1a} d + (I_1 + m_1 d^2)\omega_{1a} + I_2\omega_{2a} \end{array}}$$

Previously, we used Eq. (4.6), Newton's second axiom and solved for the angular velocity of the bat after the collision, ω_{2a}.

$$dm_1(v_{1a} - v_{1b}) = -I_2(\omega_{2a} - \omega_{2b}) \tag{4.6}$$

$$\omega_{2a} = \left\{\omega_{2b} - \frac{dm_1}{I_2}(v_{1a} - v_{1b})\right\}$$

So let us substitute this into our Conservation of Angular Momentum equation above.

$$m_1 v_{1b} d + I_1\omega_{1b} + m_1\omega_{1b} d^2 + I_2\omega_{2b} = m_1 v_{1a} d + I_1\omega_{1a} + m_1\omega_{1a} d^2 + I_2\left\{\omega_{2b} + \frac{dm_1}{I_2}(v_{1b} - v_{1a})\right\}$$

We want to solve this for the angular velocity of the ball after the collision, ω_{1a}

$$-I_1\omega_{1a} - m_1\omega_{1a}d^2 = -m_1 v_{1b} d - I_1\omega_{1b} - I_2\omega_{2b} - m_1\omega_{1b}d^2 + m_1 v_{1a} d + I_2\omega_{2b} + dm_1(v_{1b} - v_{1a})$$

Cancel the terms in color and rearrange

$$\omega_{1a}(I_1 + m_1 d^2) = \omega_{1b}(I_1 + m_1 d^2)$$

$$\boxed{\begin{array}{l} \omega_{1a} = \omega_{1b} \\ \omega_{\text{ball-after}} = \omega_{\text{ball-before}} \end{array}} \tag{4.12}$$

For the BaConLaws model, we have now proven that for a pitch with any spin about the z-axis, the spin before and after is the same. What about a pitch that has spin about the z-axis and also about the *y*-axis, like most pitches? The collision will not change ball rotation. As shown above, it will not change the spin about the *z*-axis. We could write another set of equations for angular momentum about the *y*-axis. However, the bat has no angular momentum about the y-axis, so there is nothing to affect the ball spin about the *y*-axis. {We are neglecting bat swings described as chops or uppercuts and friction. The effects of friction will be examined in Sect. 5.5, Collision with Friction.} In conclusion, a head-on collision between a bat and a ball will not change the spin on the ball (Table 4.2). Some papers have shown a relationship between ball spin before and ball spin after, but they were using oblique collisions as in configuration 3 (Nathan et al. 2012; Kensrud et al. 2016).

4.10 Simulation Results

The Excel simulation satisfies the following checks: (1) Conservation of Energy, (2) Kinetic energy lost, (3) Conservation of Linear Momentum, (4) Coefficient of Restitution, (5) Newton's second axiom, namely, an impulse changes momentum and (6) Conservation of Angular Momentum. Table 4.3 shows the kinetic energies for the same simulation.

We note that the total kinetic before (372 J) equals the kinetic energy after (176 J) plus the kinetic energy lost (196 J). However, if we set $d_{\text{cm-ip}} = 0$ in the simulation so that the impact point is at the center of mass of the bat, then Tables 4.2 and 4.3 change and produce the results of Tables 3.3 and 3.4 for configuration 1b, where the total kinetic before (346 J) equaled the kinetic energy after (169 J) plus the kinetic energy lost (177 J). This means that the whole BaConLaws model (equations, simulations, sensitivity analyses, etc.) can be reduced to be appropriate for configurations 2a, 1a and 1b by zeroing appropriate values. This is an important validation point.

4.11 Sensitivity Analysis

This section contains equations and it can be skipped without loss of continuity.

This book is about the science of baseball. So why does it have this section on sensitivity analysis? In order to understand the science of baseball, we make models. In order to validate these models we do sensitivity analyses.

The second purpose of this book is to show how the batter can buy or make an optimal baseball or softball bat. From the viewpoint of the batter, an optimum bat would produce the maximum-batted-ball velocity. The larger the batted-ball velocity, the more likely the batter will get on base safely (Baldwin and Bahill 2004). Therefore, we made the batted-ball velocity our performance criterion.

In a simple sensitivity analysis an input is changed by a small amount and the resulting change in the output is recorded. For example, in Table 4.2a when

Table 4.2 Simulation values for bat–ball collisions at the sweet spot, the BaConLaws model

	SI units	Baseball units
Inputs		
$v_{\text{ball-before}}$	−37 m/s	−83 mph
$\omega_{\text{ball-before}}$	209 rad/s	2000 rpm
$v_{\text{bat-cm-before}}$	23 m/s	52 mph
$\omega_{\text{bat-before}}$	32 rad/s	309 rpm
$vt_{\text{bat-cop-before}}$	28 m/s	62 mph
Collision Speed	65 m/s	145 mph
CoR_{2b}	0.465	0.465
Outputs		
$v_{\text{ball-after}}$	41 m/s	92 mph
$\omega_{\text{ball-after}}$	$=\omega_{\text{ball-before}}$	
$v_{\text{bat-cm-after}}$	11 m/s	24 mph
$\omega_{\text{bat-after}}$	1 rad/s	7 rpm
KE_{lost}	196 J	

Table 4.2a Incipient sensitivity analysis

Inputs	Nominal values, SI units	Nominal values, Baseball units	$v_{\text{ball-after}}$ when the input was increased by 1%. Nominal value was 91.894 mph	Percent change in $v_{\text{ball-after}}$
$v_{\text{ball-before}}$	−37 m/s	−83 mph	92.066	0.19
$\omega_{\text{ball-before}}$	209 rad/s	2000 rpm	91.894	0
$v_{\text{bat-cm-before}}$	23 m/s	52 mph	92.463	0.62
$\omega_{\text{bat-before}}$	32 rad/s	309 rpm	92.000	0.12
CoR_{2b}	0.465	0.465	92.450	0.60

Table 4.3 The BaConLaws model kinetic energies, J

KE ball linear velocity before=	100
KE bat linear velocity before=	246
KE ball angular velocity before=	1.7
KE bat angular velocity before=	25
KE before total=	372
KE ball linear velocity after=	122
KE bat linear velocity after=	53
KE ball angular velocity after=	1.7
KE bat angular velocity after=	0.01
KE after=	176
KE lost=	196
KE after + KE lost=	372

$v_{\text{bat-cm-before}}$ was increased by 1%, $v_{\text{bat-after}}$ increased by 0.62%. This was the most sensitive input in Table 4.2a.

We will now rigorously find the sensitivity of the batted-ball velocity, $v_{\text{ball-after}}$, with respect to the eight model variables and parameters, namely, $v_{\text{ball-before}}$, m_{ball}, I_{bat}, m_{bat}, $CoR_{2\text{b}}$, $d_{\text{cm-ip}}$, $v_{\text{bat-cm-before}}$ and $\omega_{\text{bat-before}}$. We will start with the equation for the ball velocity after the collision, $v_{1\text{a}}$, Eq. (4.8).

$$v_{1\text{a}} = v_{1\text{b}} - \frac{(v_{1\text{b}} - v_{2\text{b}} - \omega_{2\text{b}} d)(1 + CoR_{2\text{b}}) m_2 I_2}{m_1 I_2 + m_2 I_2 + m_1 m_2 d^2}$$

The derivatives in Sect. 4.11 require that the CoR be a constant, as in Table 4.2.

In order to perform an analytic sensitivity analysis, we need the partial derivatives of $v_{1\text{a}}$ with respect to the eight variables and parameters. These partial derivatives are often called the absolute sensitivity functions.

Let

$B = (v_{1\text{b}} - v_{2\text{b}} - \omega_{2\text{b}} d)(1 + CoR_{2\text{b}})$

$K = \left(m_1 I_2 + m_2 I_2 + m_1 m_2 d^2\right)$

Therefore,

$$v_{1\text{a}} = v_{1\text{b}} - \frac{B m_2 I_2}{K}$$

The following partial derivatives with respect to the variables are easy to derive.

$$\frac{\partial v_{1\text{a}}}{\partial v_{1\text{b}}} = 1 - \frac{(1 + CoR_{2\text{b}}) m_2 I_2}{K} \quad \text{unitless}$$

$$\frac{\partial v_{1\text{a}}}{\partial v_{2\text{b}}} = \frac{(1 + CoR_{2\text{b}}) m_2 I_2}{K} \quad \text{unitless}$$

$$\frac{\partial v_{1\text{a}}}{\partial \omega_{2\text{b}}} = \frac{(1 + CoR_{2\text{b}}) d m_2 I_2}{K} \quad \text{m}$$

$$\frac{\partial v_{1\text{a}}}{\partial CoR_{2\text{b}}} = -\frac{(v_{1\text{b}} - v_{2\text{b}} - \omega_{2\text{b}} d) m_2 I_2}{K} \quad \text{m/s}$$

In the above partial derivatives, units on the left and right sides of the equations are the same. This is a simple, but important accuracy check. We perform such a dimensional analysis on all of our equations.

For the following partial derivatives with respect to the parameters, we will need the derivative of a quotient, defined as

$$\frac{d}{dx}\left(\frac{f(x)}{g(x)}\right) = \frac{g(x)\frac{d}{dx}f(x) - f(x)\frac{d}{dx}g(x)}{[g(x)]^2}$$

Using this differential equation we getthe following partial derivatives.

$$\frac{\partial v_{1\text{a}}}{\partial d} = \frac{K \omega_{2\text{b}} (1 + CoR_{2\text{b}}) m_2 I_2 + 2 B I_2 m_1 m_2^2 d}{K^2} \quad 1/\text{s}$$

$$\frac{\partial v_{1a}}{\partial m_1} = \frac{Bm_2 I_2 (I_2 + m_2 d^2)}{K^2} \quad \text{m/kg s}$$
$$\frac{\partial v_{1a}}{\partial m_2} = \frac{-Bm_1 I_2^2}{K^2} \quad \text{m/kg s}$$
$$\frac{\partial v_{1a}}{\partial I_2} = \frac{Bm_1 m_2^2 d^2}{K^2} \quad 1/\text{kg m s}$$

4.11.1 Semirelative Sensitivity Functions

Now that we have the partial derivatives, we want to form the *semirelative sensitivity functions*, which are defined as

$$\tilde{S}_\alpha^F = \left.\frac{\partial F}{\partial \alpha}\right|_{\text{NOP}} \alpha_0$$

where NOP and the subscript 0 mean that all variables and parameters assume their nominal operating point values (Smith et al. 2008).

$$\tilde{S}_\alpha^F = \left.\frac{\partial F}{\partial \alpha}\right|_{\text{NOP}} \alpha_0$$
$$\tilde{S}_{v_{1b}}^{v_{1a}} = 1 - \left.\frac{(1 + CoR_{2b}) m_2 I_2}{K}\right|_{\text{NOP}} v_{1b_0}$$
$$\tilde{S}_{v_{2b}}^{v_{1a}} = \left.\frac{(1 + CoR_{2b}) m_2 I_2}{K}\right|_{\text{NOP}} v_{2b_0}$$
$$\tilde{S}_{\omega_{2b}}^{v_{1a}} = \left.\frac{(1 + CoR_{2b}) m_2 d I_2}{K}\right|_{\text{NOP}} \omega_{2b_0}$$
$$\tilde{S}_{CoR}^{v_{1a}} = \left.\frac{-(v_{1b} - v_{2b} - \omega_{2b} d) m_2 I_2}{K}\right|_{\text{NOP}} CoR_0$$
$$\tilde{S}_{d}^{v_{1a}} = \left.\frac{K\omega_{2b}(1 + CoR_{2b}) m_2 I_2 + 2Bm_2 I_2 m_1 m_2 d}{K^2}\right|_{\text{NOP}} d_0$$
$$\tilde{S}_{m_1}^{v_{1a}} = \left.\frac{Bm_2 I_2 (I_2 + m_2 d^2)}{K^2}\right|_{\text{NOP}} m_{1_0}$$
$$\tilde{S}_{m_2}^{v_{1a}} = \left.\frac{-Bm_1 I_2^2}{K^2}\right|_{\text{NOP}} m_{2_0}$$
$$\tilde{S}_{I_2}^{v_{1a}} = \left.\frac{Bm_1 m_2^2 d^2}{K^2}\right|_{\text{NOP}} I_{2_0}$$

Table 4.4 gives the nominal values, along with the range of physically realistic values for collegiate and professional baseball batters, and the semirelative sensitivity values computed analytically. The bigger the sensitivity is, the more important the variable or parameter is for maximizing batted-ball velocity.

Table 4.4 Typical values and first-order analytic sensitivities with respect to the batted-ball velocity for the BaConLaws model

Variables and parameters	Nominal values		Range of realistic values		$\tilde{S}_{\alpha}^{F} = \frac{\partial F}{\partial \alpha}\big\rvert_{NOP} \alpha_0$ semirelative sensitivity values
	SI units	Baseball units	SI units	Baseball units	
Inputs					
$v_{\text{ball-before}}$	−37 m/s	−83 mph	−27 to −40 m/s	−60 to −90 mph	8
$\omega_{\text{ball-before}}$	209 rad/s	2000 rpm	209 ± 21 rad/s	2000 ± 200 rpm	0
$v_{\text{bat-cm-before}}$	23 m/s	52 mph	23 ± 5 m/s	52 ± 10 mph	28
$\omega_{\text{bat-before}}$	32 rad/s	309 rpm	32 ± 11 rad/s	300 ± 100 rpm	5
$vt_{\text{bat-cop-before}}$	28 m/s	62 mph			
Parameters					
CoR_{2b}	0.465	0.465	0.465 ± 0.05	0.465 ± 0.05	25
$d_{\text{cm-cop}}$	0.134 m	5.3 in	0.134 ± 0.05 m	5.3 ± 2 in	−2
m_{ball}	0.145 kg	5.125 oz	0.145 ± 0.004 kg	5.125 ± 0.125 oz	−14
m_{bat}	0.905 kg	32 oz	0.709–0.964 kg	25–34 oz	10
$I_{\text{bat-cm}}$	0.048 kg m^2	2624 oz in^2	0.036–0.06 kg m^2	1968–3280 oz in^2	3

The right column of Table 4.4 shows that the most important property (the largest value), in terms of maximizing batted-ball velocity, is the linear velocity of the center of mass of the bat before the collision, $v_{\text{bat-cm-before}}$. This is certainly no surprise. The second most important property is the coefficient of restitution, CoR_{2b}. The least important properties are the angular velocity of the ball, $\omega_{\text{ball-before}}$, the distance between the center of mass and the impact point, $d_{\text{cm-ip}}$, and the moment of inertia of the bat, I_{bat}. The sensitivities to the distance between the center of mass and the impact point, $d_{\text{cm-ip}}$, and the mass of the ball, m_{ball}, are negative, which merely means that as they increase the batted-ball speed decreases. Cross (2011) wrote that in his model the most sensitive properties were also the bat speed followed by the *CoR*. His sensitivity to the mass of the ball was also negative.

For this operating point {meaning the nominal values given in Table 4.4 where $d_{\text{cm-ip}} = 0.134$ m}, the sensitivity of the batted-ball speed with respect to the impact point, the distance $d_{\text{cm-ip}}$, was negative. This means that as the impact point gets farther away from the center of mass the batted-ball speed falls off. This is true for all values where $d_{\text{cm-ip}} > 0.1$ m. For smaller values, the sensitivity coefficient is positive. This means that there is a point of impact that produces the maximum-batted-ball speed. This is not surprising and is a well-known fact Nathan (2003).

4.11.2 Interactions

We will now discuss interactions, or second-order partial derivatives. Once my Mother cleaned the toilet with Clorox bleach. She was pleased with the result. The next week she cleaned the toilet with ammonia. She was even happier. So then, she decided that if bleach by itself worked so well and ammonia by itself worked so well, then surely both of them together would be wonderful. She created chloramine gas and we had to get out of the house and spend the rest of the day in the desert, because this gas kills people (https://www.thoughtco.com/bleach-and-ammonia-chemical-reaction-609280). Next, don't drink ethyl alcohol and take barbiturates or acetaminophen (Tylenol) at the same time, unless you are trying to commit suicide. Finally, because grapefruit juice contains furanocoumarins it increases the absorption rate of cholesterol-lowering statins such as Zocor, which could lead to serious side effects. Interactions can amplify or attenuate the effects of drugs and chemicals. Now let us look at some interactions in the BaConLaws model.

Because $\frac{\partial v_{1a}}{\partial m_2}$ contains both I_2 and v_{2b},
and $\frac{\partial v_{1a}}{\partial I_2}$ contains both m_2 and v_{2b},
and $\frac{\partial v_{1a}}{\partial v_{2b}}$ contains both m_2 and I_2,

we see that there are interactions. How important are they? To find out, let us calculate the second-order, interaction functions for the three terms above. The first two are easy.

$$\frac{\partial^2 v_{1a}}{\partial v_{2b}\partial m_2} = \frac{(1 + CoR_{2b})I_2[K - m_2(I_2 + m_1 d^2)]}{K^2} \quad 1/\mathrm{kg}$$
$$\frac{\partial^2 v_{1a}}{\partial v_{2b}\partial I_2} = \frac{(1 + CoR_{2b})m_2[K - I_2(m_1 + m_2)]}{K^2} \quad 1/\mathrm{kg\,m^2}$$

Here, we choose the interactions of the bat mass, the moment of inertia and the bat speed, because they were expected to be large based on principles of physiology. Additionally, the forthcoming discussion on optimizing the bat suggests an interaction between the bat mass and its moment of inertia. The above two second-order partial derivatives were easy to calculate. However, it will take a bit more work to get the third part of this triad. We will now derive the interaction between bat mass and its moment of inertia, m_{bat} and I_{bat}. From before, we had

$$\frac{\partial v_{1a}}{\partial m_2} = \frac{BI_2[-K + m_2(I_2 + m_1 d^2)]}{K^2}$$

To find $\frac{\partial^2 v_{1a}}{\partial I_2 \partial m_2}$ we must first simplify $\frac{\partial v_{1a}}{\partial m_2}$. We will be dealing with I_2 so let us isolate it. But first replace K in the numerator and we get

$$K^2 \frac{\partial v_{1a}}{\partial m_2} = -\left(m_1 I_2 + m_2 I_2 + m_1 m_2 d^2\right) B I_2 + B m_2 I_2 \left(I_2 + m_1 d^2\right)$$

$$= -B\left[\left(m_1 I_2 + m_2 I_2 + m_1 m_2 d^2\right) I_2 - m_2 I_2 \left(I_2 + m_1 d^2\right)\right]$$

$$= -B\left[m_1 I_2^2 + m_2 I_2^2 + m_1 m_2 d^2 I_2 - m_2 I_2^2 - m_1 m_2 d^2 I_2\right]$$

Cancel the terms in color

$$K^2 \frac{\partial v_{1a}}{\partial m_2} = -B m_1 I_2^2$$

$$\frac{\partial v_{1a}}{\partial m_2} = \frac{-B m_1 I_2^2}{K^2}$$

Expand B and this simplification results.

$$\frac{\partial v_{1a}}{\partial m_2} = \frac{-\left(v_{1b} - v_{2b} - \omega_{2b} d\right)\left(1 + CoR_{2b}\right) m_1 I_2^2}{K^2}$$

Now, we will take the partial derivative of this function with respect to I_2.

$$\frac{\partial^2 v_{1a}}{\partial I_2 \partial m_2} = \frac{-K^2 2 B m_1 I_2 + B m_1 I_2^2 2K\left(m_1 + m_2\right)}{K^4}$$

$$= \frac{2 B m_1 I_2 K\left[-K + I_2\left(m_1 + m_2\right)\right]}{K^4}$$

substitute for the second K in the numerator

$$= \frac{2 B m_1 I_2 K\left[-\left\{m_1 I_2 + m_2 I_2 + m_1 m_2 d^2\right\} + I_2\left(m_1 + m_2\right)\right]}{K^4}$$

$$= \frac{2 B m_1 I_2 K\left[-m_1 I_2 - m_2 I_2 - m_1 m_2 d^2 + m_1 I_2 + m_2 I_2\right]}{K^4}$$

cancel the terms in color

$$= \frac{-2 B m_1^2 m_2 d^2 I_2 K}{K^4}$$

finally substitute B and K

$$\frac{\partial^2 v_{1a}}{\partial I_2 \partial m_2} = \frac{-2\left(v_{1b} - v_{2b} - \omega_{2b} d\right)\left(1 + CoR_{2b}\right) m_1^2 m_2 d^2 I_2}{\left\{m_1 I_2 + m_2 I_2 + m_1 m_2 d^2\right\}^3} \quad 1/(\mathrm{kg}^2\ \mathrm{ms})$$

This demonstrates that if we have equations for the functions, then we can do an analytic sensitivity analysis. However, for some functions it may take some effort. Fortunately, it takes no effort to calculate the following interaction terms using the partial derivatives in the previous section.

$$\frac{\partial v_{1a}}{\partial v_{1b}} = 1 - \frac{(1 + CoR_{2b}) m_2 I_2}{K}$$

$$\frac{\partial^2 v_{1a}}{\partial v_{1b} \partial CoR} = \frac{m_2 I_2}{K} \quad \text{unitless}$$

and

$$\frac{\partial v_{1a}}{\partial v_{2b}} = \frac{(1 + CoR_{2b})m_2 I_2}{K}$$
$$\frac{\partial^2 v_{1a}}{\partial v_{2b} \partial CoR} = \frac{m_2 I_2}{K} \quad \text{unitless}$$

These two partial derivatives are the same, but their semirelative sensitivity functions will be different. Let us derive one more second-order partial derivative.

$$\frac{\partial v_{1a}}{\partial m_2} = \frac{-(v_{1b} - v_{2b} - \omega_{2b} d)(1 + CoR_{2b}) m_1 I_2^2}{K^2}$$
$$\frac{\partial^2 v_{1a}}{\partial CoR\, \partial m_2} = \frac{-(v_{1b} - v_{2b} - \omega_{2b} d) m_1 I_2^2}{K^2}$$

This function does not look interesting.

Now for the above five second-order partial derivatives, we can form the following semirelative sensitivity functions for interactions:

$$\tilde{S}^{v_{1a}}_{v_{2b}-m_2} = \left. \frac{(1 + CoR_{2b}) I_2 [K - m_2(I_2 + m_1 d^2)]}{K^2} \right|_{\text{NOP}} v_{2b_0} m_{2_0}$$
$$\tilde{S}^{v_{1a}}_{v_{2b}-I_2} = \left. \frac{(1 + CoR_{2b}) m_2 [K - I_2(m_1 + m_2)]}{K^2} \right|_{\text{NOP}} v_{2b_0} I_{2_0}$$
$$\tilde{S}^{v_{1a}}_{I_2-m_2} = \left. \frac{-2(v_{1b} - v_{2b} - \omega_{2b} d)(1 + CoR_{2b}) m_1^2 m_2 d^2 I_2}{K^3} \right|_{\text{NOP}} I_{2_0} m_{2_0}$$

$$\tilde{S}^{v_{1a}}_{v_{1b}-CoR} = \left. \frac{m_2 I_2}{K} \right|_{\text{NOP}} v_{1b_0} CoR_0$$

and

$$\tilde{S}^{v_{1a}}_{v_{2b}-CoR} = \left. \frac{m_2 I_2}{K} \right|_{\text{NOP}} v_{2b_0} CoR_0$$

Table 4.5 shows values for a few of the 28 possible second-order interaction functions. They are small, which means that the model is well behaved. However, let's ask again, "What exactly what are interaction terms?" It means that the numerical value of the sensitivity of a function f to parameter α depends on the numerical value of parameter β. Often the interaction can be seen in the sensitivity function equations. In the BaConLaws model, the sensitivity of the batted-ball velocity to the mass of the bat depends on the numeric value of the moment of inertia of the bat, because it appears in the numerator of this sensitivity function.

Table 4.5 Interaction sensitivities with respect to the batted-ball velocity for the BaConLaws model computed numerically for +1% variable and parameter changes

Interacting variables and parameters	$v_{\text{ball-after}}$ with the first parameter α increased by 1%, m/s	$v_{\text{ball-after}}$ with the second parameter β increased by 1%, m/s	$\Delta v^{\alpha}_{\text{ball-after}} + \Delta v^{\beta}_{\text{ball-after}}$ Sum of columns 2 & 3	$v_{\text{ball-after}}$ with both parameters increased by 1%, m/s	$\tilde{S}^{F}_{\alpha} = \left.\frac{\partial F}{\partial \alpha}\right\|_{\text{NOP}} \alpha_0$ semirelative sensitivity values
Nominal batted-ball velocity $v_{\text{ball-after}} = 41.079$ m/s = 91.89 mph					
$v_{\text{ball-before}}$ interacting with CoR_{2b}	41.156	41.327		41.405	14
$v_{\text{ball-after-nominal}} - v_{\text{ball-after-perturbed}}$ m/s	0.077	0.248	0.325	0.326	
$v_{\text{bat-before}}$ interacting with CoR_{2b}	41.361	41.327		41.610	9
$v_{\text{ball-after-nominal}} - v_{\text{ball-after-perturbed}}$ m/s	0.282	0.248	0.530	0.531	
$v_{\text{ball-before}}$ interacting with m_{ball}	41.156	40.942		41.017	-8
$v_{\text{ball-after-nominal}} - v_{\text{ball-after-perturbed}}$ m/s	0.077	-0.137	-0.060	-0.062	
m_{bat} interacting with m_{ball}	41.182	40.942		41.044	7
$v_{\text{ball-after-nominal}} - v_{\text{ball-after-perturbed}}$ m/s	0.103	-0.137	-0.034	-0.035	
m_{bat} interacting with I_{bat}	41.182	41.114		41.216	1
$v_{\text{ball-after-nominal}} - v_{\text{ball-after-perturbed}}$ m/s	0.103	0.035	0.138	0.137	
$v_{\text{ball-before}}$ interacting with $v_{\text{bat-before}}$	41.156	41.361		41.438	0
$v_{\text{ball-after-nominal}} - v_{\text{ball-after-perturbed}}$ m/s	0.077	0.282	0.359	0.359	
$d_{\text{cm-ss}}$ interacting with I_{bat}	41.061	41.114		41.097	7
$v_{\text{ball-after-nominal}} - v_{\text{ball-after-perturbed}}$ m/s	-0.018	0.035	0.017	0.018	
CoR interacting with m_{ball}	41.327	40.942		41.189	-4
$v_{\text{ball-after-nominal}} - v_{\text{ball-after-perturbed}}$ m/s	-0.248	0.137	-0.111	-0.110	

$$\tilde{S}^{v_{1a}}_{m_2} = \left.\frac{-(v_{1b} - v_{2b} - \omega_{2b} d)(1 + CoR_{2b}) m_1 I_2^2}{K^2}\right|_{\text{NOP}} m_{2_0}$$

However, from Table 4.5, the numeric value of m_{bat} interacting with I_{bat} is only 1, which is smaller than the magnitude of the sensitivity of the batted-ball velocity to the mass of the bat by itself, which is 10 (from Table 4.4), or to the magnitude of the sensitivity of the batted-ball velocity to the moment of inertia of the bat by itself, which is 3. Thus, this interaction is unexpectedly *not* important. This model has many interactions, but fortunately, most of them are small. Interactions are hard to detect. And if they are big, they can ruin a system or a model. The most and least important interaction functions of this model are shown in Table 4.5.

Can we use this information to increase bat performance? For wooden bats, it is legal to drill a 1- to 2-inch hole into the barrel end of the bat up to 1¼ inches deep. It is also legal to taper the last 3 inches of the barrel say from 2.61 inches (6.6 cm) down to 1¾ of an inch (4.4 cm). Both of these modifications would decrease the bat weight, decrease the moment of inertia about the center of mass and would move the sweet spot closer to the knob. According to Table 4.4, the first two changes would decrease batted-ball speed, whereas the third would increase batted-ball speed. So, what is the right answer? We will not know until after we consider physiology in Sect. 4.12.4.

To complete this section on sensitivity analysis, we will now look at interactions using semirelative sensitivity functions that we will compute with *numerical* techniques instead of using the analytic equations derived above.

4.11.2.1 Empirical (or Numerical) Sensitivity Analysis

If you do not have equations for the model's functions {or for heuristic reasons as in this section}, then you can do a sensitivity analysis using numerical techniques. To estimate values for the second partial derivatives, we start with

$$\frac{\partial^2 f(\alpha_0, \beta_0)}{\partial\alpha\partial\beta} \approx \frac{f(\alpha, \beta) - f(\alpha_0, \beta) - f(\alpha, \beta_0) + f(\alpha_0, \beta_0)}{\Delta\alpha\Delta\beta}$$

from Bahill and Madni (2017). Then, for a one percent increase in the parameter α

$\Delta\alpha = 0.01\alpha_0$. Likewise, $\Delta\beta = 0.01\beta_0$. Therefore

$$\frac{\partial^2 f(\alpha_0, \beta_0)}{\partial\alpha\partial\beta} \approx \frac{f(\alpha, \beta) - f(\alpha_0, \beta) - f(\alpha, \beta_0) + f(\alpha_0, \beta_0)}{0.01\alpha_0 \times 0.01\beta_0}$$

Now to get the semirelative sensitivity function, we multiply this mixed-second partial derivative by the nominal values α_0 and β_0

$$\tilde{S}^f_{\alpha-\beta} = \left.\frac{\partial^2 f}{\partial\alpha\,\partial\beta}\right|_{\text{NOP}} \alpha_0\beta_0$$

$$\tilde{S}^f_{\alpha-\beta} \approx \left.\frac{f(\alpha, \beta) - f(\alpha_0, \beta) - f(\alpha, \beta_0) + f(\alpha_0, \beta_0)}{0.01\alpha_0 \times 0.01\beta_0}\right|_{\text{NOP}} \alpha_0\beta_0$$

$$\tilde{S}^f_{\alpha-\beta} \approx \left[f(\alpha, \beta) - f(\alpha_0, \beta) - f(\alpha, \beta_0) + f(\alpha_0, \beta_0)\right]_{NOP} \times 10{,}000$$

We used this equation to get the values for Table 4.5. The column heading $\Delta v^{\alpha}_{\text{ball-after}} + \Delta v^{\beta}_{\text{ball-after}}$ means find the change in the velocity of the batted ball after the perturbation of the parameter α and add to it the change in the velocity of the ball after the perturbation of the parameter β.

To form Table 4.5, we defined the performance criterion, chose a pair of parameters, changed the first by a fixed percentage, calculated the new performance criterion value, calculated the change in the performance criterion value, reset the first parameter, changed the second parameter by the same percentage, calculated the new performance criterion value, calculated the change in the performance criterion value, added these two changes in the performance criterion values together, then changed both parameters at the same time, calculated the performance criterion value and calculated the change in the performance criterion value.

Let us now explain the top rows of Table 4.5, the interaction of $v_{\text{ball-before}}$ with $CoR_{2\text{b}}$. If you increase $v_{\text{ball-before}}$ (call it α) by one percent, then the batted-ball speed will increase from its nominal value of 41.079 m/s to its modified value of 41.156 m/s. This is an increase of 0.077 m/s. Now reset $v_{\text{ball-before}}$ and then increase $CoR_{2\text{b}}$ (call it β) by one percent. The batted-ball speed will increase from the nominal value to its modified value of 41.327 m/s. This is an increase of 0.248 m/s. Therefore, these two changes, when performed individually, produce a total change of 0.325, highlighted in blue in Table 4.5. Now comes the important part, if you increase both $v_{\text{ball-before}}$ and $CoR_{2\text{b}}$ by one percent at the same time, then the batted-ball speed increases from the nominal value to a modified value of 41.405 m/s. This is an increase of 0.326 m/s, highlighted in green in Table 4.5. Therefore, we can see that when these two changes are performed individually they produce a total increase of 0.325, however, when performed together they produce an increase of 0.326 m/s. The whole is greater than the sum of its parts.

However, interactions do not always accentuate changes. Here is one that goes in the opposite direction; the interaction of m_{bat} with I_{bat}. Suppose that someone tells you that Eq. 4.8 shows that increasing bat mass will increase batted-ball speed. And someone else tells you that increasing the bat moment of inertia will increase your batted-ball speed. Well if each is good by itself why not do both? For instance, if you increase m_{bat} by one percent, then the batted-ball speed will increase from its nominal value of 41.079 m/s to its modified value of 41.182 m/s. This is an increase of 0.103 m/s. Now reset m_{bat} and then increase I_{bat} by one percent. The batted-ball speed will increase from the nominal value to its modified value of 41.114 m/s. This is an increase of 0.035 m/s. Therefore, these two changes, when performed individually, produce a total increase of 0.138, highlighted in blue. Now comes the important part, if you increase both m_{bat} and I_{bat} by one percent at the same time, then the batted-ball speed increases from the nominal value to a modified value of 41.216 m/s. This is an increase of 0.137 m/s, highlighted in green. Therefore, we can see that when these two changes are performed individually they produce a total increase of 0.138; however, when performed together they produce an increase of 0.137 m/s. The whole is less than the sum of its parts. Here, the interaction attenuates the individual changes.

Figure 4.3 shows the interaction of bat weight and bat moment of inertia (*MoI*) graphically. If you increase the bat weight, the batted-ball speed goes up. However, these six curves do not have the same shape. The curve for $MoI = 0.4$ starts to

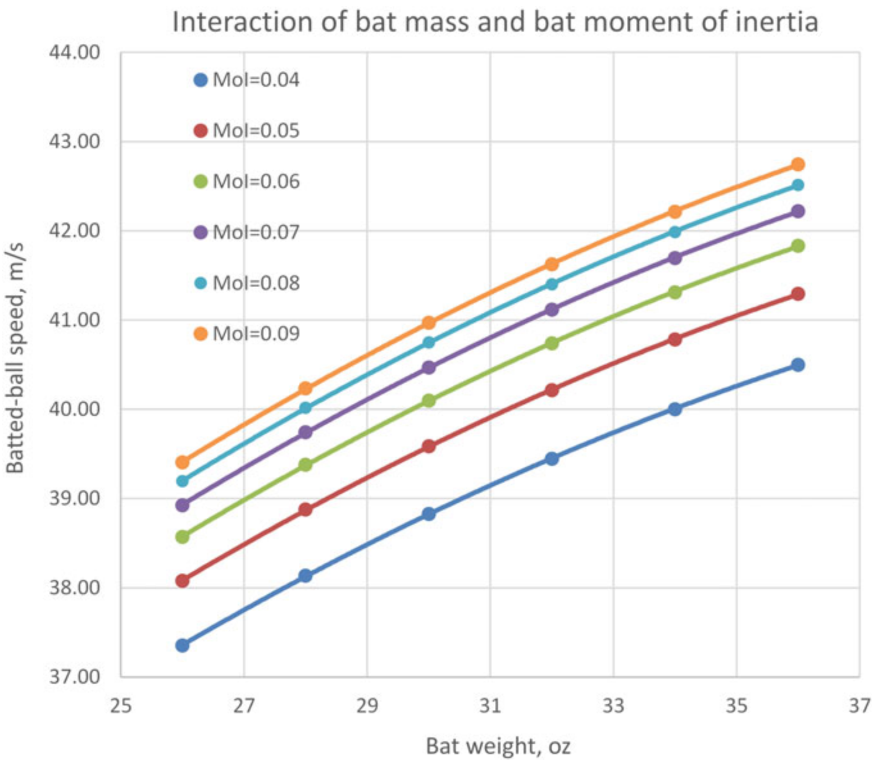

Fig. 4.3 Interaction of bat mass and bat moment of inertia

saturate at the right side. However, the curve for $MoI = 0.9$ does not flatten as much at the right side. This is the effect of the interaction. The difference in spacing of the lines is not the effect of the interaction. That is merely the dependence of the batted-ball speed on the moment of inertia (MoI).

4.11.2.2 Humidor

The Colorado Rockies store their baseballs in a humidor at 50% relative humidity and 70 °F. According to the appendix of Chap. 7, on a typical July afternoon in Denver the relative humidity is 34% and the average temperature is 88 °F. According to Alan Nathan (http://www.baseballprospectus.com/article.php?articleid=13057), compared to storing the balls in an outdoor environment, storing the balls in a humidor decreases the coefficient of restitution (because the balls get mushier, see Fig. 3.1) and increases the weight of the balls (because they absorb water): these two effects reduce the number of home runs in this stadium by 25%. However, this conclusion must be tempered, because there is an interaction between changes in CoR and m_{ball}. You cannot just say if $CoR\downarrow$, $v_{\text{ball-after}}\downarrow$ and if $m_{\text{ball}}\uparrow$, $v_{\text{ball-after}}\downarrow$ therefore if $CoR\downarrow$ and $m_{\text{ball}}\uparrow$, then $v_{\text{ball-after}}\downarrow$.

In our sensitivity analysis, we increased the value of each parameter by one percent. It told us that if you increase the *CoR* by one percent, then, according to the bottom rows of Table 4.5, the batted-ball speed will increase from its nominal value of 41.079 m/s to its modified value of 41.327 m/s. This is an increase of 0.248 m/s. Now if you increase m_{ball} by one percent, then the batted-ball speed will decrease from the nominal value to its modified value of 40.942 m/s. This is a decrease of 0.137 m/s. Therefore, these two changes, when performed individually, produce a total increase of 0.111, highlighted in blue in Table 4.5. Now comes the important part, if you increase both *CoR* and m_{ball} by one percent at the same time, then the batted-ball speed increases from the nominal value to a modified value of 41.189 m/s. This is an increase of 0.110 m/s, highlighted in green. Therefore, when these two changes are performed individually, they produce a total increase of 0.111; however, when performed together they produce an increase of only 0.110 m/s. The whole is less than the sum of its parts. Here, the interaction attenuates the changes.

Therefore, to do a proper analysis, you cannot change one parameter, change the other parameter and then add the results. In your simulation, you must change both parameters at the same time.

Okay, that is the end of the sensitivity analysis of the BaConLaws model. Now let's go back to Coors Field in Denver. From the appendix in Chap. 7, we see that the relative humidity on an average July afternoon in Denver is 34%. Alan Nathan wrote that the difference between the 50% relative humidity in the humidor and the outside air in Denver causes a decrease of 3.7% in the CoR and an increase of 1.6% in the weight of the ball.

When those changes (and the parameters of a perfect home run ball) are put into the BaConLaws model *and* the Ball in Flight model of Chap. 7, we find that decreasing the *CoR* by 3.7% percent decreases the range of the batted ball by 8.5 feet. Increasing the weight of the ball by 1.6% increases the range of the batted ball by 1.6 feet. Summing these two changes gives a range decrease of 6.9 feet. But if the changes are made in the models at the same time the result is a range decrease of 9.1 feet. The whole is greater than the sum of its parts.

The Arizona Diamondbacks are considering installing a similar humidor in their stadium in Phoenix. Therefore, we should do a similar analysis for them. In addition, we should also do an analysis of the temperature differences. We should analyze the effects of storing the balls at 70 °F versus storing them at the average daily high temperature in Phoenix in July of 104 °F. But of course, this depends on where the balls are stored if they are not in a humidor and whether the dome is open or closed.

Interactions can amplify or attenuate the effects of drugs, chemicals and parameters in a model. Interactions mean that the numerical value of the sensitivity of a function to a particular parameter depends on the numerical value of another parameter. In a well-behaved model, the interaction terms are small. If the interaction terms are large, they warn that in your analysis you cannot change one parameter, change another and then sum the results. You must have a model and simulation. And in it you must change both parameters at the same time.

4.11.3 Accuracy

An important point about this section is that we computed the semirelative sensitivity values with two techniques: analytic equations and empirical (or numerical) estimates. To compare these two techniques, we note that using the empirical method the estimate for the +1% increment of the bat speed is

$$\tilde{S}_{v_{2b}}^{v_{1a}} = \left.\frac{(1 + CoR_{2b})m_2 I_2}{K}\right|_{\mathrm{NOP}} v_{2b_0} = 28.203485470404$$

whereas the analytic method as in Table 4.4 gives the following exact value:

$$\tilde{S}_{v_{2b}}^{v_{1a}} = \left.\frac{(1 + CoR_{2b})m_2 I_2}{K}\right|_{\mathrm{NOP}} v_{2b_0} = 28.203485470399$$

With a 10% change in the variable values, the match would be worse. With a 0.1% change, the match would be better.

This analysis has only included the equations of physics. Later, in Sect. 4.12, we will consider principles of physiology. In that section, we will recommend that batters choose lightweight end-loaded bats.

The second purpose of this book is to show how the batter can buy or make an optimal baseball or softball bat. From the viewpoint of the batter, the batted-ball speed is the most important output. The larger it is, the more likely the batter will get on base safely (Baldwin and Bahill 2004).

4.11.4 Optimizing with Commercial Software

We applied *What'sBest!*, a subset of the LINGO solvers, to our model. We constrained each variable to stay within physically realistic limits under natural conditions. Such values are shown in Table 4.4. We have previously gotten good results using this technique when doing empirical sensitivity analyses (Bahill et al. 2009). Then, we asked the optimizer to give us the set of values that would maximize batted-ball speed. The optimizer applied a nonlinear optimization program. Surprisingly, the results were almost the same as in Table 4.4! That is, for variables and parameters with positive sensitivities, the optimizer chose the maximum values. For variables and parameters with negative sensitivities, the optimizer chose the minimum values. For the parameter with both negative and positive sensitivities, the optimizer chose the optimal value.

Using all of the optimal values at the same time increased the batted-ball speed from 92 to 117 mph (41–52 m/s). Using this optimal set of values changed the sensitivities, as shown in Table 4.6.

Table 4.6 Sensitivities with nominal and optimal values for the variables and parameters

Semirelative sensitives of the batted-ball velocity with respect to	With nominal values	With optimal values
Inputs		
$v_{\text{ball-before}}$	8	12
$\omega_{\text{ball-before}}$	0	0
$v_{\text{bat-cm-before}}$	28	36
$\omega_{\text{bat-before}}$	5	5
Parameters		
CoR_{2b}	25	32
$d_{\text{cm-ip}}$	−2	+0.4
m_{ball}	−14	−13
m_{bat}	10	12
$I_{\text{bat-cm}}$	3	1

1. The numerical sensitivity values mostly increased. This is a direct result of the definition of the semirelative sensitivity function where the partial derivative is multiplied by the variable or parameter value. If the variable or parameter value increases, then the sensitivity value also increases.
2. The rank order stayed the same except that the output became more sensitive to the linear velocity of the ball before the collision, $v_{\text{ball-before}}$, than to the mass of the bat, m_{bat}. In the optimal set, both of these sensitivities increased, but because the value of the linear velocity of the ball before the collision, $v_{\text{ball-before}}$, changed from 37 to 40 m/s (Table 4.4), whereas the value of the mass of the bat, m_{bat}, only changed from 0.905 to 0.964 kg, the change in the sensitivity to the linear velocity of the ball before the collision, $v_{\text{ball-before}}$, became bigger.
3. The optimizer found the optimum value for $d_{\text{cm-ip}}$ to be 10 cm (4 inches). Above this value, the semirelative sensitivity was negative; below this value, the sensitivity was positive. This is important. We could have found the same result if we had used the partial derivative of the batted-ball velocity with respect to the distance d, taken the derivative with respect to d and set it equal to zero, as in the following derivation by Ferenc Szidarovszky. We start with Eq. (4.8).

   $$v_{1a} = v_{1b} - \frac{(v_{1b} - v_{2b} - \omega_{2b} d)(1 + CoR_{2b}) m_2 I_2}{m_1 I_2 + m_2 I_2 + m_1 m_2 d^2}$$

   Let

   $$E = (1 + CoR_{2b}) m_2 I_2 \quad \text{and} \quad F = m_1 I_2 + m_2 I_2$$

   Then

   $$v_{1a} = v_{1b} - \frac{(v_{1b} - v_{2b} - \omega_{2b} d) E}{F + m_1 m_2 d^2}$$

   and the

$$\text{numerator of } \left\{\frac{\partial v_{1a}}{\partial d}\right\} = -E\left[m_1 m_2 d^2 \omega_{2b} + 2m_1 m_2 d(v_{1b} - v_{2b}) + B\omega_{2b}\right]$$

Now we set this equal to zero and solve for $d_{\text{max-velocity}}$.

$$d_{\text{max-velocity}} = \frac{(v_{1b} - v_{2b})}{\omega_{2b}} + \sqrt{\left[\frac{(v_{1b} - v_{2b})}{\omega_{2b}}\right]^2 + \frac{m_1 I_2 + m_2 I_2}{m_1 m_2}}$$

The batted-ball velocity has a maximum or a minimum at this value of d. To determine which, we derive the second partial derivative. The

$$\text{numerator of} \left\{\frac{\partial^2 v_{1a}}{\partial d^2}\right\} = -E\left[m_1^2 m_2^2 d^3 \omega_{2b} - 2Fm_1 m_2 d\omega_{2b} - \frac{F^2 \omega_{2b}}{d}\right] < 0$$

This is negative. Therefore, this value of $d_{\text{cm-ip}}$ gives the maximum-batted-ball velocity, not the minimum. Using the numbers in Table 1.1, the optimum value for $d_{\text{cm-ip}}$ is 9.2 cm (3.6 inches).

This all means that the sensitivity analysis is robust. Its results remain basically the same after big changes in the variables and parameters.

We then tried a different optimization technique. Instead of constraining each variable to stay within realistic physical limits, we allowed the optimizer to change each variable by at most ±10% and then give us the set of values that maximized batted-ball speed. The numerical values of the sensitivities changed but the rank order stayed the same, except for $v_{\text{ball-before}}$ and m_{bat} just as it did with the realistic values technique.

Both empirical sensitivity analyses and optimization can constrain each variable to stay within specified realistic physical limits or change each variable by a certain percentage. Both techniques gave the same results. However, we prefer the former technique (Bahill et al. 2009).

We found an interesting relationship between the sensitivity analyses and optimization: they gave the same results! Because the interaction terms are small, for variables and parameters with positive sensitivities, the optimizer chose the maximum values and for variables and parameters with negative sensitivities, the optimizer chose the minimum values. Where the sensitivity function had both positive and negative slopes, it found the optimal value. But of course, this finding is not original. Sensitivity analyses are commonly used in optimization studies (Choi and Kim 2005). These studies typically apply sensitivity analysis after optimization. They try to find values or limits for the objective function or the right-hand sides of the constraints that would change the decisions. However, in our study, we applied optimization after the sensitivity analysis and we had only one variable in our objective function. Therefore, our problem was much simpler than sensitivity analyses in the optimization literature.

4.12 Optimizing the Bat

The following paragraphs are from *Major League Baseball 2016 Official Baseball Rules*.

3.02 (1.10) **The Bat**

(a) The bat shall be a smooth, round stick not more than 2.61 inches in diameter at the thickest part and not more than 42 inches in length. The bat shall be one piece of solid wood.
(b) Cupped Bats. An indentation at the end of the bat up to 1¼ inches in depth is permitted and may be no wider than two inches and no less than one inch in diameter. The indentation must be curved with no foreign substance added.
(c) The bat handle, for not more than 18 inches from its end, may be covered or treated with any material or substance. Any such material or substance that extends past the 18-inch limitation shall cause the bat to be removed from the game.
(d) No colored bat may be used in a professional game unless approved by the Rules Committee.

The second purpose of this chapter is to help the batter acquire an optimal baseball or softball bat. Therefore, we ask, "How can the batter use these sensitivity and optimization results to select or customize a bat that would be optimal for him or herself?" First, it is no surprise that the speed of the bat before the collision is the most important variable in Table 4.4. Its effect is shown in Fig. 4.4, where the slope of the line is the absolute sensitivity.

For Fig. 4.4, we computed the batted-ball velocity with $v_{\text{ball-after}} = v_{\text{ball-before}} - Am_{\text{bat}}I_{\text{bat}}$ and then we plotted the batted-ball speed as a function of the total bat speed before the collision. Remember that A is not a constant, it depends on the

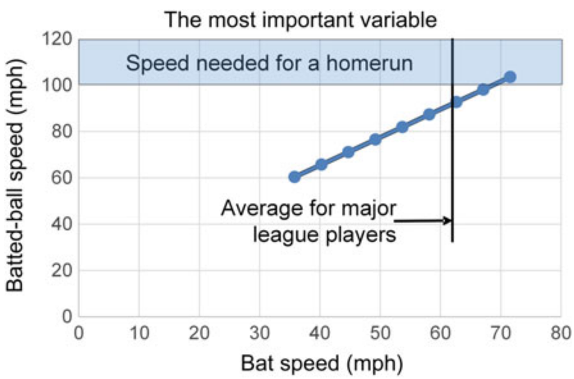

Fig. 4.4 Total bat speed before the collision is the most important variable in the BaConLaws model

three inputs: the velocity of the ball and bat before the collision and the angular velocity of the bat before the collision. Figure 4.4 is for a pitch speed of 92 mph {a ball speed at contact of 83 mph}. This figure shows that an average hit is not a home run.

For decades, Little League coaches have taught their boys to practice and gain strength so that they could increase their bat speeds. They also said that it is very important to reduce the variability in the bat swings: Every swing should be the same. “Don’t try to kill the ball.” Given our new information, we now recommend that Little League coaches continue to give the same advice: increase bat speed and reduce variation. Practice is the key. Baldwin (2007), a major-league pitcher with a career 3.08 ERA, sagaciously wrote that if you lose a game, don’t blame the umpire or your teammates; just go home and practice harder.

Using the Bat Chooser™, our measurements of over 300 batters showed that variability in the speed of the swing decreases as level of performance increases from Little League to Major League Baseball. For major leaguers, the bat speed standard deviations were typically around ±5% (Bahill and Karnavas 1989), which is a small value for physiological data.

The variable with the second largest sensitivity is the coefficient of restitution (*CoR*). The *CoR* of a bat–ball collision depends on where the ball hits the bat. It is difficult, but absolutely essential, for the batter to control this. He or she must consistently hit the ball with the sweet spot of the bat. The *CoR* also depends on the manufacturing process. The NCAA now measures the Bat–Ball Coefficient of Restitution (BBCOR) for sample lots coming off the manufacturing line. Therefore, amateurs are all going to get similar BBCORs. However, a lot can still be done with the *CoR* for aluminum and composite bats during their useful life. For example, the performance of composite bats typically improves with age because of the break-in process; repeatedly hitting the bat eventually breaks down the bat’s composite fibers and resinous glues. “Rolling” the bat also increases its flexibility. Rolling the bat stretches the composite fibers and accelerates the natural break-in process simulating a break-in period of hitting, say, 500 balls.

For wooden bats, the batter could try to influence the *CoR* by choosing the type of wood that the bat is made of. Throughout history, the most popular woods have been white ash, sugar maple and hickory. However, hickory is heavy, so most professionals now use ash or maple. A new finding about bat manufacturing is that the slope of the grain has an effect on the strength and elasticity of the bat. As a result, the wood with the straightest grain is reserved for professionals and wood with the grain up to five degrees off from the long axis of the bat is relegated to amateurs. Furthermore, the manufacturer’s emblem is stamped on the flat grain side of ash bats so that balls collide with edge grain as shown in Fig. 4.1, whereas the emblem is stamped on the edge grain side of maple wood bats (Fig. 4.6) because they are stronger when the collision is on the flat grain side.

The next largest sensitivities are for the mass of the ball and its velocity before the collision, m_{ball} and $v_{\text{ball-before}}$. However, the batter can do nothing to influence the mass of the ball or the ball velocity before the collision, so we will not concern ourselves with them. Likewise, the batter has no control over the ball spin,

$\omega_{\text{ball-before}}$, so we will ignore it when selecting bats. Now if this discussion were being written from the perspective of the pitcher (Baldwin 2007), then these three parameters would be important.

The next most important variable in Table 4.4 is the mass of the bat. Therefore, we will now consider the mass and other related properties of the bat. The sensitivity of the batted-ball speed with respect to the mass of the bat is positive, meaning (if everything else is held constant) as the mass goes up so does the batted-ball speed. However, the heavier bat cannot be swung as fast (Bahill and Karnavas 1989) due to the force–velocity relationship of human muscle, to be discussed in conjunction with Fig. 4.10. This physiological relationship was not included so far in the equations of this book because so far we only modeled the *physics* of the collision, notwithstanding physiology trumping physics in this case. The net result of physics *in conjunction with physiology* is that lighter bats are better for almost all batters (Bahill 2004).

Perhaps due to this general feeling that lighter bats are better, many professionals have "corked" their bats. This reduced the mass of the bat, but because it also reduced the moment of inertia, it did not improve performance significantly (Nathan et al. 2011). However, it is now legal to make a one- to two-inch-diameter hole 1¼ inches deep into the barrel end of the bat (see Fig. 4.6). Most batters do this because it makes the bat lighter with few adverse effects. Other bat parameters that are being studied include the type of wood (density, strength, elasticity, straightness of the grain, etc.) and type of materials (density, strength, elasticity, break-in period, durability, type of Al alloy, etc.).

For an aluminum bat, some batters reduce the thickness of the barrel wall by shaving the inside of the barrel. This reduces the bat mass, which according to physics *and* physiology increases batted-ball speed. However, it also reduces durability.

The distance between the center of mass of the bat and the center of percussion, $d_{\text{cm}-\text{cop}}$, is the next most important parameter. We presumed that the sweet spot of the bat was the center of percussion (CoP) of the bat. All batters try to hit the ball on the sweet spot of the bat. To help the batter, manufacturers of aluminum bats have been moving the CoP by moving the internal weight from the end of the bat toward the knob, http://www.acs.psu.edu/drussell/bats/cop.html. It is now an annual game of cat and mouse. The manufacturers move the CoP, then the rule makers change their rules, then the manufacturers move, etc.

Finally, we come to the moment of inertia of the bat, I_{bat}, with respect to its center of mass. The physics, revealed with the sensitivity analysis, states that although the moment of inertia is one of the least important parameters, it would help to increase its value. More importantly, physiology showed that all batters would profit from using end-loaded bats (meaning bats with higher moments of inertia) (Bahill 2004). There are many ways to change the moment of inertia of a bat. Most aluminum bats start with a common shell and then manufacturing adds a weight inside to bring the bat up to its labeled weight. The important question then becomes, *where* should the weight be added? It has been suggested that they add weight in the knob because this would comply with the regulations and would not decrease bat speed (Brancazio 1984). However, the results of Bahill (2004) show that they should add the weight in the barrel end of the bat making it *end-loaded*. This will increase the batted-ball speed. For a wooden bat, the moment of inertia can be changed by cupping out the barrel end, adding weight to the knob or tapering the barrel end. Assume that the end of the barrel of a bat is only used to "protect" the outside edge of the plate: no one hits home runs on the end of the bat. Therefore, a professional could use a bat where the last 3 in (7 cm) were tapered from 2.61 inches (6.6 cm) down to 1¾ of an inch (4.4 cm). This would decrease the weight, decrease the moment of inertia about the knob and would move the center of mass closer to the knob: these changes would probably benefit some batters. However, such modifications would have to be individually designed for each player.

At this point, it may be useful to reiterate that an end-loaded bat is not a normal bat with a weight attached to its end. Adding a weight to the end of a normal bat would increase both the weight and the moment of inertia. This would *not* be likely to help anyone. In the design and manufacture of an end-loaded bat, the weight is distributed so that the bat has a normal weight but a larger than normal moment of inertia.

Most people can feel the difference between bats with different moments of inertia. A coach with the San Francisco Giants showed us a legal custom-made bat with a large moment of inertia created by leaving it with a huge knob. He presumed that his players already understood the influence of bat weight on bat speed so he was trying to expand their understanding to the influence of bat moment of inertia on the speed of the swing. One of our University of Arizona softball players described our biggest moment of inertia bat with, "That's the one that pulls your arms out."

Our best generalization is that almost all batters would profit from using end-loaded bats. Smith and Kensrud (2014) concluded their paper with "Batter swing speed decreased with increasing bat inertia, while … the hit-ball speed increases with bat inertia."

Summarizing, these are the most important factors for understanding bat performance: bat weight, the coefficient of restitution, the moment of inertia and characteristics of humans swinging the bats.

In the future, once equations for configurations 3 and 4 have been derived, it will be possible to see how the coefficient of friction μ_f affects the batted-ball speed. Then, we will be able to decide if the varnish or paint on the bat should be made rough-textured or smooth, or if bats should be rubbed or oiled in order to improve bat performance.

To confuse fielders who are trying to locate the bat–ball collision point, perhaps the bat could be painted white with random thin red lines. Or perhaps bats could be painted pink supposedly to promote breast cancer research.

Figure 4.5 shows the outcomes of hitting the ball at different places on the front surface of the bat. We used this figure to help determine the size of the vertical sweet spot of the bat. It also suggests that putting oil on the top surface of the bat could change short pop-ups (sure outs) into innocuous foul tips.

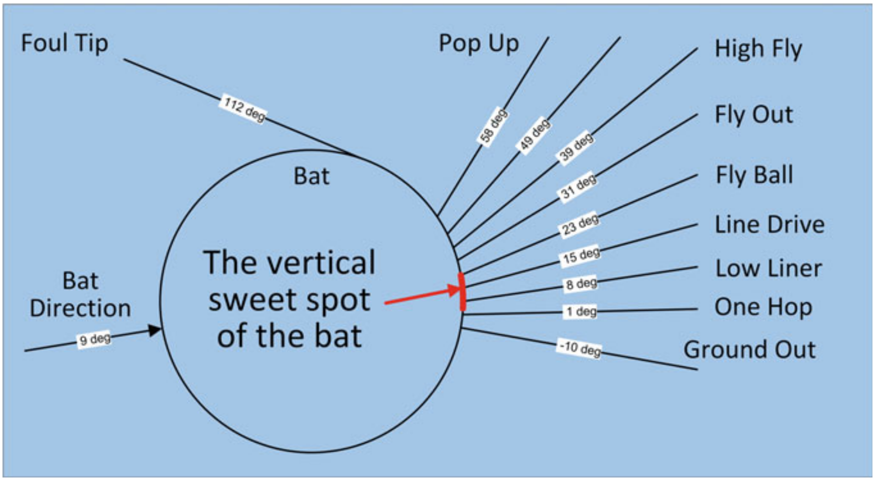

Fig. 4.5 Direction of the batted-ball as a result of hitting the ball at different places on the front surface of the bat

Fig. 4.6 Bat with an exaggerated flat front side. The actual size of the flat surface should not be larger than the vertical sweet spot, which is one-fifth of an inch high

What if the front side of the bat were flat, as in Fig. 4.6, instead of round? Then fly balls and grounders would be line drives instead. What could make the front side of the bat flat? Using sandpaper or a plane on the front side of a bat would make that front surface flat. Figure 4.7 shows that if the front of the bat were flat, then a fly ball (black lines) would be changed into a line drive (red lines). This would increase performance. Most umpires would probably not notice or might accept a bat whose front surface had been sanded or planed. This would also reduce the variability in the batted-ball trajectories, because plus or minus one millimeter would yield the same result every time.

To improve bat performance, manufacturers could reduce the variability of bat and ball parameters. Major-league bats were custom made for us by Hillerich and Bradsby Co. The manufacturing instructions were “Professional Baseball Bat, R161, Clear Lacquer, 34 inch, 32 oz, make as close to exact as possible, end

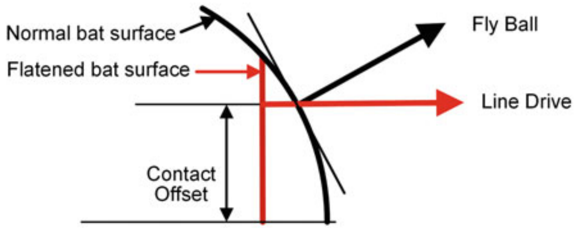

Fig. 4.7 Enlarged schematic view of a bat with a flat front and resulting ball trajectories

brand - genuine model R161 pro stock, watch weights" emphasis added. The result was six bats with an average weight of 32.1 oz and a standard deviation of 0.5! This large standard deviation surprised us. We assume there is the same variability in bats used by major-league players.

There is also variability in the ball. We might assume that the center of mass of the ball is coincident with the geometric center of the ball. However, put a baseball or softball in a bowl of water. Let the movement subside. Then put an X on the top the ball. Now spin it and let the motion subside again. The X will be on top again. This shows that for most baseballs and softballs the center of mass is *not* coincident with the geometric center of the ball.

4.12.1 Summary of Bat Selection

These sensitivity and optimality analyses showed that the most important variable, in terms of increasing batted-ball speed, is bat speed before the collision. This is in concert with ages of baseball folklore and principles of physiology. Therefore, batters should develop strength, increase coordination and practice so that their swings are fast and with low variability.

These analyses showed that the next most important variable is the coefficient of restitution, the *CoR*. Engineers and bat regulators are free to play their annual cat and mouse game of increasing *CoR* then writing rules and making tests that inhibit these changes. Indeed, most recent bat research has gone into increasing the *CoR* of bat–ball collisions.

Pitch speed, ball spin and the mass of the ball are important. However, the batter cannot control them. Therefore, they cannot help the batter to choose or modify a bat.

The next most important parameter is the bat mass, m_{bat}. However, physics recommends heavy bats, whereas the force–velocity relationship of muscle recommends light bats. In this case, physiology trumps physics. Each person's preferred bat should be as light as possible while still fitting within baseball needs, regulations and availability.

The last interesting parameter from the sensitivity analysis and the optimization study is the bat moment of inertia, I_{bat}. The sensitivity analysis suggested that a larger bat moment of inertia would be better, which contradicts studies in the physics of baseball literature that recommended smaller moments of inertia. However, an experimental physiology study stated that all players would profit from using end-loaded bats (that is, those with high moments of inertia) (Bahill 2004). Since then most studies have recommended bats with higher moments of inertia (Cross 2011; Smith and Kensrud 2014; Crisco et al. 2014).

The second purpose of this book is to show what the batter can do to achieve optimal bat performance. The most important thing is practice. Next, batters should select lightweight bats. They should then select bats that increase the *CoR* by all legal means. Finally, they should choose bats with higher moments of inertia.

4.12.2 The Ideal Bat Weight

So far, the equations in this book were equations of physics. However, we repeatedly mentioned physiology. Now it is time to look at physiology. This section is based on Bahill and Karnavas (1991).

Our instrument for measuring bat speed, the[1] Bat Chooser™, had two vertical laser beams, each with associated light detectors. Our subjects swung bats through the laser beams. A computer recorded the time between interruptions of the light beams. Knowing the distance between the light beams and the time required for the bat to travel that distance, the computer calculated the speed of the sweet spot, which we defined as the center of percussion

The computer told the batters to swing each bat as fast as they could while still maintaining control. It said, “Pretend you are trying to hit a Nolan Ryan fastball.”

In our experiments, each batter swung six bats through the light beams. The bats ran the gamut from super-light to super-heavy; yet they had similar lengths and weight distributions. In our developmental experiments, we tried about four dozen bats. We used aluminum bats, wooden bats, plastic bats, heavy metal warm-up bats, bats with holes in them, bats with lead in them, major league bats, college bats, softball bats, Little League bats, brand new bats and bats made in the 1950s.

In one of our first set of experiments (Bahill and Karnavas 1989), we used six bats of significantly different weights but which were all about 34 inches (89 cm) long, with a center of mass about 23 inches (58 cm) from the end of the handle. They are described in Table 4.7 and Fig. 4.8.

In a 20-min time interval, each subject swung each bat through the instrument five times. The order of presentation was randomized. The selected bat was announced by a speech synthesizer, for example, “Please swing bat Hank **A**aron, that is, bat **A**.” (We named our bats after famous baseball players who had names starting with the letter assigned to the bat.)

[1]Bat Chooser and Ideal Bat Weight are trademarks of Bahill Intelligent Computer Systems.

Table 4.7 Test bats used by the major league batters

Name	Weight (oz)	Mass (kg)	Distance from knob to center of mass (in)	Distance from knob to center of mass (m)	Average sweet-spot speed (mph) also given in Fig. 4.10	Average sweet-spot speed (m/s)	Description of the bat
D	49.0	1.39	22.5	0.57	60	27	Aluminum bat filled with water
C	42.8	1.21	24.7	0.63	61	27	Wooden bat with lead in the barrel
A	33.0	0.94	23.6	0.60	65	29	Wooded bat
B	30.6	0.87	23.3	0.59	65	29	Wooden bat
E	23.6	0.67	23.6	0.60	74	33	Wooden fungo bat
F	17.9	0.51	21.7	0.55	88	40	Wooden handle mounted on a light steel pipe with a six-ounce weight at the end

Fig. 4.8 Our first set of experimental bats. *Photo credit* Richard Harding

For each swing, we recorded the bat weight and the speed of the center of mass, which we converted to the speed of the center of percussion. That was as far as physics could take us; we then had to look at the principles of physiology.

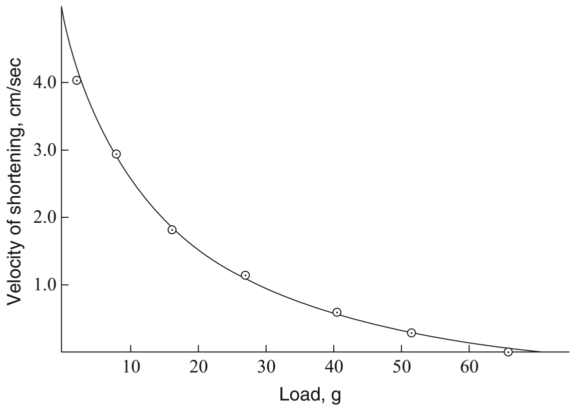

Fig. 4.9 Hill's original force–velocity relationship figure. He fit the following equation to his data: $(P + 14.35)(v + 1.03) = 87.6$ where P is the load in grams and v is the velocity in cm/s (Hill 1938)

Physiologists have long known that muscle speed decreases with increasing load as shown in Fig. 4.9. This is why bicycles have gears; gears enable the rider to maintain the muscle speed that imparts maximum power through the pedals, while the load, as reflected by the bicycle speed, varies greatly. To discover how the muscle properties of individual baseball players affect their Ideal Bat Weights, for each batter, we plotted bat speed as a function of bat weight to produce a graphical model known as a muscle force–velocity relationship as shown in Fig. 4.10. The red Xs represent the average of the five swings of each bat; the standard deviations were small for physiological data (smaller than the red Xs). These standard deviations were shown in Bahill and Karnavas (1991).

Traditionally, physiologists have used three types of equations to describe the force–velocity relationship of muscles: straight lines, hyperbolas and exponentials. Each type of equation has produced the best fit for some experimenters, under certain conditions and with certain muscles. However, usually the hyperbola fits the data best. In our experiments, we tried all three equations and chose the one that had the best fit to the data of each batter's 30 swings. For the data of the force–velocity relationship illustrated in Fig. 4.10, we found that a hyperbola provided the best fit.

These curves indicated how bat speed varied with bat weight. We now want to find the bat weight that will make the ball leave the bat with the highest speed and thus have the greatest chance of eluding the fielders (Baldwin and Bahill 2004). We call this the maximum-batted-ball-speed bat weight. To calculate this bat weight, we must couple the muscle force–velocity relationships to the equations of physics.

For the major league batter whose data are shown in Fig. 4.10, the best fit for his force–velocity data was the hyperbola, $(m_{\text{bat}} + 11) \times (v_{\text{bat-before}} - 36) = 1350$ units

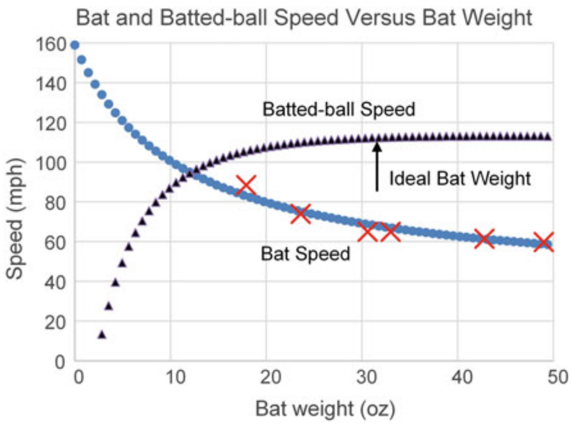

Fig. 4.10 Measured bat speed (red Xs), a hyperbolic fit to these data (blue dots) and the calculated batted-ball speed (black triangles) for a 90 mph pitch to one of the fastest San Francisco Giants

are ounces and mph, that is shown with blue dots. This batter had some of the fastest swing speeds on the team. When we substituted this equation into the batted-ball velocity equation, Eq. (4.8), we were able to plot the ball speed after a collision as a function of bat weight, shown with black triangles in Fig. 4.10.

$$(m_{\text{bat}} + 11) \times (v_{\text{bat-before}} - 36) = 1350$$

Solve for the bat velocity

$$v_{\text{bat-before}} = \left\{ \frac{36 m_{\text{bat}} + 1746}{m_{\text{bat}} + 11} \right\}$$

Now we substitute this into Eq. (4.8)

$$v_{1a} = \frac{v_{1b}(m_1 I_2 - m_2 I_2\ CoR_{2b} + m_1 m_2 d^2) + v_{2b} m_2 I_2 (1 + CoR_{2b}) + \omega_{2b} m_2 d I_2 (1 + CoR_{2b})}{m_1 I_2 + m_2 I_2 + m_1 m_2 d^2}$$

to get the batted-ball velocity

$$\begin{aligned} v_{\text{ball-after}} = v_{\text{ball-before}} & \frac{\left(m_{\text{ball}} I_{\text{cm}} - m_{\text{bat}} I_{\text{cm}}\ CoR_{2b} + m_{\text{ball}} m_{\text{bat}} d^2_{\text{cm-ip}} \right)}{K} \\ & + \left\{ \frac{36 m_{\text{bat}} + 1746}{m_{\text{bat}} + 11} \right\} \frac{m_{\text{bat}} I_{\text{cm}} (1 + CoR_{2b})}{K} \\ & + \omega_{\text{bat-before}} \frac{m_{\text{bat}} d I_{\text{cm}} (1 + CoR_{2b})}{K} \end{aligned}$$

In this equation, I_{cm} is also a function of m_{bat}.

This equation produced the curve composed of black triangles in Fig. 4.10. This curve shows that the maximum-batted-ball-speed bat weight for this batter is about 45 oz, which is heavier than that used by most batters. However, this batted-ball

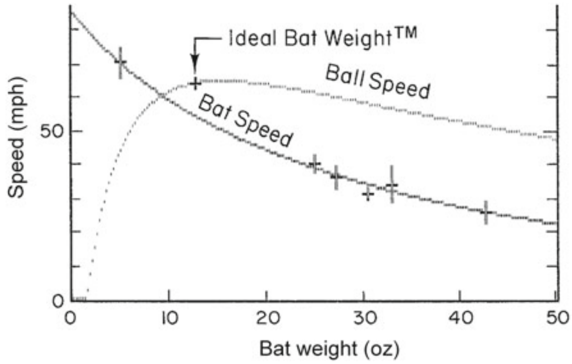

Fig. 4.11 Bat speed and calculated batted-ball speed after the collision both as functions of bat weight for a 40 mph pitch to Alex, a 10-year-old Little League player. The dots represent the average of the five swings of each bat; the vertical bars on each dot represent the standard deviations

speed curve is almost flat between 30 and 49 oz. Notably, this player normally used a 32-ounce bat. Evidently, the greater control permitted by the 32-ounce bat outweighed the one percent increase in speed that could be achieved with the 45-ounce bat.

The maximum-batted-ball-speed bat weight is not the best bat weight for any player because a lighter bat will give a batter better control and more accuracy. Obviously, a trade-off must be made between batted-ball speed and control. Because the batted-ball speed curve is so flat around the point of the maximum-batter-ball speed, we believe there is little advantage in using a bat as heavy as the maximum-batter-ball-speed bat weight. Therefore, we defined the [1]*Ideal Bat Weight*™ to be the weight where the ball speed curve drops one percent below the maximum-batted-ball speed. Using this criterion, the Ideal Bat Weight for this batter is 31.75 oz. We believe this gives a good trade-off between batted-ball speed and accuracy. For this batter, the batted-ball speed is nearly flat around the ideal bat weight. So it does not seem to be critical. But for most other batters this was not true, as is shown in Fig. 4.11.

The Ideal Bat Weight is specific to each individual; it is not correlated with height, weight, age, circumference of the upper arm or any combination of these factors, nor is it correlated with any other obvious physical factors. Nevertheless, Bahill and Morna Freitas (1995) mined their database of 163 subjects and 36 factors and determined some rules of thumb that could make suggestions. For example, for a general 9- or 10-year-old Little Leaguer, the recommended bat weight in ounces would be height in inches divided by three plus four ounces, $\textit{recommended bat weight} = \frac{\textit{height}}{3} + 4$. Table 4.8 shows their recommendations.

In conclusion, there is an ideal bat weight for each batter. It can be measured in a laboratory or it can be estimated using rules of thumb like those in Table 4.8.

Table 4.8 Simple integer models for recommending bat weights

Group	Recommended bat weight (oz)
Baseball, major league	Height/3 + 7
Baseball, amateur	Height/3 + 6
Softball, fast pitch	Height/7 + 18
Softball, slow pitch	Weight/115 + 24
Junior league (13 and 15 years)	Height/3 + 1
Little league (11 and 12 years)	Weight/18 + 16
Little league (9 and 10 years)	Height/3 + 4
Little league (7 and 8 years)	Age * 2 + 4

Age (years); height (inches); body weight (pounds)

4.12.3 Bat Moment of Inertia

The bat moment of inertia is an enigma because for most, but not all, batters as the bat moment of inertia goes up the bat speed goes down (Bahill 2004; Cross 2011; Smith and Kensrud 2014; Crisco et al. 2014). For Bahill's (2004) women batters, 80% had negative slopes for bat speed versus the moment of inertia.

Now we need a model for these data. Because of the positive and negative slopes, averaging the data makes no sense. Therefore, we chose one of the All Americans in our database as our model. Her data were fit with the equation

$$vt_{\text{sweet spot-before}} = -22 I_{\text{bat-center of mass}} + 30 \tag{4.12}$$

where the bat velocity has units of m/s and the moment of inertia has units of kg m^2. The eight bats in our variable moment of inertia experiments had moments of inertia about the center of mass in the range of 0.03–0.09 kg m^2. Typical bats used by players on this team had moments of inertia of around 0.05.

In these experiments, we used the bats described in Table 4.9. They decoupled the mass and moment of inertia, because they had nearly identical masses but different moments of inertia. That is, in each set, the masses were close to the same value, although the moments of inertia varied widely.

4.12.4 Modifying the Bat

Previously, we mentioned that, for wooden bats, it is legal to taper the last three inches of the barrel from 2.61 inches (6.6 cm) down to 1¾ of an inch (4.4 cm) (suggested in Fig. 9.1). This modification would decrease the bat weight, decrease the moment of inertia and move the center of mass closer to the knob.

Table 4.9 Properties of the variable moment of inertia bats

Name	Period of oscillation (s)	Mass (kg)	Distance from knob to center of mass, d_{k-cm} (m)	Moment of inertia with respect to the knob, I_{knob} (kg m^2)	Moment of inertia with respect to the center of mass, I_{cm} (kg m^2)
Aluminum bats					
A	1.648	0.824	0.496	0.275	0.072
B	1.682	0.824	0.494	0.286	0.085
C	1.689	0.824	0.520	0.303	0.080
D	1.702	0.833	0.526	0.316	0.086
Bats with a wooden handle and a brass disk mounted on a threaded rod, similar to bat F in Fig. 4.8					
Red bat	1.443	0.799	0.427	0.176	0.030
Blue bat	1.493	0.807	0.458	0.204	0.035
Green bat	1.563	0.801	0.493	0.239	0.044
Yellow bat	1.631	0.805	0.509	0.270	0.061

4.12.4.1 The R161 Bats

Hillerich and Bradbury made six such R161 Louisville Slugger wooden bats for us. When we compared these six bats to six of their unmodified R161 bats, we found that, on average, this modification reduced the mass by 5%, reduced the moment of inertia about the center of mass by 5.2% and reduced the distance from the knob to the center of mass by 1.6%.

That last paragraph described the measured physical changes to the bat. Next, we wanted to see how those changes coupled with human physiology to affect the bat speed. First, we used the data of Fig. 4.10 at its nominal bat weight of 31.75 oz and found that a 5% decrease in bat mass increased the bat speed by 1.7%. Next, we used Eq. (4.12) and found that a 5.2% decrease in the moment of inertia about the center of mass increased the bat speed by 0.2%. Summing these changes gave a total increase in bat speed of 1.9%. Figure 4.12 shows these numbers.

That takes care of the physical changes of the bat and how those changes couple with physiology to affect bat speed. Now, we are finally ready to use the physics captured in the BaConLaws model.

According to the sensitivity analysis of the BaConLaws model summarized in Table 4.4, decreasing m_{bat} and I_{cm} would decrease batted-ball speed, whereas decreasing the distance between the center of mass and the center of percussion (the sweet spot) would increase batted-ball speed.

Semirelative sensitivity values from Table 4.4		
m_{bat}	10	$m_{bat} \downarrow, v_{ball\text{-}after} \downarrow$
$I_{bat\text{-}cm}$	3	$I_{bat\text{-}cm} \downarrow, v_{ball\text{-}after} \downarrow$
$d_{cm\text{-}cop}$	−2	$d_{cm\text{-}cop} \downarrow, v_{ball\text{-}after} \uparrow$

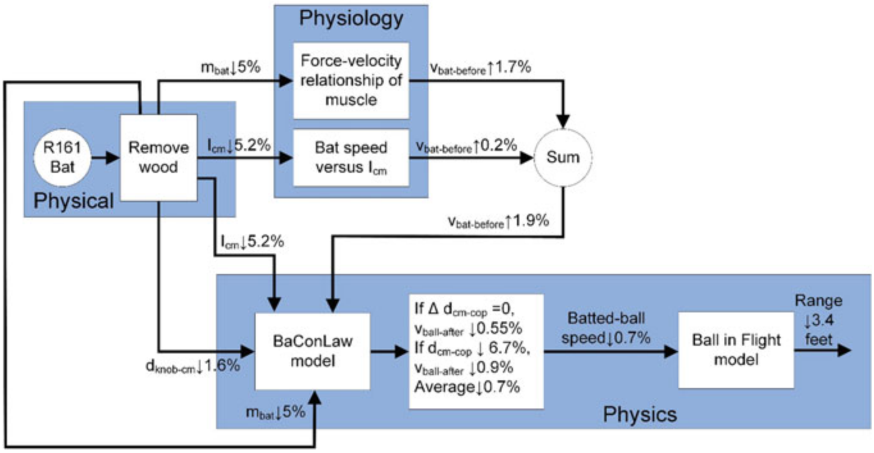

Fig. 4.12 Analysis process and numerical values for the tapered R161 bat

To see the changes in bat speed, we modified the inputs to the BaConLaws model for the modified R161 bat. We decreased the mass by 5%, decreased the moment of inertia about the center of mass by 5.2% and increased the bat speed by 1.9%. This gave us a new smaller batted-ball speed. We will now show how the distance between the knob and the center of mass affects this smaller batted-ball speed. We know that the distance from the knob to the center of mass decreased by 1.6%. However, we do not have data for the change in distance from the center of mass to the center of percussion as wood is removed from the barrel end of the bat. However, we can bracket that change. If we assume that the *distance* from the center of mass to the center of percussion stays fixed, then the batted-ball speed decreases by 0.55%. On the other hand, if we assume that the *center of percussion* stays fixed, while the distance from the knob to the center of mass decreases by 1.6%, then the distance between the center of mass and the center of percussion increases by 6.7% and the batted-ball speed decreases by 0.9%. Let us average the results of those two assumptions, and say that the new batted-ball speed decreases by an additional 0.73%.

When we put this decreased batted-ball speed into the Ball in Flight model of Chap. 7, we found that the distance of a perfectly hit home run ball *decreased by three feet!*

Vedula and Sherwood (2004) performed a finite element analysis of wooden baseball bats. They found that if they reduced the mass in the barrel end of the bat by 10%, then the distance between the center of mass and the center of percussion increases by 5% and the batted-ball speed decreases by 1.7%. This matches our results quite well.

This is a very surprising result. It states that tapering the last three inches of the barrel will *not* increase the batted-ball speed or the ball's range.

4.12.4.2 The C243 Bat

Because this result was so surprising, we repeated the analysis with another bat that had its barrel end cupped out, as shown in Fig. 4.6. We measured the volume of the cupped out hole at the end of a Louisville Slugger C243 bat. It was 25 cc. The density of white ash is 0.6 that of water. Therefore, cupping the bat reduced its mass by 15 g, or 1.7%. Theoretically, using $I_{\text{cm-after-cupping}} = I_{\text{cm-before-cupping}} - m_{\text{cup}} d^2_{\text{cm-end}}$, this should reduce the bat moment of inertia at the center of mass by 0.0012 kg m^2 or 2.2%. Finally, the last of the three parameters changed by cupping, the measured distance from the knob to the center of mass, was reduced by 1.7%.

That last paragraph described the measured physical changes to the bat. Now we want to see how those changes couple with physiology to affect the bat speed. First, we used the data of Fig. 4.10 at its nominal operating point of 31.75 oz, and found that a 1.7% decrease in bat mass increased the bat speed by 0.57%. Next, we used Eq. (4.12) and found that a 2.3% decrease in the moment of inertia about the center of mass produced a 0.1% increase in bat speed. Summing these increases gives a total increase in bat speed of 0.67%. This is probably why bat manufactures cup the ends of their bats, because they know that cupping the end of the bat increases the bat speed.

That takes care of the physical changes of the bat and how those changes couple with physiology to effect bat speed. Now, we are finally ready to use the physics captured in the BaConLaws model. To see the changes in bat speed, we modified the inputs to the BaConLaws model for the C243 bat. We decreased the mass by 1.7%, decreased the moment of inertia about the center of mass by 2.3% and increased the bat speed by 0.67%. The measured distance from the center of mass to the center of percussion increased by 4.3%. When we changed these four parameters in the BaConLaws model, the batted-ball speed decreased by 0.25%.

Finally, when we put this decreased batted-ball speed into the Ball in Flight model of Chap. 7, we found that the distance of a perfectly hit home run ball *decreased by one foot*. Figure 4.13 shows our process and captures these numbers.

Both of the bat modifications described here {tapering the barrel and cupping the barrel end} remove wood from the end of the bat. This decreases the bat mass, moment of inertia and distance from the knob to the center of mass. This should be true for any wooden bat. Physiology shows that the first two changes {reducing the mass and the moment of inertia} increase the bat speed. This is the main reason for making these modifications. Increasing the bat speed will increase the batted-ball speed.

For the tapered bat, decreasing the distance from the knob to the center of mass by 1.6% increased the distance between the center of mass and the center of percussion somewhere between zero and 6.7%. For the cupped bat, this distance was measured as an increase of 4.3%. Both methods increased the distance between the center of mass and the center of percussion. We are satisfied with these approximations, because the model is not very sensitive to this distance. Changing this distance by $\pm 4\%$ only changed the batted-ball speed by, on average, $\mp 0.08\%$.

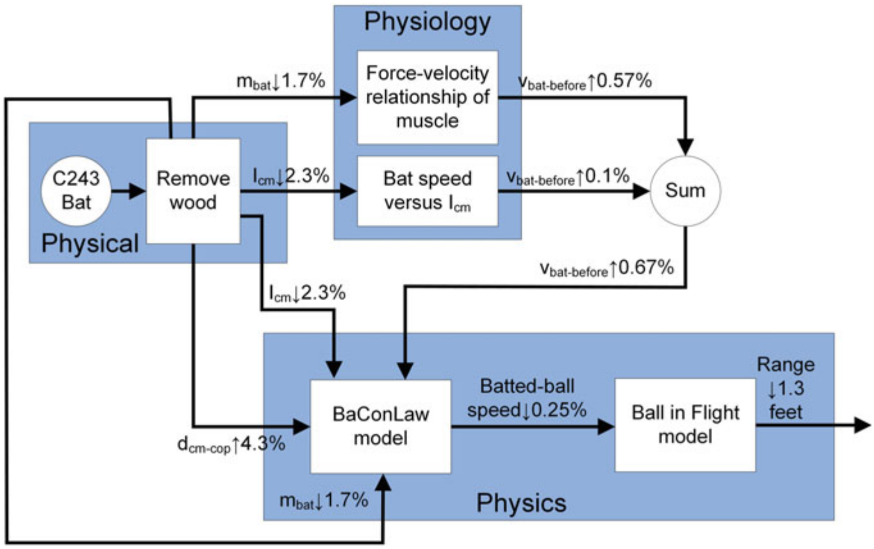

Fig. 4.13 Analysis process and numerical values for the C243 bat

There are four inputs to the BaConLaws model. When wood is removed from the end of the bat, the first two (m_{bat} and $I_{\text{bat-cm}}$) decrease, which decreases the batted-ball speed. However, the bat speed increases, which increases the batted-ball speed. The last input, the distance from the center of mass to the center of percussion, probably increases, which also decreases the batted-ball speed. Which of these four changes wins? We can only tell by deriving values for the parameters and using those in the equations of the BaConLaws model.

In the two modified bat examples that we examined in this section, the modified bats caused the batted-ball speed and therefore the ball's range to go down.

In conclusion, both tapering the barrel and cupping the barrel end of the bat decrease the batted-ball speed and subsequently decrease the range of the batted-ball. Why then would batters choose bats with the end cupped out? Perhaps, it is because they are more comfortable with the cupped bat, they don't understand the interaction of the parameters or the decrease in performance is small.

4.13 Outline of the BaConLaws Model Derivations

We started with Eq. (4.6) and solved for the bat angular velocity after the collision

$$dm_1(v_{1a} - v_{1b}) = -I_2(\omega_{2a} - \omega_{2b})$$

$$\omega_{2a} = \left\{ \omega_{2b} - \frac{dm_1}{I_2}(v_{1a} - v_{1b}) \right\}$$

Next, we used Eq. (4.5) and solved for the bat linear velocity after the collision

$$CoR_{2b} = -\frac{v_{1a} - v_{2a} - d\omega_{2a}}{v_{1b} - v_{2b} - d\omega_{2b}}$$

$$v_{2a} = v_{1a} + CoR_{2b}(v_{1b} - v_{2b} - d\omega_{2b}) - d\omega_{2a}$$

Then we substituted ω_{2a} into the above v_{2a} equation to get

$$v_{2a} = v_{1a} + CoR_{2b}\,(v_{1b} - v_{2b} - d\omega_{2b}) - d\left\{ \omega_{2b} - \frac{dm_1}{I_2}(v_{1a} - v_{1b}) \right\}$$

Finally, we used this v_{2a} in Eq. (4.4) to get Eq. (4.8) for the ball linear velocity after the collision, in terms of only the before collision variables and parameters. The linear velocity of the ball after the collision is

$$\begin{aligned} v_{\text{ball-after}} &= v_{\text{ball-before}} \\ &\quad - \frac{(v_{\text{ball-before}} - v_{\text{bat-cm-before}} - \omega_{\text{bat-before}} d_{\text{cm-ip}})(1 + CoR_{2b}) m_{\text{bat}} I_{\text{bat}}}{m_{\text{ball}} I_{\text{bat}} + m_{\text{bat}} I_{\text{bat}} + m_{\text{ball}} m_{\text{bat}} d_{\text{cm-ip}}^2} \end{aligned}$$

Then we solved Eqs. (4.4), (4.5) and (4.6) for the velocity of the bat after the collision in terms of only the before collision variables and parameters. The linear velocity of the bat after the collision is

$$\begin{aligned} v_{\text{bat-cm-after}} &= v_{\text{bat-cm-before}} \\ &\quad + \frac{(v_{\text{ball-before}} - v_{\text{bat-cm-before}} - \omega_{\text{bat-before}} d_{\text{cm-ip}})(1 + CoR_{2b}) m_{\text{ball}} I_{\text{bat}}}{m_{\text{ball}} I_{\text{bat}} + m_{\text{bat}} I_{\text{bat}} + m_{\text{ball}} m_{\text{bat}} d_{\text{cm-ip}}^2} \end{aligned}$$

Lastly, we solved Eqs. (4.4), (4.5) and (4.6) for the angular velocity of the bat after the collision, ω_{2a}, in terms of only the before collision variables and parameters. The angular velocity of the bat after the collision is

$$\begin{aligned} \omega_{\text{bat-after}} &= \omega_{\text{bat-before}} \\ &\quad + \frac{(v_{\text{ball-before}} - v_{\text{bat-cm-before}} - d_{\text{cm-ip}} \omega_{\text{bat-before}})(1 + CoR_{2b}) m_{\text{ball}} m_{\text{bat}} d_{\text{cm-ip}}}{m_{\text{ball}} I_{\text{bat}} + m_{\text{bat}} I_{\text{bat}} + m_{\text{ball}} m_{\text{bat}} d_{\text{cm-ip}}^2} \end{aligned}$$

To get a final equation for the angular velocity of the ball after the collision, ω_{1a}, we put $\omega_{2a} = \omega_{2b} - \frac{dm_1}{I_2}(v_{1a} - v_{1b})$ into the Conservation of Angular Momentum equation, Eq. (4.7s), and showed that for a head-on collision (with no friction or external forces) like this BaConLaws model, $\omega_{\text{ball-after}} = \omega_{\text{ball-before}}$.

4.14 Summary

In this chapter, we successfully incorporated Conservation of Energy into the set of bat–ball collision equations for the BaConLaws model. This Conservation of Energy equation confirmed the consistency of our set of derived equations. We also used Conservation of Energy to derive an equation for the kinetic energy lost in the collision. We derived a general equation for KE_{lost}, Eq. (4.11), and showed that if the collision were at the center of mass ($d_{\text{cm-ip}} = 0$), then this general equation reduced to an old well-known result, Eq. (3.2).

We did a sensitivity analysis on the set of equations for the BaConLaws model. It showed that the most important variable, in terms of increasing batted-ball speed, is the bat speed before the collision. Today, in the sporting world, the coefficient of restitution and the bat mass are experiencing the most experimentation for improving bat performance. However, in the future, bat moments of inertia allow for the most improvement of bat performance. Most importantly, future studies must include physics in conjunction with physiology.

The following equations comprise our BaConLaws model for bat–ball collisions. First, the kinetic energy lost or transformed.

$$KE_{\text{lost}} = \frac{1}{2}\frac{m_{\text{ball}} m_{\text{bat}} I_{\text{bat}} \left(v_{\text{ball-before}} - v_{\text{bat-cm-before}} - \omega_{\text{bat-before}} d_{\text{cm-ip}}\right)^2 \left(1 - CoR_{2b}^2\right)}{m_{\text{ball}} I_{\text{bat}} + m_{\text{bat}} I_{\text{bat}} + m_{\text{ball}} m_{\text{bat}} d_{\text{cm-ip}}^2}$$

where $d_{\text{cm-ip}}$ is the distance between the bat's center of mass and the impact point. The linear velocity of the ball after the collision is

$$v_{\text{ball-after}} = v_{\text{ball-before}} - \frac{\left(v_{\text{ball-before}} - v_{\text{bat-cm-before}} - \omega_{\text{bat-before}} d_{\text{cm-ip}}\right)(1 + CoR_{2\text{b}}) m_{\text{bat}} I_{\text{bat}}}{m_{\text{ball}} I_{\text{bat}} + m_{\text{bat}} I_{\text{bat}} + m_{\text{ball}} m_{\text{bat}} d_{\text{cm-ip}}^2}$$

The linear velocity of the bat after the collision is

$$v_{\text{bat-cm-after}} = v_{\text{bat-cm-before}} + \frac{\left(v_{\text{ball-before}} - v_{\text{bat-cm-before}} - \omega_{\text{bat-before}} d_{\text{cm-ip}}\right)(1 + CoR_{2\text{b}}) m_{\text{ball}} I_{\text{bat}}}{m_{\text{ball}} I_{\text{bat}} + m_{\text{bat}} I_{\text{bat}} + m_{\text{ball}} m_{\text{bat}} d_{\text{cm-ip}}^2}$$

The angular velocity of the bat after the collision is

$$\omega_{\text{bat-after}} = \omega_{\text{bat-before}} + \frac{\left(v_{\text{ball-before}} - v_{\text{bat-cm-before}} - d_{\text{cm-ip}} \omega_{\text{bat-before}}\right)(1 + CoR_{2\text{b}}) m_{\text{ball}} m_{\text{bat}} d_{\text{cm-ip}}}{m_{\text{ball}} I_{\text{bat}} + m_{\text{bat}} I_{\text{bat}} + m_{\text{ball}} m_{\text{bat}} d_{\text{cm-ip}}^2}$$

Our most succinct formulation of the BaConLaws model is

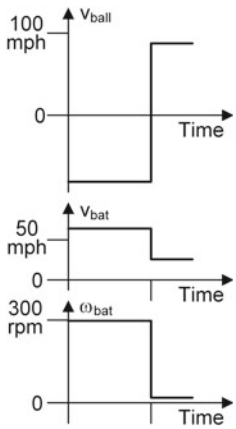

Fig. 4.14 Linear and angular velocities of the ball and bat

$$\boxed{\begin{aligned}
&A = \frac{\left(v_{\text{ball-before}} - v_{\text{bat-cm-before}} - d_{\text{cm-ip}}\,\omega_{\text{bat-before}}\right)(1 + CoR_{2b})}{m_{\text{ball}} I_{\text{bat}} + m_{\text{bat}} I_{\text{bat}} + m_{\text{ball}} m_{\text{bat}} d^2_{\text{cm-ip}}}\\
&CoR_{2b} = -\frac{v_{\text{ball-after}} - v_{\text{bat-cm-after}} - d_{\text{cm-ip}}\,\omega_{\text{bat-after}}}{v_{\text{ball-before}} - v_{\text{bat-cm-before}} - d_{\text{cm-ip}}\,\omega_{\text{bat-before}}}\\
&v_{\text{ball-after}} = v_{\text{ball-before}} - A m_{\text{bat}} I_{\text{bat}}\\
&v_{\text{bat-after}} = v_{\text{bat-before}} + A m_{\text{ball}} I_{\text{bat}}\\
&\omega_{\text{bat-after}} = \omega_{\text{bat-before}} + A m_{\text{ball}} m_{\text{bat}} d_{\text{cm-ip}}\\
&\omega_{\text{ball-after}} = \omega_{\text{ball-before}}
\end{aligned}}$$

The BaConLaws model describes the motion of the bat after the collision. This is a big deal. Many models describe the motion of the ball after the collision, but few (if any) describe the motion of the bat. When you see a batter hit a ball, do you see the jerk of the bat? Can you describe it? Well these equations do, as shown in Fig. 4.14.

This model for bat–ball collisions gives the linear and angular velocity of the bat and ball after the collision in terms of the linear and angular velocity of the bat and ball before the collision. It uses only the fundamental principles of Newtonian mechanics and the conservation laws. This chapter also fulfills the second purpose of this book, namely, to show what the batter can do to achieve an optimally performing bat, namely, select lightweight, end-loaded bats. Finally, cupping the barrel end of the bat does not increase the ball's range.

Fig. 4.15 Sir Francis Bacon the father of the scientific method, which is based on unbiased observation and induction

References

Bahill, A. T. (2004). The ideal moment of inertia for a baseball or softball bat. *IEEE Transactions on Systems, Man, and Cybernetics Part A: Systems and Humans, 34*(2), 197–204.

Bahill, A. T., Baldwin, D. G., & Ramberg, J. S. (2009). Effects of altitude and atmospheric conditions on the flight of a baseball. *International Journal of Sports Science and Engineering, 3*(2), 109–128. http://www.worldacademicunion.com/journal/SSCI/sscivol03no02paper07.pdf. ISSN 1750-9823 (print).

Bahill, A. T., & Karnavas, W. J. (1989). Determining ideal baseball bat weights using muscle force-velocity relationships. *Biological Cybernetics, 62,* 89–97.

Bahill, A. T., & Karnavas, W. J. (1991, April 6). The ideal baseball bat. *New Scientist, 130*(1763), 26–31.

Bahill, A. T., & Madni, A. M. (2017). *Tradeoff decisions in system design*. Springer Publishing Company, New York. ISBN 978-3-319-43710-1.

Bahill, A. T., & Morna Freitas, M. (1995). Two methods for recommending bat weights. *Annals of Biomedical Engineering, 23/4,* 436–444.

Baldwin, D. (2007). *Snake Jazz*. Xlibris Corporation. http://www.xlibris.com/Bookstore/BookSearchResults.aspx?Title=Snake+Jazz&Author=Baldwin&.

Baldwin, D. G., & Bahill, A. T. (2004). A model of the bat's vertical sweetness gradient. *The Engineering of Sport, 5*(2). In M. Hubbard, R. D. Mehta, & J. M. Pallis (Eds.), *Proceedings of the 5th International Engineering of Sport Conference*, September 13–16, 2004. Davis, C. A. (2004). International Sports Engineering Association (ISEA), Sheffield, England (pp. 305–311).

Brancazio, P. (1984). *Sport science: Physical laws and optimum performance*. New York: Simon and Schuster.

Choi, K. K., & Kim, M. H. (2005). *Structural sensitivity analysis and optimization 1: Linear systems*. New York, NY: Springer Science+Bussiness Media Inc.

Crisco, J. J., Rainbow, M. J., Schwartz, J. B., & Wilcox, B. J. (2014). Batting cage performance of wood and nonwood youth baseball bats. *Journal of Applied Biomechanics, 30,* 237–243. https://doi.org/10.1123/jab.2012-0178.

Cross, R. (2011). *Physics of baseball and softball*. New York: Springer.

Hill, A. V. (1938). The heat of shortening and dynamic constraints of muscle. *Proceedings of the Royal Society of London, 126B,* 136–195.

Kensrud, J. R., Nathan, A. M., & Smith, L. V. (2016, October). Oblique collisions of baseballs and softballs with a bat, *American Journal of Physics*.

Kirkpatrick, P. (1963). Batting the ball. *American Journal of Physics, 31*(8), 606–613. https://doi.org/10.1119/1.1969691.

Nathan, A. M. (2003). Characterizing the performance of baseball bats. *American Journal of Physics, 71,* 134–143.

Nathan, A. M., Smith, L. V., Faber, W. L., & Russell, D. A. (2011). Corked bats, juiced balls, and humidors: The physics of cheating in baseball. *American Journal of Physics, 79*(6), 575–580.

Nathan, A. M., Cantakos, J., Kesman, R., Mathew, B., & Lukash, W. (2012). Spin of a batted baseball. *Procedia Engineering, 34,* 182–187. In *9th Conference of the International Sports Engineering Association (ISEA)*. https://doi.org/10.1016/j.proeng.2012.04.032.

Smith, E. D., Szidarovszky, F., Karnavas, W. J., & Bahill, A. T. (2008). Sensitivity analysis, a powerful system validation technique. *The Open Cybernetics and Systemics Journal, 2,* 39–56. https://doi.org/10.2174/1874110X00802010039.

Smith, L., & Kensrud, J. (2014). Field and laboratory measurements of softball player swing speed and bat performance. *Sports Engineering, 17,* 75–82. https://doi.org/10.1007/s12283-013-0126-y.

Vedula, G., & Sherwood, J. A. (2004). An experimental and finite element study of the relationship amongst the sweet spot, COP and vibration nodes in baseball bats. In M. Hubbard, R. D. Mehta, & J. M. Pallis (Eds.), *Proceedings of the 5th Conference of Engineering of Sport* (vol. 2, pp. 626–632). International Sports Engineering Association (ISEA). ISBN 0-9547861-1-4.

Watts, R. G., & Bahill, A. T. *Keep your eye on the ball: Curveballs, knuckleballs, and fallacies of baseball*. New York: W. H. Freeman and Co., first edition, 1990, second edition 2000.

Chapter 5
Alternative Models

5.1 Introduction

Purpose: The purpose of this chapter is to present four alternatives to the BaConLaws model, explain their different purposes and explain why each might be used for a different purpose.

This chapter contains four models that are more complicated than our BaConLaws model of Chap. 4. The first one, the Effective Mass model, is an analog to the BaConLaws model. The bat Effective Mass model and the BaConLaws model both start with Newton's axioms: then they diverge. They are different: however, they yield the same rule of thumb for the batted-ball speed! This should strengthen and give people more confidence in both models. The second and third models in this chapter allow movement of the knob. The Spiral Center of Mass model shows the movement of the center of mass of the bat before the collision. The Sliding Pin model analyzes the movement of the bat with a translation and a rotation about its *knob*. It illustrates the concept of using different models for different purposes. The fourth model challenges our simple technique of using only Newton's axioms and the conservation laws. It is for a collision at the center of percussion of the bat with spin on the pitch and with consideration of friction between the bat and ball. Its purpose is to show a situation that cannot be modeled using only the conservation laws.

Modeling philosophy note. Having several alternative models helps ensure that you understand the physical system. No model is more correct than another. They just emphasize different aspects of the physical system. They are not competing models; they are synergetic.

A. T. Bahill, *The Science of Baseball*,
https://doi.org/10.1007/978-3-030-03032-2_5

5.2 Bat Effective Mass Model

Purpose: The purpose of this section is to present the bat Effective Mass model. Presently, it is the most popular physics-of-baseball model for bat–ball collisions. It will be compared to the BaConLaws model.

The bat effective mass bat–ball collision modeling community, established by Nathan (2003) and summarized nicely by Cross (2011), base their model on the concept of the effective mass of a bat. This section on the Effective Mass model is excerpted from Cross (2011). Consider Fig. 5.1 where a ball of mass m_{ball} collides with a stationary bat at a distance B from the center of mass (cm) of the bat. {Previously in this book, we have used the symbol $d_{\text{cm-ip}}$ to represent the distance between the center of mass and the impact point, or $d_{\text{cm-ss}}$ if the collision were at the sweet spot. However, in this section, to avoid confusion with the derivative operator used by Cross, we will use the letter B, as was done by Watts and Bahill (1990/2000).} Let the mass of the bat be m_{bat} and suppose that the bat is initially at rest and freely supported: that is, no one is holding the handle. In that case, the ball will bounce off the bat and the bat will be set in motion. The center of mass of the bat and the impact point on the bat both recoil. Because a bat is a rigid object, every spot on a bat will have the same linear translational velocity and the same angular rotational velocity. But each spot will have a different *total* velocity that depends on its distance from the pivot point. We define that total velocity of the bat is the sum of its linear translational velocity and its weighted angular rotation velocity: $vt_{\text{bat}} = v_{\text{cm}} + B\omega_{\text{bat}}$. We have used the symbol vt to represent the total velocity, e.g., $vt_{\text{bat-impact-after}}$, to differentiate from it from $v_{\text{bat-cm-after}}$ used in the rest of this book to indicate only the translational component of velocity. Because the bat rotates about its center of mass when it is struck by the ball, the speed of the impact point will be greater than the speed of the center of mass, $vt_{\text{impact}} > v_{\text{cm}}$. The impact point therefore accelerates faster than the center of mass of the bat, as if it were an isolated mass separate from the rest of the bat.

The whole bat is involved in the collision, but the effect on the ball is equivalent to a collision with an isolated *effective mass* M_{eff} that is less than the mass of the whole bat. Additionally, the impact point recoils as if it were a mass of M_{eff}. In

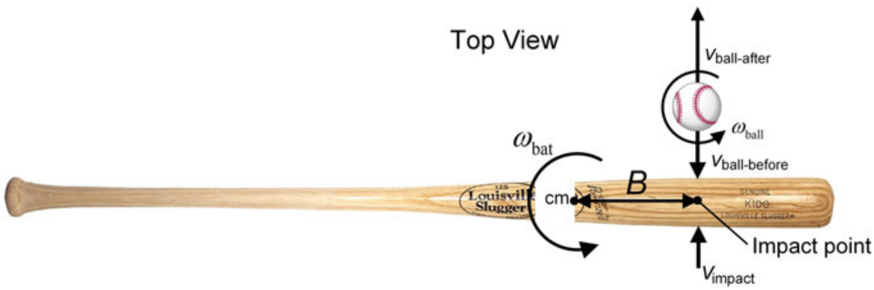

Fig. 5.1 The Effective Mass model for bat–ball collisions

other words, we can treat the collision as being equivalent to one between a ball of mass m_{ball} and an object of mass M_{eff}. We will now derive a formula for the effective mass of a bat.

Let M_{eff} be the effective mass of the bat at the impact point. A force F acting at the impact point will cause this point and the center of mass to accelerate according to these relationships $F = M_{\text{eff}} \frac{dvt_{\text{bat-impact}}}{dt}$ and $F = m_{\text{bat}} \frac{dv_{\text{bat-cm}}}{dt}$, respectively. The torque $F \times B$ causes the whole bat to rotate about its center of mass according to $F \times B = I_{\text{bat-cm}} \frac{d\omega_{\text{bat-cm}}}{dt}$ where $\omega_{\text{bat-cm}}$ is the angular velocity of the bat about its center of mass. Therefore,

$$F = M_{\text{eff}} \frac{dvt_{\text{bat-impact}}}{dt} = m_{\text{bat}} \frac{dv_{\text{bat-cm}}}{dt} = \frac{I_{\text{bat-cm}}}{B} \frac{d\omega_{\text{bat-cm}}}{dt}$$

The impact point rotates at a speed of $B\omega_{\text{bat-cm}}$ with respect to the bat's center of mass. So now, the impact point has a linear translational motion and an angular rotational motion. Hence, $vt_{\text{bat-impact}} = v_{\text{bat-cm}} + B\omega_{\text{bat-cm}}$. Taking the derivative with respect to time, we get

$$\frac{dvt_{\text{bat-impact}}}{dt} = \frac{dv_{\text{bat-cm}}}{dt} + B \frac{d\omega_{\text{bat-cm}}}{dt}$$

which can be written as

$$\frac{F}{M_{\text{eff}}} = \frac{F}{m_{\text{bat}}} + \frac{B^2 F}{I_{\text{bat-cm}}}$$

Dividing by F produces

$$\frac{1}{M_{\text{eff}}} = \frac{1}{m_{\text{bat}}} + \frac{B^2}{I_{\text{bat-cm}}}$$

which can be rearranged to give

$$M_{\text{eff}} = \frac{m_{\text{bat}}}{1 + \frac{m_{\text{bat}} B^2}{I_{\text{bat-cm}}}} \tag{5.1}$$

In summary, Fig. 5.1 suggests that a ball impacting a stationary bat, at distance B from the center of mass of the bat, will cause the bat to rotate about the center of mass. However, the speed and acceleration of the impact point are greater than that for the bat's center of mass, so the effective mass at the impact point is less than the mass of the whole bat. For the bat of Table 1.1 $M_{\text{eff}} = 0.707$ kg.

There are three important differences between this model and the BaConLaws model developed in Chap. 4. (1) In Fig. 5.1, $v_{\text{ball-before}}$ is pointing down and it is *positive* in that direction: for the rest of the book $v_{\text{ball-before}}$ was positive in the x-direction. {However, $v_{\text{ball-after}}$ is still defined to be positive in the direction of the

x-axis.} That is why there is a minus sign in front of the $m_{\text{ball}} v_{\text{ball-before}}$ term in conservation of momentum Eq. (5.2). (2) In this model, vt_{impact} is the *total* velocity of the impact point. That is, it is the sum of the translational velocity and the velocity due to rotation about the center of mass. (3) Because vt_{impact} is the sum of the translational and rotational velocities, the coefficient of restitution equation has only two terms on top and bottom, that is $e = \frac{v_{\text{ball-after}} - vt_{\text{bat-after}}}{v_{\text{ball-before}} + vt_{\text{bat-before}}}$, instead of three as in Eqs. (3.5) and (4.5).

Our next task is to get an equation for the velocity of the ball after the collision. We will start with an equation for the conservation of momentum. From here on, we no longer require a stationary bat before the collision.

$$M_{\text{eff}} vt_{\text{bat-before}} - m_{\text{ball}} v_{\text{ball-before}} = M_{\text{eff}} vt_{\text{bat-after}} + m_{\text{ball}} v_{\text{ball-after}} \tag{5.2}$$

Note this is different from the conservation of momentum equation used in the rest of this book because of the different definitions of the direction of the ball before the collision.

Next, we need the coefficient of restitution.

$$e = \frac{v_{\text{ball-after}} - vt_{\text{bat-after}}}{v_{\text{ball-before}} + vt_{\text{bat-before}}}$$

We use this expression to eliminate $vt_{\text{bat-after}}$ in Eq. (5.2). Substitute the coefficient of restitution into Eq. (5.2) and we get

$$v_{\text{ball-after}} = \left(\frac{e - \frac{m_{\text{ball}}}{M_{\text{eff}}}}{1 + \frac{m_{\text{ball}}}{M_{\text{eff}}}} \right) v_{\text{ball-before}} + \left(\frac{1 + e}{1 + \frac{m_{\text{ball}}}{M_{\text{eff}}}} \right) vt_{\text{bat-before}}$$

Plug in M_{eff}

$$v_{\text{ball-after}} = \left(\frac{e - \frac{m_{\text{ball}}}{\frac{m_{\text{bat}}}{1 + \frac{m_{\text{bat}} B^2}{I_{\text{bat-cm}}}}}}{1 + \frac{m_{\text{ball}}}{\frac{m_{\text{bat}}}{1 + \frac{m_{\text{bat}} B^2}{I_{\text{bat-cm}}}}}} \right) v_{\text{ball-before}} + \left(\frac{1 + e}{1 + \frac{m_{\text{ball}}}{\frac{m_{\text{bat}}}{1 + \frac{m_{\text{bat}} B^2}{I_{\text{bat-cm}}}}}} \right) vt_{\text{bat-before}}$$

Ten algebraic steps yield our final expression for the *batted-ball velocity*.

$$\begin{aligned} v_{\text{ball-after}} = & -v_{\text{ball-before}} \left(\frac{m_{\text{ball}} I_{\text{bat-cm}} - m_{\text{bat}} I_{\text{bat-cm}} e + m_{\text{ball}} m_{\text{bat}} B^2}{m_{\text{ball}} I_{\text{bat-cm}} + m_{\text{bat}} I_{\text{bat-cm}} + + m_{\text{ball}} m_{\text{bat}} B^2} \right) \\ & + vt_{\text{bat-before}} \left(\frac{m_{\text{bat}} I_{\text{bat-cm}} (1 + e)}{m_{\text{ball}} I_{\text{bat-cm}} + m_{\text{bat}} I_{\text{bat-cm}} + + m_{\text{ball}} m_{\text{bat}} B^2} \right) \end{aligned} \tag{5.3}$$

This is the end of the derivation of the batted-ball velocity equation using the Effective Mass model. Now, compare Eq. (5.3) with Eq. (4.8) from our BaConLaws model.

$$
\begin{aligned}
v_{\text{ball-after}} = {} & v_{\text{ball-before}} \frac{(m_{\text{ball}} I_{\text{bat}} - m_{\text{bat}} I_{\text{bat}} CoR_{2\text{b}} + m_{\text{ball}} m_{\text{bat}} d^2)}{m_{\text{ball}} I_{\text{bat}} + m_{\text{bat}} I_{\text{bat}} + m_{\text{ball}} m_{\text{bat}} d^2} \\
& + v_{\text{bat-cm-before}} \frac{m_{\text{bat}} I_{\text{bat}} (1 + CoR_{2\text{b}})}{m_{\text{ball}} I_{\text{bat}} + m_{\text{bat}} I_{\text{bat}} + m_{\text{ball}} m_{\text{bat}} d^2} \\
& + \omega_{\text{bat-before}} \frac{m_{\text{bat}} d I_{\text{bat}} (1 + CoR_{2\text{b}})}{m_{\text{ball}} I_{\text{bat}} + m_{\text{bat}} I_{\text{bat}} + m_{\text{ball}} m_{\text{bat}} d^2}
\end{aligned}
$$

The differences are that in the Effective Mass model, the first term on the right of Eq. (5.3) has a minus sign because the initial ball velocity was defined to be positive downward in Fig. 5.1. (2) In the Effective Mass model, the second term on the right is equivalent to two terms in the BaConLaws model because of the definition $vt_{\text{bat-impact-before}} = v_{\text{bat-cm-before}} + B\omega_{\text{bat-cm-before}}$. (3) Because of that definition, $e \neq CoR_{2\text{b}}$.

Returning to the exposition of Cross (2011), he then states that if a ball with velocity $v_{\text{ball-before}}$ collides with a stationary bat and bounces back with a velocity $v_{\text{ball-after}}$ then

$$
q = \frac{v_{\text{ball-after}}}{v_{\text{ball-before}}}
$$

Now, and most importantly,

$$
q = \left(\frac{e - \frac{m_{\text{ball}}}{M_{\text{eff}}}}{1 + \frac{m_{\text{ball}}}{M_{\text{eff}}}} \right) \text{ and } 1 + q = \frac{1 + e}{1 + \frac{m_{\text{ball}}}{M_{\text{eff}}}}
$$

Using this new symbol, Eq. (5.3) for $v_{\text{ball-after}}$ becomes

$$
v_{\text{ball-after}} = q v_{\text{ball-before}} + (1 + q) vt_{\text{bat-before}}
$$

This equation holds for bats that are freely suspended and rotate about their centers of mass, as shown in Fig. 5.1. Rod Cross continues with, “This is the primary physics equation that describes the outgoing speed of a struck ball, regardless of whether the ball is struck by a bat or a racquet or a club. The performance of any given striking implement depends mainly on the value of q for that implement.” However, $v_{\text{ball-before}}$ and $vt_{\text{bat-before}}$ require some considerations. For example, $vt_{\text{bat-before}}$ depends on the impact point, the mass of the ball, the mass of the bat, the moment of inertia of the bat and characteristics of the person swinging the bat. In addition, the coefficient of restitution, *e,* is not a constant. It depends on the impact point and the pivot point, as well as the speed of the collision, the relative humidity, the temperature, the deformation of the objects, the surface texture and the type of ball. However, in spite of these variabilities, Nathan (2003) and Cross (2011) found that for most baseball collisions

$$v_{\text{ball-after}} = 0.2v_{\text{ball-before}} + 1.2vt_{\text{bat-before}}$$

On the other hand, let us now use Eq. (4.8) the batted-ball velocity equation from the BaConLaws model.

$$\begin{aligned} v_{\text{ball-after}} = v_{\text{ball-before}} & \frac{(m_{\text{ball}}I_{\text{bat}} - m_{\text{bat}}I_{\text{bat}}CoR_{2\text{b}} + m_{\text{ball}}m_{\text{bat}}d^2)}{m_{\text{ball}}I_{\text{bat}} + m_{\text{bat}}I_{\text{bat}} + m_{\text{ball}}m_{\text{bat}}d^2} \\ & + v_{\text{bat-cm-before}} \frac{m_{\text{bat}}I_{\text{bat}}(1 + CoR_{2\text{b}})}{m_{\text{ball}}I_{\text{bat}} + m_{\text{bat}}I_{\text{bat}} + m_{\text{ball}}m_{\text{bat}}d^2} \\ & + d_{\text{cm-ip}}\omega_{\text{bat-before}} \frac{m_{bat}I_{bat}(1 + CoR_{2\text{b}})}{m_{\text{ball}}I_{\text{bat}} + m_{\text{bat}}I_{\text{bat}} + m_{\text{ball}}m_{\text{bat}}d^2} \end{aligned}$$

If we substitute parameter values for a major league wooden bat, as described in Table 1.1, into this equation, then the velocity of the ball after the collision becomes

$$v_{\text{ball-after}} = -0.217v_{\text{ball-before}} + 1.217\left\{v_{\text{bat-cm-before}} + d_{\text{cm-ip}}\omega_{\text{bat-before}}\right\}$$

where the units are m/s and rad/s. Remember that the velocity of the ball before the collision is a negative number. So far, we have made no approximations; everything has been exactly according to Newton's axioms and the conservation laws. In contrast, we will now create our *rule of thumb* by using pitch speed instead of the ball collision speed and using total bat speed instead of its two components.

$$\boxed{\text{batted-ball speed} = -0.19\,\text{pitch speed} + 1.22\,\text{total bat speed}}$$

The units could be m/s or mph. The pitch speed would be that determined by a radar gun focused near the pitcher's release point and announced on television. The bat speed would come from Tables such as 3.9 and 4.2. Using our typical data of Table 4.2, we have an average pitch speed of −92 mph and a total bat speed of 62 mph. Putting these numbers into our rule of thumb yields

$$\text{batted-ball speed} = 0.19 \times 92 + 1.22 \times 62 = 93\,\text{mph}$$

which is just about the average for major league hits. Using the data of Willman (2017), we found that for the 15,000 base hits in major league baseball in 2016, the average batted-ball speed was 91 mph.

The bat Effective Mass model and the BaConLaws model both start with Newton's axioms: then they diverge. They are different: however, they yield the same rule of thumb for the batted-ball speed! This should strengthen and give people more confidence in both models.

Modeling philosophy note. Having several alternative models helps ensure that you understand the physical system. No model is more correct than another. They just emphasize different aspects of the physical system. They are not competing models; they are synergetic.

5.3 The Sliding Pin Model

Purpose: The purpose of this section is to present the Spiral Center of Mass model, the moving pivot point data and the Sliding Pin model. These all use a different *type* of data from the rest of the book, namely, a translation of the knob and a rotation about the knob. The BaConLaws model of Chap. 4 assumes a free-end collision. The rotation of the bat is about its center of mass. And it is a theory-based model, whereas the sliding pin model is not for a free-end collision. Its rotation is about the knob of the bat. And it is a data-based model. Both the BaConLaws model and the Sliding Pin model derive equations for the speed and spin of the bat and ball after the collision in terms of these same variables before the collision.

5.3.1 Spiral Center of Mass Model

Cross (2009) developed an intriguing model for the swing of the bat. It is based on data from a video-camera system that measured the translation and rotation about the center of mass. The pivot point of the bat moved during the swing. In the Spiral Center of Mass model, the center of mass of the bat followed a logarithmic spiral pathway described with this equation $R = 0.25e^{0.23\theta}$. Figure 5.2 shows this movement.

The Spiral Center of Mass model models the swing of the bat and not the bat–ball collision like the BaConLaws and the Sliding Pin models do.

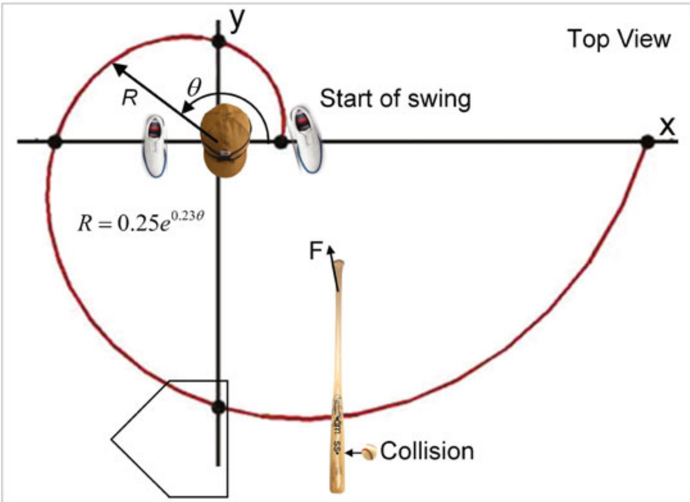

Fig. 5.2 The Spiral Center of Mass model of Cross (2009). In this top view, the batter's head is at the intersection of the x- and y-axes and his left foot is to the right

5.3.2 *The Sliding Pin Model*

With the advent of low-cost multiple-video-camera systems for making three-dimensional (3D) measurements of the movement of the bat, a new source of data became available. Using these data, the Sliding Pin model models the movement of the bat with a translation and a rotation about its *knob*. It is shown in Fig. 5.3. The bat is pinned through the knob, so it is forced to rotate about the knob. But the pin is allowed to slide along the *x*-axis (up and down in Fig. 5.4) to allow for the translational velocity of the bat.

Generalization. Imagine a baseball bat rotating in space. Because the bat is a rigid object, for any given pivot point, all points on the bat must have the same angular velocity. Next if there are no rotations just a translation, then all points on the bat will have the same linear velocity. If there are a rotation and a translation, then each point on the bat will have a total velocity that is equal to the linear velocity of the pivot point plus the angular velocity of the pivot point times its distance from the pivot point.

Fig. 5.3 Sliding Pin model for a bat pivoting about its knob

Fig. 5.4 Detail of a sliding pin joint

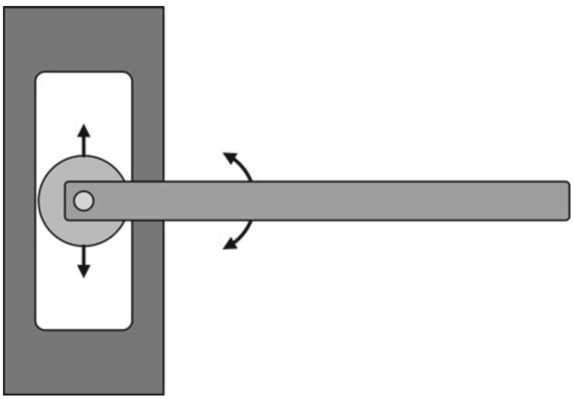

Now consider a bat that is pinned through its knob, but the pinned point is allowed to slide up and down, as in Fig. 5.4. Each spot on the bat will have a *total* velocity that depends on the location of the pivot point and the spot's distance from the pivot point.

$$vt_{\text{cm}} = v_{\text{knob}} + d_{\text{knob-cm}}\beta_{\text{bat}}$$
$$vt_{\text{cop}} = v_{\text{knob}} + d_{\text{knob-cop}}\beta_{\text{bat}}$$

5.3.3 *Moving Pivot Point Data*

Table 3.9 gave the bat sweet-spot speeds as numbers that combined the linear speed of the center of mass and the angular rotation of the bat about that point. However, data by from Fleisig et al. (2001, 2002), Cross (2009), Milanovich and Nesbit (2014), King et al. (2012) gave us a new type of data to model. They gave us simultaneous independent measurements of linear velocity and angular rotational velocity.

Milanovich and Nesbit (2014) studied 14 female collegiate softball players. They used multiple video cameras to collect data and they created three-dimensional reconstructions of bat swings. Using their Table II, which averages the data of all subjects and all swings of their aluminum bat, we will now solve for the velocity of the center of mass.

Using data from their measurements at the pivot point (the knob)

$$\beta_{\text{before}} = 29.6$$
$$vt_{\text{cm}} = v_{\text{knob}} + d_{\text{knob-cm}}\beta_{\text{before}}$$
$$vt_{\text{cm}} = 3.6 + 0.48 \times 29.6 = 17.8\,\text{m/s}$$

Using data from their measurements at the sweet spot (the center of percussion)

$$vt_{\text{cop}} = v_{\text{knob}} + d_{\text{knob-cop}}\beta_{\text{before}}$$
$$vt_{\text{cm}} = vt_{\text{cop}} - d_{\text{cm-cop}}\beta_{\text{before}}$$
$$vt_{\text{cm}} = 15.9\,\text{m/s}$$

Finally, using data from their measurements at the center of mass

$$vt_{\text{cm}} = 16.1\,\text{m/s}$$

So, their measurements for vt_{cm} of 17.8, 15.9 and 16.1 m/s are reasonably consistent.

Now, let us move on to other studies that made simultaneous independent measurements of the linear translational velocity and the angular rotational velocity.

The average sweet-spot speeds from the study of Fleisig et al. (2001, 2002) for 16 male baseball players were

$vt_{\mathrm{cop}} = 27\,\mathrm{m/s}$ and $\beta = 38\,\mathrm{rad/s}$

Cross (2009) had a single male subject with

$v_{\mathrm{cm}} = 16.5\,\mathrm{m/s}$ and $\beta = 33\,\mathrm{r/s}$

King et al. (2012) had one male subject with

$v_{\mathrm{knob}} = 6\,\mathrm{m/s}$ and $\beta = 36\,\mathrm{r/s}$

There are several reasons for differences in the experimental values. (1) Men swing the bat faster than women do. The average sweet-spot speed at impact of Milanovich and Nesbit (2014) was 20 m/s. Table 3.9 shows that male baseball players typically have higher speeds than this. Fleisig et al. (2002) measured 17 college women at 21 m/s and 16 college men at 27 m/s. Bahill (2004) measured 20 university women at 21 m/s and 28 major leaguers at 26 m/s. (2) The aluminum bat swung by the Milanovich and Nesbit (2014) subjects was lighter than the wooden bats used in the other studies. (3) Averaging data from many subjects produced slower results, particularly when the women were not elite athletes and therefore had more variability. (4) The low frame rate of the motion capture cameras low-pass filtered the data and attenuated the velocities. Further smoothing and processing reduced the velocities even more. (5) The bat rotates about a point in or nearby the knob, but there is variability in this point. Indeed, in early phases of the swing, the pivot point is outside of the knob. But when the bat reaches the collision point, the pivot point has come inside the knob. (6) They gave data for the movement of the grip, which was six inches away from the knob. (7) Figure 5.3 is not for a free-end collision. The hands are still holding the bat at the collision point and they might be applying forces to the bat. However, all of their variables (yaw, pitch, roll and v_{knob}) reach their peak values before the collision point. Therefore, if the hands were applying forces, these forces were not accelerating the bat in the x-direction. Furthermore, if the collision were at the center of percussion, then the collision would not create forces at the pivot point. (8) Experimental data are always subject to noise and measurement error.

Our most comprehensive data for bat swings come from William Clark, Founder of Diamond Kinetics (personal communication, 2017). Table 5.1 shows their data for 200 male professional baseball players swinging 33-inch wooden bats.

In this table, the variances in the angular velocity of the center of mass and sweet spot are small. These data produced this equation $vt_{\text{bat-cop-before}} = v_{\mathrm{knob}} + d_{\text{k-cop}}\beta_{\mathrm{b}} = 4.5 + 0.7 \times 41 = 33\,\mathrm{m/s} = 74\,\mathrm{mph}$, which we used in our simulations, whose outputs are shown in Tables 5.3 and 5.4. This equation has the same

Table 5.1 Linear, angular and total bat speeds for 20,000 swings by male professional batters

Variable	SI units	Baseball units
Linear knob speed, $v_{\text{bat-knob-before}}$	4.5 m/s, $\sigma = 1.7$	10.1 mph, $\sigma = 3.9$
Angular velocity, $\beta_{\text{bat-before}}$	41 rad/s, $\sigma = 5$	387 rpm, $\sigma = 51$
Total speed of the center of mass $vt_{\text{cm-before}} = v_{\text{knob-before}} + d_{\text{knob-cm}}\beta_{\text{bat-before}}$	27.9 m/s, $\sigma = 3.7$	62.3 mph, $\sigma = 8.2$
Total speed of the sweet spot $vt_{\text{cop-before}} = v_{\text{knob-before}} + d_{\text{knob-cop}}\beta_{\text{bat-before}}$	33.3 m/s, $\sigma = 4.3$	74.5 mph, $\sigma = 9.6$

six-to-one ratio of $d_{\text{k-cop}}\beta_{\text{before}}$ and v_{knob} as our frame-by-frame analysis of the swing of a major league batter. The best aspect of these data is that standard deviations are given. The worst aspect is that the angular velocity and total speed of the sweet spot are higher than those reported in Table 3.9.

5.3.4 Back to the Sliding Pin Model

Purpose: The purpose of the Sliding Pin model is to model a new type of data different from the rest of the book. Previously, the input data for our models were the translational and rotational velocities at the center of mass of the bat. The Sliding Pin model uses the translational and rotational velocities at the *knob*.

The Sliding Pin model is unique in the science of baseball literature. It has four equations and four unknowns. This new model is described in Fig. 5.3 and Table 5.2. Its purposes are (1) to show the limits of the conservation law modeling technique and (2) to model some unique new experimental data. Unlike the BaConLaws model and the Effective Mass model, it is data-driven not theory-driven.

At the beginning of this section, we must emphasize that the BaConLaws model given in Fig. 4.1 and Table 4.1 is not equivalent to the Sliding Pin model of Fig. 5.3 and Table 5.2. Although the equations may look analogous, many of them are different, because they are modeling different things. The BaConLaws model is for a free-end collision of an unsupported bat that will translate and rotate about its center of mass. The Sliding Pin model is for the collision of a restrained bat. The bat is being forced to rotate about its knob. The human is doing the restraining by applying forces on the handle during the swing. To make this perfectly clear, let us simplify the situation by ignoring translations and consider only rotations. The bat of Fig. 4.1 will rotate about its center of mass with an initial angular velocity of

Table 5.2 Synopsis of equations for the Sliding Pin, four equations and four unknowns

Inputs	$v_{\text{ball-before}},\ \omega_{\text{ball-before}},\ v_{\text{knob-before}},\ \beta_{\text{knob-before}}$ and CoR_{2c}
Outputs	$v_{\text{ball-after}},\ \omega_{\text{ball-after}},\ v_{\text{bat-ip-after}},\ \beta_{\text{knob-after}}$ and KE_{lost}
Equations	
Conservation of Linear Momentum, Eq. (5.4)	$m_{\text{ball}} v_{\text{ball-before}} + m_{\text{bat}} v_{\text{bat-before}} = m_{\text{ball}} v_{\text{ball-after}} + m_{\text{bat}} v_{\text{bat-after}}$
Definition of *CoR*, Eq. (5.5)	$CoR_{2c} = -\frac{v_{\text{ball-after}} - v_{\text{knob-after}} - d_{\text{knob-ip}}\beta_{\text{before}}}{v_{\text{ball-before}} - v_{\text{knob-before}} - d_{\text{knob-ip}}\beta_{\text{after}}}$
Newton's Second Law, Eq. (5.6)	$d_{\text{k-ip}} m_{\text{ball}} (v_{\text{ball-after}} - v_{\text{ball-before}}) = -I_{\text{knob}} (\beta_{\text{after}} - \beta_{\text{before}})$
Conservation of Angular Momentum about the z-axis, Eq. (5.7s)	$m_{\text{ball}} d_{\text{k-ip}} v_{\text{ball-before}} + \left(I_{\text{ball}} + m_{\text{ball}} d_{\text{k-ip}}^2\right) \omega_{\text{ball-before}} + (I_{\text{knob}}) \beta_{\text{before}} =$ $+ m_{\text{ball}} d_{\text{k-ip}} v_{\text{ball-after}} + \left(I_{\text{ball}} + m_{\text{ball}} d_{\text{k-ip}}^2\right) \omega_{\text{ball-after}} + (I_{\text{knob}}) \beta_{\text{after}}$

$\omega_{\text{bat-before}}$. This will give it an initial kinetic energy of $\frac{I_{\text{cm}}\omega^2_{\text{bat-before}}}{2}$, whereas the bat of Fig. 5.3 will rotate about its knob with an initial angular velocity of β_{before}. This will give it a kinetic energy of $\frac{I_{\text{knob}}\beta^2_{\text{before}}}{2}$. If the models were equivalent, then $\frac{I_{\text{cm}}\omega^2_{\text{bat-before}}}{2} = \frac{I_{\text{knob}}\beta^2_{\text{before}}}{2}$. By the parallel axis theorem $I_{\text{knob}} = I_{\text{cm}} + m_{\text{bat}}d^2_{\text{k-cm}}$, which means that the following equation would have to be true: $I_{\text{cm}}\omega^2_{\text{bat-before}} = \left(I_{\text{cm}} + m_{\text{bat}}d^2_{\text{k-cm}}\right)\beta^2_{\text{before}}$. This would require $\omega_{\text{bat-before}} = \sqrt{\beta^2_{\text{before}} + \frac{m_{\text{bat}}d^2_{\text{k-cm}}}{I_{\text{cm}}}}$. Clearly, $\omega_{\text{bat-before}} \neq \beta_{\text{before}}$ and therefore the BaConLaws model is not equivalent to the Sliding Pin model. The cause of this difference is that the BaConLaws model is for a free-end collision, whereas in the Sliding Pin model the batter is applying forces to the handle during the swing. The Sliding Pin model is more complicated than the BaConLaws model. Therefore, the Sliding Pin model takes our bat–ball collision modeling community a baby step upward.

Configuration 2c is for a collision at the sweet spot of the bat with spin on the pitch. It adds a new model for bat motion: the movement of the bat comprises a translation and a rotation about its knob. Because of this, we need a different equation for the *CoR*. This model is original. Our previous configurations, 2a and 2b, measured and used the total velocity (translational plus angular velocity) for the velocity of the sweet spot before and after the collision. However, the experimental studies examined in the previous sections gave independent linear and angular speeds of the bat about the *knob* right before the collision. We will now see if our modeling approach can accommodate this new data.

Modeling philosophy note. In general, there are two common techniques for modeling systems: the first is theory-based and the second is data-based. Here are some steps for theory-based system models. Find appropriate physical and/or physiological principles, then design, build and test a model. Design experiments to collect new data. Use these data to verify and validate the model. Use the model to make predictions and guide future data collection activities. The BaConLaws model was theory-based. The theories were the conservation laws. We found the theories first and then we gathered experimental data to support the model. The second technique for modeling a system is data-based. With this technique, the modeler starts with collecting and organizing the data and then he or she makes a model that fits that measured data. The Sliding Pin and Spiral Center of Mass models are data-based. We found the experimental data first and then we created the model to match the data. In this chapter, we give four different models for bat–ball collisions. They have different purposes and different outputs. The point is to explain to the reader that it is good to have alternative models.

5.3.5 *Coefficient of Restitution*

The Coefficient of Restitution (*CoR*) was defined by Sir Isaac Newton as the ratio of the relative velocity of the two objects after a collision to the relative velocity before the collision. The *CoR* models the energy lost in the collision.

In our models for a collision at the sweet spot of the bat, we have

$$CoR = -\frac{\text{relative velocity after collision}}{\text{relative velocity before collision}}$$

For the Sliding Pin model, we define the *CoR* with this equation (Fig. 5.5).

$$CoR_{2c} = -\frac{v_{\text{ball-after}} - v_{\text{knob-after}} - d_{\text{knob-ip}}\beta_{\text{after}}}{v_{\text{ball-before}} - v_{\text{knob-before}} - d_{\text{knob-ip}}\beta_{\text{before}}}$$

This *CoR* is a variation of the *CoR*s that we have used in previous sections.

Definition of variables

Inputs $v_{\text{ball-before}}$, $\omega_{\text{ball-before}}$, $v_{\text{bat-before}}$, $\beta_{\text{bat-before}}$ and CoR_{2c}

$v_{\text{ball-before}}$ is the linear velocity of the ball in the *x*-direction before the collision.
$\omega_{\text{ball-before}}$ is the angular velocity of the *ball about its center of mass* before the collision.
$v_{\text{bat-before}}$ is the linear translational velocity of the *knob of the* bat in the *x*-direction before the collision.
$\beta_{\text{bat-before}}$ is the angular velocity of the *bat about its knob* before the collision.
CoR_{2c} is the coefficient of restitution for this configuration.

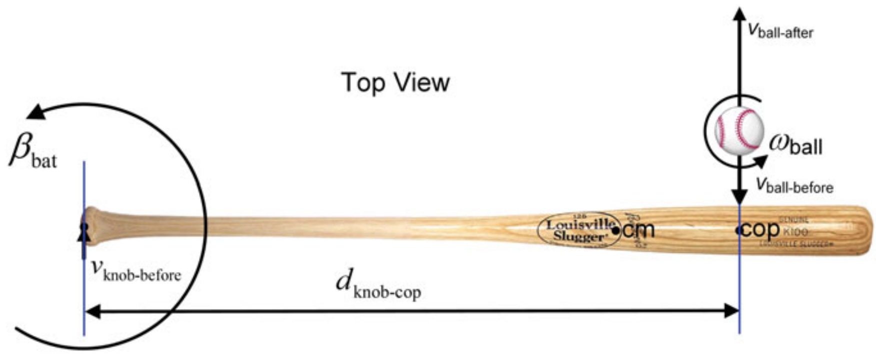

Fig. 5.5 Definition of *CoR* for the Sliding Pin model for bat–ball collisions

Outputs $\mathrm{v}_{\text{ball-after}}$, $\omega_{\text{ball-after}}$, $v_{\text{bat-after}}$, $\beta_{\text{bat-after}}$

$v_{\text{ball-after}}$ is the linear velocity of the ball in the x-direction after the collision.
$\omega_{\text{ball-after}}$ is the angular velocity of the *ball about its center of mass* after the collision.
$v_{\text{bat-after}}$ is the translational velocity of the knob of the bat in the x-direction after the collision.
$\beta_{\text{bat-after}}$ is the angular velocity of the bat *about its knob* after the collision.

We want to solve for $v_{\text{ball-after}}$, $\omega_{\text{ball-after}}$, $v_{\text{bat-after}}$, $\beta_{\text{bat-after}}$.

We will use the following fundamental equations of physics: Conservation of Linear Momentum, the Definition of *CoR*, Newton's second axiom and the Conservation of Angular Momentum.

5.3.6 Condensing Equation Notation

First, we want to simplify our notation. We will make the following substitutions:

$$d_{\text{knob-impact-point}} = d_{\text{k-ip}}$$
$$d_{\text{knob-cm}} = d_{\text{k-cm}}$$
$$I_{\text{ball}} = I_1$$
$$I_{\text{bat-cm}} = I_2 = I_{\text{cm}}$$
$$I_{\text{bat-knob}} = I_{\text{k}}$$
$$I_{\text{knob}} - m_2 d_{\text{k-cm}}^2 = I_2$$
$$m_{\text{ball}} = m_1$$
$$m_{\text{bat}} = m_2$$
$$v_{\text{ball-before}} = v_{1\text{b}}$$
$$v_{\text{ball-after}} = v_{1\text{a}}$$
$$v_{\text{bat-knob-before}} = v_{2\text{b}}$$
$$v_{\text{bat-after}} = v_{2\text{a}}$$
$$\beta_{\text{bat-before}} = \beta_{\text{b}}$$
$$\beta_{\text{bat-after}} = \beta_{\text{a}}$$

These substitutions produce the following equations.

5.3.6.1 Conservation of Linear Momentum

Assume that the bat and ball are point masses with all of their mass concentrated at the centers of mass. For now, neglect angular rotations.

$$m_{\text{ball}} v_{\text{ball-before}} + m_{\text{bat}} v_{\text{bat-cm-before}} = m_{\text{ball}} v_{\text{ball-after}} + m_{\text{bat}} v_{\text{bat-cm-after}} \tag{5.4}$$

However, from Sect. 5.3, for the linear velocity, we have

$$v_{\text{bat-cm}} = v_{\text{bat-knob}} = v_{\text{bat}} = v_2$$

Therefore,

$$m_1 v_{1\text{b}} + m_2 v_{2\text{b}} = m_1 v_{1\text{a}} + m_2 v_{2\text{a}} \tag{5.4s}$$

5.3.6.2 Definition of Coefficient of Restitution (CoR)

$$CoR_{2\text{c}} = -\frac{v_{\text{ball-after}} - v_{\text{bat-knob-after}} - d_{\text{knob-ip}}\beta_{\text{after}}}{v_{\text{ball-before}} - v_{\text{bat-knob-before}} - d_{\text{knob-ip}}\beta_{\text{before}}} \tag{5.5}$$

$$CoR_{2\text{c}} = -\frac{v_{1\text{a}} - v_{2\text{a}} - d_{\text{k-ip}}\beta_{\text{a}}}{v_{1\text{b}} - v_{2\text{b}} - d_{\text{k-ip}}\beta_{\text{b}}} \tag{5.5s}$$

5.3.6.3 Newton's Second Axiom

If we were following the development in Chap. 4, we would now apply Newton's second axiom, which states that applying an impulsive torque about an axis of rotation changes the angular momentum about that axis. However, the Sliding Pin model is not a theory-based model: it is data-based and right now we need some experimental data because the batter's hands might be applying a torque to the handle, although the Spiral Center of Mass model of Fig. 5.2 shows that at the point of impact the force applied by the batters hands is perpendicular to the direction of motion (Cross 2009). Therefore, the hands would not apply a torque to the bat. Furthermore, Milanovich and Nesbit (2014) showed that the bat's linear velocity (their Fig. 6), angular velocity (their Fig. 7) and forces (their Fig. 9) were all decreasing at the time of impact. Moreover, the torques had already reached zero by the time of impact (their Fig. 9). In summary, because of the experimental data, we will ignore the possibility of the hands applying a torque to the bat at the time of impact and we will continue our derivation with Newton's second axiom.

Newton's second axiom states that applying an impulsive torque about an axis of rotation changes the angular momentum about that axis. We can apply this axiom to a collision at the sweet spot with rotation about the knob of the bat.

$$d_{\text{knob-ip}} m_{\text{ball}} (v_{\text{ball-after}} - v_{\text{ball-before}}) = -I_{\text{knob}} (\beta_{\text{after}} - \beta_{\text{before}}) \tag{5.6}$$

$$d_{\text{k-ip}} m_1 (v_{1\text{a}} - v_{1\text{b}}) = -I_{\text{k}} (\beta_{\text{a}} - \beta_{\text{b}}) \tag{5.6s}$$

Solve for β_{a}

$$\beta_{\text{a}} = \beta_b - \frac{(v_{1\text{a}} - v_{1\text{b}}) m_1 d_{\text{k-ip}}}{I_{\text{k}}}$$

$$\beta_{\text{after}} = \beta_{\text{before}} - \frac{(v_{\text{ball-before}} - v_{\text{bat-cm-before}}) m_{\text{ball}} d_{\text{k-ip}}}{I_{\text{knob}}}$$

5.3.6.4 Abbreviations

For simplicity (especially when doing derivations by hand), the following temporary simplifications will be used in the derivations. Because they are analogous to the abbreviation used in Chap. 4, these will have a bar over the letter.

$$\bar{A} = \frac{(v_{1\text{b}} - v_{2\text{b}} - d_{\text{k-ip}} \beta_{\text{b}})(1 + CoR_{2\text{c}})}{m_1 I_{\text{k}} + m_2 I_{\text{k}} + m_1 m_2 d_{\text{k-ip}}^2} \quad \frac{1}{\text{kg}^2\,\text{m}\,\text{s}}$$

$$\bar{C} = v_{1\text{b}} - v_{2\text{b}} - d_{\text{k-ip}} \beta_{\text{b}} \quad \text{m/s}$$

$$\bar{D} = \frac{m_1 d_{\text{k-ip}}^2}{I_k} \quad \text{unitless}$$

$$\bar{G} = +v_{2\text{b}} m_2 I_k (1 + CoR_{2\text{c}}) + \beta_{\text{b}} m_2 I_k d_{\text{k-ip}} (1 + CoR_{2\text{c}}) \quad \text{kg}^2\,\text{m}^3/\text{s}$$

$$\bar{K} = (m_1 I_k + m_2 I_k + m_1 m_2 d_{\text{k-ip}}^2) \quad \text{kg}^2\,\text{m}^2$$

The units are for dimensional analysis. Note that none of these constants contains the outputs $\text{v}_{\text{ball-after}}$, $v_{\text{bat-after}}$ or $\beta_{\text{bat-after}}$. One of the purposes of this book is to show how complex these collisions can be, while still being modeled using only Newton's axioms and the conservation laws. The most useful simplifications are the ones that are constants independent of velocities after the collision. These simplifications are only used during the derivations. They are removed from the output equations. We will now use the Newtonian axioms in Eqs. (5.4), (5.5) and (5.6) and the conservation laws to find $\text{v}_{\text{ball-after}}$, $\omega_{\text{ball-after}}$, $v_{\text{bat-after}}$ and $\beta_{\text{bat-after}}$.

5.3.6.5 Conservation of Angular Momentum

We will now use the law of Conservation of Angular Momentum about the axis through the knob of the bat. When the ball contacts the bat, as shown in Fig. 5.3, the ball has linear momentum of $m_{\text{ball}} v_{\text{ball-before}}$. Therefore, following tradition, we will model the ball as rotating about the bat's knob at a distance $d = d_{\text{k-ip}}$. Thus, the ball has an initial angular momentum of $m_{\text{ball}} d_{\text{knob-ip}} v_{\text{ball-before}}$. In addition, it is possible to throw a curveball so that it spins about the vertical, z-axis, as also shown in Fig. 5.5. We call this a purely horizontal curveball (although it will still drop due to gravity, more than it will curve horizontally). The curveball will have angular momentum of $I_{\text{ball}} \omega_{\text{ball-before}}$ about an axis parallel to the z-axis. However, this is momentum about the center of mass of the *ball* and we want the equivalent momentum about the knob of the *bat*. So, we use the parallel axis theorem producing $\left(I_{\text{ball}} + m_{ball} d_{\text{k-ip}}^2\right) \omega_{\text{ball-before}}$.

The bat has an initial angular momentum reflecting the rotation about the knob. The symbol used for angular momentum is L. Therefore, the initial angular momentum for the bat–ball system about the axis through the knob of the bat is

$$L_{\text{initial}} = m_1 d_{\text{k-ip}} v_{1\text{b}} + \left(I_1 + m_1 d_{\text{k-ip}}^2\right) \omega_{1b} + I_{\text{knob}} \beta_{\text{b}}$$

All of these momenta are positive, pointing out of the page. (Remember that $v_{1\text{b}}$ is a negative number.) Please refer to Fig. 5.5 now.

For the final angular momentum, we will treat the ball, as before, as an object rotating around the axis through the knob of the bat with angular momentum, $m_{\text{ball}} d_{\text{k-ip}} v_{\text{ball-before}}$. Now we could treat the bat as a long slender rod with a moment of inertia of $m_{\text{bat}} d_{\text{bat}}^2 / 12$ where d_{bat} is the bat length. However, this is only an approximation and we have actual experimental data for the bat moment of inertia. Thus, our final angular momentum about the knob of the bat is

$$L_{\text{final}} = m_1 d_{\text{k-ip}} v_{1\text{a}} + \left(I_1 + m_1 d_{\text{k-ip}}^2\right) \omega_{1\text{a}} + I_{\text{knob}} \beta_{\text{a}}$$

As we did in the section on Newton's second axiom, we will ignore the possibility of the hands applying a torque to the bat handle at the time of impact. So now, we apply the law of Conservation of Angular Momentum, which states that when no external torque acts on an object the initial angular momentum about some axis equals the final angular momentum about that axis.

$$\begin{aligned} &L_{\text{initial}} = L_{\text{final}} \\ &m_1 d_{\text{k-ip}} v_{1\text{b}} + \left(I_1 + m_1 d_{\text{k-ip}}^2\right) \omega_{1\text{b}} + I_{\text{k}} \beta_{\text{b}} = \\ &\quad + m_1 d_{\text{k-ip}} v_{1\text{a}} + \left(I_1 + m_1 d_{\text{k-ip}}^2\right) \omega_{1\text{a}} + I_{\text{k}} \beta_{\text{a}} \end{aligned} \tag{5.7s}$$

Now, we solve this Conservation of Angular Momentum equation for the angular velocity about the knob after the collision, β_{a}.

$$-I_{\text{k}}\beta_{\text{a}} = m_1 d_{\text{k-ip}} v_{1\text{a}} + \left(I_1 + m_1 d_{\text{k-ip}}^2\right)\omega_{1\text{a}} - m_1 d_{\text{k-ip}} v_{1\text{b}} - \left(I_1 + m_1 d_{\text{k-ip}}^2\right)\omega_{1b} - I_{\text{k}}\beta_{\text{b}}$$

divide by minus I_k

$$\beta_{\text{a}} = \frac{-m_1 d_{\text{k-ip}} v_{1\text{a}} - \left(I_1 + m_1 d_{\text{k-ip}}^2\right)\omega_{1\text{a}} + m_1 d_{\text{k-ip}} v_{1\text{b}} + \left(I_1 + m_1 d_{\text{k-ip}}^2\right)\omega_{1b} + I_{\text{k}}\beta_{\text{b}}}{I_{\text{k}}}$$

$$\beta_{\text{a}} = \beta_{\text{b}} - \frac{m_1 d_{\text{k-ip}}(v_{1\text{a}} - v_{1\text{b}}) + \left(I_1 + m_1 d_{\text{k-ip}}^2\right)(\omega_{1\text{a}} - \omega_{1b})}{I_{\text{k}}}$$

This equation was derived from Eq. (5.7s) Conservation of Angular Momentum. In Sect. 4.9, we showed that for a head-on bat–ball collision the ball spin before the collision is the same as the ball spin after the collision. Well, this is a head-on collision. Therefore, $(\omega_{1\text{a}} = \omega_{1\text{b}})$ and the above equation reduces to

$$\beta_{\text{a}} = \beta_b - \frac{(v_{1\text{a}} - v_{1\text{b}})m_1 d_{\text{k-ip}}}{I_{\text{k}}}$$

$$\beta_{\text{after}} = \beta_{\text{before}} - \frac{(v_{\text{ball-before}} - v_{\text{bat-cm-before}})m_{\text{ball}} d_{\text{k-ip}}}{I_{\text{knob}}}$$

which is the same equation that we derived from Eq. (5.6), Newton's second axiom.

5.3.7 *Ball Velocity After the Collision*

We will now find the ball velocity after the collision. We start with Eq. (5.5) and solve for the bat translational velocity after the collision, $v_{2\text{a}}$

$$CoR_{2\text{c}} = -\frac{v_{1\text{a}} - v_{2\text{a}} - d_{\text{k-ip}}\beta_{\text{a}}}{v_{1\text{b}} - v_{2\text{b}} - d_{\text{k-ip}}\beta_{\text{b}}}$$

Let $\bar{C} = v_{1\text{b}} - v_{2\text{b}} - d_{\text{k-ip}}\beta_{\text{b}}$

$$v_{2\text{a}} = v_{1\text{a}} + CoR_{2\text{c}}\bar{C} - d_{\text{k-ip}}\beta_{\text{a}}$$

Now we substitute the β_a that we just derived.

$$v_{2\mathrm{a}} = v_{1\mathrm{a}} + CoR_{2\mathrm{c}}\bar{C} - d_{\text{k-ip}}\left\{\beta_b - \frac{d_{\text{k-ip}}m_1(v_{1\mathrm{a}} - v_{1\mathrm{b}})}{I_k}\right\}$$

$$v_{2\mathrm{a}} = v_{1\mathrm{a}} + CoR_{2\mathrm{c}}\bar{C} + \frac{m_1 d_{\text{k-ip}}^2(v_{1\mathrm{a}} - v_{1\mathrm{b}})}{I_k} - d_{\text{k-ip}}\beta_b$$

$$v_{2\mathrm{a}} = v_{1\mathrm{a}}\left(1 + \frac{m_1 d_{\text{k-ip}}^2}{I_k}\right) - \frac{m_1 d_{\text{k-ip}}^2 v_{1\mathrm{b}}}{I_k} + CoR_{2\mathrm{c}}\bar{C} - d_{\text{k-ip}}\beta_b$$

Let $\bar{D} = \dfrac{m_1 d_{\text{k-ip}}^2}{I_k}$

$$v_{2\mathrm{a}} = v_{1\mathrm{a}}(1 + \bar{D}) - v_{1\mathrm{b}}\bar{D} + CoR_{2\mathrm{c}}\bar{C} - d_{\text{k-ip}}\beta_b$$

Use this $v_{2\mathrm{a}}$ in Eq. (5.4) to get the ball velocity after the collision, $v_{1\mathrm{a}}$.

Prepare to substitute this $v_{2\mathrm{ka}}$ into Eq. (5.4) by multiplying by the bat mass, m_2

$$v_{2\mathrm{a}}m_2 = v_{1\mathrm{a}}m_2(1 + \bar{D}) - v_{1\mathrm{b}}m_2\bar{D} + m_2 CoR_{2\mathrm{c}}\bar{C} - \beta_b m_2 d_{\text{k-ip}}$$

Now substitute this $v_{2a}m_2$ into Eq. (5.4)

$$m_1 v_{1\mathrm{b}} + m_2 v_{2\mathrm{b}} = m_1 v_{1\mathrm{a}} + m_2 v_{2\mathrm{a}}$$

$$v_{1\mathrm{b}}m_1 + v_{2\mathrm{b}}m_2 = v_{1\mathrm{a}}m_1 + \left\{v_{1\mathrm{a}}m_2(1 + \bar{D}) - v_{1\mathrm{b}}m_2\bar{D} + m_2 CoR_{2\mathrm{c}}\bar{C} - \beta_b m_2 d_{\text{k-ip}}\right\}$$

Rearrange

$$+v_{1\mathrm{a}}m_1 + v_{1\mathrm{a}}m_2(1 + \bar{D}) = +v_{1\mathrm{b}}m_1 + v_{1\mathrm{b}}m_2\bar{D} + v_{2\mathrm{b}}m_2\text{-}m_2 CoR_{2\mathrm{c}}\bar{C} + \beta_b m_2 d_{\text{k-ip}}$$

Replace the dummy variables $\bar{C}$ and $\bar{D}$

$$+v_{1\mathrm{a}}m_1 + v_{1\mathrm{a}}m_2\left(1 + \left\{\frac{m_1 d_{\text{k-ip}}^2}{I_k}\right\}\right) =$$

$$+v_{1\mathrm{b}}m_1 + v_{1\mathrm{b}}m_2\left\{\frac{m_1 d_{\text{k-ip}}^2}{I_k}\right\}$$

$$+v_{2\mathrm{b}}m_2$$

$$-m_2 CoR_{2\mathrm{c}}\left\{v_{1\mathrm{b}} - v_{2\mathrm{b}} - d_{\text{k-ip}}\beta_{\mathrm{b}}\right\}$$

$$+\beta_{\mathrm{b}}m_2 d_{\text{k-ip}}$$

Rearrange

$$v_{1\mathrm{a}}\left[m_1 + m_2\left(1 + \left\{\frac{m_1 d_{\text{k-ip}}^2}{I_k}\right\}\right)\right]$$

$$= +v_{1\mathrm{b}}\left[m_1 + m_2\left\{\frac{m_1 d_{\text{k-ip}}^2}{I_k}\right\} - m_2 CoR_{2\mathrm{c}}\right]$$

$$+v_{2\mathrm{b}}m_2(1 + CoR_{2\mathrm{c}})$$

$$+\beta_{\mathrm{b}}m_2 d_{\text{k-ip}}(1 + CoR_{2\mathrm{c}})$$

Multiply by the moment of inertia of the bat, I_k.

$$
\begin{aligned}
&v_{1\mathrm{a}}\left[m_1 I_k + m_2 I_k + m_1 m_2 d_{\text{k-ip}}^2\right] = \\
&+ v_{1\mathrm{b}}\left[m_1 I_k - m_2 I_k CoR_{2\mathrm{c}} + m_1 m_2 d_{\text{k-ip}}^2\right] \\
&+ v_{2\mathrm{b}} m_2 I_k (1 + CoR_{2\mathrm{c}}) \\
&+ \beta_{\mathrm{b}} m_2 I_k d_{\text{k-ip}} (1 + CoR_{2\mathrm{c}})
\end{aligned}
$$

$$
v_{1\mathrm{a}} = \frac{v_{1\mathrm{b}}\left[m_1 I_k - m_2 I_k CoR_{2\mathrm{c}} + m_1 m_2 d_{\text{k-ip}}^2\right] + v_{2\mathrm{b}} m_2 I_k (1 + CoR_{2\mathrm{c}}) + \beta_{\mathrm{b}} m_2 I_k d_{\text{k-ip}} (1 + CoR_{2\mathrm{c}})}{m_1 I_k + m_2 I_k + m_1 m_2 d_{\text{k-ip}}^2}
$$

This is the normal form of the equation for $v_{1\mathrm{a}}$. However, we now want to rearrange this equation into our canonical form. Let

$$
\begin{aligned}
&\bar{K} = (m_1 I_k + m_2 I_k + m_1 m_2 d_{\text{k-ip}}^2) \\
&\bar{G} = \ + v_{2\mathrm{b}} m_2 I_k (1 + CoR_{2\mathrm{c}}) + \beta_{\mathrm{b}} m_2 I_k d_{\text{k-ip}} (1 + CoR_{2\mathrm{c}})
\end{aligned}
$$

Then

$$
v_{1\mathrm{a}} = \frac{v_{1\mathrm{b}}\left[m_1 I_k - m_2 I_k CoR_{2\mathrm{c}} + m_1 m_2 d_{\text{k-ip}}^2\right] + \bar{G}}{\bar{K}}
$$

add $\left\{ v_{1\mathrm{b}} - \frac{v_{1\mathrm{b}}\bar{K}}{\bar{K}} \right\}$ to the right side

$$
\begin{aligned}
v_{1\mathrm{a}} &= \{v_{1\mathrm{b}}\} + \frac{v_{1\mathrm{b}}\left(m_1 I_k - m_2 I_k CoR_{2\mathrm{c}} + m_1 m_2 d_{\text{k-ip}}^2\right)}{\bar{K}} \left\{ - \frac{v_{1\mathrm{b}}\left(m_1 I_k + m_2 I_k + m_1 m_2 d_{\text{k-ip}}^2\right)}{\bar{K}} \right\} + \frac{\bar{G}}{\bar{K}} \\
v_{1\mathrm{a}} &= v_{1\mathrm{b}} + \frac{v_{1\mathrm{b}}\left(m_1 I_k - m_2 I CoR_{2\mathrm{c}} + m_1 m_2 d_{\text{k-ip}}^2\right) - v_{1\mathrm{b}}\left(m_1 I_k + m_2 I_k + m_1 m_2 d_{\text{k-ip}}^2\right)}{\bar{K}} + \frac{\bar{G}}{\bar{K}} \\
v_{1\mathrm{a}} &= v_{1\mathrm{b}} + \frac{v_{1\mathrm{b}}\left(m_1 I_k - m_2 I_k CoR_{2\mathrm{c}} + m_1 m_2 d_{\text{k-ip}}^2 - m_1 I_k - m_2 I_k - m_1 m_2 d_{\text{k-ip}}^2\right)}{\bar{K}} + \frac{\bar{G}}{\bar{K}} \\
v_{1\mathrm{a}} &= v_{1\mathrm{b}} + \frac{v_{1\mathrm{b}}(-m_2 I_k - m_2 I_k CoR_{2\mathrm{c}})}{\bar{K}} + \frac{\bar{G}}{\bar{K}} \\
v_{1\mathrm{a}} &= v_{1\mathrm{b}} + \frac{-v_{1\mathrm{b}} m_2 I_k (1 + CoR_{2\mathrm{c}}) + \bar{G}}{\bar{K}}
\end{aligned}
$$

Replace the dummy variable $\bar{G}$ and we get the following equation:

$$
v_{1\mathrm{a}} = v_{1\mathrm{b}} - \frac{(v_{1\mathrm{b}} - v_{2\mathrm{b}}) m_2 I_k (1 + CoR) - \beta_{\mathrm{b}} m_2 I_k d_{\text{k-ip}} (1 + CoR_{2\mathrm{c}})}{m_1 I_k + m_2 I_k + m_1 m_2 d_{\text{k-ip}}^2}
$$

Simplify and our final equation for the batted-ball velocity becomes

$$v_{1a} = v_{1b} - \frac{\left(v_{1b} - v_{2b} - \beta_b d_{\text{k-ip}}\right)(1 + CoR_{2c})m_2 I_k}{m_1 I_k + m_2 I_k + m_1 m_2 d^2_{\text{k-ip}}}$$

$$v_{\text{ball-after}} = v_{\text{ball-before}} - \frac{\left(v_{\text{ball-before}} - v_{\text{bat-before}} - \beta_{\text{before}} d_{\text{k-ip}}\right)(1 + CoR_{2c})m_{\text{bat}} I_{\text{knob}}}{m_{\text{ball}} I_{\text{knob}} + m_{\text{bat}} I_{\text{knob}} + m_{\text{ball}} m_{\text{bat}} d^2_{\text{k-ip}}}$$

or if we let

$$\bar{A} = \frac{\left(v_{1b} - v_{2b} - d_{\text{k-ip}}\beta_b\right)(1 + CoR_{2c})}{m_1 I_k + m_2 I_k + m_1 m_2 d^2_{\text{k-ip}}}$$

$$v_{1a} = v_{1b} - \bar{A} m_2 I_k$$

$$v_{\text{ball-after}} = v_{\text{ball-before}} - \bar{A} m_{\text{bat}} I_{\text{knob}}$$

Nothing in this derivation depended on the collision being at the sweet spot of the bat. Therefore, $d_{\text{k-ip}}$ could be replaced with the distance from the knob to any arbitrary impact point. This equation was derived from Eqs. (5.4), (5.5) and (5.6).

This $\bar{A}$ differs from the A of the BaConLaws model in that it uses I_k instead of I_2, $d_{\text{k}-\text{ss}}$ instead of $d_{\text{cm-ss}}$ and CoR_{2c} instead of CoR_{2b}.

5.3.8 *Bat Translational Velocity After the Collision*

Now, we will derive an equation for the translational velocity of the bat after the collision. We start with Eq. (5.5) and solve for the bat translational velocity after the collision, v_{2a}

$$CoR_{2c} = -\frac{v_{1a} - v_{2a} - d_{\text{k-ip}}\beta_a}{v_{1b} - v_{2b} - d_{\text{k-ip}}\beta_b}$$

$$v_{2a} = v_{1a} + CoR_{2c}\left(v_{1b} - v_{2b} - d_{\text{k-ip}}\beta_b\right) - d_{\text{k-ip}}\beta_a$$

First, get rid of β_a by substituting this β_a that we derived above.

$$\beta_a = \beta_b - \frac{d_{\text{k-ip}} m_1 (v_{1a} - v_{1b})}{I_k}$$

$$v_{2a} = v_{1a} + CoR_{2c}\left(v_{1b} - v_{2b} - d_{\text{k-ip}}\beta_{\text{b}}\right) - d_{\text{k-ip}}\left\{\beta_b - \frac{d_{\text{k-ip}}m_1(v_{1a} - v_{1b})}{I_k}\right\}$$

$$v_{2a} = v_{1a} + CoR_{2c}\left(v_{1b} - v_{2b} - d_{\text{k-ip}}\beta_{\text{b}}\right) + \frac{m_1 d_{\text{k-ip}}^2(v_{1a} - v_{1b})}{I_k} - d_{\text{k-ip}}\beta_b$$

$$v_{2a} = v_{1a}\left(1 + \frac{m_1 d_{\text{k-ip}}^2}{I_k}\right) - v_{1b}\left(\frac{m_1 d_{\text{k-ip}}^2}{I_k} - CoR_{2c}\right) - v_{2b}CoR_{2c} - d_{\text{k-ip}}\beta_b(1 + CoR_{2c})$$

Let $\bar{D} = \dfrac{m_1 d_{\text{k-ip}}^2}{I_k}$

$$v_{2a} = v_{1a}(1 + \bar{D}) - v_{1b}(\bar{D} - CoR_{2c}) - v_{2b}CoR_{2c} - d_{\text{k-ip}}\beta_b(1 + CoR_{2c})$$

Now get rid of v_{1a} by substituting this v_{1a} that we derived above.

$$v_{1a} = \left\{v_{1b} - \frac{\left(v_{1b} - v_{2b} - d_{\text{k-ip}}\beta_{\text{b}}\right)(1 + CoR_{2c})m_2 I_k}{m_1 I_k + m_2 I_k + m_1 m_2 d_{\text{k-ip}}^2}\right\}$$

$$\begin{aligned} v_{2a} = &\left\{v_{1b} - \frac{\left(v_{1b} - v_{2b} - d_{\text{k-ip}}\beta_{\text{b}}\right)(1 + CoR_{2c})m_2 I_k}{m_1 I_k + m_2 I_k + m_1 m_2 d_{\text{k-ip}}^2}\right\}(1 + \bar{D}) \\ &- v_{1b}(\bar{D} - CoR_{2c}) - v_{2b}CoR_{2c} - d_{\text{k-ip}}\beta_b(1 + CoR_{2c}) \end{aligned}$$

$$\begin{aligned} \bar{K}v_{2a} = &\ \bar{K}v_{1b}(1 + \bar{D}) - \left(v_{1b} - v_{2b} - d_{\text{k-ip}}\beta_{\text{b}}\right)(1 + CoR_{2c})(1 + \bar{D})m_2 I_k \\ &- v_{1b}\bar{K}(\bar{D} - CoR_{2c}) - v_{2b}\bar{K}CoR_{2c} - d_{\text{k-ip}}\beta_b\bar{K}(1 + CoR_{2c}) \end{aligned}$$

Let $MM = (1 + CoR_{2c})m_2 I_k$

$$\begin{aligned} \bar{K}v_{2a} = &\ v_{1b}[\bar{K}(1 + \bar{D}) - MM(1 + \bar{D}) - \bar{K}\bar{D} + \bar{K}CoR_{2c}] \\ &+ v_{2b}[MM(1 + \bar{D}) - \bar{K}CoR_{2c}] \\ &+ d_{\text{k-ip}}\beta_{\text{b}}[MM(1 + \bar{D}) - \bar{K}(1 + CoR_{2c})] \end{aligned}$$

$$\begin{aligned} \bar{K}v_{2a} = &\ v_{1b}[\bar{K} - MM(1 + \bar{D}) + \bar{K}CoR_{2c}] \\ &+ v_{2b}[MM(1 + \bar{D}) - \bar{K}CoR_{2c}] \\ &+ \beta_{\text{b}}d_{\text{k-ip}}[MM(1 + \bar{D}) - \bar{K}(1 + CoR_{2c})] \end{aligned}$$

$$\begin{aligned} \bar{K}v_{2a} = &\ v_{1b}[\bar{K}(1 + CoR_{2c}) - MM(1 + \bar{D})] \\ &- v_{2b}[\bar{K}CoR_{2c} - MM(1 + \bar{D})] \\ &- d_{\text{k-ip}}\beta_{\text{b}}[\bar{K}(1 + CoR_{2c}) - MM(1 + \bar{D})] \end{aligned}$$

Add $\{+v_{2b}\bar{K} - v_{2b}\bar{K}\}$ to the right side

$$\begin{aligned}\bar{K}v_{2\mathrm{a}} = v_{1\mathrm{b}}[\bar{K}(1 + CoR_{2\mathrm{c}}) - MM(1 + \bar{D})] \\ - v_{2\mathrm{b}}[\bar{K}CoR_{2\mathrm{c}} - MM(1 + \bar{D})] + \{v_{2\mathrm{b}}\bar{K} - v_{2\mathrm{b}}\bar{K}\} \\ - d_{\text{k-ip}}\beta_{\mathrm{b}}[\bar{K}(1 + CoR_{2\mathrm{c}}) - MM(1 + \bar{D})]\end{aligned}$$

$$\begin{aligned}\bar{K}v_{2\mathrm{a}} = v_{1\mathrm{b}}[\bar{K}(1 + CoR_{2\mathrm{c}}) - MM(1 + \bar{D})] \\ - v_{2\mathrm{b}}[\bar{K}(1 + CoR_{2\mathrm{c}}) - MM(1 + \bar{D})] + v_{2\mathrm{b}}\bar{K} \\ - d_{\text{k-ip}}\beta_{\mathrm{b}}[\bar{K}(1 + CoR_{2\mathrm{c}}) - MM(1 + \bar{D})]\end{aligned}$$

Let $Q = \bar{K}(1 + CoR_{2\mathrm{c}}) - MM(1 + \bar{D})$

$$\bar{K}v_{2\mathrm{a}} = v_{2\mathrm{b}}\bar{K} + v_{1\mathrm{b}}Q - v_{2\mathrm{b}}Q - \beta_{\mathrm{b}}d_{\text{k-ip}}Q$$

divide by $\bar{K}$

$$v_{2\mathrm{a}} = v_{2\mathrm{b}} + \frac{\left(v_{1\mathrm{b}} - v_{2\mathrm{b}} - d_{\text{k-ip}}\beta_{\mathrm{b}}\right)Q}{\bar{K}}$$

That looks good. So, let's work on Q for a while.

$$Q = \bar{K}(1 + CoR_{2\mathrm{c}}) - MM(1 + \bar{D})$$
$$MM = m_2 I_k(1 + CoR_{2\mathrm{c}})$$
$$\bar{D} = \frac{m_1 d_{\text{k-ip}}^2}{I_k}$$
$$MM(1 + \bar{D}) = m_2 I_k(1 + CoR_{2\mathrm{c}})\left(1 + \frac{m_1 d_{\text{k-ip}}^2}{I_k}\right)$$
$$MM(1 + \bar{D}) = \left[m_2 I_k(1 + CoR_{2\mathrm{c}}) + m_1 m_2 d_{\text{k-ip}}^2(1 + CoR_{2\mathrm{c}})\right]$$
$$Q = \bar{K}(1 + CoR_{2\mathrm{c}}) - \left[m_2 I_k(1 + CoR_{2\mathrm{c}}) + m_1 m_2 d_{\text{k-ip}}^2(1 + CoR_{2\mathrm{c}})\right]$$
$$\bar{K} = m_1 I_k + m_2 I_k + m_1 m_2 d_{\text{k-ip}}^2$$
$$Q = \left(m_1 I_k + m_2 I_k + m_1 m_2 d_{\text{k-ip}}^2\right)(1 + CoR_{2\mathrm{c}}) - \left[m_2 I_k(1 + CoR_{2\mathrm{c}}) + m_1 m_2 d_{\text{k-ip}}^2(1 + CoR_{2\mathrm{c}})\right]$$

cancel equal terms

$$Q = m_1 I_k(1 + CoR_{2\mathrm{c}})$$

$$v_{2\mathrm{a}} = v_{2\mathrm{b}} + \frac{\left(v_{1\mathrm{b}} - v_{2\mathrm{b}} - d_{\text{k-ip}}\beta_{\mathrm{b}}\right)m_1 I_k(1 + CoR_{2\mathrm{c}})}{\bar{K}}$$

$$v_{2\mathrm{a}} = v_{2\mathrm{b}} + \frac{\left(v_{1\mathrm{b}} - v_{2\mathrm{b}} - d_{\text{k-ip}}\beta_{\mathrm{b}}\right)m_1 I_k(1 + CoR_{2\mathrm{c}})}{m_1 I_k + m_2 I_k + m_1 m_2 d_{\text{k-ip}}^2}$$

If we let

$$\bar{A} = \frac{\left(v_{1b} - v_{2b} - d_{\text{k-ip}}\beta_b\right)(1 + CoR_{2c})}{m_1 I_k + m_2 I_k + m_1 m_2 d_{\text{k-ip}}^2}$$

$$v_{2a} = v_{2b} + \bar{A} m_1 I_k$$

$$v_{\text{bat-after}} = v_{\text{bat-before}} + \bar{A} m_{\text{ball}} I_{\text{knob}}$$

5.3.9 Bat Angular Velocity After the Collision

Now, we will derive an equation for the rotational velocity of the bat after the collision. We start with the previously derived equation for β_a.

$$\beta_a = \beta_b - \frac{d_{\text{k-ip}} m_1 (v_{1a} - v_{1b})}{I_k}$$

Now we must get rid of the term with the *after* subscript. Multiply by I_k

$$\beta_a I_k = \beta_b I_k - d_{\text{k-ip}} m_1 (v_{1a} - v_{1b})$$

Substitute the previously derived expression for v_{1a}.

$$v_{1a} = \left\{ v_{1b} - \frac{\left(v_{1b} - v_{2b} - \beta_b d_{\text{k-ip}}\right)(1 + CoR_{2c}) m_2 I_k}{\overline{K}} \right\}$$

$$\beta_a I_k = \beta_b I_k - d_{\text{k-ip}} m_1 \left(\left\{ v_{1b} - \frac{\left(v_{1b} - v_{2b} - \beta_b d_{\text{k-ip}}\right)(1 + CoR_{2c}) m_2 I_k}{\overline{K}} \right\} - v_{1b} \right)$$

Cancel $\left(v_{1b} - v_{1b}\right)$ and multiply by $\overline{K}$

$$\beta_a I_k \overline{K} = \beta_b I_k \overline{K} - d_{\text{k-ip}} m_1 \left(-\left(v_{1b} - v_{2b} - \beta_b d_{\text{k-ip}}\right)(1 + CoR_{2c}) m_2 I_k \right)$$

Distribute the $-d_{\text{k-ip}} m_1$ term

$$\beta_a I_k \overline{K} = \beta_b I_k \overline{K} + \left(v_{1b} - v_{2b} - \beta_b d_{\text{k-ip}}\right) d_{\text{k-ss}} m_1 m_2 I_k (1 + CoR_{2c})$$

Collect similar terms

$$\beta_a I_k \overline{K} = \beta_b I_k \overline{K}$$
$$+ v_{1b} m_1 m_2 d_{\text{k-ip}} I_k (1 + CoR_{2c})$$
$$- v_{2b} m_1 m_2 d_{\text{k-ip}} I_k (1 + CoR_{2c})$$
$$- \beta_b d_{\text{k-ss}} m_1 m_2 d_{\text{k-ip}} I_k (1 + CoR_{2c})$$

Divide by $I_k\bar{K}$

$$\begin{aligned}\beta_a = \beta_b &\\ &+ v_{1b}\frac{(1+CoR_{2c})m_1 m_2 d_{\text{k-ip}}}{\bar{K}}\\ &- v_{2b}\frac{(1+CoR_{2c})m_1 m_2 d_{\text{k-ip}}}{\bar{K}}\\ &\quad - \beta_b d_{\text{k-ip}}\frac{(1+CoR_{2c})m_1 m_2 d_{\text{k-ip}}}{\bar{K}}\end{aligned}$$

$$\beta_a = \beta_b + \frac{(v_{1b} - v_{2b} - \beta_b d_{\text{k-ss}})(1+CoR_{2c})m_1 m_2 d_{\text{k-ip}}}{m_1 I_k + m_2 I_k + m_1 m_2 d_{\text{k-ip}}^2}$$

Let

$$\bar{A} = \frac{\left(v_{1b} - v_{2b} - \beta_b d_{\text{k-ip}}\right)(1+CoR_{2c})}{m_1 I_k + m_2 I_k + m_1 m_2 d_{\text{k-ip}}^2}$$

$$\beta_a = \beta_b + \bar{A} m_1 m_2 d_{\text{k-ip}}$$

$$\beta_{\text{bat-after}} = \beta_{\text{bat-before}} + \bar{A} m_{\text{ball}} m_{\text{bat}} d_{\text{k-ip}}$$

5.3.10 Conservation of Energy

The following equation is for the kinetic energy lost:

$$0 = m_1 v_{1b}^2 + m_2 v_{2b}^2 + I_k \beta_b^2 - m_1 v_{1a}^2 - m_2 v_{2a}^2 - I_k \beta_a^2 - 2KE_{\text{lost}}$$

These are our equations for the outputs:

$$\begin{aligned}v_{1a} &= v_{1b} - \bar{A} m_2 I_k\\ v_{2a} &= v_{2b} + \bar{A} m_1 I_k\\ \beta_a &= \beta_b + \bar{A} m_1 m_2 d_{\text{k-ip}}\\ \omega_{1a} &= \omega_{1b}\end{aligned}$$

Substituting the linear velocity of the ball after the collision, v_{1a}, the linear velocity of the bat after the collision, v_{2a} and the angular velocity of the bat after the collision, ω_{2a} into this Conservation of Energy equation yields

$$KE_{\text{lost}} = \frac{1}{2}\left\{\begin{array}{c} m_1 v_{1b}^2 + m_2 v_{2b}^2 + I_k \beta_b^2 - m_1\left(v_{1b} - \bar{A} m_2 I_k\right)^2 \\ -m_2\left(v_{2b} + \bar{A} m_1 I_k\right)^2 - I_k\left(\beta_b + \bar{A} m_1 m_2 d_{\text{k-ip}}\right)^2 \end{array}\right\}$$

Substitute for $\bar{A}$

$$\bar{A} = \frac{\left(v_{1\mathrm{b}} - v_{2\mathrm{b}} - d_{\text{k-ip}}\beta_{\mathrm{b}}\right)(1 + CoR_{2\mathrm{c}})}{m_1 I_{\mathrm{k}} + m_2 I_{\mathrm{k}} + m_1 m_2 d_{\text{k-ip}}^2}$$

After a little bit of algebra that follows the development in Chap. 4, we get

$$KE_{\mathrm{lost}} = \frac{1}{2}\frac{m_1 m_2 I_{\mathrm{k}}}{m_1 I_{\mathrm{k}} + m_2 I_{\mathrm{k}} + m_1 m_2 d_{\text{k-ip}}^2}\left[\left(v_{1\mathrm{b}} - v_{2\mathrm{b}} - \beta_{\mathrm{b}} d_{\text{k-ip}}\right)^2 (1 - CoR_{2\mathrm{c}}^2)\right]$$

or expanding the abbreviations gives

$$KE_{\mathrm{lost}} = \frac{1}{2}\frac{m_{\mathrm{ball}} m_{\mathrm{bat}} I_{\mathrm{knob}}}{m_{\mathrm{ball}} I_{\mathrm{knob}} + m_{\mathrm{bat}} I_{\mathrm{knob}} + m_{\mathrm{ball}} m_{\mathrm{bat}} d_{\text{k-ip}}^2}\left[\left(v_{\text{ball-before}} - v_{\text{bat-before}} - \beta_{\mathrm{before}} d_{\text{k-ip}}\right)^2 (1 - CoR_{2\mathrm{c}}^2)\right]$$

5.3.11 Summary: The Output Equations

Our final equation for the batted-ball velocity is

$$v_{1\mathrm{a}} = v_{1\mathrm{b}} - \frac{\left(v_{1\mathrm{b}} - v_{2\mathrm{b}} - \beta_{\mathrm{b}} d_{\text{k-ip}}\right)(1 + CoR_{2\mathrm{c}}) m_2 I_k}{m_1 I_k + m_2 I_k + m_1 m_2 d_{\text{k-ip}}^2}$$

Expanding the subscripts, we get

$$v_{\text{ball-after}} = v_{\text{ball-before}} - \frac{\left(v_{\text{ball-before}} - v_{\text{bat-before}} - \beta_{\mathrm{before}} d_{\text{k-ip}}\right) m_{\mathrm{bat}} I_{\mathrm{knob}} (1 + CoR_{2\mathrm{c}})}{m_{\mathrm{ball}} I_{\mathrm{knob}} + m_{\mathrm{bat}} I_{\mathrm{knob}} + m_{\mathrm{ball}} m_{\mathrm{bat}} d_{\text{k-ip}}^2}$$

Our final equation for the translational bat velocity after the collision is

$$v_{2\mathrm{a}} = v_{2\mathrm{b}} + \frac{\left(v_{1\mathrm{b}} - v_{2\mathrm{b}} - d_{\text{k-ip}}\beta_{\mathrm{b}}\right)(1 + CoR_{2\mathrm{c}}) m_1 I_k}{m_1 I_k + m_2 I_k + m_1 m_2 d_{\text{k-ip}}^2}$$

or

$$v_{\text{bat-after}} = v_{\text{bat-before}} + \frac{\left(v_{\text{ball-before}} - v_{\text{bat-before}} - \beta_{\mathrm{before}} d_{\text{k-ip}}\right)(1 + CoR_{2\mathrm{c}}) m_{\mathrm{ball}} I_{\mathrm{knob}}}{m_{\mathrm{ball}} I_{\mathrm{knob}} + m_{\mathrm{bat}} I_{\mathrm{knob}} + m_{\mathrm{ball}} m_{\mathrm{bat}} d_{\text{k-ip}}^2}$$

Our final equation for the rotational velocity of the bat after the collision is

$$\beta_{\mathrm{a}} = \beta_b + \frac{\left(v_{1\mathrm{b}} - v_{2\mathrm{b}} - \beta_{\mathrm{b}} d_{\text{k-ip}}\right)(1 + CoR_{2\mathrm{c}}) m_1 m_2 d_{\text{k-ip}}}{m_1 I_k + m_2 I_k + m_1 m_2 d_{\text{k-ip}}^2}$$

$$\beta_{\text{bat-after}} = \beta_{\text{bat-before}} + \frac{\left(v_{\text{ball-before}} - v_{\text{bat-before}} - \beta_{\text{before}} d_{\text{k-ip}}\right)(1 + CoR_{2\mathrm{c}}) m_{\text{ball}} m_{\text{bat}} d_{\text{k-ip}}}{m_{\text{ball}} I_{\text{knob}} + m_{\text{bat}} I_{\text{knob}} + m_{\text{ball}} m_{\text{bat}} d_{\text{k-ip}}^2}$$

These three equations have a common term

$$\bar{A} = \frac{\left(v_{\text{ball-before}} - v_{\text{bat-before}} - \beta_{\text{before}} d_{\text{k-ip}}\right)(1 + CoR_{2\mathrm{c}})}{m_{\text{ball}} I_{\text{knob}} + m_{\text{bat}} I_{\text{knob}} + m_{\text{ball}} m_{\text{bat}} d_{\text{k-ip}}^2}$$

We can summarize with the following:

If we let

$$\bar{A} = \frac{\left(v_{1\mathrm{b}} - v_{2\mathrm{b}} - d_{\text{k-ip}} \beta_{\mathrm{b}}\right)(1 + CoR_{2\mathrm{c}})}{m_1 I_{\mathrm{k}} + m_2 I_{\mathrm{k}} + m_1 m_2 d_{\text{k-ip}}^2}$$

Then our set of equations becomes

$$CoR_{2\mathrm{c}} = -\frac{v_{1\mathrm{a}} - v_{2\mathrm{a}} - d_{\text{k-ip}} \beta_{\mathrm{a}}}{v_{1\mathrm{b}} - v_{2\mathrm{b}} - d_{\text{k-ip}} \beta_{\mathrm{b}}}$$

$$v_{1\mathrm{a}} = v_{1\mathrm{b}} - \bar{A} m_{\text{bat}} I_{\mathrm{k}}$$

$$v_{2\mathrm{a}} = v_{2\mathrm{b}} + \bar{A} m_{\text{ball}} I_{\mathrm{k}}$$

$$\beta_{\mathrm{a}} = \beta_{\mathrm{b}} + \bar{A} m_{\text{ball}} m_{\text{bat}} d_{\text{k-ip}}$$

$$\omega_{1\mathrm{a}} = \omega_{1\mathrm{b}}$$

5.4 Differences Between the BaConLaws and Sliding Pin Models

The purpose of Chap. 4 was to develop the BaConLaws model that explains bat–ball collisions with precise, correct equations. The BaConLaws model described head-on bat–ball collisions at the sweet spot of the bat. It gave the speed and spin of the bat and ball before and after collisions. The purpose of the Sliding Pin model of Chapter 5 was to model a new type of data. Previously, the input data for our models were the total velocities of the center of mass or the center of percussion of the bat. However, the Sliding Pin model used the translational and rotational velocities at the *knob*. The experimental data produced different nominal values for the inputs. Because these two models had different purposes and inputs, we would not expect them to be equivalent. And they are not. Here are some of the differences between these two models.

The BaConLaws model. If you toss a bat into the air, it will have linear motion and it will rotate about its center of mass. Because the bat is a rigid object, all points on the bat must have the same angular velocity. If there is no rotation just a translation, then all points on the bat will have the same linear velocity. If there is a rotation about the center of mass and a translation, then each point on the bat will have a total velocity that is equal to the linear velocity of the center of mass plus the angular velocity of the center of mass times its distance from the center of mass. For example, the total velocity of the center of percussion, vt_{cop}, is

$$vt_{\text{cop}} = v_{\text{cm}} + d_{\text{cm-cop}}\omega_{\text{cm}}$$

If a bat tossed into the air were hit by a ball, it would be a free-end collision because there are no other forces acting on the bat. The BaConLaws model uses a free-end collision because of the simplicity. We need not search for other forces on the bat, because there are none. The BaConLaws model and the Effective Mass model both assume free-end collisions with no external forces and with rotation about the center of mass.

The Sliding Pin model. Now imagine a bat that is pinned through its knob, but the pinned point is allowed to slide along the x-axis, as in Fig. 5.3. This bat will have linear motion and it will rotate about its knob. Therefore, each point on the bat will have a total velocity that is equal to the linear velocity of the knob plus the angular velocity of the knob times its distance from the knob. For example,

$$vt_{\text{cm}} = v_{\text{knob}} + d_{\text{knob-cm}}\beta_{\text{knob}}$$

$$vt_{\text{cop}} = v_{\text{knob}} + d_{\text{knob-cop}}\beta_{\text{knob}}$$

When the bat is swung, there will be forces on the pin. This makes the Sliding Pin model more complicated than the BaConLaws model. Forces in the x-direction are not worrisome: they are known to be small (Milanovich and Nesbit 2014). Two of the forces on the pin will be along the y-axis. The centrifugal force due to the bat's rotation about the pin will be in the negative y-direction. The human will be applying an approximately equal and opposite centripetal force in the positive y-direction, as shown in Fig. 5.2. But at the time of the collision, these forces will not affect the bat's velocity $\bar{v}_{\text{bat}}$ because they are perpendicular to it. The Sliding Pin model assumes negligible forces on the pin and rotations about the knob.

Let us compare the BaConLaws model of Fig. 4.1 and the Sliding Pin model of Fig. 5.3. For the time being, let us ignore the translational movements and consider only rotational movements. Suppose you want to move the sweet spot forward a distance x. The BaConLaws model of Fig. 4.1 would require a rotation through an angle θ_{cm} where the $\tan\theta_{\text{cm}} = \frac{x}{d_{\text{cm-ip}}}$, whereas the Sliding Pin model of Fig. 5.3 would require a rotation through an angle ψ_{knob} where the $\tan\psi_{\text{knob}} = \frac{x}{d_{\text{knob-ip}}}$. Now the angular velocity of the BaConLaws model is $\omega_{\mathrm{cm}} = \frac{d\theta_{\mathrm{cm}}}{dt}$, whereas the angular velocity of the Sliding Pin model is $\beta_{\mathrm{knob}} = \frac{d\psi_{\mathrm{knob}}}{dt}$. Clearly $\omega_{\mathrm{cm}} \neq \beta_{\mathrm{knob}}$.

The Sliding Pin model is analogous to the BaConLaws model, but it is not equivalent.

$$A \neq \bar{A}$$

$$A = \frac{\left(v_{1\mathrm{b}} - v_{2\mathrm{b}} - d_{\text{cm-ip}}\omega_{2\mathrm{b}}\right)(1 + CoR_{2\mathrm{b}})}{m_1 I_{\text{bat-cm}} + m_2 I_{\text{bat-cm}} + m_1 m_2 d_{\text{cm-ip}}^2}$$

$$\bar{A} = \frac{\left(v_{1\mathrm{b}} - v_{2\mathrm{b}} - d_{\text{knob-ip}}\beta_{\mathrm{b}}\right)(1 + CoR_{2\mathrm{c}})}{m_1 I_{\text{knob}} + m_2 I_{\text{knob}} + m_1 m_2 d_{\text{knob-ip}}^2}$$

Therefore, the two $v_{\text{ball-after}}$ equations yield different numerical values. From the BaConLaws model of Chap. 4, we have

$$v_{\text{ball-after}} = v_{\text{ball-before}} - A m_{\text{bat}} I_{\text{bat-cm}}$$

And from the Sliding Pin model of this chapter, we have

$$v_{\text{ball-after}} = v_{\text{ball-before}} - \bar{A} m_{\text{bat}} I_{\text{knob}}$$

Because $A m_{\text{bat}} I_{\text{bat-cm}} \neq \bar{A} m_{\text{bat}} I_{\text{knob}}$, the $v_{1\mathrm{a}}$ of the BaConLaws model is different from the $v_{\text{ball-after}}$ of the Sliding Pin model.

For the angular momentum $L_{\text{initial}} = L_{\text{final}}$ for both models, but the numerical values are different. Numerically, the CoRs are the same although their equations are different.

$$CoR_{2\mathrm{b}} = -\frac{v_{\text{ball-after}} - v_{\text{bat-cm-after}} - d_{\text{cm-ip}}\omega_{\text{bat-after}}}{v_{\text{ball-before}} - v_{\text{bat-cm-before}} - d_{\text{cm-ip}}\omega_{\text{bat-before}}}$$

$$CoR_{2\mathrm{c}} = -\frac{v_{\text{ball-after}} - v_{\text{knob-after}} - d_{\text{knob-ip}}\beta_{\text{after}}}{v_{\text{ball-before}} - v_{\text{knob-before}} - d_{\text{knob-ip}}\beta_{\text{before}}}$$

where the subscript "ip" stands for the impact point.

The *CoR* and KE_{lost} are properties of the collision and not of the model used for collision analysis. Therefore, their values should be the same for the BaConLaws model and the Sliding Pin model. So, this provides an easy consistency check between the two models. In our simulations, the *CoRs* were 0.465 and 0.453 and the KE_{lost} were 196 and 207 J, respectively. These values are close given that the BaConLaws model used input data from Table 4.2 and the Sliding Pin model used input data from Table 5.1. At this point, it may be useful to note that the Sliding Pin model is original with this book. It has not been published in peer-reviewed journals yet. So, there are still some rough edges. In the future, once we determine a gold-standard input dataset for bat swings, we will compare the BaConLaws and the Sliding Pin models in detail.

Inputs and outputs for the BaConLaws model from Table 4.1	
Inputs	$v_{\text{ball-before}}$, $\omega_{\text{ball-before}}$, $v_{\text{bat-cm-before}}$, $\omega_{\text{bat-before}}$ and CoR_{2b}
Outputs	$v_{\text{ball-after}}$, $\omega_{\text{ball-after}}$, $v_{\text{bat-ip-after}}$, $\omega_{\text{bat-after}}$, and KE_{lost}

Inputs and outputs for the Sliding Pin model from Table 5.1	
Inputs	$v_{\text{ball-before}}$, $\omega_{\text{ball-before}}$, $v_{\text{knob-before}}$, $\beta_{\text{knob-before}}$ and CoR_{2c}
Outputs	$v_{\text{ball-after}}$, $\omega_{\text{ball-after}}$, $v_{\text{bat-ip-after}}$, $\beta_{\text{knob-after}}$ and KE_{lost}

The BaConLaws and Sliding Pin models are analogous, but they are not equivalent. The derivations followed the same processes and the outputs have similar forms but the numerical values are different.

The BaConLaws model states that the maximum-batted-ball speed will occur for a collision 0.66 m from the knob, while the Sliding Pin model states that the maximum-batted-ball speed will occur for a collision 0.68 m from the knob. Once again, the models are different.

From our sensitivity analyses, we have, for the BaConLaws model,

$$\frac{\partial v_{1a}}{\partial I_2} = \frac{B m_1 m_2^2 d_{\text{cm-cop}}^2}{K^2}$$

and for the sliding pin model

$$\frac{\partial v_{1a}}{\partial I_k} = \frac{B m_1 m_2^2 d_{\text{knob-ip}}^2}{\bar{K}^2}$$

Once again, the results are different.

Perhaps, we are making too big of a deal about this, but at the risk of pressing our luck, let us do one more analysis of the difference between the BaConLaws model and the Sliding Pin model. Please refer to Fig. 5.6.

Assume that we took two top-view photographs of a bat in motion as shown in Fig. 5.6. Then, we took a ruler and measured the distances. If the distances were

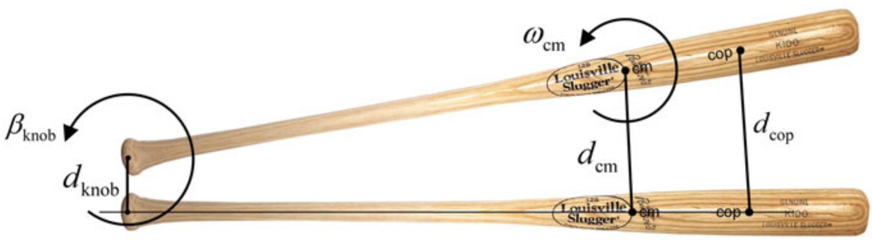

Fig. 5.6 Positions in space for a bat at two different times

small (smaller than shown in the figure), then we could approximate $\frac{\Delta x}{\Delta t} \approx v$ and then we could fit these data with the BaConLaws model.

$$\begin{aligned} vt_{\text{cop}} &= vt_{\text{cm}} + d_{\text{cm-cop}}\omega_{\text{cm}} \\ \omega_{\text{cm}} &= \frac{vt_{\text{cop}} - vt_{\text{cm}}}{d_{\text{cm-cop}}} \\ vt_{\text{cm}} &= vt_{\text{cop}} - d_{\text{cm-cop}}\omega_{\text{cm}} \end{aligned}$$

For the BaConLaws model, $vt_{\text{cm}} = v_{\text{cm}}$. From the measurements, we could find v_{cm} and ω_{cm}.

We could also fit these same data with the Sliding Pin model.

$$\begin{aligned} vt_{\text{cop}} &= vt_{\text{knob}} + d_{\text{knob-cop}}\beta_{\text{knob}} \\ \beta_{\text{knob}} &= \frac{vt_{\text{cop}} - v_{\text{knob}}}{d_{\text{knob-cop}}} \\ vt_{\text{knob}} &= vt_{\text{cop}} + d_{\text{knob-cop}}\beta_{\text{knob}} \end{aligned}$$

For the Sliding Pin model $vt_{\text{knob}} = v_{\text{knob}}$. From the measurements, we could find v_{knob} and β_{knob}.

Now the whole point of this discussion is that we have two valid models that we can apply to this set of experimental data. Which one is correct? They are both correct. Which you should choose depends on your purpose and your data.

5.4.1 Simulation Results

Tables 5.3 and 5.4 show the results of our Excel simulation of the Sliding Pin model equations using the Diamond Kinetics input data from Table 5.1. These

Table 5.3 Simulation values for bat–ball collisions of the Sliding Pin model

	SI units (m/s, rad/s)	Baseball units (mph, rpm)
Inputs		
$v_{\text{ball-before}}$	−37.1	−83.0
$\omega_{\text{ball-before}}$	209	2000
$v_{\text{knob-before}}$	4.5	10
β_{before}	41	387
CoR_{2c}	0.453	0.453
Outputs		
$v_{\text{ball-after}}$	37.2	83.4
$\omega_{\text{ball-after}}$	$= \omega_{\text{ball-before}}$	
$v_{\text{knob-after}}$	−7	−17
β_{after}	18	175

Table 5.4 Comparison of inputs and outputs of the Sliding Pin model and the BaConLaws model

	SI units (m/s, rad/s)	Baseball units (mph, rpm)
Sliding Pin model		
Inputs		
$v_{\text{knob-before}}$	4.5	10
β_{before}	41	387
$vt_{\text{bat-ip-before}}$	33.4	75
Outputs		
$v_{\text{knob-after}}$	−7	−17
β_{after}	18	175
BaConLaws model		
Inputs		
$v_{\text{bat-cm-before}}$	23	52
$\omega_{\text{bat-before}}$	32	309
$vt_{\text{bat-ip-before}}$	28	62
Outputs		
$v_{\text{bat-cm-after}}$	11	24
$\omega_{\text{bat-after}}$	1	7

Table 5.5 Kinetic energies for the Sliding Pin model collision, Joules

KE of ball linear velocity before, $v_{\text{ball-before}}$	100
KE of bat linear translational velocity before, $v_{\text{bat-trans-before}}$	9
KE of ball angular velocity before, $\omega_{\text{ball-before}}$	1.7
KE of bat angular velocity before, β_{b}	280
KE before, total	391
KE of ball linear velocity after, $v_{\text{ball-after}}$	100
KE of bat linear translational velocity after, $v_{\text{bat-trans-after}}$	25
KE of ball angular velocity after, $\omega_{\text{ball-after}}$	1.7
KE of bat angular velocity after, β_{a}	57
KE after, total	184
KE lost	207
KE before minus (KE after plus KE lost)	391

It is just a coincidence that the KE of the ball linear velocity before and after are nearly the same

results are similar to those in Tables 4.2 and 4.3 for the BaConLaws model except that the batted-ball speed $v_{\text{ball-after}}$ is smaller, 83 mph (37.2 m/s) versus 92 mph (41 m/s).

The kinetic energies of the bat linear velocity and the bat angular velocity in Table 5.4 are different from those in Table 4.3, because the experimental input data for the variables are different. Otherwise, the numbers in Table 5.4 are comparable to those of Table 4.3. This shows that our analysis and equations are consistent.

Modeling philosophy note. Earlier we noted that, if we set $d_{\text{cm-ip}} = 0$ in the simulation of the BaConLaws model so that the impact point was at the center of mass of the bat, then Tables 4.2 and 4.3 changed and produced the results of Tables 3.3 and 3.4 for configuration 1b. This means that the whole BaConLaws model (equations, simulations, sensitivity analyses, results, etc.) can be reduced to be appropriate for configurations 1a, 1b and 2a by zeroing appropriate values. However, this does not work for all models. For example, we cannot set variables and parameters in the Sliding Pin model so that it is equivalent to the BaConLaws model or the Effective Mass model. The Sliding Pin model is analogous to the BaConLaws model, but it is not equivalent.

5.5 Collision with Friction

Purpose: The purpose of this section is to present the Collision with Friction model. Our modeling technique could not handle this configuration because our model is only good for a point before the collision and a point after the collision. It cannot handle behavior during the collision. The BaConLaws model of Chap. 4 fulfilled part of the first purpose of this book. It showed a complex configuration for which our technique did work. This section completes the fulfillment of this purpose by showing a configuration for which our technique is too simple.

One of the purposes of this book is to find how complicated our configurations can be and still be solvable using only Newton's axioms and the conservation laws. The BaConLaws model passed this test. So now, let us try configuration 2d, the Collision with Friction model. This model is for a collision at the sweet spot of the bat with spin on the pitch and with consideration of friction between the bat and ball, as shown in Fig. 5.7. The inputs, outputs and equations are given in Table 5.5.

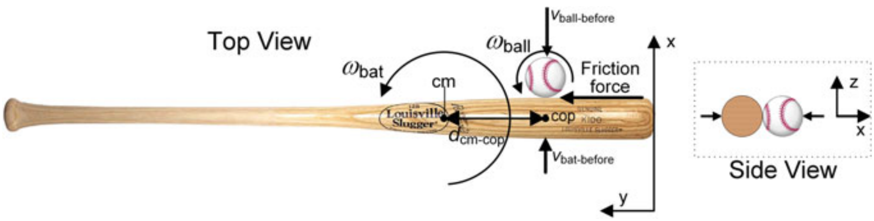

Fig. 5.7 Model of the bat–ball collision with the addition of friction between the bat and ball. The arrows show that angular momenta are positive when pointing out of the page

Table 5.5 Equations for the Collision with Friction model, two equations and one unknown

Inputs	$v_{\text{ball-before}},\ \omega_{\text{ball-before}},\ vt_{\text{bat-ss-before}},\ \omega_{\text{bat-ip-before}}$
Outputs	$\omega_{\text{ball-after}}$
Equations	
Newton's Second Law, Eq. (5.6)	$\Delta t'(r_{\text{ball}} \times F_{\text{friction}}) = -(I_{\text{ball}}\omega_{\text{ball-after}} - I_{\text{ball}}\omega_{\text{ball-before}})$
Conservation of Angular Momentum, Eq. (5.7s)	$L_{\text{initial}} = L_{\text{final}}$ $m_1 v_{1\text{b}} d + (I_1 + m_1 d^2)\omega_{1b} + I_2\omega_{2b} - 0.1\mu_f m_1 r_1 \lvert v_{1\text{b}}\rvert + m_1 d^2 \omega_{1b}$ $= +m_1 v_{1\text{a}} d + (I_1 + m_1 d^2)\omega_{1a} + I_2\omega_{2\text{a}} + 0.1\mu_f m_1 r_1 \lvert v_{1\text{a}}\rvert - m_1 d^2 \omega_{1a}$

5.5.1 Using Newton's Axioms

During the collision, the ball velocity changes from $v_{\text{ball-before}}$ to $v_{\text{ball-after}}$. Assume that the ball velocity reaches zero somewhere in the middle of the collision. Therefore, during this first part of the collision, the velocity changes from $v_{\text{ball-before}}$ to 0. By Newton's second axiom, we can write the force that the ball exerts on the bat normal to the tangent plane of the collision is $F_{\text{normal}} = \frac{m_{\text{ball}} v_{\text{ball-before}}}{\Delta t}$. We postulate that during the first part of the collision the ball is sliding across the bat. Therefore, the friction force acting on the ball is

$$F_{\text{friction}} = F_{\text{normal}}\mu_f$$
$$F_{\text{friction}} = \left|\frac{m_1 v_{1\text{b}} \mu_f}{\Delta t}\right|$$

The absolute value sign is necessary because friction always opposes motion. I experimentally measured the dynamic coefficient of friction between a wooden baseball bat and a baseball to be $\mu_f = 0.5$. We will use this numerical value in the simulation. According to Newton's second law, this friction force, shown in Fig. 5.6, creates a torque that reduces the angular momentum of the ball. The amount depends on how long we apply the torque, $\Delta t'$.

$$\Delta t'(r_{\text{ball}} \times F_{\text{friction}}) = -(I_1\omega_{1\text{a}} - I_1\omega_{1\text{b}})$$

As always, omega, ω, stands for the rotational velocity of an object about its center of mass. This friction force only exists when the ball is sliding across the surface of the bat, not when it is rolling or griping. Figure 5.8 shows how the ball is deformed during the collision. This suggests that the ball is sliding on the bat during only a short part of the collision (maybe the first 10% of the total collision duration), then it grips the bat tightly.

We can solve the above equation for $\omega'_{1\text{a}}$. This omega has a prime symbol on it because it is not the omega after the whole collision. It is the omega after only the

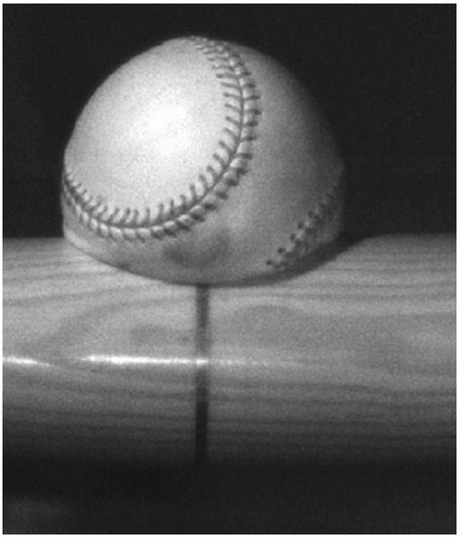

Fig. 5.8 A bat–ball collision showing how much the baseball is deformed during a collision. The collision lasts about one millisecond. *Photo Credit* UMass Lowell Baseball Research Center. From https://student.societyforscience.org/sites/student.societyforscience.org/files/main/articles/ballbat.jpg

first part of the collision where the ball is sliding on the bat. Let $\Delta t'$ be the duration of sliding and Δt be the duration of this part of the collision.

$$I_1\omega'_{1a} = I_1\omega_{1b} - \Delta t' F_{\text{friction}} r_{\text{ball}}$$

$$I_1\omega'_{1a} = I_1\omega_{1b} - \Delta t' \left|\frac{m_1 v_{1b}\mu_f}{\Delta t}\right| r_1$$

Assume that $\Delta t' = \Delta t/10$

$$I_1\omega'_{1a} = I_1\omega_{1b} - |0.1 m_1 v_{1b}\mu_f r_1|$$

$$\omega'_{1a} = \omega_{1b} - \frac{0.1\mu_f m_1 r_1}{I_1}|v_{1b}|$$

This result does not depend on Δt. Near the end of the collision, the friction force rearises, but in the opposite direction (Cross 2011; Kensrud et al. 2016). This *in*creases the ball spin.

$$F_{\text{normal}} = \frac{m_1 v_{1a}}{\Delta t}$$

$$F_{\text{friction}} = \left|\frac{m_1 v_{1a}\mu_f}{\Delta t}\right|$$

This time the ω'_{1b} has the prime symbol because it is not the omega before the whole collision. It is the omega before only this part of the collision.

$$I_1\omega_{1a} = I_1\omega'_{1b} + \Delta t' F_{\text{friction}} r_{\text{ball}}$$
$$I_1\omega_{1a} = I_1\omega'_{1b} + \Delta t' \left|\frac{m_1 v_{1a} \mu_f}{\Delta t}\right| r_1$$
Again assume $\Delta t' = \Delta t/10$
$$I_1\omega_{1a} = I_1\omega'_{1b} + \left|0.1 m_1 v_{1a} \mu_f r_1\right|$$
$$\omega_{1a} = \omega'_{1b} + \frac{0.1\mu_f m_1 r_1}{I_1}|v_{1a}|$$

Now, we ignore all of the time when the ball is not sliding across the bat and ω'_{1a} becomes ω'_{1b} and we can combine these equations to get

$$\omega_{1a} = \omega_{1b} + \frac{\mu_f m_1 r_1}{10 I_1}(|v_{1a}| - |v_{1b}|)$$
or by expanding the subscripts
$$\omega_{\text{ball-after}} = \omega_{\text{ball-before}} + \frac{\mu_{\text{friction}} m_{\text{ball}} r_{\text{ball}}}{10 I_{\text{ball}}}(|v_{\text{ball-after}}| - |v_{\text{ball-before}}|)$$

However, this whole analysis depends on how long the ball slides on the bat before it switches to rolling or griping.

5.5.2 *Conservation of Angular Momentum*

Most of the equations for the BaConLaws model also apply to the Collision with Friction model. The exceptions are Conservation of Energy and kinetic energy lost. As in the BaConLaws model, at the instant when the ball contacts the bat, as shown in Fig. 5.3, the ball has a linear translational velocity of $v_{\text{ball-before}}$ that, as before, we model as the ball rotating about the bat's center of mass at a distance $d = d_{\text{cm-ip}}$. When it comes time to substitute a value for d, we will use either $d = d_{\text{cm-ip}}$ or $d = \sqrt{d^2_{\text{dm-ip}} + r^2_{\text{bat}}}$. However, the sensitivity analysis has shown that this is one of the least significant parameters in the model. Therefore, which we use is not important. The ball also has angular momentum because of its spin: we use the parallel axis theorem to compute the moment of inertia with respect to the center of mass of the bat, $(I_{\text{ball}} + m_{\text{ball}} d^2)\omega_{\text{ball-before}}$. The bat has initial angular momentum, $I_2\omega_{2b}$. Now we add a new term due to the friction between the bat and ball, $r_{\text{ball}} \times F_{\text{friction}}$. This term exists during the collision, not before. Nevertheless, we will lump it in with the initial angular momentum. Therefore, we can write the sum of the initial angular momenta of the bat–ball system about an axis through the center of mass of the bat parallel to the z-axis. In Fig. 5.3, positive moments will be pointing out of the page.

$$L_{\text{initial}} = m_1 v_{1\text{b}} d + \left(I_1 + m_1 d^2\right)\omega_{1b} + I_2\omega_{2b} - F_{\text{friction}} r_1 \Delta t$$
$$L_{\text{initial}} = m_1 v_{1\text{b}} d + \left(I_1 + m_1 d^2\right)\omega_{1b} + I_2\omega_{2b} - \left|0.1\mu_f m_1 v_{1\text{b}} r_1\right|$$

Assume that the last term is$I_1\omega_{1b}$ about the center of mass of the ball. To relate it to an axis through the center of mass of the bat, use the parallel axis theorem.

$$L_{\text{initial}} = m_1 v_{1\text{b}} d + \left(I_1 + m_1 d^2\right)\omega_{1b} + I_2\omega_{2b} - \left(I_1 - m_1 d^2\right)\omega_{1b}$$
$$L_{\text{initial}} = m_1 v_{1\text{b}} d + \left(I_1 + m_1 d^2\right)\omega_{1b} + I_2\omega_{2b} - I_1\omega_b + m_1 d^2\omega_{1b}$$
$$L_{\text{initial}} = m_1 v_{1\text{b}} d + \left(I_1 + m_1 d^2\right)\omega_{1b} + I_2\omega_{2b} - \left|0.1\mu_f m_1 v_{1\text{b}} r_1\right| + m_1 d^2\omega_{1b}$$

For the final angular momentum after the collision, we will treat the ball, as before, as an object orbiting the center of mass of the bat with angular momentum, $m_{\text{ball}} v_{\text{ball-after}} d_{\text{cm-ip}}$. The ball also has angular momentum because of its spin: we use the parallel axis theorem to compute the moment of inertia with respect to an axis through the center of mass of the bat, $(I_{\text{ball}} + m_{\text{ball}} d^2)\omega_{\text{ball-after}}$. The bat angular momentum is $I_{\text{bat}}\omega_{\text{bat-after}}$. The sum of the angular momenta after the collision is

$$L_{\text{final}} = m_1 v_{1\text{a}} d + \left(I_1 + m_1 d^2\right)\omega_{1a} + I_2\omega_{2a} + F_{\text{friction}} r_1 \Delta t$$
$$L_{\text{final}} = m_1 v_{1\text{a}} d + \left(I_1 + m_1 d^2\right)\omega_{1a} + I_2\omega_{2a} + \left|0.1\mu_f m_1 v_{1\text{a}} r_1\right|$$

Assume that the last term is $I_1\omega_{1b}$ about the center of mass of the ball.
To relate it to an axis through the center of mass of the bat, use the parallel axis theorem.

$$L_{\text{final}} = m_1 v_{1\text{a}} d + \left(I_1 + m_1 d^2\right)\omega_{1a} + I_2\omega_{2a} + \left(I_z - m_1 d^2\right)\omega_{1a}$$
$$L_{\text{final}} = m_1 v_{1\text{a}} d + \left(I_1 + m_1 d^2\right)\omega_{1a} + I_2\omega_{2a} + I_z\omega_a - m_1 d^2\omega_{1a}$$
$$L_{\text{final}} = m_1 v_{1\text{a}} d + \left(I_1 + m_1 d^2\right)\omega_{1a} + I_2\omega_{2a} + \left|0.1\mu_f m_1 v_{1\text{a}} r_1\right| - m_1 d^2\omega_{1a}$$

Now for the whole bat–ball collision, we know that the initial angular momentum must equal the final angular momentum.

$$L_{\text{initial}} = L_{\text{final}}$$
$$\begin{aligned} m_1 v_{1\text{b}} d + \left(I_1 + m_1 d^2\right)\omega_{1b} + I_2\omega_{2b} - 0.1\mu_f m_1 r_1 |v_{1\text{b}}| + m_1 d^2\omega_{1b} \\ = +m_1 v_{1\text{a}} d + \left(I_1 + m_1 d^2\right)\omega_{1a} + I_2\omega_{2\text{a}} + 0.1\mu_f m_1 r_1 |v_{1\text{a}}| - m_1 d^2\omega_{1a} \end{aligned}$$

Previously, we used Newton's Second Law, $dm_1(v_{1\text{a}} - v_{1\text{b}}) = -I_2(\omega_{2\text{a}} - \omega_{2\text{b}})$, and solved for $\omega_{2\text{a}}$, $\omega_{2\text{a}} = \omega_{2\text{b}} + \frac{dm_1}{I_2}(v_{1\text{b}} - v_{1\text{a}})$. So let us substitute this into our Conservation of Angular Momentum equation above.

$$m_1 v_{1b} + \left(I_1 + m_1 d^2\right)\omega_{1b} + I_2\omega_{2b} - \left|\mu_f m_1 v_{1b} r_1\right| + m_1 d^2 \omega_{1b}$$
$$= m_1 v_{1a} d + \left(I_1 + m_1 d^2\right)\omega_{1a} + I_2\left\{\omega_{2b} + \frac{dm_1}{I_2}(v_{1b} - v_{1a})\right\} + \left|\mu_f m_1 v_{1a} r_1\right| - m_1 d^2 \omega_{1a}$$

We want to solve this for the angular velocity of the ball after the collision, ω_{1a}

$$-\left(I_1 + m_1 d^2\right)\omega_{1a} + m_1 d^2 \omega_{1a}$$
$$= -m_1 v_{1b} d - \left(I_1 + m_1 d^2\right)\omega_{1b} - I_2\omega_{2b} - \left|0.1\mu_f m_1 v_{1b} r_1\right| + m_1 d^2 \omega_{1b}$$
$$+ m_1 v_{1a} d + I_2 \omega_{2b} + dm_1(v_{1b} - v_{1a}) + \left|0.1\mu_f m_1 v_{1a} r_1\right|$$

Cancel the terms in color, multiply by -1 and rearrange

$$\omega_{1a}(I_1 + m_1 d^2) - m_1 d^2 \omega_{1a} = \omega_{1b}(I_1 + m_1 d^2) + \left|0.1\mu_f m_1 v_{1b} r_1\right| - m_1 d^2 \omega_{1b} - \left|0.1\mu_f m_1 v_{1a} r_1\right|$$
$$\omega_{1a} I_1 = \omega_{1b}(I_1 + m_1 d^2) + \left|0.1\mu_f m_1 v_{1b} r_1\right| - m_1 d^2 \omega_{1b} - \left|0.1\mu_f m_1 v_{1a} r_1\right|$$
$$\omega_{1a} I_1 = \omega_{1b} I_1 + \left|0.1\mu_f m_1 v_{1b} r_1\right| - \left|0.1\mu_f m_1 v_{1a} r_1\right|$$
$$\boxed{\omega_{1a} = \omega_{1b} + \frac{\mu_f m_1 r_1}{10 I_1}\left(\left|v_{1a}\right| - \left|v_{1b}\right|\right)}$$

This is the same equation that we derived earlier using Newton's axioms. This result does not depend on d. Table 5.6 shows the simulation results using this equation. The top two rows show the nominal input values. The next two rows show before and after values for an initial ball spin of 209 rad/s. The next two rows show before and after values for an initial ball spin of 0 rad/s. The final two rows show before and after values for an initial ball spin of −209 rad/s. We know that these numbers are not exact, but they are probably within an order of magnitude. If we put $\omega_{\text{ball}} = -1874$ rpm into the simulation for Fig. 7.13, we find that the difference in range is 1%. The purpose of this table is to estimate the magnitude of error introduced by our Sect. 3.5 derivation of $\omega_{\text{ball-after}} = \omega_{\text{ball-before}}$.

Table 5.6 Simulation values for bat–ball collisions at the sweet spot for the Collision with Friction model

	SI units (m/s or rad/s)	mph or rpm
Inputs		
$v_{\text{ball-before}}$	−37	−83
$vt_{\text{bat-ip-before}}$	28	62
Results		
$\omega_{\text{ball-before}}$	209	2000
$\omega_{\text{ball-after}}$	222	2126
$\omega_{\text{ball-before}}$	0	0
$\omega_{\text{ball-after}}$	13	126
$\omega_{\text{ball-before}}$	−209	−2000
$\omega_{\text{ball-after}}$	−196	−1874

The equations for (1) $v_{\text{ball-after}}$ the linear velocity of the ball after the collision, (2) $v_{\text{bat-ss}-\text{after}}$ the linear velocity of the sweet spot of the bat after the collision, (3) $\omega_{\text{bat-after}}$ the angular velocity of the bat about its center of mass after the collision and (4) *CoR* the coefficient of restitution are the same as those derived for the BaConLaws model.

This section on the Collision with Friction model assumed that the ball slides (does not roll) across the surface of the bat during the collision. However, that is a bad assumption because the ball could slip, slide, roll or grip, or flip from one mode to another during the collision (Cross 2011; Kensrud et al. 2016). To make matters even worst, Rod Cross (personal communication 2016) pointed out that when a ball grips the bat as in Fig. 5.8 there is a large static friction force acting and it can even reverse direction during the impact. Furthermore, presently, the behavior of the bat and ball *at game speeds* is not known. Therefore, although the equations are consistent, we are going to say that the analysis is not valid because we know so little about the actual bat and ball behavior during the collision.

Modeling philosophy note. The Collision with Friction model includes friction during the collision. Our modeling technique cannot handle this configuration because our model is only good for a point before the collision and a point after the collision. It cannot handle behavior *during* the collision. Chapter 4 fulfilled part of the first purpose of this book. It showed a complex configuration for which our technique did work. Chapter 5 completed the fulfillment of this purpose by showing a configuration for which our technique was too simple. From a modeling perspective, this is an important section because few studies show failures. In this section, I show a failure. I tried to model an event, but was unsuccessful. Then I explain why I was unsuccessful.

5.6 Summary

The bat Effective Mass model and the BaConLaws model both start with Newton's axioms: then they diverge. They are different: however, they yield the same rule of thumb for the batted-ball speed! This should strengthen and give people more confidence in both models.

Modeling philosophy note. Having several alternative models helps ensure that you understand the physical system. No model is more correct than another. They just emphasize different aspects of the physical system. They are not competing models; they are synergetic.

This chapter presented alternative models. The Effective Mass model (Fig. 5.1) was similar to the BaConLaws model of Chap. 4, except that it did not have the algebraic equations. The fundamental model for both was that of a free-end collision of a bat and ball that produced a translation and a rotation of the bat about its center of mass. They produced the same rule of thumb for the speed of the batted ball. For a major league wooden baseball bat, the speed of the ball after the collision is

$$\text{batted-ball speed} = -0.19\,\text{pitch speed} + 1.22\,\text{total bat speed} \tag{5.8}$$

The units could be either m/s or mph.

The next two alternative models in this chapter were data-based models. They allowed forces on the bat handle. The Spiral Center of Mass model (Fig. 5.2) matched data for the swing of the bat where the center of mass of the bat followed a spiral trajectory. The Sliding Pin model (Fig. 5.3) used a translation and a rotation about the knob of the bat. It also allowed the batter to apply forces on the handle during the swing. These three models modeled different aspects of the swing and collision. Therefore, they gave different results for outputs such as batted-ball speed.

The last model in this chapter included friction during the collision. Our modeling technique could not handle this configuration because our model is only good for a point before the collision and a point after the collision. It cannot handle behavior during the collision.

Chapter 4 fulfilled part of the first purpose of this book. It showed a complex configuration for which our technique did work. This chapter completed the fulfillment of this purpose by showing a configuration for which our technique was too simple.

References

Bahill, A. T. (2004). The ideal moment of inertia for a baseball or softball bat. *IEEE Transactions on Systems, Man, and Cybernetics Part A: Systems and Humans, 34*(2), 197–204.

Cross, R. (2009). Mechanics of swinging a bat. *American Journal of Physics, 77*(1), 36–43.

Cross, R. (2011). *Physics of baseball and softball*. New York: Springer.

Fleisig, G. S., Zheng, N., Stodden, D. F., & Andrews, J. R. (2001). Relationship between bat mass properties and bat velocity. In *Biomechanics Symposia 2001*, University of San Francisco.

Fleisig, G. S., Zheng, N., Stodden, D. F., & Andrews, J. R. (2002). Relationship between bat mass properties and bat velocity. *Sports Engineering, 5,* 1–8. 10.1046/j.1460-2687.2002.00096.x.

Kensrud, J. R., Nathan, A. M., & Smith, L. V. (2016, October). Oblique collisions of baseballs and softballs with a bat. *American Journal of Physics*.

King, K., Hough, J., & McGinnis, R. (2012). A new technology for resolving the dynamics of a swinging bat. *Sports Engineering, 15,* 41–52.

Milanovich, M., & Nesbit, S. M. (2014, January). A three-dimensional kinematic and kinetic study of the college-level female softball swing. *Journal of Sports Science & Medicine, 13*(1), 180–191. PMCID: PMC3918556.

Nathan, A. M. (2003). Characterizing the performance of baseball bats. *American Journal of Physics*, *71*, 134-143.

Watts, R. G., & Bahill, A. T. *Keep your eye on the ball: Curveballs, knuckleballs, and fallacies ofbaseball*. New York: W. H. Freeman and Co., first edition, 1990, second edition 2000.

Willman, D. (2017). BaseballSavant, https://baseballsavant.mlb.com/statcast_search. Last accessed August 2018.

Chapter 6
Synopsis

6.1 Introduction

Purpose: The purpose of this chapter is to compare the models presented in the first five chapters and shows links to other studies in the physics of baseball literature.

The first five chapters of this book presented many models for the swing of the bat and bat–ball collisions. Chapter 1 presented Newton's axioms and laid the groundwork for analyzing bat–ball collisions. It introduced ten different models for the swing of the bat. These ten models had different purposes, inputs and outputs. Each modeled a different aspect of the swing of the bat. None modeled all aspects of the swing. However, studied as a whole, they should provide a good understanding of the swing of a baseball bat. Having alternative models helps ensure that the modeler understands the physical system. No model is more correct than another. They just emphasize different views of the physical system.

Using text and figures, Chap. 2 explained nine common configurations of bat–ball collisions. In Chap. 3, we started developing sets of equations for those configurations. Configuration 1b was for a very simple collision at the center of mass of a translating bat. Configuration 2a added a rotation of the bat and moved the collision point to the sweet spot of the bat. Chapter 3 also presented nine different models for the sweet spot of the bat. It explained that they were based on different physical principles but indicated a general area of the bat. A common theme shown so far in this book is the use of multiple models for each aspect being studied.

In Chap. 4, we developed our complete model for bat–ball collisions. The following equations comprise our BaConLaws model for bat–ball collisions.

A. T. Bahill, *The Science of Baseball*,
https://doi.org/10.1007/978-3-030-03032-2_6

$$
\boxed{
\begin{aligned}
KE_{\text{lost}} &= \frac{1}{2}\frac{m_{\text{ball}}m_{\text{bat}}I_{\text{bat}}\left(v_{\text{ball-before}}-v_{\text{bat-cm-before}}-\omega_{\text{bat-before}}d_{\text{cm-ip}}\right)^2\left(1-CoR_{2b}^2\right)}{m_{\text{ball}}I_{\text{bat}}+m_{\text{bat}}I_{\text{bat}}+m_{\text{ball}}m_{\text{bat}}d_{\text{cm-ip}}^2}\\
CoR_{2\text{b}} &= -\frac{v_{\text{ball-after}}-v_{\text{bat-cm-after}}-d_{\text{cm-ip}}\omega_{\text{bat-after}}}{v_{\text{ball-before}}-v_{\text{bat-cm-before}}-d_{\text{cm-ip}}\omega_{\text{bat-before}}}\\
\text{Let } A &= \frac{\left(v_{\text{ball-before}}-v_{\text{bat-cm-before}}-d_{\text{cm-ip}}\omega_{\text{bat-before}}\right)\left(1+CoR_{2\text{b}}\right)}{m_{\text{ball}}I_{\text{bat}}+m_{\text{bat}}I_{\text{bat}}+m_{\text{ball}}m_{\text{bat}}d_{\text{cm-ip}}^2}\\
v_{\text{ball-after}} &= v_{\text{ball-before}} - Am_{\text{bat}}I_{\text{bat}}\\
v_{\text{bat-after}} &= v_{\text{bat-before}} + Am_{\text{ball}}I_{\text{bat}}\\
\omega_{\text{bat-after}} &= \omega_{\text{bat-before}} + Am_{\text{ball}}m_{\text{bat}}d_{\text{cm-ip}}\\
\omega_{\text{ball-after}} &= \omega_{\text{ball-before}}
\end{aligned}
}
$$

In this set of equations, the *CoR* needs values for velocities *after* the collision. This means that either the value of the *CoR* must be determined experimentally or else an initial value must be assumed and then updated incrementally.

This BaConLaws model for bat–ball collisions gives the linear and angular velocities of the bat and ball after the collision in terms of these same variables before the collision. Its development used only Newtonian mechanics and the conservation laws. It was assumed that there are no external forces and no friction. The fundamental principle and limiting condition for the BaConLaws model was our assumption that the bat–ball collision is a free-end collision. That means that the bat acts as if no one is applying forces to its knob. To visualize this, imagine that the bat is laying on a sheet of ice and you are looking down on top of it, as in Fig. 4.1. Then, a baseball slams into the bat at 80 mph. This collision produces a translation and a rotation of the bat about its center of mass.

Chapter 5 contained four alternative models for bat–ball collisions. The bat Effective Mass model used the same fundamental principles of Newtonian mechanics as the BaConLaws model and the same limiting assumption that the bat–ball collision is a free-end collision. Therefore, its equation and results are similar to the BaConLaws model. For the BaConLaws model, the inputs and outputs are the linear velocity of the bat, the angular rotational velocity of the bat and the velocity of the ball, whereas, for the bat Effective Mass model, the input is the total velocity (meaning translation plus rotation) of the bat and the output is usually only the velocity of the ball. Both of these models produce the following extremely simplified equation:

$$\text{batted} - \text{ball speed} = -0.19\,\text{pitch speed} + 1.22\,\text{total bat speed}$$

The units could be either m/s or mph.

The Spiral Center of Mass model and the Sliding Pin model are data-based, not theory-based. They use a different *type* of data from the previous models. These data provide independently calculated translations and rotations about a specified point on the bat during the swing. They allow rotation about the knob of the bat. Most distinctively, they do not assume a free-end collision. The Spiral Center of Mass model represents the movement of the bat through three-dimensional space during the swing. This motion is not the simple translation and rotation about the center of mass used by the BaConLaws and Effective Mass models. The Spiral Center of Mass model stops when the collision begins. The Sliding Pin model starts when the collision begins.

The purpose of the BaConLaws model was to describe head-on bat–ball collisions at the sweet spot of the bat. It gave the speed and spin of the bat and the ball before and after collisions. The inputs for the BaConLaws model were the translational and rotational velocities at the center of mass of the bat. The purpose of the Sliding Pin model was to model a new type of data. The Sliding Pin model used the translational and rotational velocities at the knob. Because these two models had different purposes, inputs and outputs, they are not equivalent. However, both of them give equations for the speed and spin of the bat and ball after the collision in terms of these same variables before the collision. In the third edition of this book, once we create a gold-standard input dataset for swings of the bat, we will compare the BaConLaws and the Sliding Pin models using this gold standard.

Finally, the Collision with Friction model considered friction during the collision. It was shown that this type of collision cannot be modeled precisely using only the conservation laws. Therefore, this model completes the fulfillment of the first purpose of this book, to show a configuration that is too complex for our simple technique.

6.2 Limitations

We showed that the BaConLaws model for bat–ball collisions could be modeled using only Newton's axioms and the conservation laws, whereas configurations 2d, 3 and 4 will have to use additional details such as those presented in physics of baseball papers of Adair (2002), Brach (2007), Cross (2011), Hubbard (http://faculty.engineering.ucdavis.edu/hubbard/), Nathan (http://baseball.physics.illinois.edu/), Russell (http://www.acs.psu.edu/drussell/), Sherwood (https://www.uml.edu/Engineering/Mechanical/faculty/sherwood-james.aspx) and Smith (http://www.mme.wsu.edu/people/faculty/faculty.html?smith). This current book is at a higher level of abstraction (Bahill et al. 2008) than those physics of baseball papers, because it ignores details during the collision, such as (1) the ball can slip, slide, roll or grip the bat, and the ball switches between these modes, (2) the coefficient of friction can change from dynamic to static, (3) the bat and ball deform (Mustone and Sherwood 2003), (4) the collision has normal and tangential components and (5) the bat has a twist or a rotation about its long axis. This book ignores the difference between a half-dozen parameters that have commonly been used for collision analysis such as the *kinetic* coefficient of restitution, the *energetic* coefficient of restitution, μ or e_{T} that models the energy loss due to tangential forces and e_m that models the losses in angular momentum. This book grouped all of the energy losses into one parameter, the *kinematic* Coefficient of Restitution (*CoR*). This book models the variables of the bat and ball at a time just before the collision and at a time just after the collision, not during the collision.

The authors mentioned in the previous paragraph are, for the most part, members of the bat Effective Mass modeling community. The bat Effective Mass model for bat–ball collisions was developed by Alan Nathan. The people in this community think that it is an intuitive model. It was presented at the beginning of Chap. 5. The bat Effective Mass model usually produces only the batted-ball speed, whereas the BaConLaws model also gives equations for the bat linear and angular velocities after the collision. However, I come from a different background. I am an engineer and a modeler. Back in the 1970s, engineers would not design with integrated circuits that did not have a second source. Therefore, integrated circuit manufacturers *gave* their masks to their competitors! That way there would be a second source for the integrated circuits in case the first manufacturer's process went sour. From that experience, I learned to cherish alternative models. Chapters 1– 5 of this book provide alternative models for bat–ball collisions. The BaConLaws model of Chap. 4 was based on the conservation laws. Its derivations are completely different, yet it yields similar results to the bat Effective Mass model. This should allow people to put more faith in both models. They are not competing models: they are synergistic.

A model is a simplified representation of a particular view of a real system. No model matches all views of its real system perfectly. If it did, then there would be no advantage to using the model. In modeling theory, there is *never one* correct model. Good modelers always embrace alternative models. This enhances the probability of the models being useful.

The terms in Table 1.1 should be understandable by high-school students, undergraduates and all other students of the science of baseball. These terms are all you need to know to understand this book. This book does not obfuscate with jargon, rules of thumb or esoteric terms such as *swing weight* (moment of inertia about a pivot point six inches from the knob), *swing speed* (the angular speed of the bat), the *trampoline effect* (hollow aluminum and composite bats are more elastic than wooden bats), *hoop frequency* (vibration of the barrel), the Ball–Bat Coefficient of Restitution (BBCOR), collision efficiency, rebound power, intrinsic power, bounce factor and recoil factor. By using only fundamental principles and no jargon, it is hoped that the reader will gain intuition about the behavior of the bat and ball before and after collisions.

6.3 Summary

One purpose of this book was to show how complicated bat–ball collisions could be while still being modeled using only Newton's axioms and the conservation laws. We were successful. The BaConLaws model was the pinnacle of our models, whereas the Collision with Friction model involved actions *during* the collision. Because our technique is only valid for points before and after the collision, we concluded that the Collision with Friction model is inappropriate for our simple Newtonian technique. Therefore, the BaConLaws model is the most complex configuration for which our technique, based only on Newton's axioms and the conservation laws, is valid. Our configurations were explained in Chap. 2. The five equations that we used are listed in Table 4.1. These equations were used for configurations 2a, 2b, 2c and 2d. Additionally, all of these results can be simplified to be appropriate for previous configurations. We derived these equations for the BaConLaws model of configuration 2b. But most importantly, if we set, for example, the initial ball spin equal to zero, then they satisfy configuration 2a. If we let $d_{\text{cm-ip}} = 0$ the resultant equations are the same as those we derived for configurations 1a and 1b. This is a validation of the equations of the BaConLaws model.

A second purpose of this book was to show how the individual batter could select or create the optimal baseball or softball bat for him or herself. The sensitivity analysis and optimization study of this book showed that the most important variable, in terms of increasing batted-ball speed, is bat speed before the collision. However, in today's world, the coefficient of restitution and the bat mass are experiencing the most experimentation in trying to improve bat performance, although the bat moment of inertia provides more room for future improvement. Above all, future studies must include physics in conjunction with physiology in order to improve bat performance.

References

Adair, R. K. (2002). *The physics of baseball* (3rd ed.). New York: HarperCollins.

Bahill, A. T., Szidarovszky, F., Botta, R., & Smith, E. D. (2008). Valid models require defined levels. *International Journal of General Systems, 37*(5), 533–571.

Brach, R. M. (2007). *Mechanical impact dynamics: Rigid body collisions.* Hoboken: Wiley.

Cross, R. (2011). *Physics of Baseball and Softball.* Berlin: Springer.

Mustone, T. J., & Sherwood, J. A. (2003). *A method to evaluate and predict the performance of baseball bats using finite elements* (MS Thesis). University of Massachusetts Lowell.

Chapter 7
The Ball in Flight Model

7.1 Introduction

Purpose: One purpose of this chapter was to derive equations and develop the Ball in Flight model. This model was then used to show how altitude, temperature, barometric pressure and relative humidity affect air density, and consequently how air density affects the flight of the ball.

7.2 Movement of the Ball in Flight

Baseball batters say that the pitch hops, drops, curves, breaks, rises, sails or tails away. Baseball pitchers say that they throw fastballs, screwballs, curveballs, drop curves, flat curves, knuckle curveballs, sliders, backup sliders, backdoor sliders, changeups, palm balls, split-fingered fastballs, splitters, forkballs, sinkers, cutters, two-seam fastballs and four-seam fastballs. This sounds like a lot of variation. However, no matter how the pitcher grips or throws the ball, once it is in the air its motion depends only on gravity, its velocity and its spin. In engineering notation, these pitch characteristics are described, respectively, by a gravity vector, a linear velocity vector and an angular velocity vector, each with magnitude and direction. The magnitude of the linear velocity vector is called pitch speed and the magnitude of the angular velocity vector is called the spin rate. These vectors produce a force acting on the ball that causes a deflection of the ball's trajectory. This chapter is based on Bahill et al. (2009).

Figures 7.1 and 7.2 show the effects of spin on the pitch. During the pitch of a major league baseball, the ball falls about three feet due to gravity ($d = ½\ at^2$). However, the fastball has backspin that opposes gravity and the curveball has top spin that aids the fall due to gravity. The simulations for these figures were run at standard temperature and pressure (STP).

A. T. Bahill, *The Science of Baseball*,
https://doi.org/10.1007/978-3-030-03032-2_7

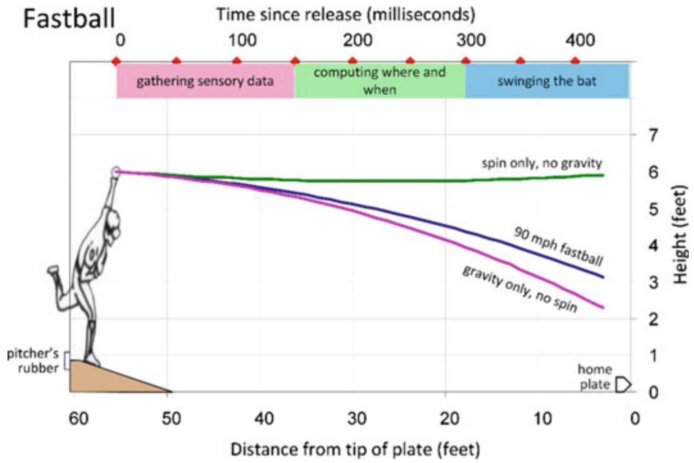

Fig. 7.1 A 90 mph (40 m/s) overhand fastball launched one-degree downward with 1200 rpm of backspin

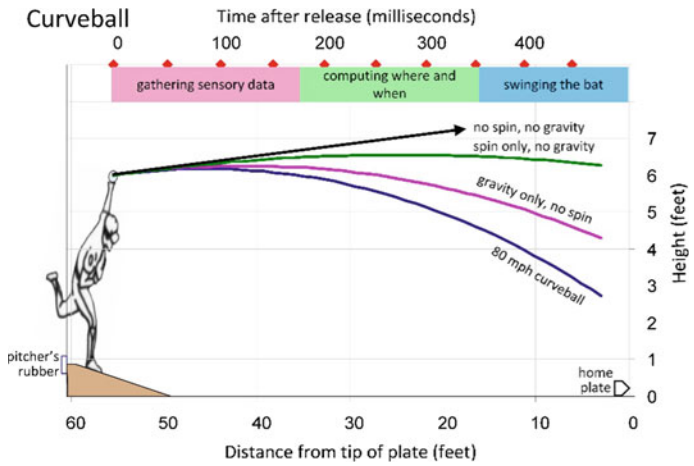

Fig. 7.2 An 80 mph (36 m/s) overhand curveball launched two-degrees upward with 2000 rpm of topspin

In the simulations of Figs. 7.1 and 7.2, the pitcher releases the ball five feet (1.5 m) in front of the pitcher's rubber at a height of six feet (1.8 m). The batter hits the ball 1.5 feet (0.5 m) in front of home plate. These figures also show what the batter's brain is doing during the pitch. During the first third of the pitch, he is gathering sensory information (mostly with his eyes) about the velocity and spin of the pitch. During the middle third of the pitch, he is computing where and when the ball will cross the plate. During the last third, he is swinging the bat and can do little to alter its trajectory.

For a half-century, our models were hampered by limited data for the spin of the ball. The best published experimental data for the spin rate of different pitched baseballs came from Selin's cinematic measurements of baseball pitches (Selin 1959). But now there is a plethora of data. The two biggest surprises from these new data were that the average fastball has almost the same spin rate as the average curveball and that the changeup is not really slow.

Table 7.1 presents data for pitches thrown in 2016 in the Arizona Diamondback's stadium. These numbers came from Willman (2017) BaseballSavant. The numbers for the changeup were surprising because their glossary states, "A changeup is one of the slowest pitches thrown in baseball…" Therefore, I computed several datasets and consulted several sources. The numbers were similar. However, please note that the standard deviations for both the velocity and the spin rate are large.

For readers who are familiar with statistics, please allow me this aside for those that are not. By using the term standard deviation in Table 7.1, I assumed that, for example, the velocity data for curveballs were normally distributed. See Fig. 3.4. This means that 68% of the data points were within plus or minus one standard deviation of the average, 79 mph: meaning that 68% of the curveball velocities were between 83 and 75 mph. However, this also means that 16% of major league curveballs had velocities below 75 mph.

The number of pitches column shows the relative popularity of each type of pitch. Of the dozen types of pitches listed in Willman (2017), Table 7.1 only gives data for five. The two-seam and the four-seam fastballs are both listed, just to show that there is little physical difference between the two. The difference must be psychological (meaning visual) (Bahill et al. 2005).

Figure 7.3 shows photographs of spinning baseballs. The simulated four-seam fastball in the top of Fig. 7.3 appears to be a gray blur with thin vertical red lines about 1/7 of an inch apart. These are the individual stitches of the baseball. In contrast, the two-seam fastball (bottom) seems to exhibit two big red vertical stripes about 3/8 of an inch wide. These stripes are evident because they represent seams

Table 7.1 Values for representative major league pitches from Willman (2017)

	Speed of the pitch at the pitcher's release point			Pitch spin rate, absolute values		Number of pitches
Type of pitch	Average (mph)	Standard deviation	Average (m/s)	Average (rpm)	Standard deviation	
4-seam fastball	93.6	2.3	41.8	2169	363	10,215
2-seam fastball	92.7	2.4	41.4	2148	321	2959
Slider	85	3.1	38	745	346	4072
Changeup	85	3.5	38	1714	419	2370
Curveball	79	3.8	35	1286	461	1865

rather than individual stitches. They provide easily perceived information to the batter for determining the angle of the spin and the direction of the resultant deflection. In an experiment with 104 laypeople, our subjects could distinguish the pink stripes of the two-seam fastball on average 43 feet from the ball, whereas they could only see the pink lines of the four-seam fastball on average 17 feet away. In the bottom of Fig. 7.3, the red stripes are vertical. Were the stripes at an angle, they would indicate the horizontal direction in which the ball would curve. Therefore, the big difference between four-seam and two-seam fastballs is that (because of the visibility of vertical red stripes) the batter may be able to perceive the spin on the two-seam fastball. Videos of these simulated fastballs are available at http://sysengr.engr.arizona.edu/baseball/index.html.

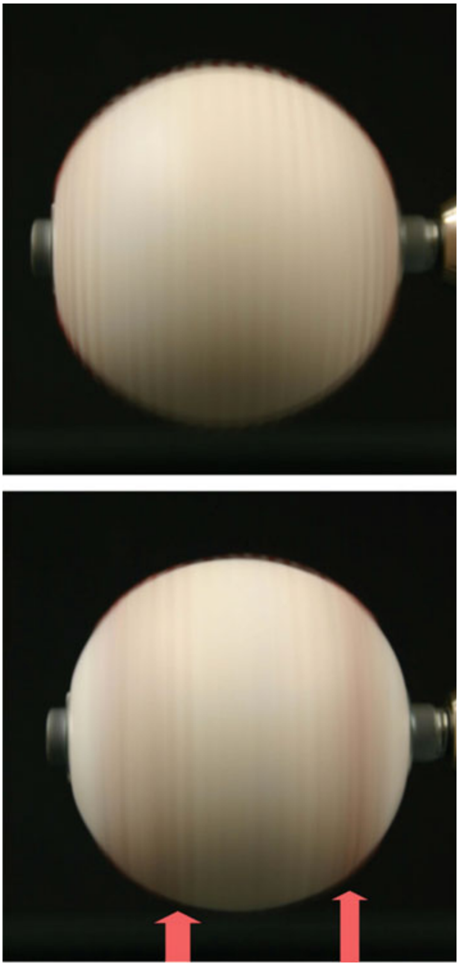

Fig. 7.3 Photographs of spinning balls simulating a fastball thrown with (top) a four-seam grip and (bottom) a two-seam grip. The balls are being rotated at 1200 rpm (20 times per second). The camera exposures are about 0.25 s

Table 7.2 Major league averages from Statcast

Type of pitch	Average, speed at the release point (mph)	Average spin rate (rpm)
4-seam fastball	92.9	2226
2-seam fastball	91.9	2123
Slider	84.6	2090
Changeup	83.9	1746
Curveball	78.2	2308

Table 7.2 presents 2015 data from the Statcast system (Petriello 2016). It has higher spin rates for the slider and the curveball than Table 7.1. This reiterates the fact that the numbers given in Tables 7.1 and 7.2 are still just estimated values subject to theoretical and measurement errors. Although they did not present their data, we presume that these systems measured the air density and wind speed at field level for every pitch.

7.3 Right-Hand Rules for a Spinning Ball in Flight

We will now apply the right-hand rules to the linear velocity vector and the angular velocity vector in order to describe the direction of the spin-induced deflection of the spinning ball in flight. First, we use the angular right-hand rule to find the direction of the spin axis. As shown in Fig. 7.4, if you curl the fingers of your right hand in the direction of spin, your extended thumb will point in the direction of the spin axis.

Next, we use the coordinate right-hand rule to determine the direction of the spin-induced deflection force. Point the thumb of your right hand in the direction of the spin axis (as determined from the angular right-hand rule), and point your index finger in the direction of forward motion (Fig. 7.4). Bend your middle finger so that it is perpendicular to your index finger. Your middle finger will be pointing in the direction of the spin-induced deflection (of course, the ball also drops due to gravity). The spin-induced deflection force will be in a direction represented by the cross product of the angular velocity vector (the spin axis) and the linear velocity vector of the ball: Angular velocity × Linear velocity = Spin-induced deflection force. Or mnemonically, **S**pin **a**xis × **D**irection = **S**pin-**i**nduced **d**eflection (SaD Sid). This acronym only gives the direction of spin-induced deflection. The equations yielding the magnitude of the spin-induced deflection force are discussed in Sect. 7.6.

The right-hand rules apply to all spinning balls whether thrown by a right-handed pitcher or a left-handed pitcher. They apply to baseballs, softballs, golf balls, soccer balls, tennis balls and even bocce balls.

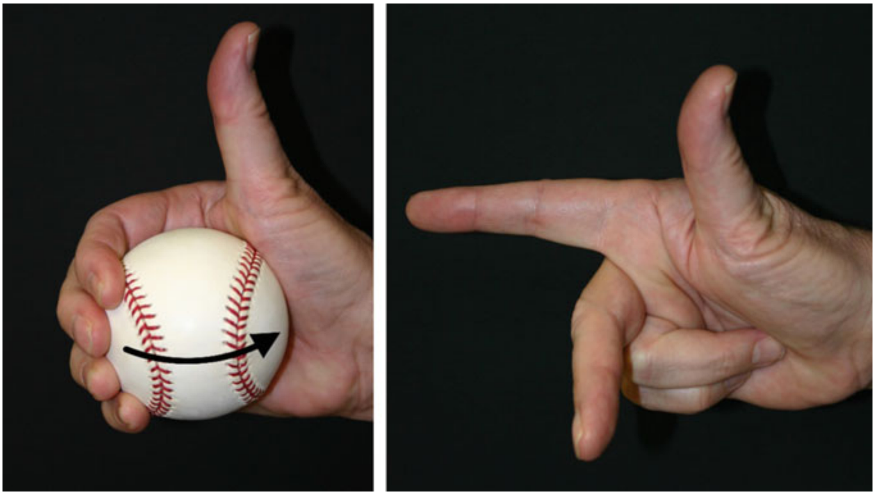

Fig. 7.4 The angular right-hand rule (left). When the fingers are curled in the direction of rotation, the thumb points in the direction of the spin axis. The coordinate right-hand rule (right). If the thumb points in the direction of the spin axis and the index finger points in the direction of forward motion, then the middle finger will point in the direction of the spin-induced deflection. Photographs by Zach Bahill

7.4 Direction of Forces on Specific Pitches

Figures 7.5 and 7.6 show the directions of spin (circular red arrows) and spin axes (straight black arrows) of some common pitches from the perspective of a camera in center field or the pitcher (Fig. 7.5 represents a right-hander's view and Fig. 7.6 a left-hander's view). We will now consider the direction of the spin-induced deflection of each of these pitches.

The spin on the ball is produced by the grip of the fingers and the motion of the pitcher's arm and wrist. This is the difference between all types of pitches (Kindall 1983). When a layperson throws a ball, the fingers are the last part of the hand to touch the ball. If the ball is thrown with an overhand motion, then the fingertips touching the bottom of the ball will impart backspin to the ball. The overhand fastball shown in Fig. 7.6 has predominantly backspin, which gives it lift, thereby decreasing its fall due to gravity as shown in Fig. 7.1. However, most pitchers throw the fastball with a three-quarter arm delivery, which means the arm does not come straight over-the-top, but rather it is in between over-the-top and sidearm. This delivery rotates the spin axis from the horizontal as shown for the fastball in Fig. 7.5. This rotation of the axis reduces the lift and also introduces lateral deflection, to the right for a right-handed pitcher.

The curveball can also be thrown with an overhand delivery, but this time the pitcher rolls his wrist and causes the fingers to sweep in front of the ball. This produces a spin axis as shown for the overhand curveball of Fig. 7.5. This pitch will

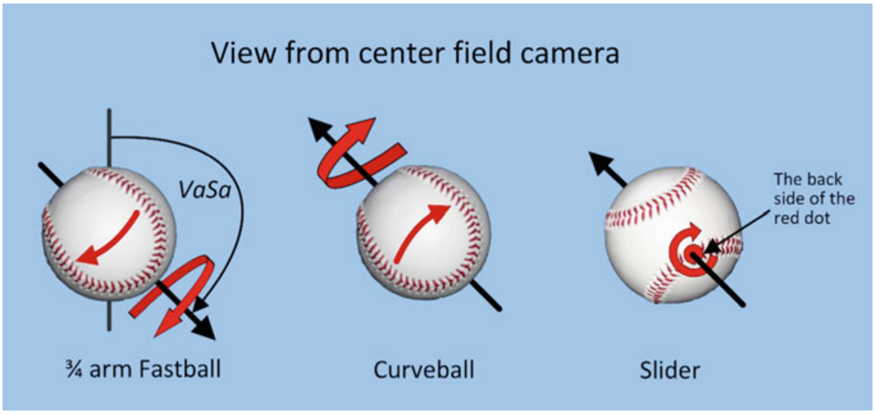

Fig. 7.5 The direction of spin (circular red arrows) and the spin axes (straight black arrows) of a three-quarter arm fastball, an overhand curveball and a slider, all from the perspective of a right-handed pitcher, meaning the ball is moving into the page. VaSa is the angle between the Vertical axis and the Spin axis (VaSa). The spin axes could be labeled spin vectors, because they suggest both direction and magnitude

Fig. 7.6 The direction of spin (circular arrows) and the spin axes (straight arrows) of an overhand fastball, an overhand curveball, a slider and a screwball thrown by a left-handed pitcher. The ball would be moving into the page

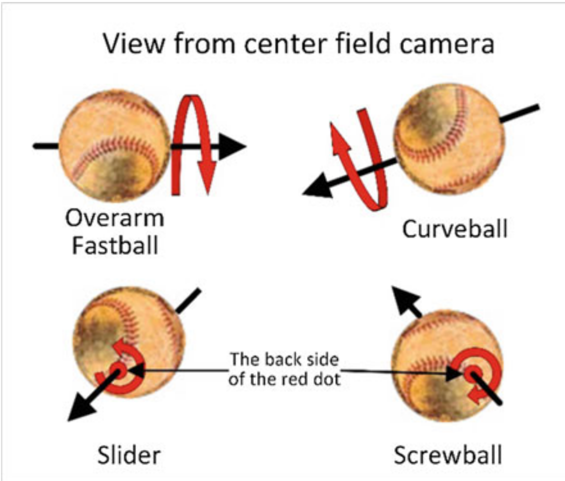

curve at an angle from upper right to lower left as seen by a right-handed pitcher or a camera in center field. Thus, the ball curves diagonally. The advantage of the drop in a pitch is that the sweet area of the bat is about two inches long (5 cm), see Sect. 3.3.1.1 (Bahill 2004) but only one-fifth of an inch (5 mm) high, see Chap. 9. Thus, when the bat is swung in a horizontal plane, a vertical drop is more effective than a horizontal curve at taking the ball away from the bat's sweet area.

The slider is an enigmatic pitch. It is thrown somewhat like a football. Unlike the fastball and curveball, the spin axis of the slider is not perpendicular to the direction

Fig. 7.7 The batter's view of a slider thrown by a right-handed pitcher: the ball is coming out of the page. The red dot alerts the batter that the pitch is a slider

of forward motion. As the angle between the spin axis and the direction of motion decreases, the magnitude of deflection decreases, but the direction of deflection remains the same. If the spin axis is coincident with the direction of motion, as for the backup slider (Bahill and Baldwin 2007, footnote 3), the ball spins like a bullet and experiences no deflection. Therefore, a right-handed pitcher usually throws the slider so that he sees the axis of rotation pointed up and to the left. This causes the ball to drop and curve from the right to the left. Rotation about this axis allows some batters to see a red dot at the spin axis on the upper-right-side of the ball (see Fig. 7.7). Baldwin et al. (2005, 2007) show pictures of this spinning red dot. Videos of this spinning red dot are on Bahill's website http://sysengr.engr.arizona.edu/baseball/index.html. Seeing this red dot is important—if the batter can see this red dot, then he will know the pitch is a slider and he can better predict its trajectory.

7.5 Magnitude of Forces on a Spinning Ball in Flight

Watts and Baroni (1989) proposed that three forces affect the ball in flight, as shown in Fig. 7.8: gravity pulls the ball downward, air resistance or drag operates in the opposite direction of the ball's motion and, if the ball is spinning, there is a Magnus force perpendicular to the direction of motion. Equations for these forces are often written as

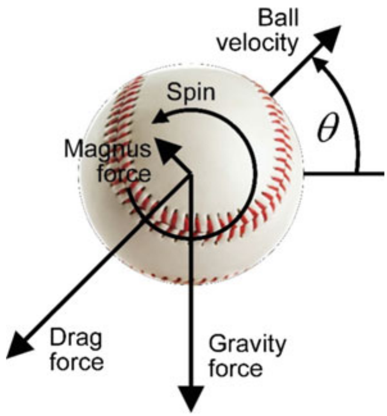

Fig. 7.8 The forces acting on a spinning ball flying through the air

$$F_{\text{gravity}} = m_{\text{ball}} g$$
$$F_{\text{drag}} = 0.5\pi\rho r_{\text{ball}}^2 v_{\text{ball}}^2 C_{\text{D}}$$
$$F_{\text{Magnus}} = 0.5\pi\rho r_{\text{ball}}^3 \omega_{\text{ball}} v_{\text{ball}} C_{\text{M}}$$

7.5.1 The Force of Gravity

The force of gravity is downward, $F_{\text{gravity}} = m_{\text{ball}} g$, where m_{ball} is the mass of the ball and g is the acceleration due to gravity (9.718 m/s^2 at the University of Arizona): the magnitude of F_{gravity} is the ball's weight, as in Table 7.3a.

Table 7.3a Typical baseball and softball parameters for line drives using baseball units (Bahill and Baldwin 2007)

	Major league baseball	Little league	[a]NCAA softball
Ball type	Baseball	Baseball	Softball
Ball weight (oz)	5.125	5.125	6.75
Ball weight, F_{gravity}, (lb)	0.32	0.32	0.42
Ball radius (in)	1.45	1.45	1.9
Ball radius, r_{ball} (ft)	0.12	0.12	0.16
Pitch speed (mph)	85	50	65
Pitch speed, v_{ball} (ft/s)	125	73	95
Distance from front of rubber to tip of plate (ft)	60.5	46	43
Pitcher's release point: (distance from tip of plate, height) (ft)	(54.5, 6)[b]	(42.5, 5)	(40.5, 2.5)
Bat–ball collision point: (distance from tip of plate, height) (ft)	(3, 3)	(3, 3)	(3, 3)
Bat type	Wooden C243	Aluminum	Aluminum
Typical bat weight (oz)	32	23	25
Maximum bat radius (in)	1.3	1.125	1.125
Speed of sweet spot (mph)	57–69[c]	45	50
Backspin of batted ball (rpm)	1800–2500[c]	1800–2500	1800–2500
Launch angle (degrees)	8–20[c]	8–20	8–20
Initial batted-ball velocity, v_{ball} (mph)	85–100[c]	70–80	70–80
Coefficient of Restitution (CoR)	0.55–0.49	0.5	0.44
Desired ground contact point from the plate (ft)	120–240	80–140	80–150
[d]Air mass density, ρ (lb-s^2/ft^4)	0.0023	0.0023	0.0023

[a]NCAA stands for the National Collegiate Athletic Association, which is the governing body for university sports in the United States
[b]http://m.mlb.com/statcast/leaderboard#avg-pitch-velo calls this point the "extension"
[c]From Willman (2017)
[d]Air density depends on altitude, temperature, barometric pressure and humidity

Our tactics are to use baseball units (e.g., feet, mph and pounds, Table 7.3a) for inputs, SI units (e.g., meters, kilograms and seconds, Table 7.3b) for computations, and baseball units for outputs.

7.5.2 The Magnus Force

In 1671, Sir Isaac Newton (1671) noted that spinning tennis balls experienced a lateral deflection mutually perpendicular to the direction of flight and to the direction of spin. Later, in 1742, Robins (1742) bent the barrel of a musket to produce spinning musket balls and also noted that the spinning balls experienced a lateral deflection perpendicular to the direction of flight and to the direction of spin. In 1853, Gustav Magnus studied spinning artillery shells fired from rifled artillery pieces and found that the range depended on crosswinds. A crosswind from the right lifted the shell and gave it a longer range: a crosswind from the left made it drop short. In 1902, the Polish-born Martin Kutta and independently in 1906 Nikolai Joukowski studied cylinders spinning in an airflow. They were the first to model this force with an equation. Although these four experiments sound quite different (and they did not know about each other's work), they were all investigating the same underlying force. This force, now commonly called the Magnus force, operates when a spinning object (like a baseball) moves through a fluid (like air) which results in it being pushed sideways.

The earliest empirical equation for this transverse force on a spinning object moving in a fluid is the Kutta–Joukowski Lift Theorem.

$$\boldsymbol{L} = \rho \boldsymbol{U} \times \boldsymbol{\Gamma} \tag{7.1}$$

where $\boldsymbol{L}$ is the lift force per unit length of a cylinder, ρ is the fluid density, $\boldsymbol{U}$ is the fluid velocity and $\boldsymbol{\Gamma}$ is the circulation around the cylinder, which is analogous to the angular velocity. The boldface font indicates that $\boldsymbol{L}, \boldsymbol{U}$ and $\boldsymbol{\Gamma}$ are vectors.

The original Sikorsky and Lightfoot 1949 C_{lift} and circulation data were given in Alaways (2008).

A little bit of mathematics can change this equation for the force on a cylinder to the force on a sphere (NASA https://www.grc.nasa.gov/WWW/K-12/airplane/beach.html) $\boldsymbol{F}_{\text{Magnus}} = 0.5\pi\rho r_{\text{ball}}^3(\boldsymbol{\omega}_{\text{ball}} \times \boldsymbol{v}_{\text{ball}})C_{\text{M}}$, where C_{M} is a constant. This is an experimental, not a theoretical equation. This is the form that is given in Watts and Ferrer (1987), Watts and Bahill (2000, p. 80) and Sarafian (2015).

A second approach for deriving an equation for the force on a spinning object in a moving fluid stream is to use balls thrown through the air or spun in a wind tunnel. This approach usually starts with an equation of the form $F_{\text{lift}} = 0.5\pi\rho r_{\text{ball}}^2 v_{\text{ball}}^2 C_{\text{lift}}$. Then the experimenters try to find relationships between

Table 7.3b Typical baseball and softball parameters for line drives (SI units)

	Major league baseball	Little league	NCAA softball
Ball type	Baseball	Baseball	Softball
Ball mass, m_{ball} (kg)	0.145	0.145	0.191
Ball radius, r_{ball} (m)	0.037	0.037	0.048
Pitch speed, v_{ball} (m/s)	38	22	29
Distance from front of rubber to tip of plate (m)	18.4	14.0	13.1
Pitcher's release point: distance from tip of plate and height	17 m out 2 m up	13 m out 1.5 m up	12 m out 0.8 m up
Bat–ball collision point: distance from tip of plate and height	1 m out 1 m up	1 m out 1 m up	1 m out 1 m up
Bat type	Wooden C243	Aluminum	Aluminum
Typical bat mass (kg)	0.9	0.6	0.7
Maximum bat radius (m)	0.033	0.029	0.029
Speed of sweet spot (m/s)	25–31	20	22
Backspin of batted ball, ω_{ball} (rad/s)	188–262	188–262	188–262
Launch angle (degrees)	8–20	8–20	8–20
Initial batted-ball velocity, v_{ball} (m/s)	38–45	31–36	31–36
CoR	0.55–0.49	0.5	0.44
Desired ground contact point: distance from the plate (m)	37–73	24–43	24–46
Air density, ρ (kg/m^3) This is the average air density for a game played in a major league stadium on a July afternoon	1.045	1.045	1.045

Air density depends on altitude, temperature, barometric pressure and humidity

the parameters by measuring forces on a ball in a wind tunnel or by measuring the trajectory of a ball in free flight with cameras and then estimating the forces. From these forces, the lift coefficient can be calculated, if you know the air density. The lift coefficient is usually plotted as a function of the spin parameter. The spin parameter is defined as the ratio of the spin velocity to the linear velocity, $SP = \left|\frac{r_{\text{ball}}\omega_{\text{ball}}}{v_{\text{ball}}}\right|$. We use the symbol SP for the spin parameter, whereas some other authors use the symbol S. Using typical values from Tables 7.1 and 7.2 the spin parameters for a major league fastball and curveball are, respectively, $SP = 0.2$ and $SP = 0.25$. Table 7.4 shows spin parameters for other flying baseballs.

There is a large literature showing the lift coefficient for a variety of experimental conditions. We are only interested those that used spinning baseballs. Those

Table 7.4 Spin parameter and Reynolds number for average balls in flight

Type of launch	Initial Speed (mph)	Spin rate (rpm), absolute values	Spin parameter (SP)	[a]Reynolds number (Re, times 10^{-5})
Fastball	93	2200	0.20	1.685
Slider	85	2000	0.20	1.540
Curveball	79	2300	0.25	1.431
Changeup	85	1700	0.17	1.540
Knuckle ball	65	30	0.00	1.178
Batted ball, home run, initial values	98	2000	0.18	1.776
Home run, ball hitting the ground	55	1760	0.28	0.996
Slow line drive	85	2500	0.25	1.540
Fast line drive	100	1800	0.16	1.812
Extreme pop-up	70	6000	0.74	1.268
NCAA softball pitch	65	1200	0.21	1.538

[a]The Reynolds number will be discussed in the next section

with cricket balls, golf balls, smooth balls or nonspinning baseballs are of little use to us. Furthermore, we are only interested in data where the spin parameter was between 0.1 and 0.3. Other values are outside our game of baseball. The knuckleball and the pop-up are governed by effects that are not covered in this book. They are covered, respectively, by Watts and Sawyer (1975) and McBeath et al. (2008). Clanet (2015) analyzed both.

Experimental data for spinning major league baseballs, with $0.1 < SP < 0.3$, show $C_{\text{lift}} \approx 1.2 \times SP$ (Watts and Ferrer 1987; Sawicki et al. 2003; Nathan 2008; Kensrud 2010). We called the numerical value in this equation C_{M}. Therefore, $C_{\text{lift}} = C_{\text{M}} SP = \frac{C_{\text{M}} r_{\text{ball}} \omega_{\text{ball}}}{v_{\text{ball}}}$. Remember, we started with $F_{\text{lift}} = 0.5\pi\rho r_{\text{ball}}^2 v_{\text{ball}}^2 C_{\text{lift}}$. These experiments contained primarily horizontal motions, so $F_{\text{Magnus}} \approx F_{\text{lift}}$. Substituting $C_{\text{lift}} = \frac{C_{\text{M}} r_{\text{ball}} \omega_{\text{ball}}}{v_{\text{ball}}}$ into this lift force equation produces

$$F_{\text{Magnus}} = 0.5\pi\rho r_{\text{ball}}^3 \omega_{\text{ball}} v_{\text{ball}} C_{\text{M}} \tag{7.2}$$

where C_{M} is a constant around 1.2. This is the same equation that we derived above from the Kutta–Joukowski Lift Theorem. This is our final equation for the Magnus force.

7.5.3 The Drag Force

Figure 7.8 also shows a force directly opposite to the direction of motion. This force is called the drag force, or air resistance. The magnitude of this drag force is

$$F_{\mathrm{drag}} = 0.5\pi\rho r_{\mathrm{ball}}^2 v_{\mathrm{ball}}^2 C_{\mathrm{D}} \tag{7.3}$$

where ρ is air mass density, v_{ball} is the ball velocity and r_{ball} is the radius of the ball (Watts and Bahill 2000, p. 161). Typical values for these parameters are given in Tables 7.3a, b. For the aerodynamic drag coefficient, C_{D}, we use a value of 0.4.

Kagan and Nathan (2014) analyzed data from the Pitchf/x system (the camera computer system that overlays pitch trajectories on television replays). For one particular pitch that was analyzed in detail, they computed $C_{\mathrm{D}} = 0.34$. They stated that Nathan's website had Pitchf/x data for 8000 pitches. The C_{D} values varied from 0.28 to 0.58. Kensrud (2010), Figs. 4.35 and 4.38, showed spinning baseball C_{D} at 0.4 and 0.3, respectively. Kensrud et al. (2015) measured $C_{\mathrm{D}} \approx 0.35$ for a major league baseball at 98 mph. There is a lot of variability in these data because the drag coefficient depends on ball speed, ball spin, roughness of the ball surface, height of the seams (Kensrud et al. 2015), orientation of the seams and for a golf ball the shape and number of dimples.

Thrown and batted balls can achieve speeds above 100 mph (147 m/s) and at high speeds the drag coefficient gets smaller (Frohlich 1984; Watts and Bahill 2000, p. 157; Adair 2002; Sawicki et al. 2003, 2004). There are no wind-tunnel data showing the drag coefficient of spinning baseballs over the entire range of velocities and spin rates that characterize major league pitches and hits. Data taken from a half-dozen studies of spinning baseballs, nonspinning baseballs and other balls showed C_{D} between 0.15 and 0.55 (Sawicki et al. 2003). In the data of Nathan et al. (2006), the drag coefficient can be fit with a straight line of $C_{\mathrm{D}} = 0.45$, although there is considerable scatter in these data. The drag force causes the ball to lose about 10% of its speed en route to the plate. The simulations of Alaways, Mish and Hubbard (2001) also studied this loss in speed. Data shown in their Fig. 7.9 for the speed lost en route to the plate can be nicely fit with $\mathit{Percent\,Speed\,Lost} = 20C_{\mathrm{D}}$, which implies $C_{\mathrm{D}} = 0.5$. Clanet (2015). gives a value of 0.38 for baseballs. In summary, the literature has a lot of variation in the coefficient of drag for a spinning baseball. However, most of the numbers are between 0.3 and 0.5.

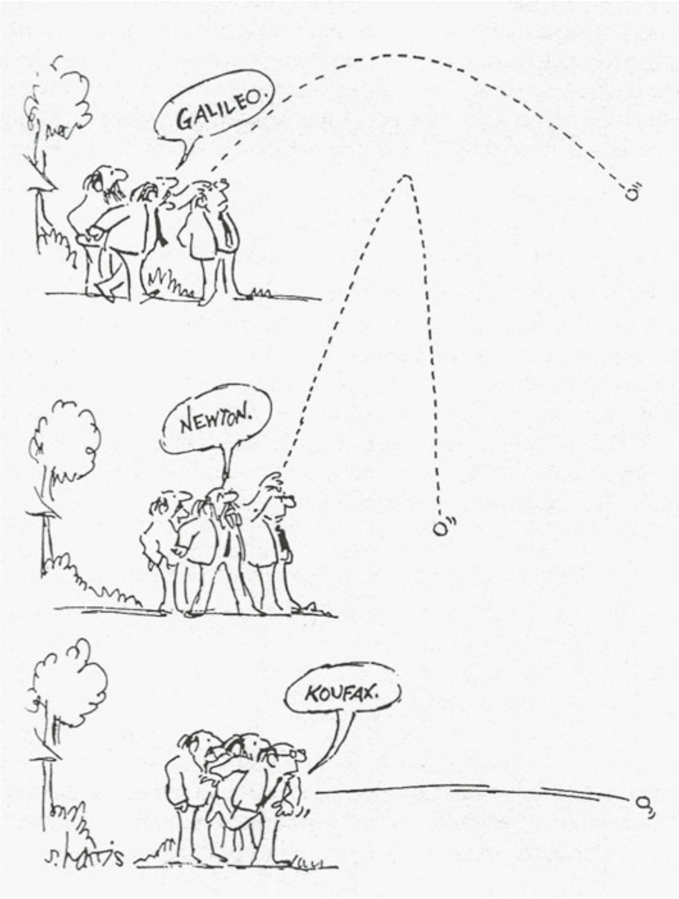

Fig. 7.9 A Sydney Harris (1986) cartoon, © ScienceCartoonsPlus.com, used with permission

Fig. 7.10 He even dreams about that stupid ball

7.5.3.1 The Reynolds Number

The drag on an object in a moving airflow depends on how the air flows around the object. For example, the boundary layer flow around the object could be laminar or turbulent. The drag also depends on the points where the airflow separates from the surface of the object. How the air flows around an object is a function of how fast the air flows. More specifically, the drag is a function of the Reynolds number as shown in Fig. 7.11.

The Reynolds number is defined as $Re = \frac{2r_{\mathrm{ball}}v_{\mathrm{ball}}}{\nu}$ where ν is the *kinematic* viscosity of air. We use $1.8 \times 10^{-5}\ \mathrm{m^2/s}$ or $2 \times 10^{-4}\ \mathrm{ft^2/s}$ for a baseball at 85 °F. The Reynolds number is also written as $Re = \frac{2\rho r_{\mathrm{ball}}v_{\mathrm{ball}}}{\mu}$ where μ is the *dynamic* viscosity of air in kg/m s. The Reynolds number is used to assert whether a flow is laminar or turbulent. Where the flow is laminar, viscous forces dominate and *Re* is low. Where the flow is turbulent, inertial forces dominate and *Re* is high. The Reynolds number is named after the British physicist and engineer Osborne Reynolds who discovered the relationship in 1883. This might all sound complicated, therefore, when I write, Reynolds number, you, the reader, should think scaled ball velocity.

In Fig. 7.11, for smooth balls, the circles of Achenbach (1972), the drop in C_{D} starts at $Re = 3 \times 10^5$ and ends at 4×10^5. This sharp change in drag is bound to arouse curiosity. Frohlich (1984) wrote that if the pitch went through this "drag crisis," en route to the plate, then the ball would surely exhibit a strange trajectory. Figure 7.11 also shows linearized drag coefficient data for seven other data analyses. The Watts and Bahill (2000) analysis for spinning baseballs (Fig. 52, data of

Fig. 7.11 The drag coefficient varies with the Reynolds Number. The circles and the line fit to the them are copies of Achenbach's original figure (1972). The green circles represent the initial ball speeds at the pitcher's release point for a 95 mph fastball and the red squares show the final ball speeds when the ball crosses the plate. The gray box is then the region for the flight of the pitch

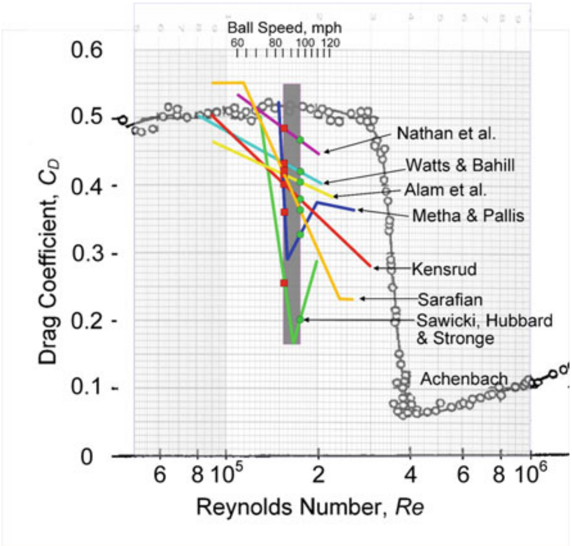

Gonzalez) did not have a sharp drop in the drag coefficient. Metha and Pallis (2001) showed a critical Reynolds number at $Re = 1.7 \times 10^5$ for nonspinning baseballs in wind tunnels. Sawicki et al. (2004) referenced the flight of baseballs in Olympic baseball games. Their calculated drag coefficient for a spinning baseball decreased precipitously at $Re = 1.6 \times 10^5$. Nathan et al. (2006) show drag coefficients around 0.45 for all Reynolds numbers. Kensrud (2010, Fig. 4.50) shows the minimum drag coefficient for nonspinning MLB baseballs at $Re = 2.3 \times 10^5$. The newest experimental data, by Alam et al. (2012), show the minimum drag coefficient for nonspinning MLB baseballs at $Re = 2 \times 10^5$. Sarafian (2015) has a theoretical curve with a minimum drag coefficient at $Re = 2.6 \times 10^5$. Good linear fits to these sets of data are given in Fig. 7.11. Many studies have shown that roughening the surface of the ball or spinning the ball moves the middle and the right parts of the Achenbach curve up and to the left.

Now comes the most important part of this analysis. How much would the drag coefficient change *during* a variety of pitches? If a major league fastball started with a speed of 95 mph, then it would cross the plate with a speed of 85.5 mph. (This ten-percent reduction in ball speed from the pitchers release point until the ball crosses the plate is universal.) Parameters of such a pitch are displayed in Table 7.5 and in the gray box of Fig. 7.11.

The percent increases in the drag coefficient en route to the plate were small, averaging 9%.

The replication crisis The results shown in Fig. 7.11 and Table 7.5 are quite different. Such failures to replicate previous findings are common in science, particularly, in the psychological literature, where half of the important findings could not be replicated (https://en.wikipedia.org/wiki/Replication_crisis; also

Table 7.5 Range of drag coefficient values for a fastball

Authors	Characteristics of the ball	C_D for a 95-mph fastball at the pitcher's release point, green circles	C_D when the ball crosses home plate at 85.5 mph, red squares	Percent change in drag coefficient en route to the plate (%)
Achenbach (1972)	Smooth, nonspinning balls			
Watts and Bahill (1990), Fig. 52	Nonspinning baseballs	0.42	0.43	2
Metha and Pallis (2001)	Nonspinning baseballs	0.33	0.36	9
Sawicki (2004)	Spinning baseballs	0.20	0.25	25
Nathan et al. (2006)	Spinning baseballs	0.47	0.48	2
Kensrud (2010), Fig. 7.50	Nonspinning baseballs	0.38	0.40	5
Alam et al. (2012)	Nonspinning baseballs	0.40	0.41	1
Sarafian (2015)	Theoretical calculations	0.36	0.42	17

Kahneman 2014). This is called the *replication crisis*. However, in the physical sciences, we would expect a much greater replication rate. Therefore, in this physics of baseball endeavor, either some fundamental physical parameter is misunderstood or there is no desire to replicate previous experimental results.

To enhance replicability, Stodden et al. (2016) recommended that we "share data, software, workflows, and details of the computational environment that generate published findings in open trusted repositories." Details include things like the treatment of outliers and missing data values. A good counter-example to this is the Major League Baseball database based on Pitchf/x, etc., that not only does not share data, software and workflows, but it also hides computations and calls them proprietary. From the viewpoint of the scientific community, this is awful behavior by Major League Baseball.

The papers cited in Fig. 7.11 and Table 7.5 generally refer the previous papers, but they do not explain why their new results are different from the old results. Maybe the physics of baseball is too immature to expect replicability. For the most part, the experimental procedures are different and many fundamental details, such as air density, are not even given.

So far, this discussion of the drag coefficient has been in terms of the pitch. During the pitch, the drag coefficient changes only by 9%, on average. Now we want to consider the batted ball. The home run is the batted ball that will be affected the most by changes in the drag coefficient because it will be in the air the longest, it will have the biggest changes in velocity and it will, therefore, have the biggest changes in the drag coefficient.

Major League Baseball (MLB) is releasing many new data that show ball speeds above 100 mph. In 2016, MLB measured over 700,000 pitches Willman (2017). Of these 1400 or 0.2% had initial speeds over 100 mph. It also had 140,000 balls hit into play (30% of these were base hits). Of these batted balls, 3.6% had initial batted-ball speeds (exit velocities) greater than 100 mph. These comprise 0.2% of pitches and 3.6% of batted balls. To accommodate these high velocities we could consider the following alternative models for the drag coefficient.

$C_{\mathrm{D}} = 0.4$ as a simple model or we could let

$$C_{\mathrm{D}} = \begin{cases} 0.5 \text{ for ball speed} \leq 85 \text{ mph} \\ 0.3 \text{ for ball speed} > 85 \text{ mph} \end{cases}$$

A more complicated model following a gestalt of Fig. 7.11 would be

$$C_{\mathrm{D}} = \begin{cases} 0.5 \quad \text{for} \quad v_{\mathrm{ball}} \leq 60 \text{ mph} \\ -0.005 v_{\mathrm{ball}} + 0.8 \quad \text{for} \quad 60 < v_{\mathrm{ball}} < 100 \text{ mph} \\ 0.3 \quad \text{for} \quad v_{\mathrm{ball}} \geq 100 \text{ mph} \end{cases}$$

Another complicated model using the data of Alam et al. (2012) is

$$C_{\mathrm{D}} = \begin{cases} 0.5 \quad \text{for} \quad v_{\mathrm{ball}} \leq 30 \text{ mph} \\ -0.004 v_{\mathrm{ball}} + 0.6 \quad \text{for} \quad 30 < v_{\mathrm{ball}} < 90 \text{ mph} \\ 0.25 \quad \text{for} \quad v_{\mathrm{ball}} \geq 90 \text{ mph} \end{cases}$$

However, by Ockham's razor, this added complexity without added validation is useless (Jefferys and Berger 1992). Therefore, until Chap. 8 we will use $C_{\mathrm{D}} = 0.4$.

Figure 7.12 shows the drag coefficient as a function of the Reynolds number for a simulated home run. The green circle in Fig. 7.12 represents the initial batted-ball velocity at the launch point where $v_{\mathrm{ball}} = 97$ mph and $C_D = 0.3$. The red square indicates the coordinates when the ball hits the ground with a $Range = 380$ feet, $v_{\mathrm{ball}} = 55$ mph and $C_{\mathrm{D}} = 0.5$. Compared to pitches where the average change of C_{D} was 9%, for this batted ball the change of C_{D} is 40%. Therefore, the change in the drag coefficient during the *pitch* is not likely to be important, however, for the *batted ball*, it might be more significant.

The BaConLaws model of Chap. 4 is linked to the Ball in Flight model of this chapter. Equation (4.8) from Chap. 4 showed that the *batted-ball velocity* depends on the pitch speed, pitch spin and bat speed. Now this chapter shows that the distance that the batted ball will travel depends on the *batted-ball velocity*, the batted-ball spin rate, the launch angle, the Magnus coefficient, the drag coefficient and air density.

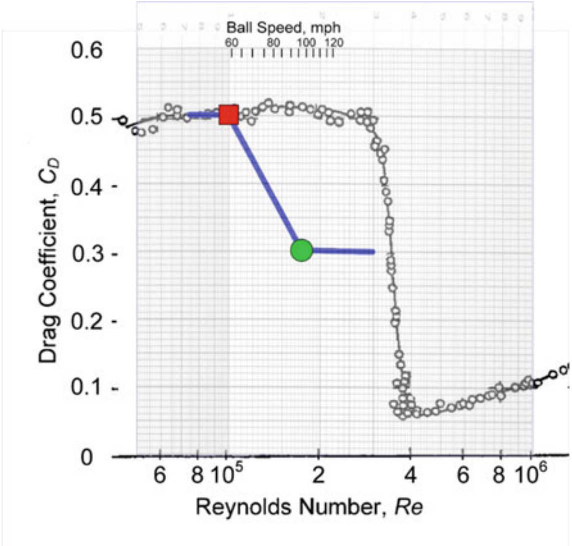

Fig. 7.12 Drag coefficient as a function of the Reynolds Number for a home run

7.6 Sensitivity Analysis

In Sect. 4.11, we performed both an analytic and an empirical (or numerical) sensitivity analysis for the BaConLaws model. First, we chose our performance criterion, the batted-ball speed. Then we calculated the partial derivatives of that performance criterion with respect to the eight model parameters. Finally, we multiplied the partial derivatives by the nominal values of those parameters and evaluated those semirelative sensitivity functions. In that section, our performance criteria, the batted-ball speed, was the result of one of our equations. Therefore, it was easy to calculate the partial derivatives. However, in this chapter for our Ball in Flight model, our chosen performance criterion, the range, is not a result of any single equation. It would be possible but difficult to create such an equation. Therefore, in this chapter, we run the model by simulation and we do an empirical (or numerical) sensitivity analysis.

To do a sensitivity analysis of a model we first select a performance criterion. For the Ball in Flight model, we chose the range, meaning how far the batted-ball travels before it hits the ground. We used our standard pitch and swing of Chap. 4 that produced a batted-ball speed of 92 mph, a backspin rate of 2000 rpm, a launch angle of 34° and a launch height of 3 feet. We used the midlevel or average air density for major league stadiums, $\rho = 0.00205\,\text{lb-s}^2/\text{ft}^4$ (or slugs/ft^3) or $\rho = 1.0582\,\text{kg}/\text{m}^3$. We changed each variable by +1% and computed the new range. Our results are shown in Table 7.6. The range numbers are large because our parameter values are for optimal athletes performing optimally. Few major league batting events would have values as large as these. Laypeople could not come close.

The right column of Table 7.6 shows that the most important variable, in terms of maximizing the batted-ball range, is the batted-ball speed. This is certainly no

Table 7.6 Results of a numerical sensitivity analysis of the Ball in Flight model for a +1% increase in the parameter values

Parameters	Nominal values	Nominal values increased by +1%	Altered range (ft)	Change in range (ft)	Semirelative sensitivity values
Range (ft)	384.87				
Batted-ball speed (mph)	91.9	92.819	389.56	4.69	469
Ball diameter (inches)	2.90	2.9336	382.59	−2.28	−228
Drag coefficient (C_d)	0.4	0.404	383.16	−1.71	−171
Ball weight, oz	5.125	5.1763	386.18	1.31	131
Air density, ρ (kg/m^3)	1.0582	1.0688	383.65	−1.22	−122
Slope of lift coefficient curve (CM)	1.2	1.212	385.37	0.50	50
Ball spin (rpm)	−2000	−2020	385.37	0.50	50
Ball spin (rpm)	−2000	−1980	384.37	−0.50	−50
Launch angle (degrees)	34	34.34	384.39	−0.48	−48
Launch height (feet)	3	3.03	384.90	0.03	3

surprise. The second most important variable is the diameter of the ball. The least important parameters are the launch height and the launch angle. As you can remember, we did not have very good data for the Magnus lift coefficient, so we are happy that its sensitivity is small. The sensitivities to some of the variables and parameters are negative, which merely means that as they increase the range decreases. The results of this sensitivity analysis show that the model is well behaved. The most and least important variables and parameters are as expected. There are no unexpectedly large or small sensitivities. Comparing Tables 4.4 and 7.6, we see that the Ball in Flight model is more sensitive to its parameters than the BaConLaws model is.

Of the 36 possible interaction sensitivities, the most important are (1) the batted-ball speed,v_{1a}, and the ball diameter; (2) the ball weight and the drag coefficient, C_d; (3) the ball weight and air density, ρ; (4) and the ball weight and the Magnus coefficient, CM.

The interaction of the ball spin and the launch angle is small. Figure 7.13 shows its effect graphically. Because of the interactions, the three lines are not the same shape and they peak at different values for the launch angle. These curves are very flat near their peak values, illustrating the small sensitivity to the launch angle at the nominal operating point. For this figure, I choose to use the batted-ball spin rate and the launch angle because that matches Fig. 55 of Watts and Bahill (2000) and is analogous to Nathan (2016).

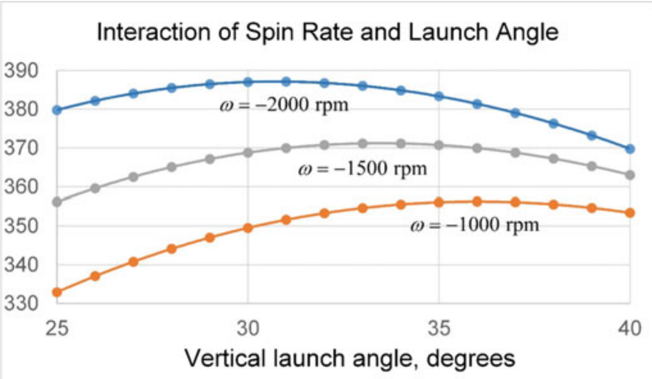

Fig. 7.13 Interaction of spin rate and launch angle

Figure 7.13 shows the interaction of the spin rate and the vertical launch angle. On the left side of this figure, when the launch angle increases, the range goes up. However, these three curves do not have the same shape. The curve for the 2000 rpm spin rate has a steeper drop on the right side. This is the effect of the interaction. The difference in spacing of the lines is not the effect of the interaction. That is merely the dependence of the batted-ball speed on spin rate.

7.7 Numerical Values

This section presents numerical values for the three forces that act on the ball in flight. Its purpose is merely to create familiarity with the numbers. If US customary units are to be used in Eqs. (7.1)–(7.7), then ρ should be in lb-s^2/ft^4 (or slugs/ft^3), v_{ball} should be in ft/s, r_{ball} should be in ft and ω_{ball} should be in rad/s, then F_{drag} would be in lb. Let us now present a simple numerical example. Let us use the average fastball from Table 7.4. When the pitcher releases the ball is going 93 mph (136 ft/s) with 2200 rpm (230 rad/s) of backspin.

$$F_{\text{drag}} = 0.5\pi\rho r_{\text{ball}}^2 v_{\text{ball}}^2 C_{\text{D}}$$
$$F_{\text{drag}} = (0.5)(3.14)(0.002)(0.12)^2(136)^2(0.4) = 0.35 \text{ lb}$$

Near the beginning of the pitch, the Magnus force will be straight up in the air, that is, pure lift.

$$F_{\text{Magnus}} = 0.5\pi\rho r_{\text{ball}}^3 \omega_{\text{ball}} v_{\text{ball}} C_{\text{M}}$$
$$F_{\text{Magnus}} = (0.5)(3.14)(0.002)(0.12)^3(230)(136)(1.2) = 0.07 \text{ lb}$$

The force of gravity is

$$F_{\text{gravity}} = m_{\text{ball}}g = 0.32\,\text{lb}$$

For this fastball, the Magnus force is about one-fifth the force of gravity and one-fifth of the drag force. This is consistent with Tables 7.7a, b where the sixth column shows the drop due to drag and spin. This drop is due to a combination of $F_{\text{drag}} \sin\theta + F_{\text{Magnus}} \cos\theta$.

These simulations were run at standard temperature and pressure (STP). Therefore, the numerical values are different from those in other tables.

Using SI units and Table 7.3b, produces

$$F_{\text{drag}} = 0.5\pi\rho r_{\text{ball}}^2 v_{\text{ball}}^2 C_{\text{D}}$$
$$F_{\text{drag}} = (0.5)(3.14)(1.06)(0.037)^2(42)^2(0.4) = 1.56\ \text{N}$$

and

Table 7.7a Gravity-induced and spin-induced drop for overhand pitches (with the United States customary units) (Bahill and Baldwin 2007)

Pitch speed and type	Spin rate (rpm)	Duration of flight (ms)	Drop due to gravity (ft)	Spin-induced vertical drop (ft)	Total drop (ft)
95 mph fastball	−1200	404	2.63	−0.91	1.72
90 mph fastball	−1200	426	2.92	−0.98	1.94
85 mph slider	+1400	452	3.29	+0.74	4.03
80 mph curveball	+2000	480	3.71	+1.40	5.11
75 mph curveball	+2000	513	4.24	+1.46	5.70

Table 7.7b Gravity-induced and spin-induced drop for overhand pitches (with SI units)

Pitch speed and type	Spin rate (rpm)	Duration of flight (ms)	Drop due to gravity (ft)	Spin-induced vertical drop (ft)	Total drop (ft)
42.5 m/s fastball	−126	404	0.80	−0.28	0.52
40.2 m/s fastball	−126	426	0.89	−0.30	0.59
38.0 m/s slider	+147	452	0.95	+0.23	1.23
35.8 m/s curveball	+209	480	1.13	+0.43	1.56
33.5 m/s curveball	+209	513	1.29	+0.45	1.74

$$F_{\text{Magnus}} = 0.5\pi\rho r_{\text{ball}}^3 \omega_{\text{ball}} v_{\text{ball}} C_{\text{M}}$$
$$F_{\text{Magnus}} = (0.5)(3.14)(1.06)(0.037)^3(230)(42)(1.2) = 0.32\ \text{N}$$

For this fastball, the Magnus force is about one-fifth the force of gravity, which is

$$F_{\text{gravity}} = m_{ball}\text{g} = 0.145 \times 9.718 = 1.41\ \text{N}$$

As a rule of thumb, we offer the following, over a wide range of conditions, the drag force and the force of gravity have about the same magnitude and the Magnus force is about one-fifth as large.

When the ball's spin axis is not horizontal, the Magnus force should be decomposed into a force lifting the ball up and a lateral force pushing it sideways.

$$F_{\text{upward}} = 0.5\pi\rho r_{\text{ball}}^3 \omega v_{\text{ball}} C_{\text{M}} \sin VaSa \tag{7.4}$$

where VaSa is the angle between the vertical axis and the spin axis (Fig. 7.5). The magnitude of the lateral force is

$$F_{\text{sideways}} = 0.5\pi\rho r_{\text{ball}}^3 \omega v_{\text{ball}} C_{\text{M}} \cos VaSa \tag{7.5}$$

Finally, if the spin axis is not perpendicular to the direction of motion (as in the case of the slider), the magnitude of the cross product of these two vectors will depend on the angle between the **S**pin **a**xis and **D**irection of motion, this angle is called SaD (Fig. 7.14). In aeronautics, it is called the angle of attack. Finally, we get

$$F_{\text{lift}} = 0.5\pi\rho r_{\text{ball}}^3 \omega v_{\text{ball}} C_{\text{M}} \sin VaSa \sin SaD \tag{7.6}$$

$$F_{\text{lateral}} = 0.5\pi\rho r_{\text{ball}}^3 \omega v_{\text{ball}} C_{\text{M}} \cos VaSa \sin SaD \tag{7.7}$$

These equations comprise our Ball in Flight model.

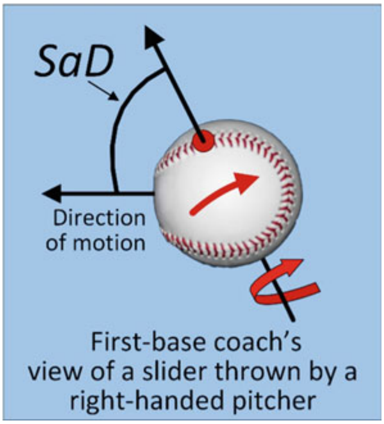

Fig. 7.14 The first-base coach's view of a slider thrown by a right-handed pitcher. This illustrates the definition of the angle SaD

The spin-induced force on the ball changes during the pitch. Its magnitude decreases because the drag force slows the ball down by about 10%. Its direction changes, because gravity is continuously pulling the ball downward, which changes the direction of motion of the ball by 5 to 10 degrees. However, the ball acts like a gyroscope, so the spin axis does not change. This means that, for a slider, the angle SaD increases and partially compensates for the drop in velocity in Eqs. (7.6) and (7.7).

The right-hand rules for the lateral deflection of a spinning ball and Eqs. (7.1)–(7.7) apply to pitched and also batted balls, except it is harder to make predictions about the magnitude of deflection of batted balls because the data about the spin of batted balls are poor. The right-hand rules and these equations can also be applied to soccer, tennis and golf, where speeds, spins and deflections are similar to baseball. However, the right-hand rules and these equations would be inappropriate for American football, because the spin axis of a football is almost coincident with the direction of motion. Therefore, the angle SaD is near zero, and consequently the spin-induced deflections of a football are small (Rae 2004).

7.8 Effects of Air Density on a Spinning Ball in Flight

The distance that a fly ball travels is inversely related the air density. However, the explanation for this is not straightforward. Equations (7.1) and (7.3) show that both the drag and Magnus forces are directly proportional to the air density. Therefore, if air density gets smaller, the drag force gets smaller, this allows the ball to go farther. But at the same time, as air density gets smaller, the Magnus force also gets smaller, which means that the ball will not be held aloft as long and will therefore not go as far. So these two effects are in opposite directions. We have built a computer simulation that implements the above equations. This simulation shows that the change in the drag force has a greater influence on the trajectory of the ball than the change in the Magnus force does; therefore, as air density goes down, the range of a potential home run ball increases. A ten-percent decrease in air density produces a four-percent increase in the distance of a home run ball; however, the increase is less than this for pop-ups and greater than this for line drives. This section is based on Bahill, Baldwin and Ramberg (2009).

Air density is inversely related to altitude, temperature and humidity, and is directly related to barometric air pressure. We derived an equation for these relationships. It came from the WeatherLink Software (2017) and the CRC Handbook of Chemistry and Physics (1980–81) with a correction from Nathan (personal correspondence, 2016). It agrees with the results from Shelquist (2017). Equation (7.8) shows how air density depends on altitude, temperature, humidity and barometric air pressure.

$$Air\ Density = \rho = 1.2929 \times \frac{273}{Temp + 273} \times \frac{Air\ Pres - 0.379(SVP \times RH/100)}{760} \tag{7.8}$$

where *Air Density* is in kg/m^3.
Temp is temperature in degrees Celsius.
Air Pres is the pressure of the air in mm of Hg and is given in Eq. (7.9).
SVP is saturation vapor pressure in mm Hg and is given in Eq. (7.10).
RH is relative humidity as a percentage.

This equation uses the absolute (or actual) atmospheric air pressure, which is also called station pressure because it is the air pressure at a particular weather station. It can be computed from the U.S. Weather Service sea-level corrected barometric pressure (which is given in newspapers, on television and on personal computers) with the following formula.

$$Air\,Press = Barometric\ Pressure\ \left[e^{\frac{-\mathrm{gM}\,Altitude}{\mathrm{R}\,(Temp+273.15)}}\right] \tag{7.9}$$

where g is the Earth's gravitational acceleration (9.80665 m/s^2 at sea level),
M is the molecular mass of air (0.0289644 kg/mole),
R is the Universal Gas Constant (8.31447 J/°K mole),
Altitude is the altitude of the ballpark in meters,
and *Temp* is the temperature in °C.

However, what is *Temp* the temperature of? As a simple approximation in the following examples, we have used the temperature of the baseball stadium. But the above equation should be integrated with respect to the time-averaged temperature from the baseball stadium to mean sea level. Because this is impossible, the National Weather Service (2001) uses nine different approximations: about them they write, "There is no single true, correct solution of Sea Level Pressure … only estimates." For any given time and place, the most accurate measure of air pressure for Eq. (7.8) would be a local barometer that is not corrected to sea level (i.e., with its altitude set to 0), which is what a household barometer usually indicates.

Dozens of equations have been fit to the experimental saturation vapor pressure (SVP) data. Here is one by Buck (1981).

$$SVP = 4.5841\ e^{\frac{\left(18.687-\frac{Temp}{234.5}\right)*Temp}{257.14+Temp}} \tag{7.10}$$

As before, Temp is in degrees Celsius and SVP is in mmHg.

Air density is inversely related to altitude, temperature and humidity, and is directly related to barometric pressure. For the range of values in major league ballparks, the altitude is the most important of the four input parameters. Table 7.8 gives values for a typical late-afternoon summer game, assuming that the stadium roofs are open and there are no storms. For these examples, baseball units are used instead of SI units. A more comprehensive table is given in the appendix of this chapter.

Table 7.8 Air density in some typical baseball stadiums

	Altitude (feet above sea level)	Average daily high temperature (degrees Fahrenheit) in July	Relative humidity, on an average July afternoon (%)	Average barometric pressure in July (inch of Hg)	Air density (kg/m^3)
Denver	5190	88	34	29.98	0.96
Houston	45	94	63	29.97	1.11
Minneapolis	815	83	59	29.96	1.11
Phoenix	1086	104	20	29.81	1.07
San Francisco	0	68	65	29.99	1.19
Seattle	10	75	49	30.04	1.18

Weather data such as these can be obtained from http://www.weather.com and http://www.wunderground.com/. The multiyear average July afternoon relative humidity and barometric pressure data came from internet databases that are no longer accessible. Estimates of barometric pressure are also available at http://www.usairnet.com/weather/maps/current/barometric-pressure/. Programs that calculate air density can be downloaded from Linric Company (http://www.linric.com/) or they can be used on-line at http://www.uigi.com/WebPsycH.html or https://wahiduddin.net/calc/calc_da_rh.htm.

In physics, we typically reference constants at standard temperature and pressure (STP). However, this reference point is not as a common a condition as one might think. It is actually unusual. The density of dry air at STP of 0 °C (32 °F) and sea level is 1.2754 kg/m^3. At the International Standard Atmosphere, (dry air at 15 °C, 59 °F, at sea level) the density of air is 1.225 kg/m^3. Both of these are bigger than for any baseball game, as shown in Table 7.9. In our computer programs, the default air density is that at midlevel in Table 7.9, namely 1.0582 kg/m^3, or 0.00205 slug/ft^3.

For a potential home run ball, both the drag and the lift (Magnus) forces are the greatest in San Francisco, where the park is just at sea level, and smallest in the "mile high" city of Denver. However, as previously stated, the drag force is more important than the Magnus force. Therefore, if all collision parameters (e.g., pitch speed, bat speed, collision point, etc.) are equal, a potential home run will travel the farthest in Denver and the shortest in San Francisco.

These values were chosen to show realistic numbers with natural variation. On any given afternoon in July, it is almost certain that baseball games will be played at the high and low ends of all these ranges.

To understand how the four fundamental variables, altitude, temperature, humidity and barometric pressure determine the air density, these equations were evaluated at eighty-one experimental points in a spreadsheet. These points were

Table 7.9 Values used in the simulations

	Altitude (feet above sea level)	Temperature (degrees Fahrenheit)	Relative humidity (%)	Barometric pressure (inch Hg)	Air density (kg/m^3)	Air density, percent change from midlevel
Low altitude	0	85	50	29.92	1.16	9.4
Low temperature	2600	70	50	29.92	1.09	2.9
Low humidity	2600	85	10	29.92	1.06	0.7
Low barometric pressure	2600	85	50	29.33	1.04	−2.0
Lowest density	5200	100	90	29.33	0.91	−14.0
Midlevel	2600	85	50	29.92	1.06	0.0
Highest density	0	70	10	30.51	1.22	15.5
High barometric pressure	2600	85	50	30.51	1.08	2.0
High humidity	2600	85	90	29.92	1.05	-0.7
High temperature	2600	100	50	29.92	1.03	-2.9
High altitude	5200	85	50	29.92	0.97	-8.6

selected at the low, middle and high values of the fundamental variables, or at 3^4 or 81 points. An edited regression output is given in Table 7.10.

Surprisingly, a simple linear equation explains most of the changes, or variability, in the air density values. The linear algebraic equation for air density obtained by least squares analysis is

$$\begin{aligned}
&\Delta\,\text{Air density}(\text{percent change from mean level}) = \\
&-0.0035(\text{Altitude} - 2600) \\
&-0.2422(\text{Temperature} - 85) \\
&-0.0480(\text{Relative Humidity} - 50) \\
&+3.4223(\text{Barometric Pressure} - 29.92)
\end{aligned} \tag{7.11}$$

where Δ Air density is stated as a percent change from mean level of 1.045, Altitude is in feet, Temperature is in degrees Fahrenheit, Relative Humidity is in

Table 7.10 Edited regression summary for linear approximation (from JMP and excel)

Summary of fit				
RSquare	0.993			
RSquare adjusted	0.993			
Root mean square error	0.71			
Observations (or sum weights)	81			
Analysis of variance				
Source	DF	Sum of squares	Mean square	F ratio
Model	4	5662	1415	2783
Error	76	39	0.51	
C. total	80	5701		
Parameter estimates				
Term	Estimate	Standard error	t ratio	
Intercept	0.0			
Altitude (ft) − 2600	−0.0035	0.0000	−94	
Temperature (°F) − 85	−0.2422	0.0065	−37	
Relative Humidity (%) − 50	−0.0480	0.0024	−20	
Sea-level corrected barometric pressure (inch Hg) − 29.92	3.4223	0.1643	21	

percent and Barometric Pressure is in inches of Hg. The parameter estimates are taken from Table 7.10. This equation can be reexpressed to give the air density in kg/m^3

$$\begin{aligned}
&\text{Air density} = \rho = 1.045 + 0.01045\{ \\
&- 0.0035\,(\text{Altitude} - 2600) \\
&- 0.2422\,(\text{Temperature} - 85) \\
&- 0.0480\,(\text{Relative Humidity} - 50) \\
&+ 3.4223\,(\text{Barometric Pressure} - 29.92)\}
\end{aligned} \tag{7.12}$$

This Air density is ρ in Table 7.3b and Eqs. (7.1)–(7.8).

Note that the factors are in different dimensions with different ranges. Hence, the magnitudes of the coefficients should be interpreted in this light. That is, a coefficient with a larger magnitude does not necessarily mean it has a greater impact on the response. Also, keep in mind that the equations that yield the air density values are deterministic. That is, there is no random variation. Hence, the sum of squares residual is the variation remaining after predicting the response from the linear approximation. There is no pure error, but rather simply lack of fit to the true model. The least squares analysis differentiates between the variables for the range of the eighty-one observations as follows. Altitude explains 80% of the variation between the equation and the 81 data points; temperature explains 13%, barometric pressure accounts for 4% and relative humidity accounts for 3%.

Since Eq. (7.11) is linear, the impact of each factor can be shown graphically. Figure 7.15 shows the changes in air density that should be expected over the range of parameter values that would be typical for a baseball stadium on an afternoon in July in North America. It shows that altitude is the most important factor, followed by temperature, barometric pressure and relative humidity. Since the factor ranges given are indicative of their natural variation, larger absolute slopes means stronger effects. These results are for baseball and should not be used for other purposes, such as calculating safe takeoff parameters for a small airplane.

The linear Eq. (7.11) explains 99.3% of the variation in air density across our 81 setting. However, the unexplained variation, as given by the prediction standard error is 0.71%, suggesting that a further minor improvement is possible. (It is possible to obtain a very high R^2 and still have unexplained variability.)

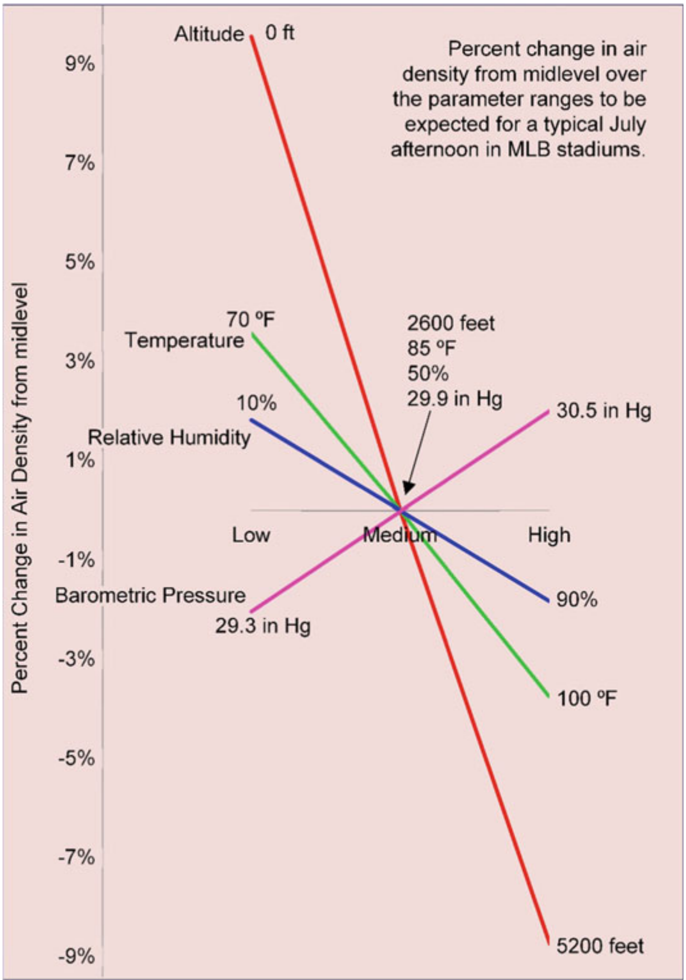

Fig. 7.15 Air density depends on altitude, temperature, barometric pressure and relative humidity

Figure 7.16 shows a quadratic pattern between the residuals and the predicted values of the linear approximation, suggesting that second-order terms might be helpful. Since altitude is the most important factor, the square of its value is a likely candidate. After fitting a regression to the complete quadratic model, that also includes four pure square terms and six cross-product terms, the conjecture is confirmed, the square of altitude does play a role. In addition, the cross product term between altitude and temperature is even more important, although they are a magnitude smaller than the linear altitude and temperature terms in their effect.

The impact of augmenting the model with these two second-order terms raises the percentage of explained variation only slightly (from 99.3 to 99.5%), but it decreases the unexplained variation, as measured by the prediction standard error from 0.71 to 0.61. The corresponding model is given by Eq. (7.13).

$$\begin{aligned}
&\Delta\,\text{Air density}(\text{percent change from mean level}) = \\
&-0.0035(\text{Altitude} - 2600) \\
&-0.2422(\text{Temperature} - 85) \\
&-0.0480(\text{Relative Humidity} - 50) \\
&+3.4223(\text{Barometric Pressure} - 29.92) \\
&+0.000000061\left\{(\text{Altitude} - 2600)^2 - 4506667\right\} \\
&+0.000012(\text{Altitude} - 2600)\bullet(\text{Temperature} - 85)
\end{aligned} \tag{7.13}$$

This is a confirmation of the correctness of our model. It shows that increasing the complexity of our model, increases the accuracy of the model. This should be true for all good models.

Many people erroneously think that humid air is heavier than normal air. They say things like, “Boy it’s humid. Feel how heavy the air is.” But in reality, humid air is lighter than normal air. Consider this. Each cubic meter of air contains the same number of molecules, about 10^{25} molecules. Air is primarily composed of

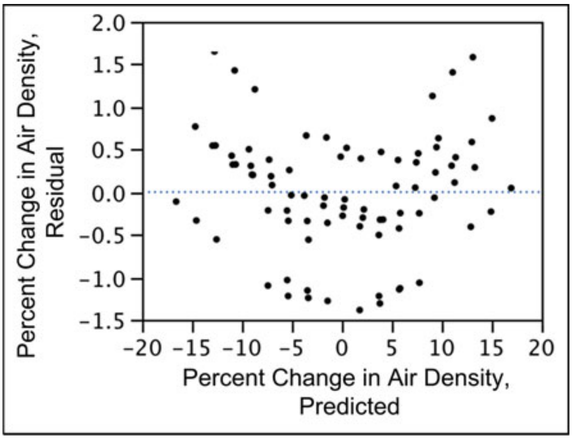

Fig. 7.16 Residuals versus predicted air density for the linear approximation

nitrogen and oxygen (with atomic weights of 14 and 16, respectively). However, both of these gasses are diatomic, meaning that in air two nitrogen atoms are bound together, N_2, and two oxygen atoms are bound together, O_2, (yielding molecular weights of 28 and 32, respectively). Now if you introduce some water vapor, H_2O, (with a molecular weight of 18) into this cubic meter of air, lighter water molecules will displace heavier nitrogen and oxygen molecules. The nitrogen and oxygen molecules with molecular weights of 28 and 32 will be displaced by water molecules with a molecular weight of 18. Thus, humid air is less dense than regular air.

Please note that this section is not a traditional sensitivity analysis. In a sensitivity analysis, each parameter would be changed by a certain percent, and then the resulting changes in the output would be calculated (Smith et al. 2008). For baseball, if we change each parameter by 5% we find that the semirelative sensitivity of air density with respect to barometric pressure, temperature, altitude and relative humidity are, respectively, 1.07, −0.21, −0.1 and −0.02. The reason for the different results is that the high, medium and low barometric pressures that could be expected on a July afternoon in a major league baseball stadium are 775, 760 and 745 mmHg. These changes are much less than 5% whereas, the high, medium and low altitudes that could be expected in a major league baseball stadium are 5200, 2600 and 0 feet. These changes are much more than 5%. Stated simply, there would be a greater change in air density due to moving from San Francisco to Denver than there would be due to moving from fair weather to stormy weather.

The *range* of a batted ball is defined as the distance from home plate to the spot where the ball first hits the ground. Table 7.11 shows the range for perfectly hit simulated baseballs. The pitch, from Table 4.2, was a fastball with 2000 rpm backspin that was going 83 mph (37 m/s) when it hit the sweet spot of the bat, which was going 62 mph (28 m/s): the CoR was 0.465. From Table 4.2, we can see that (if all other things were equal) such a collision could produce a home run ball launched optimally at 34° at 92 mh with 2000 rpm of backspin. This is a potential home run ball. Reducing the air density by 10% from 1.0 to 0.9 increased the range of this potential home run ball by 12 feet or three percent.

For Table 7.11, the home run was launched at 92 mph (41 m/s) at an upward angle of 34° with a backspin of 2000 rpm. The pop-up was launched at 70 mph (31 m/s) at an upward angle of 70° with a backspin of 5000 rpm. The line drive was launched at 90 mph (40 m/s) at an upward angle of 15° with a backspin of 2000 rpm.

Table 7.11 Range as a function of air density

Air density (kg/m^3)	Range (ft)			Range (m)		
	Home run	Pop-up	Line drive	Home run	Pop-up	Line drive
1.3	372	59	266	113	18	81
1.2	382	67	268	117	20	82
1.1	394	75	269	120	23	82
1.0	406	84	271	124	26	83
0.9	418	94	272	128	29	83
0.8	432	104	274	132	32	84

Replication crisis To make our results more replicable, we should have deposited our 81-point spreadsheet into an on-line repository. The sources of our weather data were given, but our workflows were not. We gave names of the software packages we used for the statistical regression analysis of the 81-point spreadsheet, namely JMP and Excel, but we did not give details. We gave atmospheric conditions for most of our simulations.

In this section, average values were used. Of course, ball games are not played at average values and the actual values are not constant throughout the game. In particular, wind speed and direction could change on a minute-by-minute basis. In this section, the effects of prevailing winds or height and distance of the outfield walls were not modeled. Chambers et al. (2003) have written that for most games played at Colorado Rockies stadium in Denver there was a slight breeze (e.g., 5 mph, 2.2 m/s) blowing from center field toward home plate. They further stated that the outfield walls at in Denver were farther back than in most stadiums. They concluded that these two factors together reduced the number of home runs by three to four percent, which nearly compensated for Denver's high altitude. The greatest wind effects in major league stadiums are in San Francisco where the average is a gentle breeze blowing from home plate into the right-center field stands at 10 mph (4.5 m/s).

7.9 Vertical Deflections of Specific Pitches

The magnitude of the gravity and spin-induced drops for three kinds of pitches at various speeds are shown in Tables 7.3a and 7.3b. Our simulations included air density, the force of gravity, the drag force and the vertical and horizontal spin-induced forces (Bahill and Karnavas 1993; Watts and Bahill 2000; Bahill and Baldwin 2004). Looking at one particular row of Tables 7.3a and 7.3b, a 90 mph (40.2 m/s) fastball is in the air for 426 ms, so it drops 2.92 feet (0.89 m) due to gravity (½ gt^2, where the gravitational constant g is 32.2 ft/s^2 or 9.8 m/s^2 and t is the time from release until the time of bat–ball collision). But the backspin lifts this pitch 0.98 feet (0.3 m), producing a total drop of 1.94 feet (0.59 m) as shown in Tables 7.3a and 7.3b. In the spin rate column, negative numbers are backspin and positive numbers are top spin. In the spin-induced vertical drop column, negative numbers mean the ball is being lifted up by the Magnus force. All of the pitches in Tables 7.3a and 7.3b were launched horizontally—that is, with a launch angle of zero: that is why they are different from the pitches in Figs. 7.1 and 7.2. The angle VaSa was also set to zero (simulating an overhand delivery); therefore, pitches thrown with a three-quarter arm delivery would have smaller spin-induced deflections than given in Tables 7.3a and 7.3b.

A batter's failure to hit safely is most likely caused by his fallibility in predicting where and when the ball will reach the bat–ball contact point. Vertical misjudgment of this potential bat–ball contact point is the most common cause of batters' failure (Bahill and Baldwin 2003; Baldwin and Bahill 2004). The vertical differences between the curveballs and fastballs in Tables 7.3a and 7.3b are greater than three feet (1 m), whereas the difference produced by the two speeds of fastballs is around three inches (7 cm) and the difference produced by the two speeds of curveballs is around seven inches (18 cm). However, the batter is more likely to make a vertical error because speed has been misjudged than because the kind of pitch has been misjudged (Bahill and Baldwin 2003, 2004). A vertical error of as little as one-third of an inch (8 mm) in the batter's swing will generally result in a failure to hit safely (Bahill and Baldwin 2003, 2004); see Fig. 4.5.

The spin on the pitch causes both vertical and horizontal deflections of the ball's path. When a batter is deciding whether to swing, the horizontal deflection is more important than the vertical because the umpire's judgment with respect to the distinct sides of the plate may have more precision than his or her judgment regarding the fuzzy top and bottom of the strike zone. However, after the batter has decided to swing and is trying to track and hit the ball, the vertical deflection becomes more important because the sweet spot of the bat is wider than it is tall.

7.10 Effects of Air Density on Specific Pitches

A reduction in air density would reduce the drag and the Magnus forces on the pitch. Table 7.12 shows the speed and the height of the ball when it crosses the front edge of the plate for a 93 mph (42 m/s) fastball launched downward at 1.5° from a point 6 feet high with 2200 rpm of backspin using an overarm delivery and for a 79 mph (35 m/s) curveball launched upward at one degree with 2300 rpm of pure top spin. In Table 7.12 the speed is the vector velocity, meaning it is the sum of the horizontal and vertical velocities.

A ten-percent decrease in air density, for example, from 1.0 to 0.9, produces a fastball that is one percent faster when it crosses the plate and two percent lower. Such a change in air density produces a curveball that is also one percent faster when it crosses the plate with a drop that is seven percent smaller. Earlier in this chapter we wrote, if all other things were equal, a ten-percent decrease in air density would produce a three-percent increase in the distance of a home run ball. Now it can be seen that all other things will not be equal: the ball collision speed will be larger (the bat speed will not change). Using the higher ball collision speed increases the range of the home run ball by one foot.

Table 7.12 Pitch variations with air density

Air density (kg/m^3)	Fastball released at 93 mph		Curveball released at 79 mph	
	Speed at the plate (mph)	Height above the plate (ft)	Speed at the plate (mph)	Height above the plate (ft)
1.3	83.5	3.18	71.3	1.84
1.2	84.2	3.08	71.9	1.97
1.1	84.9	2.98	72.5	2.1
1.0	85.7	2.93	73.1	2.24
0.9	86.5	2.86	73.7	2.39
0.8	87.3	2.81	74.6	2.52

Table 7.13 Two rows from Table 7.8 for an average July afternoon in two major league baseball stadiums

City	Altitude (feet above sea level)	Average daily high temperature (°F)	Average relative humidity (%)	Average barometric pressure (inch of Hg)	Average air density (kg/m^3)
Denver	5190	88	34	29.98	0.96
San Francisco	0	68	65	29.99	1.19

Table 7.14 A tale of two cities

City	Air density (kg/m^3)	Computed range in feet for a home run ball	Computed range in meters for a home run ball
Denver	0.96	423	129
San Francisco	1.19	399	122

Table 7.11 showed that decreasing the air density by ten percent, for example, from 1.0 to 0.9, could increase the distance of a home run ball by, for example, 12 feet. Now Table 7.12 shows that decreasing the air density from 1.0 to 0.9 could allow the fastball to retain more of its speed when it crosses the plate. This higher speed (86.5 compared to 85.7) allows the home run ball to travel one foot farther. Considering both of these effects, reducing the air density from 1.0 to 0.9, would allow the home run ball to travel 13 feet or three-percent farther.

I hate to use extreme examples because people tend to latch onto them and consider them typical. However, our readers might not relate to a ten-percent change in air density. So regrettably, I will now present in Tables 7.13 and 7.14 the most extreme example for major league stadiums.

For Table 7.14, we used an average major league home run as described by Willman (2017): it was launched at 97 mph (43 m/s) at an upward angle of 28° with a backspin of 2000 rpm. In 2016, the computed range of typical home runs (meaning if the stands and the fans were not there) was between 340 and 430 feet, so the ranges in Table 7.14 are realistic.

Because of the difference in the air densities, if all other things were equal, the optimally launched home run ball would travel about 24 feet farther in Denver than in San Francisco. However, in Denver, the *pitch* would not slow down as much. The difference in pitch speeds would add another two feet to the range in Denver. We hope there is enough detail in this section to make our result replicable.

We now know enough about the flight of the ball to make some generalizations. The Magnus, gravity and drag forces on the ball are continuous. Therefore, the ball follows a parabolic path in both the horizontal and vertical planes. This means that there is no such thing as a “late breaking” pitch. The pitcher does not have a string attached to the ball that he can pull at the last second to make the ball jump. All pitches, except for the knuckleball, follow a smooth almost parabolic pathway from the pitcher’s release point to the plate.

7.11 Modeling Philosophy

A model is a simplified representation of a particular view of a real system. No model perfectly matches all views of its real system. If it did, then there would be no advantage to using the model. Although the equations and numerical values in this chapter might imply great confidence and precision in our numbers, it is important to note that our equations are only models. The Kutta–Joukowski lift equation and subsequent derivations are not theoretical equations, they are only approximations fit to experimental data.

There are many models for the flight of the baseball. The models of Frohlich (1984), Watts and Bahill (1990, 2000), Adair (2002, 2004), Sawicki et al. (2003, 2004), Nathan (2000), Bahill and Baldwin (2007) and McBeath et al. (2008) give different numerical results. However, we believe, they all give the same comparative results. Meaning they all should show that a ten-percent decrease in air density produces about a three-percent increase in the distance of a home run ball with the increase being less for pop-ups and greater for line drives.

Our models only considered certain aspects of the baseball in flight. We ignored the possibility that air flowing around certain areas of the ball (due to perhaps a scuffmark) might change from laminar to turbulent flow *en route* to the plate. Our equations did not include effects of *shifting* the wake of turbulent air behind the ball *during* the flight. En route to the plate, the ball loses 10% of its linear velocity (Watts and Bahill 2000) and 2% of its angular velocity (McBeath et al. 2008): we did not include this reduction in angular velocity in our simulation. We ignored the stabilizing gyroscopic effect and the precession of the spin axis. Furthermore, we ignored the difference between the center of mass and the geometrical center of the baseball. We ignored possible differences in the moments of inertia of different balls. In computing velocities due to bat–ball collisions, we ignored deformations of the bat and ball, and energy dissipated when the ball grips the bat.

The implied precision suggested by the home run trajectories shown by Willman (2017) would need to answer all of the above issues as well accommodate wind velocity and its changes with height and perhaps even temperature gradients.

Our numerical values were only estimates because so many factors affect them. For example, the outputs of the BaConLaws and Ball in Flight models vary with the particular bat that was used. In Sect. 4.12.4, we discussed C243 and R161 bats. They were similar in length, weight and moment of inertia, yet with our standard pitch speed of 83 mph and swing speed of 61 mph, the C243 bat produced a batted-ball range of 387 feet whereas the R161 bat drove the ball 389 feet.

Table 4.12 was for head-on collisions. However, a launch angle of 34° would require an oblique collision that would produce a lower launch speed (Kensrud et al. 2016). Consequently, producing a launch speed of 97 mph would require a higher swing speed. Obligingly, Willman (2017) shows many swing speeds that are higher.

The importance of this present chapter lies in comparisons rather than in absolute numbers. Our model emphasizes that the right-hand rules show the direction of forces acting on a spinning ball in flight. The model provides predictive power and comparative evaluations of the behavior of different types of pitches.

The order of determining values Variables and parameters used in Chaps. 1–6, but not used in Chap. 7, include bat mass, bat moment of inertia, ball moment of inertia, CoR and the location of the collision point. Outputs of Chaps. 1–6 that are inputs for Chap. 7 include launch velocity, launch angle and launch spin. Now we had to find numerical values for the other Chap. 7 variables and parameters. The order of determining them is important because it is impossible to correctly derive the values in the wrong order. The correct order is shown in Table 7.15.

We first had to choose a default state: we used the midlevel values given in Table 7.9. Of course, in our simulations, particular variables and parameters were changed for particular stadiums or circumstances, but the default values were usually used. The biggest mistake that we made in the last 30 years was using standard temperature and pressure (STP) as the default for air density in the early years. Next, we needed values for altitude, temperature, relative humidity and barometric pressure; they were given in Tables 7.8 and 7.9 and the appendix of this chapter. These values were then used to compute air density, the dynamic viscosity of air (μ) and the kinematic viscosity of air (υ). The dynamic viscosity is also called the absolute viscosity or just the viscosity: it depends on temperature. The kinematic viscosity of air depends on both temperature and pressure. In the early years, we used the kinematic viscosity of air, but it was difficult to get good values for all stadiums, therefore we switched to the dynamic viscosity. We found internet sites that gave authoritarian values for the dynamic viscosity of air. This is the statistical summary for the dynamic viscosity of air at 85 °F and 2600 feet altitude.

$$\bar{\mu} = 1.922 \times 10^{-5}\ \text{kg/m} \cdot \text{s or N} \cdot \text{s/m}^2$$
$$\sigma = 0.13 \times 10^{-5}$$
$$n = 8$$

We used the official rules of major league baseball for the mass and diameter of the ball, which were given in Table 1.1. Typical ball speeds and spins came from Table 4.2. Now we had enough data to compute the spin parameter and the Reynolds number for particular pitches and hits as given in Table 7.4. We determined that for major league pitches and hits (with the exception of knuckleballs and extreme pop-ups) the

$$0.1 < SP < 0.3$$

and

$$10^5 < \text{Re} < 2 \times 10^5$$

We used these numbers to access the literature and find lift, drag and Magnus coefficients, as given in Sect. 7.6. Although it was not important, we tried to get the

Table 7.15 The order of determining numerical values for the variables and parameters

Variable		Value in SI units	Value in US customary units	
Default state		Midlevel	Midlevel	
Altitude		792 m	2600 ft	
Temperature		29.4° C	85° F	
Relative Humidity		50 %	50 %	
Barometric pressure		760 mm Hg	29.92 inch Hg	
		$\Rightarrow$ divide by 515.4		
Air density		$\rho = 1.0582$ kg/m^3	$\rho = 0.00205$ slugs/ft or lbgs^2 /ft^4	
		$\Rightarrow$ multiply by 2.09×10^{-2}		
Dynamic viscosity of air	$\Downarrow$ divide by $\rho = 1.0582$	$\bar{\mu} = 1.922\times10^{-5}$ kg/mgs or Ngs/m^2	$\mu = 4.017\times10^{-7}$ lbfgs/ft^2	$\Downarrow$ divide by $\rho = 0.00205$
		$\Rightarrow$ multiply by 10.7638		
Kinematic viscosity of air		$\upsilon = 1.816\times10^{-5}$ m^2/s	$\upsilon = 1.955\times10^{-4}$ ft^2/s down then right $\upsilon = 1.959\times10^{-4}$ ft^2/s right then down	
Diameter of a baseball		0.07366 m	2.9 in	
Mass of a baseball		0.145 kg	5.125 oz	
Launch speed		43 m/s	97 mph	
Launch angle		34 degrees	34 degrees	
Launch spin		-209 rad/s	-2000 rpm	
Reynolds number		$10^5 < \mathrm{Re} < 2\times10^5$		
Spin parameter		$0.1 < SP < 0.3$		
C_M		1.2		
C_D		0.4		

earth's gravitational constant at each home plate. It would have been nice to also have had the wind speed at home plate for each pitch.

The order in which these values were gathered is important because, for example, the air density cannot be computed until after the altitude, temperature, humidity and barometric pressure are known, furthermore small mistakes in the beginning would propagate throughout the whole process. Once we had values for the variables and parameters, we could start developing and running the model. First, we needed input values for the launch velocity, lunch angle and launch spin. For one of the longest possible batted-ball examples, we used the following inputs from Table 4.12. The home run was launched at 97 mph (43 m/s) at an upward angle of 34° with a backspin of 2000 rpm. The results are given in Table 7.11.

Not only are numerical values important, but their variability is also important. For example, the variation in the earth's gravitation constant is small between stadiums, whereas the variation in the diameter of actual balls in play is comparatively large. Furthermore, the time scale of change is important. The wind speed changes from pitch to pitch, the temperature and barometric pressure change from inning to inning and the altitude and the earth's gravitational constant vary on a geological scale.

The numerical values used for the parameters in our equations have uncertainty. However, the predictions of the equations match baseball trajectories quite well. When better experimental data become available for parameters such as the drag coefficient and spin rate, then the equations or the values of *other* parameters will have to be adjusted to maintain the match between the equations and actual baseball trajectories. A well-developed model is an interconnected system. You should not try to improve one parameter at a time.

So far, experimental data have driven the development of the model and the simulation. However, as shown in Fig. 7.17, modeling is not a one-way street. The theorists should be sending advice to the experimentalists. For example, the worst data used in developing the model is probably that for determining values for the drag coefficient, C_D. The results of the seven studies shown in Fig. 7.11 are different: none replicated earlier results. Therefore, there is a need for someone to show the drag coefficient varying as a function of the Reynolds number for spinning baseballs with the care and precision exhibited by Achenbach (1972). It is important that they explicitly cover the realistic baseball range of spin parameters, $0.1 < SP < 0.3$. As a second example, modelers should point out that the huge Major League Baseball databases contradict each other. In particular, the spin rates for curveballs must be wrong. Table 7.1, using data from Willman (2017), gives an average spin rate for the curveball of 1300 rpm with a standard deviation of 500: this is a huge standard deviation. Whereas, Table 7.2, with data from Statcast (Petriello 2016), gives an average spin rate of 2300 rpm for the curveball. Each of these databases contains an entire year of data. Therefore, the differences are not due to an inadequate sample size. Both of these are for the curveball, which should

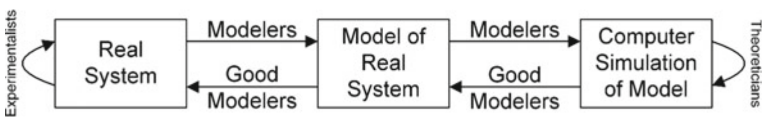

Fig. 7.17 The modeling process

be easy to identify and hard to confuse with other types of pitches. Therefore, the discrepancy is significant. It suggests a fundamental flaw in the system.

As for replicability, we acknowledge that some areas of science (like Psychology) are more difficult to study and are less mature than other areas because of the lack of basic theory to guide us. However, this is definitely not the case for the science of baseball.

Stark (1968) explained that models are ephemeral: they are created, they explain a phenomenon, they stimulate discussion, they foment alternatives and then they are replaced by new models. When there are better wind-tunnel data for the forces on a spinning baseball, then our equations for the lift and drag forces on a baseball might be updated with newer parameters. However, we think our models, based on the right-hand rules showing the direction of the spin-induced deflections, will have permanence: they are not likely to be superseded.

Planck (1948) wrote, "A new scientific truth does not triumph by convincing its opponents and making them see the light, but rather because its opponents eventually die, and a new generation grows up that is familiar with it."

7.12 Which Can Be Thrown Farther a Baseball or a Tennis Ball?

We now have all the tools necessary to analyze the different flight paths of heavy and light balls. If you type, "Which can be thrown farther a heavy ball or a light ball?" into a Google search box, you will get over a million answers: most of them are probably wrong. So let's try to answer this question now.

The force–velocity relationship of muscle shown in Fig. 4.9 does *not* suggest that a light ball can be thrown farther than a heavy ball. For example, given a tennis ball, a baseball, a softball, a bocce ball and a woman's shot put, we suspect that the baseball can be thrown the farthest. The tennis ball with a low weight would be at the left side of a force–velocity diagram like Fig. 4.10. It would have a high speed, but the force applied to it by the muscles would be small. Whereas, the shot put would be on the right side of Fig. 4.10. It would have a large force applied to it, but its speed would be small.

Figure 4.9 gives the force–velocity relationship for a single isolated muscle in controlled laboratory conditions. Figure 4.10 gives the force–velocity relationship for a whole intact human being swinging a bat. This similarity has been reproduced in many physiological experiments. In Fig. 7.18, we apply it to humans throwing balls.

Physics textbooks state that an ideal projectile-launch on the moon at a 45-degree angle would yield a maximum range of $R_{\max} = \frac{v_0^2}{g}$, which does not depend on the mass of the projectile. Let us see if we can be more realistic. The *range* of a batted ball is defined as the distance from home plate to the spot where the ball first hits the ground. What determines the range of a batted ball? In a major

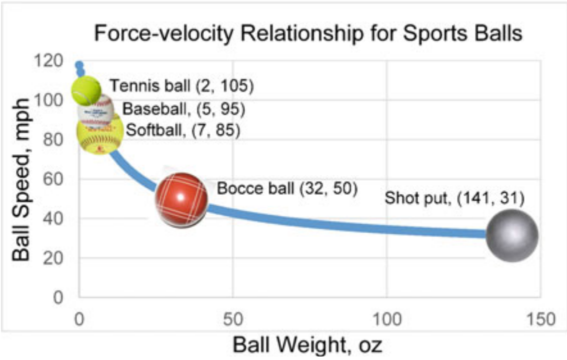

Fig. 7.18 Launch speed versus weight for different sports balls. The numbers in parentheses are weight and speed. The equation for the blue line is $(weigh + 12.5) \times (speed - 24) = 1171$ where *weight* is in ounces and *speed* is in mph. These five balls are similar in size. Therefore, they *could* all be thrown with an overhand motion producing backspin

league baseball stadium, the range depends on the time that the ball is in the air and that depends on the vertical component of the velocity. The height of the ball is given by $z = z_0 + \dot{z}t + 0.5\ddot{z}t^2$ where $\dot{z}$ means the derivative of z with respect to time, $\frac{dz}{dt}$, the vertical velocity, and $\ddot{z}$ means the second derivative of z with respect to time, $\frac{d^2z}{dt^2}$, the vertical acceleration. Typical ball trajectories derived from equations like this are shown in Fig. 7.19.

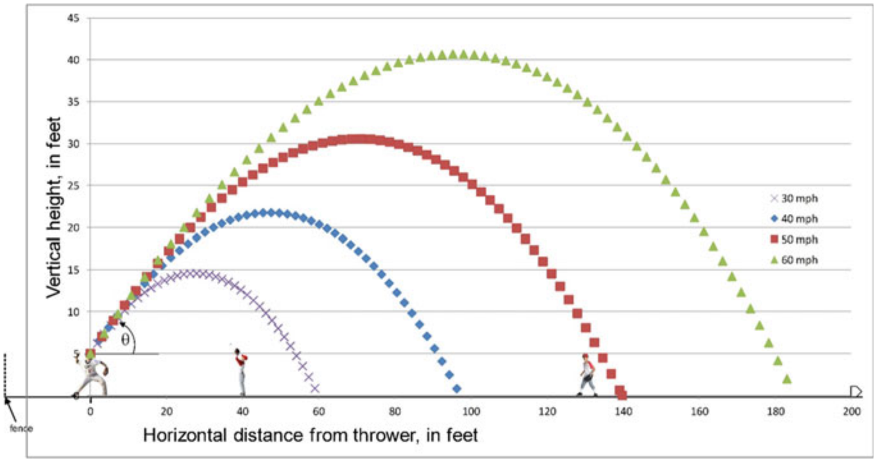

Fig. 7.19 Simulated trajectories for balls thrown from the outfield by a Little Leaguer at various launch velocities. The launch angle is 34°, but it does not look like that on the figure, because the horizontal and vertical scales are not the same

When the ball is going up we have

$$F_{\text{down}} = -F_{\text{lift}} + F_{\text{gavity}} + F_{\text{drag}} \sin\theta$$

where θ is the angle between the direction of motion and the horizontal. The lift force is the vertical component of the Magnus force. Therefore,

$$F_{\text{down}} = -F_{\text{Magnus}} \cos\theta + F_{\text{gavity}} + F_{\text{drag}} \sin\theta$$

From Sect. 7.5.2, we have

$$F_{\text{Magnus}} = 0.5\pi\rho r_{\text{ball}}^3 \omega_{\text{ball}} v_{\text{ball}} C_{\text{M}}$$

assuming that the spin axis is perpendicular to the direction of motion, that is pure backspin.

$$F_{\text{gravity}} = m_{\text{ball}} g$$

$$F_{\text{drag}} = 0.5\pi\rho r_{\text{ball}}^2 v_{\text{ball}}^2 C_{\text{drag}}$$

Therefore,

$$F_{\text{down}} = -0.5\pi\rho r_{\text{ball}}^3 \omega_{\text{ball}} v_{\text{ball}} C_{\text{M}} \cos\theta + m_{\text{ball}} g + 0.5\pi\rho r_{\text{ball}}^2 v_{\text{ball}}^2 C_{\text{D}} \sin\theta$$

Now the vertical acceleration is related to the downward force by

$$\ddot{z} = \frac{-F_{\text{down}}}{m_{\text{ball}}}$$

Therefore,

$$\begin{aligned} z = z_0 + \dot{z}t \\ - \frac{t^2}{2m_{\text{ball}}}\left(-0.5\pi\rho r_{\text{ball}}^3 \omega_{\text{ball}} v_{\text{ball}} C_{\text{M}} \cos\theta + m_{\text{ball}} g + 0.5\pi\rho r_{\text{ball}}^2 v_{\text{ball}}^2 C_{\text{D}} \sin\theta\right) \end{aligned}$$

In order to simulate this equation, we needed values for C_{D} and C_{L}. We took these values from Fig. 7.20, which came from Clanet (2015). We also used $C_{\text{M}} = 0.7$.

Once we had values for these three constants, we ran our simulation and produced the numbers in Table 7.16. We ran the simulation in dry air at 85 °F at sea level, yielding $\rho = 1.14\,\text{kg/m}^3$. This detail aids replicability.

The weak link in this section is the launch speeds. The reliability of these data decreases from baseballs to shot puts to softballs to bocce balls to tennis balls. We have the most confidence in the launch speed of the baseball at 95 mph. Many television viewers are familiar with this number. Many professional baseball players can throw a baseball at this speed: few laypeople can. Regardless, we do not want the

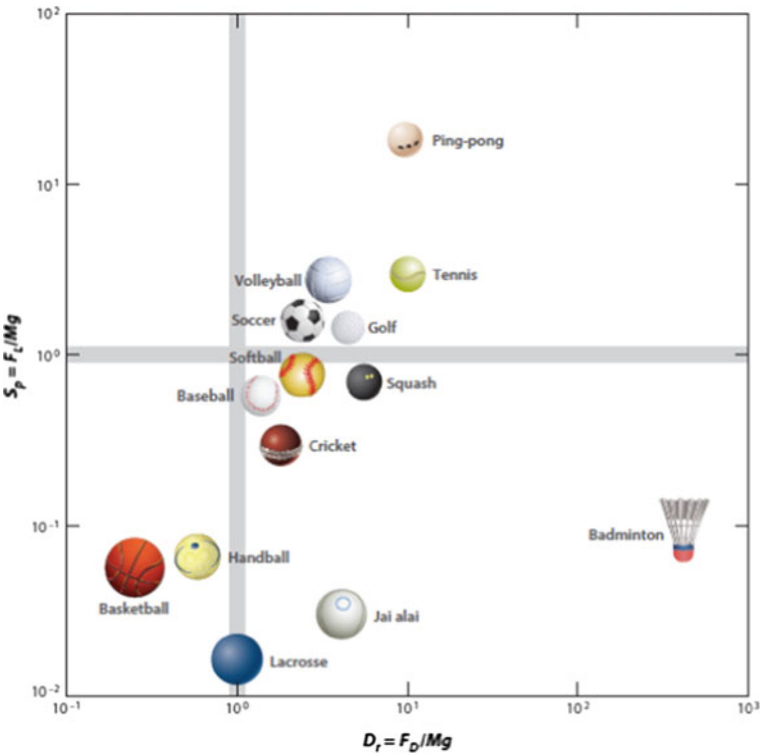

Fig. 7.20 Normalized lift and drag coefficients for various sports balls. From Clanet (2015) ©. *Annual Reviews of Fluid Mechanics,* used with permission

average speed of a thousand random people, nor do we want outliers like *Rocky Colavito* who routinely threw the baseball over 400 feet. To state it differently, we are studying optimal athletes doing what they do optimally. This removes a lot of variabilities. Therefore, we are comfortable with a 95 mph launch speed for a baseball. With this speed, the baseball is in the low drag region of Fig. 7.11, around 0.38.

The data for the shot put are for Michelle Carter who won the gold medal in the 2016 Olympics with a throw of 20.63 meters (68 feet). Using our simulation, we found values that would produce her actual output of 20.63 meters. These values were a 30.81 mph launch speed at a 43-degree angle. She could also have produced that throw with a higher speed and a different launch angle. However, if this throw won the gold medal, then it was probably close to optimal. The shot put has little spin and therefore little lift, but it does have drag (as indicated by the optimal launch angle of 43 instead of 45°). These numbers are not apocryphal or outliers. They represent an optimal athlete performing optimally. Therefore, a shot put launch speed of 31 mph is realistic.

Premier women pitchers throwing the softball *underhand* have maximum speeds that range between 70 and 75 mph. We ignore outliers like Eddie Feigner and Ty Stofflet who supposedly threw the softball over 100 mph. Additionally, there are

Table 7.16 Simulation parameters for baseballs, tennis balls, softballs, bocce balls and shot puts thrown by elite athletes

Parameter	Baseball, nominal values	Baseball, mass increased by 10%	Baseball, mass +10% and reduced launch velocity	Tennis ball	Softball	Bocce ball	Women's shot put
Ball weight (oz)	5.125	5.637	5.637	2.03	6.75	32.45	141
Ball mass, m_{ball} (kg)	0.15	0.16	0.16	0.06	0.19	0.92	4.00
Launch speed (mph), from Fig. 7.16	95	95	93	105	85	55	30.81
Launch speed (m/s), from Fig. 7.16	42.5	42.5	41.6	46.9	38.0	24.6	13.8
Ball diameter (in)	2.90	2.90	2.90	2.51	3.84	4.21	4.04
Ball diameter (m)	0.07	0.07	0.07	0.06	0.10	0.11	0.10
Nominal drag coefficient, C_{D}, from Clanet (2015) for baseball, tennis and softball	0.38	0.38	0.38	0.56	0.4	0.4	0.4
Air density, ρ (slugs/ft^3)	0.002	0.002	0.002	0.002	0.002	0.002	0.002
Air density, ρ, (kg/m^3)	1.045	1.045	1.045	1.045	1.045	1.045	1.045
Nominal lift coefficient, C_{M} from Nathan (2008) and C_{L} from Clanet (2015)	0.7	0.7	0.7	1	0.75	0.8	0.8
Ball spin, ω_{ball} (rpm)	−2000	−2000	−2000	−2200	−1800	−1200	−12

(continued)

Table 7.16 (continued)

Parameter	Baseball, nominal values	Baseball, mass increased by 10%	Baseball, mass +10% and reduced launch velocity	Tennis ball	Softball	Bocce ball	Women's shot put
Ball spin, ω_{ball} (rad/s)	−209	−209	−209	−209	−157	−63	−0.6
launch angle (degrees)	34	34	34	34	34	34	43
Launch height (feet)	5	5	5	5	5	5	5
Launch height (m)	1.5	1.5	1.5	1.5	1.5	1.5	1.5
Flight duration (seconds)	5.26	5.24	5.15	5.49	5.13	3.02	2.06
Range (ft)	372	384	374	250	297	186	68
Range (m)	113	117	114	76	90	57	20.67

Table 7.17 Summary lines from Table 7.16

Parameter	Baseball	Heavy baseball	Tennis ball	Softball	Bocce ball	Women's shot put
Launch speed (mph)	95	93	105	85	55	31
Range (feet)	372	374	250	297	186	68

internet sites showing overhand softball throws of over 300 feet. Therefore, we chose a launch speed of 85 mph for men throwing a softball overhand.

Table 7.17 shows the most important data from Table 7.16.

The size of the bocce ball is similar to the other balls, so we expect it to be gripped the same. However, estimated speed and spin for the bocce ball are a wag.

The least reliable data are for the launch speed of the tennis ball. The 105 mph value was derived from several internet videos and Clanet (2015). The tennis ball has a fuzzy surface, which produces a high drag coefficient of 0.56 (Clanet 2015). This difference in drag may be the main reason that the baseball can be thrown farther despite the tennis ball's higher launch speed.

In summary, the baseball can be thrown farther than the tennis ball. This conclusion depends on the force–velocity relationship of muscle and properties of the ball such as mass, and the coefficients of lift and drag. However, that really does not answer the original question, "Which can be thrown farther a heavy ball or a light ball?" The sensitivity analysis of Table 7.5 suggested that a heavier ball would go farther. To answer this question thoroughly, we ran the simulation with only the mass being different. The results in Table 7.16 show that the heavier ball can go slightly farther.

How is it even possible for a heavy ball to go farther than a light ball? There are two explanations based on physics. First, if the balls were launched with the same velocity, then the heavier ball must have been given more energy. Therefore, it will have more momentum and it will take more force and time to slow it down. Second, the only terms in our equations that depend on mass are the acceleration terms. At the beginning of motion, the ball with the bigger mass has smaller accelerations:

$$\ddot{z} = \frac{F_{\text{down}}}{m_{\text{ball}}} \text{ and } \ddot{x} = \frac{F_{\text{retard}}}{m_{\text{ball}}}$$

Both of these will be smaller for the heavier ball. Which means that the horizontal and vertical velocities will not slow down as fast. Both of these effects will make the heavier ball go farther. However, the system is dynamic. Both the horizontal and vertical velocities decrease with time. And both the Magnus and the drag forces are functions of velocity. Therefore, for the rest of the trajectory, we will drop the textural argument and revert to the simulation. We increased the mass of the baseball by 10% as shown in column 3 of Table 7.16. While we kept the launch speed the same. The heavier ball traveled 384 instead of 372 feet.

Now it is time to look at physiology. Recall the force–velocity relationship of muscle. Our muscles will produce a lower velocity for a heavier load than for a lighter load. According to Fig. 7.18, the 10% heavier baseball will be launched at 93 mph instead of 95 mph. As shown in column 4 of Table 7.16, this reduced launch velocity will reduce the range from 384 to 374 feet. In conclusion, increasing the baseball's mass by 10% increased the range by 12 feet. However, the concurrent reduction in launch velocity caused by the force–velocity relationship of muscle decreased the range by 10 feet. Therefore, if a human is throwing balls of about the same mass, then the heavier ball might go *slightly* farther.

At this point in our experiments, someone objected and said, "Yah, but you launched the normal ball and the heavy ball at the same angle. What if you were to launch each at its optimal angle?" Therefore, we reran our simulations and found the optimal angle for the normal ball was 34° producing a range of 372 feet, whereas the optimal angle for the heavy ball launched at 93 mph was 35°, which increased the range from 373.9 to 374.0. Our conclusion remained the same: if a human is throwing balls of about the same mass, then they will go about the same distance.

Of course, there are other physiological factors that could affect this conclusion, such as the size of the hands, the size of the ball, the grip, the throwing motion and familiarity. For example, most American males, who grew up playing baseball, thought that they could throw a baseball farther than a tennis ball, whereas most others thought the opposite.

In conclusion, because of the difference in the drag coefficient, the baseball can definitely be thrown farther than a tennis ball. In addition, if all other parameters are held constant, a lighter ball cannot be thrown farther than a heavier ball.

Technical note: The numbers in this book should not be compared between tables, because the tables have different purposes. Therefore, they may have used different versions of the model and different parameter values. For example, the nominal range of the home run ball in Table 7.6 is 385 feet: the air density was 1.0582 kg/m^3, the drag coefficient was 0.4, the Magnus coefficient was 1.2 and the nominal launch speed was 92 mph. Whereas, the nominal range of the home run ball in Table 7.16 is 372 feet, but that is for an air density of 1.045 kg/m^3, a drag coefficient 0.38, a Magnus coefficient of 0.7 and the launch speed depended on properties of the ball. Table 7.11 gave the nominal range for six different air densities: 0.8, 0.9, 1.0, 1.1 and 1.2 kg/m^3. Finally, Table 7.14 gave the nominal range for two air densities: 0.96 and 1.19 kg/m^3. Numerical values are not as important as the comparisons that are made using the numerical values in the tables.

7.13 Summary

According to our Ball in Flight model, during its flight, the ball is subjected to the following forces

$$F_{\text{gravity}} = m_{\text{ball}} g$$
$$F_{\text{drag}} = 0.5\pi \rho r_{\text{ball}}^2 v_{\text{ball}}^2 C_{\text{D}}$$
$$F_{\text{Magnus}} = 0.5\pi \rho r_{\text{ball}}^3 \omega_{\text{ball}} v_{\text{ball}} C_{\text{M}}$$

For major league baseball stadiums, the air density is inversely related to altitude, temperature and humidity, and is directly related to barometric pressure, according to this equation.

$$-\,0.0480(\text{Relative Humidity} - 50) + 3.4223(\text{Barometric Pressure} - 29.92)\}.$$

A plea was made for science of baseball experimentalists to try to replicate previous experiments and explain the reasons if they cannot.

Both the drag force (Eq. 7.3) and the Magnus force (Eq. 7.2) are directly proportional to the air density. Therefore, if air density gets smaller, the drag force gets smaller, this allows the ball to go farther: But at the same time, as air density gets smaller, the Magnus force also gets smaller, which means that the ball will not be held aloft as long and will therefore not go as far. These two effects are in opposite directions. Simulation shows that the change in the drag force affects the trajectory of the ball more than the change in the Magnus force. Therefore, as air density goes down, the range of a potential home run ball increases. On a typical July afternoon in a major league baseball stadium, a ten-percent decrease in air density can produce a three-percent increase in the distance of a home run ball. A home run ball might go 26 feet farther in Denver than in San Francisco.

Finally, we note that a baseball can be thrown farther than a tennis ball. Additionally, if a human is throwing balls of about the same mass, then the heavier ball might go *slightly* farther.

Appendix: Weather Data for Major League Baseball Stadiums

City/State	Team name	Altitude of home plate (ft)	Altitude of home plate (m)	Average daily high temperature in July (°F)	Average daily high temperature in July (°C)	SVP, mm Hg	Relative Humidity on an average July afternoon (%)	Average sea-level corrected Barometric pressure (inch Hg)	Average sea-level corrected Barometric Pressure psia	Average sea-level corrected Barometric pressure (mm Hg)	Average absolute pressure, mm Hg. Not sea-level corrected	Air density (kg/m^3)
Arizona	Diamondbacks	1061	323	104	40	55	20	29.81	14.64	757	730	1.077
Atlanta	Braves	942	287	90	32	36	59	29.99	14.73	762	738	1.111
Baltimore	Orioles	36	11	87	31	33	53	29.99	14.73	762	761	1.154
Boston	Red Sox	16	5	82	28	28	57	29.93	14.70	760	760	1.164
Chicago	Cubs	601	183	84	29	30	60	29.93	14.70	760	745	1.135
Chicago	White Sox	595	181	84	29	30	60	29.93	14.70	760	745	1.135
Cincinnati	Reds	490	149	86	30	32	58	30.00	14.74	762	748	1.136
Cleveland	Indians	653	199	81	27	27	57	30.05	14.76	763	746	1.145
Colorado	Rockies	5186	1581	88	31	34	34	29.98	14.72	761	638	0.967
Detroit	Tigers	578	176	84	29	30	54	30.06	14.76	763	748	1.141
Houston	Astros	21	6	94	34	41	63	29.97	14.72	761	760	1.133
Kansas City	Royals	857	261	90	32	36	64	29.97	14.72	761	739	1.111
Los Angeles	Angels	146	45	84	29	30	52	29.94	14.70	760	756	1.155
Los Angeles	Dodgers	501	153	84	29	30	52	29.94	14.70	760	747	1.140
Miami	Marlins	5	2	91	33	37	63	30.00	14.73	762	762	1.143
Milwaukee	Brewers	618	188	81	27	27	64	30.00	14.74	762	746	1.144

(continued)

(continued)

City/State	Team name	Altitude of home plate (ft)	Altitude of home plate (m)	Average daily high temperature in July (°F)	Average daily high temperature in July (°C)	SVP, mm Hg	Relative Humidity on an average July afternoon (%)	Average sea-level corrected Barometric pressure (inch Hg)	Average sea-level corrected Barometric Pressure psia	Average sea-level corrected Barometric pressure (mm Hg)	Average absolute pressure, mm Hg. Not sea-level corrected	Air density (kg/m^3)
Minnesota	Twins	827	252	83	28	29	59	29.96	14.71	761	740	1.130
New York	Mets	12	4	84	29	30	55	30.02	14.74	763	762	1.163
New York	Yankees	33	10	84	29	30	55	30.00	14.73	762	760	1.160
Oakland	Athletics	0	0	73	23	21	55	29.95	14.71	761	761	1.188
Philadelphia	Phillies	0	0	86	30	32	54	30.01	14.74	762	762	1.157
Pittsburgh	Pirates	726	221	83	28	29	54	30.00	14.73	762	742	1.134
Saint Louis	Cardinals	438	134	90	32	36	60	29.98	14.73	762	750	1.128
San Diego	Padres	15	5	76	24	23	67	29.88	14.68	759	758	1.175
San Francisco	Giants	8	2	68	20	18	65	29.99	14.73	762	762	1.201
Seattle	Mariners	17	5	75	24	22	49	30.04	14.75	763	763	1.187
Tampa Bay	Rays	44	13	90	32	36	64	30.08	14.77	764	764	1.149
Texas	Rangers	543	166	96	36	44	53	29.97	14.72	761	747	1.112
Toronto	Blue Jays	268	82	80	27	26	55	30.00	14.73	762	755	1.161
Washington	Nationals	6	2	88	31	34	53	30.00	14.73	762	761	1.152

References

Achenbach, E. (1972). Experiments on the flow past spheres at very high Reynolds numbers. *Journal of Fluid Mechanics, 54*(3), 565–575.

Adair, R. K. (2002). *The physics of baseball*. New York: HarperCollins.

Adair, R. K. (2004). Comments on "How to hit home runs: Optimum baseball bat swing parameters for maximum range trajectories". In G. S. Sawicki, M. Hubbard, & W. J. Stronge (Eds.) *American Journal of Physics*, *73*(2), 184–185.

Alam, F., Ho, H., Smith, L., Subic, A., Chowdhury, H., & Kumar, A. (2012). A study of baseball and softball aerodynamics. *Procedia Engineering, 34,* 86–91.

Alaways, L. W. (2008). Aerodynamics of a curve-ball: The Sikorsky/Lightfoot lift data. In *Proceedings of 7th ISEA Conference*. Biarritz, June 2–6, 2008.

Alaways, L. W., Mish, S. P., & Hubbard, M. (2001). Identification of release conditions and aerodynamic forces in pitched-baseball trajectories. *Journal of Applied Biomechanics, 17,* 63–76.

Bahill, A. T. (2004). The ideal moment of inertia for a baseball or softball bat. *IEEE Transactions* on *Systems*, *Man, and Cybernetics—Part A Systems and Humans*, *34*(2), 197–204.

Bahill, A. T., & Baldwin, D. G. (2003). The vertical illusions of batters. *Baseball Research Journal, 32,* 26–30.

Bahill, A. T., & Baldwin, D. G. (2004). The rising fastball and other perceptual illusions of batters. In G. Hung & J. Pallis (Eds.), *Biomedical engineering principles in sports* (pp. 257–287). New York: Kluwer Academic.

Bahill, A. T., & Baldwin, D. G. (2007). Describing baseball pitch movement with right-hand rules. *Computers in Biology and Medicine, 37,* 1001–1008.

Bahill, A. T., & Baldwin, D. G. (2008) Mechanics of baseball pitching and batting (Chap. 16). In D. Ghista (Ed.), *Applied biomedical engineering mechanics* (pp. 445–488). Boca Raton: CRC Press and Taylor & Francis Asia Pacific.

Bahill, A. T., Baldwin, D. G., & Ramberg, J. S. (2009). Effects of altitude and atmospheric conditions on the flight of a baseball. *International Journal of Sports Science and Engineering*, *3*(2), 109–128. ISSN 1750-9823.

Bahill, A. T., Baldwin, D. G., & Venkateswaran, J. (2005). Predicting a baseball's path. *American Scientist, 93*(3), 218–225.

Bahill, A. T., & Karnavas, W. J. (1993). The perceptual illusion of baseball's rising fastball and breaking curveball. *Journal of Experimental Psychology: Human Perception and Performance, 19,* 3–14.

Baldwin, D. G., & Bahill, A. T. (2004). A model of the bat's vertical sweetness gradient. In M. Hubbard, R. D. Mehta & J. M. Pallis (Eds.), *The Engineering of Sport 5*, Vol. 2 (pp. 305–311). *Proceedings of the 5th International Engineering of Sport Conference, September 13–16, 2004*, Davis, CA: International Sports Engineering Association (ISEA), Sheffield, UK. ISBN 0-9547861-1-4.

Baldwin, D. G., Bahill, A. T., & Nathan, A. (2007). Nickel and dime pitches. *Baseball Research Journal, 35,* 25–29.

Barkla, H., & Auchterlonie, L. (1971). The Magnus or Robins effect on rotating spheres. *Journal of Fluid Mechanics, 47,* 437–447.

Buck, A. L. (1981). New equations for computing vapor pressure and enhancement factor. *Journal of Applied Meteorology and Climatology*, *20*, 1527–1532. Buck fine-tuned his equation in 1996.

Chambers, F., Page, B., & Zaidins, C. (2003). Atmosphere, weather, and baseball: How much farther do baseballs really fly at Denver's Coors Field? *The Professional Geographer, 55*(4), 491–508.

Clanet, C. (2015). Sports ballistics. *Annual Reviews of Fluid Mechanics, 47,* 455–478. https://doi.org/10.1146/annurev-fluid-010313-141255.

CRC handbook of chemistry and physics (1980–1981). (61st ed., p. F-10). Boca Raton: CRC Press.
Frohlich, C. (1984). Aerodynamic drag crisis and its possible effect on the flight of baseballs. *American Journal of Physics, 52*(4), 325–334.
Harris, S. (1986). A century of scientific research. *American Scientist*, *74*(5), 542–545. Retrieved from http://www.jstor.org/stable/27854344.
Jefferys, W. H., & Berger, J. O. (1992). Ockham's razor and Bayesian analysis. *American Scientist, 80,* 64–72.
Kagan, D., & Nathan, A. M. (2014). Simplified models for the drag coefficient of a pitched baseball. *The Physics Teacher, 52,* 278–280. https://doi.org/10.1119/1.4872406.
Kahneman, D. (2014). A new etiquette for replication. *Social Psychology, 45*(4), 12–13.
Kensrud, J. R. (2010). *Determining aerodynamic properties of sports balls in situ* (*Master of Science thesis in mechanical engineering*). Washington State University.
Kensrud, J. R., Nathan, A. M., & Smith, L. V. (2016). Oblique collisions of baseballs and softballs with a bat. *American Journal of Physics*, arXiv:1610.03464 [physics.pop-ph].
Kensrud, J. R., Smith, L. V., Nathan, A., & Nevins, D. (2015). Relating baseball seam height to carry distance. *Procedia Engineering, 112,* 406–411.
Kindall, J. (1983). *Sports illustrated baseball*. New York: Harper & Row.
McBeath, M. K., Nathan, A. M., Bahill, A. T., & Baldwin, D. G. (2008). Paradoxical pop-ups: Why are they difficult to catch? *American Journal of Physics, 76*(8), 723–729.
Mehta, R. D., & Pallis, J. M. (2001). Sports ball aerodynamics: Effects of velocity, spin and surface roughness. In E. H. Froes & S. J. Haake (Eds.), *Materials and science in sports* (pp. 185–197). Warrendale, PA:TIMIS.
Nathan, A. M. (2000). Dynamics of the baseball-bat collision. *American Journal of Physics, 68* (11), 979-990.
Nathan, A. M. (2008). The effect of spin on the flight of a baseball. *American Journal of Physics, 76*(2), 118–124.
Nathan, A. M. (2016). Going deep on goin' deep. *The Hardball Times*. Retrieved April 6, 2016 from http://www.hardballtimes.com/going-deep-on-goin-deep/.
Nathan, A. M., Hopkins, J., & Chong, L., Kaczmarski, H. (2006). The effect of spin on the flight of a baseball. In *SABR Conference*. Seattle, June 2006.
Newton, I. (1671–1672). A letter of Mr. Isaac Newton, of the University of Cambridge, containing his new theory about light and colors. *Philosophical Transactions of the Royal Society*, *7* (1671–1672), 3075–3087.
NOAA's National Weather Service. (2001). Surface pressure analysis … clearing the confusion in the presence of different solutions. Retrieved April, 2009 from http://www.crh.noaa.gov/unr/?n=mslp.
Petriello, M. (2016). The spectrum of Statcast: Spin versus velocity. Retrieved January 11th, 2016 from http://m.mlb.com/news/article/160896926/statcast-spin-rate-compared-to-velocity/.
Planck, M. (1948, 1949). *Wissenschaftliche Selbstbiographie. Mit einem Bildnis und der von Max von Laue gehaltenen Traueransprache* (p. 22). Leipzig: Johann Ambrosius Barth Verlag. *Scientific autobiography and other papers* (pp. 33–24) (F. Gaynor, Trans.). New York (as cited in T. S. Kuhn, *The structure of scientific revolutions*).
Rae, W. J. (2004). Mechanics of the forward pass. In G. Hung & J. Pallis (Eds.), *Biomedical engineering principles in sports* (pp. 291–319). New York: Kluwer Academic.
Robins, B. (1742). New principles of gunnery: Containing, the determination of the force of gun-powder, and investigation of the difference in the resisting power of the air to swift and slow motions. London: J. Nourse. Available online through Early English Books Online.
Sarafian, H. (2015). Impact of the drag force and the magnus effect on the trajectory of a baseball. *World Journal of Mechanics, 5,* 49–58. https://doi.org/10.4236/wjm.2015.54006.
Sawicki, G. S., Hubbard, M., & Stronge, W. J. (2003). How to hit home runs: Optimum baseball bat swing parameters for maximum range trajectories. *American Journal of Physics, 71*(11), 1152–1162.

Sawicki, G. S., Hubbard, M., & Stronge, W. J. (2004). Reply to comments on "How to hit home runs: Optimum baseball bat swing parameters for maximum range trajectories". *American Journal of Physics, 73*(2), 185–189.

Selin, C. (1959). An analysis of the aerodynamics of pitched baseballs. *The Research Quarterly, 30*(2), 232–240.

Shelquist, R. (2017). *Density altitude calculator*. Shelquist Engineering. Retrieved January, 2017 from https://wahiduddin.net/calc/calc_da_rh.htm.

Smith, E. D., Szidarovszky, F., Karnavas, W. J., & Bahill, A. T. (2008). Sensitivity analysis, a powerful system validation technique. *The Open Cybernetics and Systemics Journal*, *2*, 39–56. Retrieved from https://doi.org/10.2174/1874110x00802010039.

Stark, L. (1968). *Neurological control systems, studies in bioengineering*. New York: Plenum Press.

Stodden, V., McNutt, M., Bailey, D, H., Dellman, E., Gil, Y., Hanson, B., et al. (2016). Enhancing reproducibility for computational methods, *Science*, *354*(6317), 1240–1241.

Watts, R. G., & Bahill, A. T. (1990). *Keep your eye on the ball: The science and folklore of baseball*. New York: W. H. Freeman and Co.

Watts, R. G., & Bahill, A. T. (2000). *Keep your eye on the ball: Curveballs, knuckleballs and fallacies of baseball*. New York: W. H. Freeman.

Watts, R. G., & Baroni, S. (1989). Baseball-bat collisions and the resulting trajectories of spinning balls. *American Journal of Physics, 57*(1), 40–45. https://doi.org/10.1119/1.15864.

Watts, R. G., & Ferrer, R. (1987). The lateral force on a spinning sphere: Aerodynamics of a curveball. *American Journal of Physics, New Orleans, 55*(1), 40–44.

Watts, R. G., & Sawyer, E. (1975). Aerodynamics of a knuckleball. *American Journal of Physics, New Orleans, 43*(11), 960–963.

WeatherLink Software. (2017). Retrieved February, from http://www.davisnet.com/weather/products.

Willman, D. (2017). BaseballSavant. Retrieved March, from https://baseballsavant.mlb.com/statcast_search.

Chapter 8
Accuracy of Simulations

8.1 Introduction

Purpose: The purpose of this chapter is to investigate the accuracy of simulations of the flight of the baseball that is shown in this book and on MLB television broadcasts and internet sites. When the television announcer says, for example, that home run went 431.1 feet. Our readers will know that he should have said, that the *true* range of that home run was 430 plus or minus 30 feet. This chapter also shows which parameters of the simulations are the most and least important. This will allow scientists and engineers to focus their time and efforts on the most important variables and parameters.

The results of simulations of the flight of baseballs were given in Chap. 7. Simulations of the flight of baseballs are also used by Major League Baseball (MLB), where television broadcasts and internet sites frequently present simulations of the trajectories of batted balls, particularly of home runs. Often the trajectories shown on television predict the final impact point and therefore the range of the home run ball, if there were no fans or stands in the way. In this chapter, we investigate the accuracy of these simulations. As always, the accuracy of the outputs depends on the accuracy of the inputs. So now our question becomes, "What *are* the inputs to these simulations and how accurate are they?"

8.2 Simulation Inputs

The first three inputs of interest for analyzing the accuracy of flight of baseball simulations describe the launch of the baseball immediately after the bat–ball collision, namely, the launch speed, the launch angle and the initial spin of the batted ball. For the Ball in Flight model of Chap. 7, values for these parameters came from the BaConLaws model of Chap. 4, and another model presented in

A. T. Bahill, *The Science of Baseball*,
https://doi.org/10.1007/978-3-030-03032-2_8

Chap. 9. For the television and internet simulations, these values are estimated from outputs of the Doppler radar systems mounted in the MLB stadiums, the same computer systems that provide the trajectories of the pitches during televised baseball games.

In Sect. 1.2.1, we distinguished between *parameters* and *variables*. Variables have equations that give them values. Our variables contain parameters whose different values produce different sets of equations. In Chap. 4 we described the input variables to the BaConLaws model for bat–ball collisions as $v_{\text{ball-before}}$, $\omega_{\text{ball-before}}$, $v_{\text{bat-cm-before}}$, $\omega_{\text{bat-before}}$ and CoR.

$v_{\text{ball-before}}$ is the linear velocity of the pitched-ball before the bat–ball collision. Pitch speed is a negative number because the x-axis points from home plate to the pitcher's rubber.
$\omega_{\text{ball-before}}$ is the angular velocity of the ball about its center of mass before the collision.
$v_{\text{bat-cm-before}}$ is the linear velocity of the center of mass of the bat in the x-direction before the collision.
$\omega_{\text{bat-before}}$ is the angular velocity of the bat about its center of mass before the collision.
CoR is the coefficient of restitution for the particular collision configuration.

Also in Chap. 4 we described the output variables from the BaConLaws model as $\mathrm{v}_{\text{ball-after}}$, $\omega_{\text{ball-after}}$, $v_{\text{bat-cm-after}}$ and $\omega_{\text{bat-after}}$.

$v_{\text{ball-after}}$ is the linear velocity of the ball in the x-direction after the bat–ball collision.
$\omega_{\text{ball-after}}$ is the angular velocity of the ball about its center of mass after the collision.
$v_{\text{bat-cm-after}}$ is the linear velocity of the center of mass of the bat in the x-direction after the collision.
$\omega_{\text{bat-after}}$ is the angular velocity of the bat about its center of mass after the collision.

These output variables of the BaConLaws model of Chap. 4 were input variables for the Ball in Flight model of Chap. 7.

The following are *parameters* used in our equations: launch speed, launch angle, launch spin rate, mass and moment of inertia of the bat and ball, air density and the Magnus coefficient. For each invocation of an equation, they will have fixed values. We refer to variables and parameters collectively as *properties* of the model.

To find the rest of the Ball in Flight model inputs, we examine the following equations for the three basic forces acting on the ball in flight (Watts and Bahill 2000).

$$F_{\text{gravity}} = m_{\text{ball}} g$$
$$F_{\text{drag}} = 0.5\pi\rho r_{\text{ball}}^2 v_{\text{ball}}^2 C_{\text{D}}$$
$$F_{\text{Magnus}} = 0.5\pi\rho r_{\text{ball}}^3 \omega_{\text{ball}} v_{\text{ball}} C_{\text{M}}$$

Many scientists write the Magnus force equation as

$$F_{\text{lift}} = 0.5\pi\rho r_{\text{ball}}^2 v_{\text{ball}}^2 C_{\text{L}}$$

where the lift coeficient is not a constant, but rather $C_{\text{L}} = \dfrac{C_{\text{M}} r_{\text{ball}} \omega_{\text{ball}}}{v_{\text{ball}}}$

These force equations depend upon the following properties

- the mass of the ball, m_{ball}, which equals the weight of the ball divided by the earth's gravitational acceleration, g,
- the air density, ρ, which depends on altitude, temperature, relative humidity and barometric pressure,
- the radius of the ball, r_{ball},
- the ball velocity, v_{ball}, whose initial value is the launch velocity, $v_{\text{ball-after}}$, from the BaConLaws model,
- the wind velocity, which may vary throughout the flight,
- the drag coefficient (or air resistance), C_{D}, which depends on the Reynolds number and therefore on the ball velocity,
- the spin of the ball, ω_{ball}, whose initial value is $\omega_{\text{ball-after}}$ from the BaConLaws model and
- the Magnus coefficient C_{M}, (for the lift force).

These properties must be measured at home plate for each batted ball and they must be given along with the batted-ball trajectory, otherwise the displayed batted-ball trajectory is nonsense. Table 8.4 gives nominal values for these properties.

Launch parameters. For the Ball in Flight model, values for the launch speed, the launch angle (θ in Fig. 8.1) and the launch spin rate of the batted ball come from

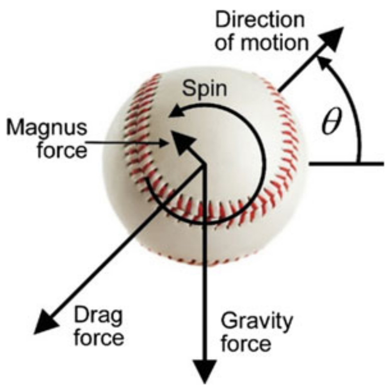

Fig. 8.1 Forces acting on the ball in flight

the BaConLaws model (for example, from Table 4.2). For the television and internet simulations, these values are computed from outputs of the Doppler radar systems mounted in MLB stadiums. The spin on the batted ball has a lot of variabilities. It also decreases a by a few percent during the flight, but we ignore this decrease (McBeath et al. 2008).

Earth's gravitational acceleration. In MLB stadiums, the Earth's gravitational acceleration (colloquially called the Earth's gravity), g, varies from, for example, 9.79197 m/s^2 in Houston to 9.81145 m/s^2 in Seattle. These differences are relatively small. The Ball in Flight model uses the *standard* gravitational acceleration of 9.80665 m/s^2.

Radius of the baseball. MLB rules state that the radius of the baseball shall be 1.45 ± 0.02 inches. The radius of each baseball will not be measured before each pitch, so it will be an uncontrolled variable in the simulations.

Weight of the baseball. There are two sources of variation in the weight of the baseball: manufacturing variability and variability due to the storage environment. To accommodate manufacturing variability, MLB rules allow the weight of the baseball to vary between 5.0 and 5.25 ounces ±2.4%. Now, on top of that, the storage environment can cause additional variation. On a typical July afternoon outdoors in Denver, the relative humidity is 34% with an average temperature of 88 °F. The Colorado Rockies take their baseballs from this environment and put them in a humidor at 50% relative humidity and 70 °F. This higher humidity could cause the baseballs to absorb water in the humidor and increase their weights by as much as 1.6% (Nathan 2011, 2017). Each ball in flight trajectory depends on the weight of the baseball, which in turn depends on the temperature and humidity of the place where the baseballs have been stored and on how long the baseballs have been out of that controlled environment. Adding these two effects would allow the ball weight to vary by ±4%.

Coefficient of restitution. There are two sources of variation in the baseball's contribution to the coefficient of restitution (CoR) of a bat–ball collision: manufacturing variability and variability due to the storage environment. To accommodate manufacturing variability, MLB rules allow the CoR to vary by ±3.2% in a specified test. Now, on top of that, the storage environment causes additional variation. On a typical July afternoon, outdoors in Denver, the relative humidity is 34% with an average temperature of 88 °F. The Colorado Rockies take their baseballs from this environment and put them in a humidor at 50% relative humidity and 70 °F. This higher humidity could cause the baseballs to absorb water in the humidor and become mushier, decreasing the CoR by as much as 3.7% (Nathan 2011, 2017). Adding these two effects would allow the CoR to vary by ±6.9%. This is a large variation.

Air density. Air density is inversely related to altitude, temperature and humidity, and is directly related to barometric pressure. The following linear equation from Chap. 7 is a very good fit for air density (Bahill et al. 2009; Shelquist 2017).

$$\begin{aligned}\text{Air density} = \rho = 1.045 + 0.01045 \\ \{-0.0035(\text{Altitude} - 2600) \\ - 0.2422(\text{Temperature} - 85) \\ - 0.0480(\text{Relative Humidity} - 50) \\ + 3.4223(\text{Barometric Pressure} - 29.92)\}\end{aligned} \tag{8.1}$$

where Air Density is in kg/m^3, Altitude is in feet, Temperature is in degrees Fahrenheit, Relative Humidity is a percentage and Barometric Pressure is in inches of Hg. These parameters should be measured at home plate for each batted ball. Each of these parameters (except for altitude) could be different for each batted ball. We assume that in the simulations the altitude is set for each stadium and remains constant throughout the game. Table 8.1 gives typical values in some MLB stadium late-afternoon games in July if the stadium roofs are open and there are no storms.

In our simulations, we used values for altitude, temperature, relative humidity and barometric pressure that would span the range of values that would be typical for a MLB game on any given afternoon in July. Low, middle and high altitudes that should be expected in MLB stadiums are 0, 2600 and 5200 feet. Low, middle and high temperatures that should be expected in MLB stadiums are 70, 85 and 100 °F. Low, middle and high relative humidities that should be expected in MLB stadiums are 10, 50 and 90%. Low, middle and high barometric pressures that should be expected in MLB stadiums are 29.33, 29.92 and 30.51 inches of Hg. These values were chosen to show realistic numbers with natural variation. On any given afternoon in July, it is almost certain that baseball games will be played at the high and low ends of these ranges and at values in between (Table 8.2).

To understand how the four fundamental weather variables (altitude, temperature, humidity and barometric pressure) determine the air density, we evaluated our equations at eighty-one theoretical points in a spreadsheet. These points were selected to be at the low, middle and high values of the fundamental variables producing 3^4 or 81 points.

Table 8.1 Typical weather parameter values in some MLB stadiums for afternoon games in July

City	Altitude (feet above sea level)	Average daily high temperature in July (°F)	Relative humidity, on an average July afternoon (%)	Average barometric pressure in July (inches of Hg)	Air density (kg/m^3)
Denver	5190	88	34	29.98	0.96
Houston	45	94	63	29.97	1.11
Minneapolis	815	83	59	29.96	1.11
Phoenix	1086	104	20	29.81	1.07
San Francisco	0	68	65	29.99	1.19
Seattle	10	75	49	30.04	1.18

Table 8.2 Some weather parameter values used in the simulations

Condition	Altitude (feet above sea level)	Temperature (degrees Fahrenheit)	Relative Humidity (%)	Barometric pressure (inches of Hg)	Air density (kg/m^3)	Air density, percent change from midlevel
Low altitude	0	85	50	29.92	1.16	9.4
Low temperature	2600	70	50	29.92	1.09	2.9
Low humidity	2600	85	10	29.92	1.06	0.7
Low barometric pressure	2600	85	50	29.33	1.04	−2.0
Lowest density	5200	100	90	29.33	0.91	−14.0
Midlevel	2600	85	50	29.92	1.06	0.0
High barometric pressure	2600	85	50	30.51	1.08	2.0
High humidity	2600	85	90	29.92	1.05	−0.7
High temperature	2600	100	50	29.92	1.03	−2.9
High altitude	5200	85	50	29.92	0.97	−8.6
Highest density	0	70	10	30.51	1.22	15.5

The impact of each factor in Eq. (8.1) can be shown graphically. Figure 8.2 shows the changes in air density that should be expected over the range of parameter values that would be typical for a MLB stadium on an afternoon in July. It shows that altitude, having the largest slope, is the most important factor, followed by temperature, barometric pressure and relative humidity. Since the factor ranges given are indicative of their natural variation, larger absolute slopes mean stronger effects. These results are for baseball and should not be used for other purposes, such as calculating safe takeoff parameters for a small airplane.

Wind velocity. The wind speed and direction should be measured at home plate for each batted ball and these values should be given along with the displayed batted-ball trajectory. However, it would be difficult to measure these variables at home plate. Therefore, some other place might be used, such as a place in the stands behind home plate where the radar units are mounted or at the top of the flagpole. However, to make things worse, these variables are likely to vary with elevation throughout the flight of the ball. As a rough approximation, in Sect. 7.7, we gave typical wind speed values of 0, 5 and 10 mph. However, for this present sensitivity

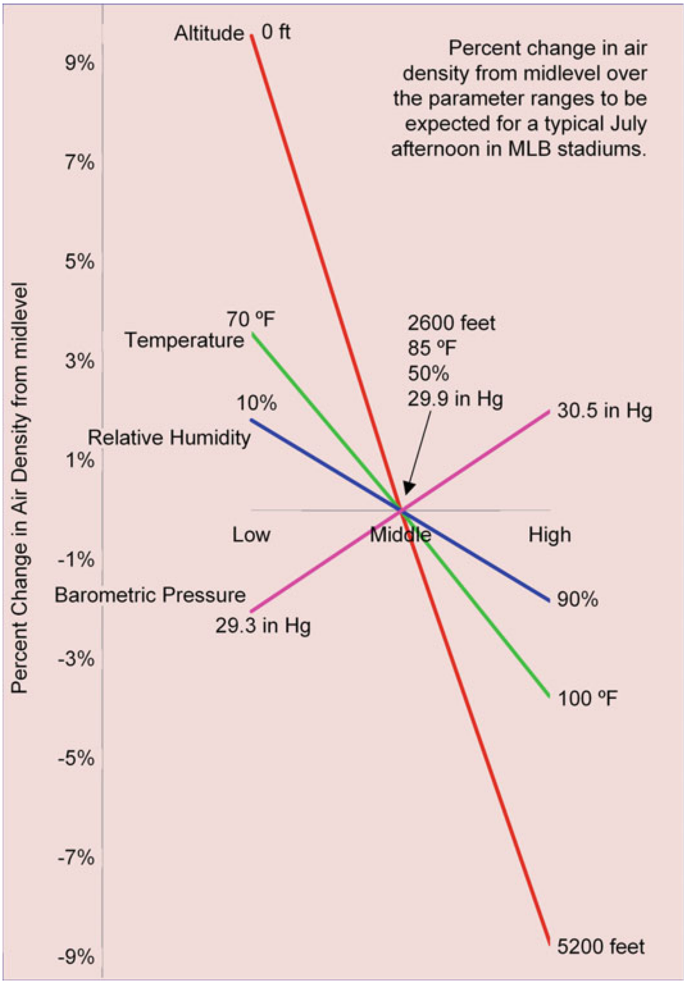

Fig. 8.2 Air density depends on altitude, temperature, barometric pressure and relative humidity in that order

analysis, we reduced these values for wind speed to 0, 3 and 5 mph. As shown in Table 8.3 and Fig. 8.3, winds of one to three mph are barely perceptible by humans. As a demonstration of this, while you are inside a building, walk 10–20 feet at a normal three to four mph pace. Did you feel the "wind" on your face? Probably not.

Drag coefficient. The drag coefficient (or air resistance), C_D, depends on the Reynolds number, which in turn depends on ball velocity. As shown in Fig. 8.4, for a home run ball the Reynolds number decreases from about 200,000 at the beginning of flight (green disk) to 100,000 at the end (red square).

Table 8.3 Beaufort wind speed scale

Force number	Wind speed, (mph)	Name	Effects
1	1–3	Light air	The wind direction will be shown by the drift of smoke but not by wind vanes: tree leaves will not move: flags will hang limp
2	4–7	Slight breeze	A slight breeze will be felt on the face and wind vanes will be moved by the wind: tree leaves will rustle: flags will stir
3	8–12	Gentle breeze	Leaves and twigs will be in constant motion: flags will occasionally extend

Fig. 8.3 Flag behavior for wind speeds of 1–3 mph (left), 4–7 mph (middle) and 8–12 mph (right)

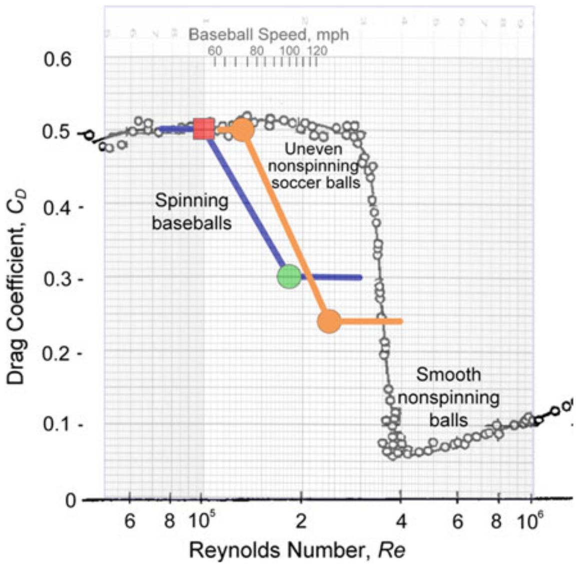

Fig. 8.4 Drag coefficient as a function of the Reynolds number for different experimental conditions

A recent study of the Reynolds number for sports balls (Naito et al. 2018) provided data for soccer balls that we have added to Fig. 7.12 to produce Fig. 8.4. Their data confirm the general shape of the curve. This figure also nicely shows something that has been known for a century that in going from smooth non-spinning balls, to uneven nonspinning balls, to rough spinning balls (changing the boundary layer flow from turbulent to laminar), the lower-right corner of the Reynolds number curve moves up and to the left.

Given this additional data, we modified our Ball in Flight model: we added the following equation, fit to the data of Fig. 8.4.

$$C_{\mathrm{D}} = \begin{cases} 0.5 \text{ for } v_{\mathrm{ball}} \leq 55\,\text{mph} \\ -0.0044 v_{\mathrm{ball}} + 0.744 \text{ for } 55 < v_{\mathrm{ball}} < 100\,\text{mph} \\ 0.3 \text{ for } v_{\mathrm{ball}} \geq 100\,\text{mph} \end{cases}$$

Making the equation logarithmic instead of linear did not improve the model.

Magnus coefficient. The Magnus coefficient, C_{M}, is used in the lift force equation. In this chapter, we use low, middle and high values of 0.71, 0.81 and 0.91.

8.3 Sensitivity Analysis

The shaded boxes in Table 8.4 indicate the most important properties in the simulation of the interconnected BaConLaws and Ball in Flight models. They are, in decreasing order of importance, the CoR, Wind velocity (ignoring the 5-mph wind, because it would be noticeable), Air density, Initial spin of the batted ball, Launch speed and the Drag coefficient. The coefficient of restitution (CoR) is the most important property. It is affected by manufacturing variability and it might be changed by the humidors that are being installed in some MLB stadiums. This introduces more uncontrolled properties because the CoR depends on the temperature and humidity of the place where the baseballs have been stored and on how long the baseballs have been out of that controlled environment. The wind velocity is the second most important property in the simulation: unfortunately, data are not available to allow the simulation to control for a changing wind velocity. The third most important property, the air density, is easily controlled for in the simulation: all we must do is supply the altitude, temperature, relative humidity and barometric pressure at home plate for each batted ball. The fourth most important property, the initial spin of the batted ball is problematic: we do not have good data for it. Finally, the initial launch speed and the drag coefficient are important, but they are easy to deal with in the simulations.

Table 8.5 shows the most important properties in this overarching simulation of the interconnected BaConLaws and Ball in Flight models which are, in decreasing order of importance, CoR, Wind velocity, Air density, Initial spin rate of the batted ball, Launch speed and the Drag coefficient.

Table 8.4 Variations in parameters and variables for perfectly-hit home run balls

Parameters and variables	Sub parameters	Symbols	Parameter values	Range (feet)	Change in range (feet)	1
			High value			2
			Nominal value			3
			Low value			4
Nominal range				375.56		5
Results from changing values in the Ball in Flight model						
Launch speed (mph)		High value	94	387.43	11.87	7
		Nominal value	92		0	8
		Low value	90	363.61	-11.95	9
Launch angle (degrees)		θ	28	377.05	1.49	10
			27		0	11
			26	373.55	-2.01	12
Initial spin of the batted-ball (rpm)		ω_{ball}	2500	389.90	14.34	13
			2000		0	14
			1500	360.23	-15.33	15
Earth's gravitational acceleration (m/s2)	Seattle	g	9.8296	374.69	-0.87	16
	Standard		9.8066		0	17
	Houston		9.7943	376.03	0.47	18
Radius of the baseball (inches)		r_{ball}	1.47	373.37	-2.19	19
			1.45		0	20
			1.43	377.68	2.12	21
Air density(kg/m^3)		below is resulting air density, ρ	1.223	358.85	-16.71	22
			1.058		0	23
			0.910	390.65	15.09	24
	Altitude (feet above sea level)	0.967	5200	384.88	9.32	25
		1.058	2600		0	26
		1.158	0	365.39	-10.17	27
	Air temperature (degrees Fahrenheit)	1.027	100	378.73	3.17	28
		1.058	85		0	29
		1.089	70	372.41	-3.15	30
	Barometric pressure (inch Hg)	1.079	30.51	373.41	-2.15	31
		1.058	29.92		0	32
		1.037	29.33	377.71	2.15	33

	Relative humidity (percentage)	1.051	90	376.29	0.73	34
		1.058	50		0	35
		1.065	10	374.82	-0.74	36
Wind velocity (mph)		v_{wind}	5 toward centerfield	405.10	29.54	37
			3 toward centerfield	393.34	17.78	38
			0		0	39
			3 from centerfield	357.60	-17.96	40
			5 from centerfield	345.55	-30.01	41
Drag coefficient slope			0.005	386.19	10.63	42
			0.0044		0	43
			0.004	368.03	-7.53	44
Drag coefficient intercept			0.8	364.48	-11.08	45
			0.744		0	46
			0.7	385.45	9.89	47
Magnus coefficient		C_{M}	0.86	379.21	3.65	48
			0.81		0	49
			0.76	371.84	-3.72	50
Results from changing values in the BaConLaws model						
		Launch speed, mph				53
Range of CoR allowed by MLB rules ±3.2%	high value	93.78	0.480	386.11	10.55	54
	nominal	92	0.465		0	55
	Low value	90.22	0.45	364.94	-10.62	56
Change in CoR due to humidor ±3.7%		94.06	0.482	387.76	12.2	57
		92	0.465		0	58
		89.95	0.448	363.28	-12.28	59
CoR range allowed by MLB rules plus humidor changes, ±6.9%		95.83	0.497	398.31	22.75	60
		92	0.465		0	61
		88.17	0.433	352.66	-22.90	62

Results from changing values in both the BaConLaws model and the Ball in Flight model						
Range of weight allowed by MLB rules (ounces) ±2.4%	high value	91.25	5.250	373.58	-1.98	65
	nominal	92	5.125		0	66
	Low value	92.76	5	377.39	1.83	67
Change in weight due to humidor (ounces) ±1.6%		91.51	5.207	374.28	-1.28	68
		92	5.125		0	69
		92.48	5.043	376.62	1.06	70
Weight of the ball allowed by MLB rules plus humidor changes, (ounces) ±4%		90.75	5.334	372.37	-3.19	71
		92	5.125		0	72
		93.25	4.920	378.29	2.73	73

Table 8.5 The most important parameters and variables for perfectly hit home run balls

Parameters and variables	Parameter values	Range (feet)	Change in range (feet)
Nominal range		376	
CoR range allowed by MLB rules plus humidor changes, ±6.9%	0.497	398	22.7
	0.465		0
	0.433	353	−23.0
Wind velocity (mph)	3 mph toward centerfield	393	17.8
	0		0
	3 mph from centerfield	358	−18.0
Air density (kg/m^3)	1.223	359	−16.7
	1.058		0
	0.910	391	15.1
Initial spin of the batted ball (rpm)	2500	390	14.3
	2000		0
	1500	360	−15.3
Launch speed (mph)	94	387	11.9
	92		0
	90	364	−12.0
Drag coefficient intercept	0.8	364	−11.1
	0.744		0
	0.7	385	9.9
Drag coefficient slope	0.005	386	10.6
	0.0044		0
	0.004	368	−7.5

8.4 Batted-Ball Range

8.4.1 Technical Note

Numbers in scientific publications should have at least two parts. The first is the magnitude or value. The second part should indicate the reliability, confidence, uncertainty, range of validity, tolerance, direction (for vectors), variance, standard deviation, sample size, margin of error, skewness, or some combination of these qualifiers. For example, in Table 8.5 it was written that in a normal MLB game the CoR might *range* from 0.4 to 0.5. Earlier we wrote that MLB rules allow the radius of the baseball to be 1.45 ± 0.02 inches (*tolerance*). In Table 7.16, we described the typical launch velocity of a batted ball as having a magnitude of 92 mph and a launch angle of 30 degrees (*direction*). Figure 4.10 indicated the mean and *variance* of swing speeds. Table 5.1 gave means and *standard deviations*.

8.4.2 Range of the Batted Ball

The distance that a baseball travels from the bat–ball collision point to where it first touches the ground is its *measured range*. We now have the need to qualify this term. We will use *estimated range* for instance when the ball does not hit the ground (for example, when it hits the stadium seats or is caught by a fielder) and the last part of its trajectory is estimated with a simulation. To make comparisons in the record books it will be necessary to remove external effects such as wind velocity. We will say that the *measured range* is equal to the *true range* increased or decreased by the wind velocity and other effects.

Most MLB stadiums have outfield walls at 325 feet or more down the foul lines and at 400 feet or more in center field. These walls are about nine feet high. Therefore, we have used a nominal range of 375 feet for a home run. The home run trajectory must have a range that is large enough to reach the wall at a height that is enough to clear the wall.

As a simple example, using the nominal values of Table 8.4, our home run ball had a nominal range of 376 feet. However, if there were a barely detectable three-mph wind blowing out toward center field, then this wind would have added 17 feet to the true range. Therefore, the true range would have been $376 - 17 = 359$ feet. If the temperature, relative humidity and barometric pressure were not recorded, then the nominal range could be six feet less or 370 feet. If both abnormal sets of data occurred at the same time, then the true range might have only been 352 feet. In other words, if the range was measured at 376 feet then the true range that should be put in the record books would be only 352 feet with a $\pm 6\%$ margin of error.

8.5 Other Models and Measurement Systems

Alan Nathan has an excellent ball in flight simulation on his website, http://baseball.physics.illinois.edu/, named the Trajectory Calculator, which you are free to use. It is like our Ball in Flight model, except that (1) his drag coefficient C_D is a constant at 0.374, (2) his lift coefficient is not a constant, he uses $C_L = C_M \frac{r_{ball}\omega_{ball}}{v_{ball}}$, (3) we use the Runge–Kutta integration method, he presumably uses something else, and (4) his launch point is at the tip of the plate, whereas our bat–ball collision point is 1.5 feet in front of the plate. However, in spite of these differences, his results are like ours. When our nominal parameter values of Table 8.4 are put into his Trajectory Calculator, it produces a range of 378.3 feet with a hang time of 4.784 s, compared to our Ball in Flight range of 375.6 with a hang time of 4.768. The difference in the ranges is 2.7 feet which is nearly the same as the distance from the tip of the plate to our collision point 1.5 feet in front of the plate, namely 2.9 feet.

Television and internet sites frequently present simulations of the trajectories of MLB batted balls, particularly of home runs. Often the trajectories shown on television predict the final impact point and therefore the estimated range of the home run ball, if there were no fans or stands in the way. In this section, we investigate the accuracy of these trajectories.

Most MLB teams use TrackMan Baseball, which is a three-dimensional (3D) Doppler radar system that measures the ball's distance, velocity, elevation angle and azimuth angle. It uses these measurements to compute values for the launch speed, the launch angle, the spin of the batted ball and the ball's trajectory. The TrackMan radar unit is typically mounted behind home plate on the front of the second deck. It covers the field from the left- to the right-field foul lines and the air above the fielders' heads. Therefore, practically the only thing in its field of view is the ball in flight. The physiological and psychological effects of this radar on humans sitting below it have not been published. To assess the accuracy of Trackman we will compare its results with the results of the Trajectory Calculator and the Ball in Flight model.

We do not know how Trackman computes the spin rate. But if the radar frequency were high enough, they could measure the speed at the top of the ball and the speed at the bottom of the ball and from these compute the spin rate.

In order for MLB and Statcast to be scientific, they would have to define all of their metrics and they would have to state the measurements and calculation that were used to derive their numbers. Furthermore, they would have to publish the variability in their data.

Evidently, TrackMan has difficultly computing spin particularly for the slider because their spin axis is in the y–z plane, meaning this axis is not leaning toward the batter. If this were the actual case, then the batter would never see the telltale red dot of the slider shown in Fig. 7.7 (Baldwin et al. 2007). Nathan http://baseball.physics.illinois.edu/ gives a technique for calculating this forward leaning angle.

Trackman measures the position of the ball in space until it hits the stadium, a seat, a sign or is caught by a fan. Thereafter, it uses a simulation to extrapolate the trajectory to ground level. It uses this projected impact point to estimate the range.

Kagan and Nathan (2017) repeated Statcast data and analyzed Alex Rodriguez's longest home run of the 2015 season. Its stated parameters were

Estimated distance	470.5 ft
Launch speed	107.3 mph
Maximum height	96.0 ft

What do you think was the *true* range of this home run ball? Unless they also stated measured values for altitude, temperature, relative humidity, barometric pressure, wind speed and the weight of the baseball, then the most reasonable estimate of the baseball's true range would be 470 ± 50 feet.

Let us now reanalyze Alex Rodriguez's home run of April 17, 2015 with its estimated distance of 470.5 feet using the values in Table 8.4. Suppose the actual baseball that he hit was lighter and smaller than the average baseball. The smaller radius would have allowed it to go 2.1 feet farther than an average baseball. The lighter weight would have allowed it to go 2.7 feet farther than an average baseball. Suppose there was a light air of 3 mph blowing toward centerfield, this would be barely noticeable and would certainly not be noteworthy: this could have caused it to go 17.8 feet farther than average. The baseball's contribution to the coefficient of restitution (CoR) of the bat–ball collision could have been larger than the average due to both manufacturing variability and variability due to the storage environment. This could have allowed it to go 22.7 feet farther than an average baseball. Suppose the barometric pressure was low (add 2.2 feet) and the humidity was high (add 0.7 feet). For this home run, the ball's trajectory from where the ball hit the stadium to where it would have hit the ground if there were no obstructions, had to be simulated. Assume the whole trajectory was 90% measured and 10% simulated. Suppose the simulation for the 10% segment had extreme values for the drag coefficient (add 2 feet) and the Magnus coefficient (add 0.4 feet). The total of these deviations from the norm is 50 feet. Therefore, when Statcast stated that this ball's range was 470.5 feet, *we* know that its true range might have only been 420 feet. The extra 50 feet could have been artifact. Now, it is unlikely that all of these properties would have been at their extremes and in the same direction at the same time, but it is possible. The important point of this section is that the values stated on television broadcasts and internet sites for the range of a home run ball are not accurate! First, there should be no numbers after the decimal point: numbers after the decimal point are evidence of the mental mistake of implying false precision. Second, an estimated margin of error should be stated, in this case, it would be $\pm 10\%$.

Television announcers and commentators make a big deal about the difference between, for example, a 98-mph pitch and a 100-mph pitch, sometimes even stating digits after the decimal point, like 100.1 mph. They should state where their speeds were measured (perhaps 10 feet in front of the rubber or perhaps at the pitcher's release point) because the pitch loses 10% of its speed en route to the plate. The results of this chapter have indicated that this two-mph difference is awash in the noise. For instance, a two-mph wind could cause the same difference: and a two-mph wind might not even be perceived by a spectator, much less by an announcer in a glass-enclosed booth. Therefore, unless the wind speed is reported, the announcer should not adulate the pitcher for differences between a 98 and a 100-mph pitch. Let us be very clear here. A 98-mph pitch with an imperceptible 2-mph wind from center field is exactly the same as a 100-mph pitch with no wind. Note that in this chapter we did not even consider the effects of crosswinds.

Today's pitchers are probably faster than those of yesteryears. Television announcers and commentators make a big deal about this difference. However, they should admit that some of this increase in speed is due to better measurement techniques. For example, in the 1910s the speed at home plate of Walter Johnson's fastball was measured as 83 and 92 mph. In 1939 Bob Feller's fastball was measured as near 100 mph. The technique for this measurement was racing his fastball against a police motorcycle. The motorcycle was going 86 mph and Feller's fastball caught up to and passed the motorcycle. In 1946 they used equipment from the U. S. Army Ordinance Department and measured his fastball near home plate at 98.6 mph. In 1974, Nolan Ryan entered the Guinness Book of Records with a 100.9 mph pitch. That speed was measured by a radar gun when the ball was around 10 feet in front of the plate. In the next decades, the radar gun technique improved and the point at which the speed of the ball was measured became standardized at around ten feet in front of the pitcher's rubber: the measured pitch speeds got faster. Around 2016 MLB introduced 3D Doppler radar in their stadiums. Nowadays, the speed of a fastball, measured at the pitcher's release point, thrown by dozens of pitchers, routinely exceeds 100 mph. Over the past century, the measurement techniques and the pitchers have gotten better. Therefore, the measured speed of the fastball has increased.

8.6 Causes of Inaccuracies

Most of the inaccuracies reported in this chapter, were caused by omitting variables and parameters, and by not stating assumptions. For example, the biggest source of error in computing the range of a home run ball was assuming that there was no wind.

We have said little about inaccuracies in the BaConLaws model because there are none. The BaConLaws model merely converts inputs into outputs. If the inputs are accurate, then the outputs will be accurate. The two major assumptions of the BaConLaws model were stated as the bat–ball collision is a free-end collision and it only models the speed and spin of the bat and ball just after the collision in terms of these same variables just before the collision. There are no important unstated assumptions. In the BaConLaws model the user supplies values for $d_{\text{cm-ip}}, I_{\text{cm}}, m_{\text{ball}}, m_{\text{bat}}, r_{\text{ball}}, r_{\text{bat}}, v_{\text{ball-before}}, v_{\text{bat-cm-before}}, \omega_{\text{bat-before}}$ and COR and the model returns corresponding accurate output values.

In contrast, when the Ball in Flight model is used to analyze a particular, for example, home run ball, values for $d_{\text{cm-ip}}, I_{\text{cm}}, m_{\text{ball}}, m_{\text{bat}}, r_{\text{ball}}, r_{\text{bat}}, COR$, launch speed, *angle* and spin must be guessed.

So the difference in the accuracy of the BaConLaws model and Ball in Flight model is in how they are used. For the BaConLaws model, inputs are provided and it produces appropriate outputs, whereas the Ball in Flight model used in Sects. 8.4 and 8.5 was being used to replicate a particular batted-ball trajectory and values for the variables and parameters were not known: they had to be guessed.

8.7 People Want Stories

This section is a digression from baseball. It involves human thinking, which was the topic of Chap. 2 of Bahill and Madni (2017). People like stories. Would you rather read the technical description in the previous sections written by a scientist/engineer or the following story written by a sports writer?

> April 17, 2015, St. Petersburg Florida
>
> Alex Rodriguez is back after his year-long suspension for using performance enhancing drugs. And he is back with a blast. On Friday night, in the second inning, on an 0-1 pitch from Tampa Bay starter Nate Karns, he blasted a 92-mph letter-high fastball onto the Captain Morgan party deck in left-center at Tropicana Field to give the Yankees a 1-0 lead. This blast was a moonshot: it was absolutely crushed. In fact, according to the MLB tracking system, that was the longest home run in baseball this season, measuring 471 feet. A-Rod hit his second home run of the night in the sixth. That ball jumped off his bat at 115 mph, tied for the hardest hit home run of the season. So in one night, A-Rod hit the farthest homer and the hardest hit homer of the 2015 season. He is now sitting on 658 career home runs, two behind Willie Mays on the all-time list. When he ties Willie Mays he is entitled to a $6 million marketing bonus.

Most people prefer the story. They do not want to think about assumptions, simulation accuracy and confounding factors. They want stories.

8.8 Comparison of Sensitivity Analyses

In Sect. 4.11, we performed both an analytic (Table 4.4) and an empirical (Table 4.5) sensitivity analysis for the BaConLaws model for bat–ball collisions. For the analytic sensitivity analysis, we first choose the performance criterion, the batted-ball speed. Then, we calculated the partial derivatives of that performance criterion with respect to the eight model properties. Finally, we multiplied the partial derivatives by the nominal values of those properties and computed the semirelative sensitivity values. We found that the most important properties were the bat velocity before the collision and the coefficient of restitution (CoR). The least important properties were the distance between the center of mass of the bat and the bat–ball collision point, and the moment of inertia of the bat. In summary, this sensitivity analysis suggested that we spend more time and effort trying to improve the data and models for the swing of the bat and less time worrying about the exact impact point, which has a lot of variability anyway.

Then we performed an empirical (or numeric) sensitivity analysis on the BaConLaws model in order to see the effects of interactions between the properties, meaning what happens when two properties are changed at the same time. We used the same performance criterion, the batted-ball speed. We varied the properties by 1%, and then computed the semirelative sensitivity values (Table 4.5). The most important interaction was that between the ball velocity before the collision (the pitch speed) and the CoR. However, this sensitivity was smaller than the sensitivity to the single variable bat velocity. This was a welcome result because large interactions increase the complexity of models.

In Chap. 7, for the Ball in Flight model, the chosen performance criterion, the range of the batted ball, was not the result of any single equation. It would have been possible, but difficult to create such an equation. Therefore, in Chap. 7, we simulated the model and did an empirical sensitivity analysis. We changed each property by 1% and computed the semirelative sensitivity values. The results, given in Table 7.6, showed that the most important property, in terms of maximizing the batted-ball range, was the batted-ball speed. This was certainly no surprise. The second most important property was the diameter of the baseball, over which we, unfortunately, have no control. The least important properties were the launch height and the launch angle. As you can remember, we did not have good data for the Magnus lift coefficient, so we were happy that its sensitivity was small. The sensitivities to some of the properties were negative, which merely means that as they increased the range decreased. The results of this sensitivity analysis showed that the model was well behaved. The most and least important properties were as expected. There were no unexpectedly large or small sensitivities.

In this, we did a sensitivity analysis of the interconnected BaConLaws model of Chapter 4 and the Ball in Flight model of Chap. 7. As before, our performance criterion was the range of the batted ball. Because we do not have an equation for this range, we could not do an analytic sensitivity analysis. Therefore, we did an empirical sensitivity analysis. However, this time, instead of changing each of the properties by 1%, we choose realistic numbers with natural variation for the values. The results of this analysis are shown in Table 8.4.

8.9 Accuracy of the Speed and Spin Rate of the Pitch

Velocity and spin of the ball are vectors so they have two components: a magnitude and a direction. Velocity has a magnitude, called speed, and a direction as shown in Fig. 8.1. The spin has a magnitude, called the spin rate, and an axis of rotation.

How accurate are the measurements of speed and spin rate of the pitch? Table 8.6 presents data for pitches thrown in 2017 in MLB. These numbers came from Willman (2018). They look reasonable.

Thirty years ago (Watts and Bahill 1990, Table 1), we did not have high-tech three-dimensional Doppler radar systems to measure the speed and spin rate of the pitch. We had to estimate speed and spin rate using whatever was available in the

Table 8.6 2017 MLB Pitching statistics from Statcast

	Speed of the pitch at the pitcher's release point			Pitch backspin rate		Number of pitches (×1000)
Type of pitch	Average, mph	Standard deviation	Average, m/s	Average, rpm	Standard deviation	
4-seam fastball	92.9	2.6	41.6	2235	151	253
2-seam fastball	92.8	2.5	41.5	2195	153	95
Sinker fastball	91.3	2.7	40.8	2112	150	49
Cut fastball	88.6	2.8	39.6	2306	204	36
Slider	84.4	3	37.7	−2342	227	108
Changeup	84.9	3.2	38	1762	254	71
Curveball	77.8	3.4	34.8	−2438	264	58

These data are the average of the average values of the pitch speeds and spins for each pitcher who had at least 100 total pitches in 2017. These are not weighted averages

scientific literature. We expected no overlap in the speed and spin rate of the fastball, slider, changeup and curveball. Therefore, we thought that speed and spin rate would differentiate these four types of pitches. Our speed estimates for the fastball, slider and curveball overlap the mean values given in Table 8.6. However, we estimated the changeup to be slower. The spin rates given in Table 8.6 are all higher than we had estimated. Furthermore, and most surprisingly, the spin rates in Table 8.6 for different types of pitches overlap each other. Except for the changeup, all of the absolute spin rates for the pitches in Table 8.6 are within their standard deviation of the fastball average spin rate. That means that spin rate cannot be used to distinguish between the different types of pitches. Statcast has not revealed their algorithms for distinguishing between types of pitches (this is probably the weak link in their analysis). Knowledge of their algorithms would be essential to instill trust their data.

Decades ago, we designed a system to help the batter distinguish different types of pitches based on acoustic frequency. The curveball has a higher spin rate, 2440 rpm, than the changeup, 1760 rpm. These different spin rates produce different sounds. A frequency of 2489 Hz is the 79th key on a piano, D#7. 1760 Hz is the 73rd key on the piano, A6. It is easy to distinguish between D#7 and A6. We think that a batter, perhaps wearing a programmed hearing aid, can distinguish between these frequencies. However, because the spin rates of the different pitches overlap so much and the standard deviations are so large, this technique will not help identify the type of pitch.

Here are some comments on this dataset. It is good that the numbers for the 2-seam fastball and the sinker are so similar because they are basically the same pitch except for the arm angle at the release point. The size of this dataset is impressive: over a half-million pitches thrown by over 600 pitchers over a whole season. Possible uncontrolled factors that could be responsible for variability in the data include measurement error, physiological differences between pitchers, differences in the intent of the pitchers, and most importantly the wind speed and direction.

The data in Table 8.6 make sense. This is fortunate because presently all baseball authors are using this same data set. There is no independent confirmation of these numbers. The only confirmation that we have is that most of the numbers for 2015 (Table 7.2), 2016 (Table 7.1) and 2017 (Table 8.6) are similar. The exceptions are the two pitches with negative backspin rates. The spin rates for the slider and the curveball computed in 2017 for the 2016 season (Table 7.1) and in 2018 for the 2017 season (Table 8.6) were far apart. We think Statcast changed their algorithm and subsequently their 2016 data.

In summary, we are pleased with these data. Together they make sense, except for the changeup that still has a high average speed.

8.10 Summary

The most important properties in this simulation of the interconnected BaConLaws and Ball in Flight models are, in decreasing order of importance, CoR, Wind velocity, Air density, Initial spin of the batted ball, Launch speed and the Drag coefficient. These properties affect the range of the batted ball. The values stated on television broadcasts and internet sites for the range of home run balls probably have an estimated margin of error of around $\pm 10\%$.

References

Bahill, A. T., Baldwin, D. G., & Ramberg, J. S. (2009). Effects of altitude and atmospheric conditions on the flight of a baseball. *International Journal of Sports Science and Engineering*, *3*(2), 109–128. ISSN 1750-9823.

Baldwin, D. G., Bahill, A. T., & Nathan, A. (2007). Nickel and dime pitches. *Baseball Research Journal, 35*, 25–29.

Kagan, D., & Nathan, A. M. (2017). Statcast and the baseball trajectory calculator. *The Physics Teacher, 55*(3), 134–136.

McBeath, M. K., Nathan, A. M., Bahill, A. T., & Baldwin, D. G. (2008). Paradoxical pop-ups: Why are they difficult to catch? *American Journal of Physics, 76*(8), 723–729.

Naito, K., Hong, S., Koido, M., Nakayama, M., Sakamoto, K., Asai, T. (2018). Effect of seam characteristics on critical Reynolds number in footballs. *Japanese Mechanical Engineering Journal*, *5*. https://doi.org/10.1299/mej.17-00369.

Nathan, A. M. (2011). Baseball ProGUESTus: home runs and humidors: Is there a connection? Baseball Prospectus, February 25, 2011, http://www.baseballprospectus.com/article.php?articleid=13057/.

Nathan, A. M. (2017). *A Humidor at Chase Field: What's Up with That? The Hardball Times*, April 17, 2017, https://www.fangraphs.com/tht/a-humidor-at-chase-field-whats-up-with-that/.

Shelquist, R. (2018). Density Altitude Calculator, Shelquist Engineering, https://wahiduddin.net/calc/calc_da_rh.htm, accessed November 2018.

Watts, R. G., & Bahill, A. T. (1990). *Keep Your Eye on the Ball: the Science and Folklore of Baseball*. New York: W. H. Freeman, Table 1.

Watts, R. G., & Bahill, A. T. (2000). *Keep your eye on the ball: Curveballs, Knuckleballs and Fallacies of baseball*. New York: W. H. Freeman.

Willman, D. (2018). *BaseballSavant*, https://baseballsavant.mlb.com/statcast_search, last accessed November 2018.

Chapter 9
The Bat's Vertical Sweetness Gradient

9.1 Introduction

Purpose: The purposes of this chapter are to present a model for determining the batter's probability of success depending on the bat–ball collision offset and to show that the sweet spot of the bat is one-fifth of an inch high. The size of the sweet spot determines the required swing accuracy for batter success.

Warren Spahn summed up his pitching strategy with a pithy aphorism, "Hitting is timing. Pitching is upsetting timing." The great pitching coach Johnny Sain advised his pitchers to avoid showing batters consecutive pitches of the same speed.[1] Judging the speed of the pitch is the most difficult part of the batter's task and this must be done in the first third its flight (Adair 2002; Bahill and Baldwin 2004). Once the batter begins the swing, he cannot alter the timing or the trajectory of the swing. This chapter is based on the models created by Major League Baseball (MLB) pitcher Dave Baldwin (Baldwin and Bahill 2004).

The batter must determine pitch speed in order to estimate the ball's height at the bat–ball collision point. Misjudgment of the pitch speed results in a vertical error in the swing (e.g., underestimating pitch speed results in swinging under the ball). The vertical collision offset (see Fig. 9.1) between the velocity vector of the ball and the velocity vector of the bat is the major factor determining the launch parameters of the ball after a collision with the bat.

How is this collision offset related to the batter's probability of success? We next describe a Bat–Ball Oblique Collision model relating this collision offset and several other collision parameters to the behavior of the batted ball, which, in turn, is associated with the batter's probability of success. Batter *success* is defined as getting a base hit and *sweetness* is the probability of success for a given bat–ball collision.

[1]Yes, these are the pitchers immortalized in the phrase "Spahn and Sain and pray for rain."

A. T. Bahill, *The Science of Baseball*,
https://doi.org/10.1007/978-3-030-03032-2_9

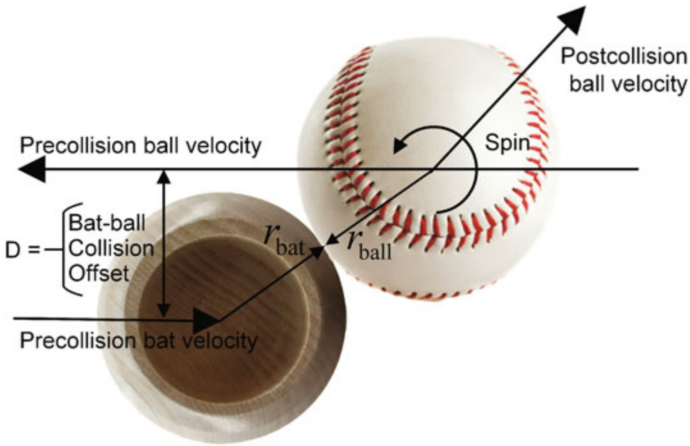

Fig. 9.1 The offset between the bat and ball velocity vectors during a collision

9.2 Performance Criteria

Problem statement We need a high-level criterion for batting success that shows the relative importance of bat weight, bat shape, the coefficient of friction, bat speed, the swing angle (usually an uppercut) and bat–ball collision offset at impact. These are all under the batter's control.

In most engineering studies, the most important design decision is choosing the performance criterion. What might be the best performance criterion for a batter hitting a baseball? In various previous models, we have used kinetic energy imparted to the ball, momentum imparted to the ball, batted-ball speed, accuracy and variability of the swing, launch speed, launch angle, batted-ball spin rate, batted-ball spin axis and the distance from the plate to where the ball hit the ground (the range). For the most previous science of baseball studies, the performance criterion has been maximizing batted-ball speed. Where in baseball would other performance criteria be more appropriate?

The efficiency of energy transfer might be another performance criterion. The batter wants to swing the bat so that as much energy as possible is transferred from the bat to the ball *in a particular direction*. Ball velocity perpendicular to this direction is not helpful (pop-ups and grounders). This performance criterion wants the batted-ball direction to be the same as the bat's direction before the collision, i.e., it wants a ten-degree uppercut and zero collision offset.

Knockdown power might be another performance criterion and kinetic energy would be an appropriate metric for it. The Colt .45 automatic pistol was designed for battles in the Philippines in the early years of the twentieth century, with the performance criterion of, "Knock down the charging Moro warrior before he can chop off your head with a machete." The existing .38 would kill the warrior, but he would chop off your head before he would die. A solution for this problem was the

Colt .45 caliber APC cartridge with a muzzle kinetic energy of 500 J (368 ft-lb$_m$). (The kinetic energy of bullets is given in units of foot-pounds, but the pounds are not pounds-force, rather they are pounds-mass. So, one ft-lb$_m$ = 1.36 J). In contrast, a baseball traveling at 97 mph (43 m/s) has 137 J (101 ft-lb$_m$) of kinetic energy. This explains why a hit-batter can be hurt, but not knocked down by a pitch. As an aside, the rotational kinetic energy stored in a baseball spinning at 2200 rpm is 2 J (1.5 ft-lb$_m$), which is much less than the translational energy.

Here are some potential performance criteria for an MLB *pitcher*: (1) maximize batter intimidation, (2) minimize the number of pitches per inning, by getting batters to hit early pitches for grounders; this would reduce batters' opportunities to learn the pitches and lessen pitcher fatigue, (3) minimize the number of runs and (4) generate impressive statistics (e.g., pitch speed, strikeouts, wins, ERA and saves) that would generate high salaries.

The old batter performance criterion of maximizing batted-ball speed worked well for home runs, but less than 5% of MLB base hits are home runs. Therefore, in this chapter, we develop a new performance criterion, the probability of getting a base hit.

9.3 Bat–Ball Oblique Collision Model

The simulations of this chapter use the four interconnected models shown in Fig. 9.2. We will first discuss the Bat–ball Oblique Collision model.

Interconnecting four models posed some difficulties. If any part of the interconnection were implemented manually, then the precision of the data was important. To avoid noise confounding, we had to use two or three digits after the decimal point.

Baseball and softball batters swing a narrow cylinder with the axis more or less parallel with the ground. Thus, the curvature of the bat's face (the hitting surface) is a

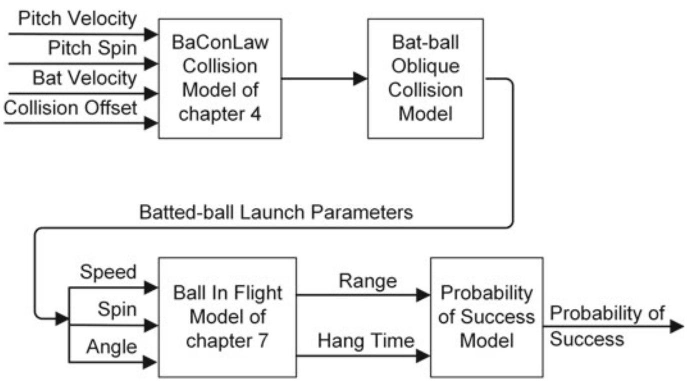

Fig. 9.2 The bat–ball collision model comprising four interconnected submodels

vertical arc. This vertical arc, in combination with the vertical collision offset of the bat and ball trajectories, determines the ball's launch speed, launch angle and spin. These launch variables are included in a vector describing a specific point on the bat's face; a vector field specifies the launch characteristics of all the points on the face. Each vector determines the batted-ball behavior: the distance it travels in the air, until it first strikes the ground (*range*) , how long it stays in the air (*hang time*), and for ground balls, the time taken for the ball to reach the infielders *(ground time*).

The set of success probabilities associated with a specific vertical arc on the bat's face is called the *vertical sweetness gradient* of that arc. The face's vector field represents sweetness gradients in both the longitudinal (horizontal) and transverse (vertical) dimensions of the bat. Section 3.2 dealt with the horizontal aspects of the sweet spot, therefore in this chapter, we restrict our discussion to vertical aspects of collisions and the placement of the ball in play in fair territory.

The basic principle of the Bat–Ball Oblique Collision model is to decompose the bat and ball velocities into components normal to the collision plane and components tangential to the collision plane (see Fig. 9.3). And then, apply conservation of energy and conservation of linear and angular momentum in each direction.

Figures 9.1, 9.3 and 9.4 illustrate the vertical configuration of a bat and ball collision. The inputs for the Bat–Ball Oblique Collision model are illustrated in Fig. 9.4 and are described here.

1. Initial velocity vector of the bat $(\mathbf{v}_{\text{bat-before}})$.
2. Initial normal component of the bat's velocity vector $(\mathbf{v}_{\text{bat-before-normal}})$.
3. Initial tangential component of the bat's velocity vector $(\mathbf{v}_{\text{bat-before-tangent}})$.
4. Initial velocity vector of the ball $(\mathbf{v}_{\text{ball-before}})$. $\mathbf{v}_{\text{ball-before}}$ is the velocity of the ball immediately before the bat–ball collision. This is about 10% smaller than the pitch speed measured at the pitcher's release point 5.5 feet in front of the rubber.

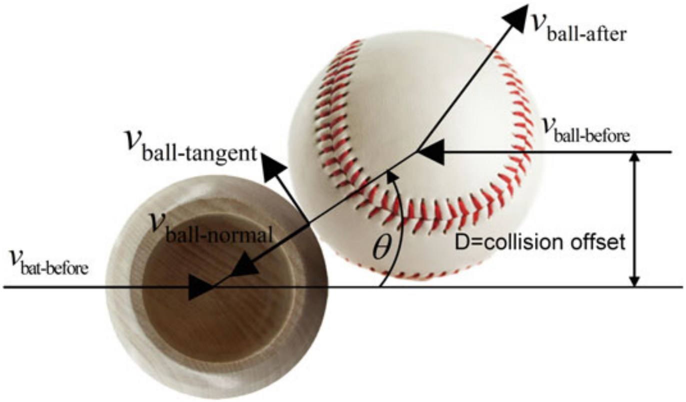

Fig. 9.3 The bat's velocity and the ball's velocity are decomposed into components normal to the collision plane and components tangent to it

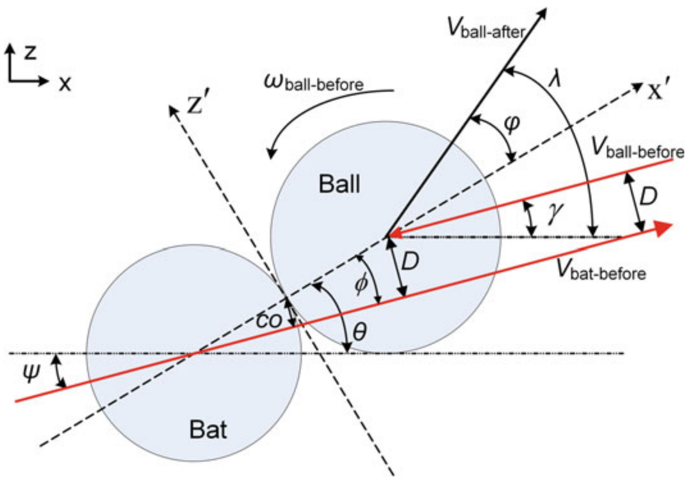

Fig. 9.4 Illustration of angles and directions. To allow room for labels, this drawing is not to scale: for example, the real-world angle ψ is about ten degrees but, in this illustration, it is about 15°

5. Initial normal component of the ball's velocity vector ($\mathbf{v}_{\text{ball-before-normal}}$).
6. Initial tangential component of the ball's velocity vector ($\mathbf{v}_{\text{ball-before-tangent}}$).
7. Collision offset distance (D) from $\mathbf{v}_{\text{bat-before}}$ to $\mathbf{v}_{\text{ball-before}}$ (see Figs. 9.1 and 9.3).
8. Vertical angle (θ) between the line connecting the bat and ball centers (line of centers) and the horizontal plane.
9. Vertical angle (γ) between $\mathbf{v}_{\text{ball-before}}$ and the horizontal plane.
10. Vertical angle (ψ) between $\mathbf{v}_{\text{bat-before}}$ and the horizontal plane.
11. Mass of bat (m_{bat}).
12. Mass of ball (m_{ball}).
13. Radius of bat at collision point (r_{bat}).
14. Radius of ball (r_{ball}).
15. Coefficient of Restitution (CoR) of the bat–ball collision.
16. Coefficient of friction (μ) of the bat–ball collision.
17. Angular velocity of the pitch ($\boldsymbol{\omega}_{\text{ball-before}}$).

The parameters m_{ball}, r_{ball}, CoR and μ are constants. The values of CoR and μ were derived empirically. Nominal values for these variables and parameters were given in Tables 1.1 and 8.4.

The outputs of the Bat–Ball Oblique Collision model are:

1. Resultant velocity vector of the bat ($\mathbf{v}_{\text{bat-after}}$).
2. Resultant normal component of the bat's velocity vector ($\mathbf{v}_{\text{bat-after-normal}}$).

3. Resultant tangential component of the bat's velocity vector $(\mathbf{v}_{\text{bat-after-tangent}})$.
4. Resultant velocity vector of ball $(\mathbf{v}_{\text{ball-after}})$. This is called the *launch velocity*.
5. Resultant normal component of the ball's velocity vector $(\mathbf{v}_{\text{ball-after-normal}})$.
6. Resultant tangential component of the ball's velocity vector $(\mathbf{v}_{\text{ball-after-tangent}})$.
7. Vertical angle (φ) between the line of centers and $\mathbf{v}_{\text{ball-after}}$
8. Vertical angle (λ) between the horizontal plane ($z = 0$) and $\mathbf{v}_{\text{ball-after}}$. This is called the *launch angle*. In this chapter we use λ not θ as we did in previous chapters.
9. Angular velocity of the batted ball $(\boldsymbol{\omega}_{\text{ball-after}})$, whose magnitude is called the *spin rate*.

The model is set in the x-z plane of a coordinate system with its origin at the collision point, three feet in front of the tip of home plate at a height of three feet. The positive z-axis points upward, the positive x-axis points toward the pitcher and the positive y-axis points from first base to third base. In Fig. 9.4, the x-z plane is rotated so the x′-axis lies along the bat–ball line of centers and the z′-axis is tangential to the bat–ball collision plane. Angular velocity is positive for pitch topspin and for batted-ball backspin. *D* is positive if the bat undercuts the ball. The angle of descent (γ) of an average pitch is about ten degrees even for a submarine pitcher like Dave Baldwin or a National Collegiate Athletic Association (NCAA) softball pitcher. Batters intentionally uppercut the bat by the same amount (ψ). Which means the bat and ball are traveling in opposite directions at the time of contact. This helps control the collision offset distance. This Bat–Ball Oblique Collision model is based on Goldsmith (1960) and is implemented in spreadsheets developed by Alan Nathan.

The bat swing angle is important. We assume that the angle of descent (γ) of an average pitch when it crossed the front edge of home plate is about ten degrees downwards and that batters intentionally swing the bat upward by the same amount (ψ).

$$\gamma = \psi = 10^\circ$$

Which means the bat and ball will be traveling in opposite directions at the time of the collision. Figure 9.5 shows the difference between swinging level and upper cutting the ball. On the left side of this figure, the ball is coming down at a ten-degree angle (red path) and the bat is being swung level (blue path). The good hitting area (green) is the intersection of the bat path and the ball path. On the right side of Fig. 9.5, the ball is also coming down at a ten-degree angle, however, the bat is being swung upward at a ten-degree angle. This time, the good hitting area (green) is larger.

We assumed that the pitch was coming down at a ten-degree angle when it crossed the plate. Then we assumed that the batter would swing the bat in the exact opposite direction. However, all pitches do not have a ten-degree angle of descent.

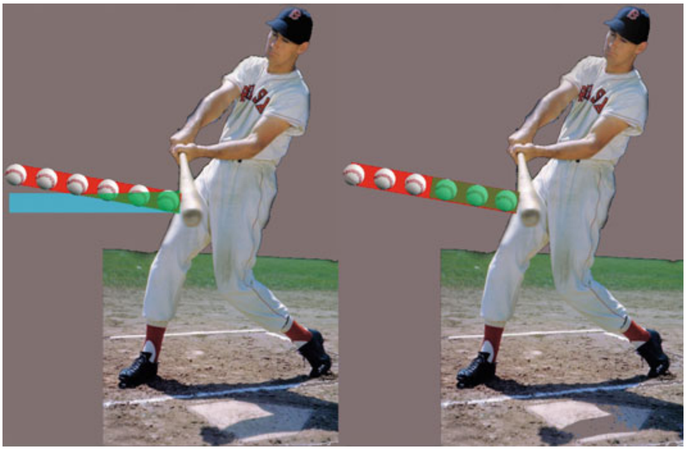

Fig. 9.5 In the left side of this figure, the ball is coming down at a ten-degree angle and the bat is being swung level. The good hitting area (green) is the intersection of the bat path (blue) and the ball path (red). On the right side, the ball is also coming down at a ten-degree angle, however, the bat is being swung upward

The extremes are a rise ball in NCAA softball and a curveball in MLB. At one extreme, the rise ball can cross the plate horizontally, at an angle of zero degrees. At the other extreme, a 75 mph MLB curveball has an angle of descent of 10° or 11°. Somewhere in the middle, a 90 mph MLB fastball has an angle of descent of 5° or 6°. It is not known if batters can adjust their bat swing angles between pitches. They probably do not, because they want machine-like consistent swings.

At this point, it is appropriate to caution young players that we are not recommending that they ignore their coaches' advice to "Swing level." Coaches and parents have difficulty differentiating between level horizontal swings and those with a ten-degree upward angle. The coach's admonition means do not swing with a 30° or 40° upward angle. In this context, "Swing level," means swing with about a ten-degree upward angle.

This Bat–Ball Oblique Collision model is a consistent elaboration (Wymore Wymore 1993) of the BaConLaws model of Chap. 4. It is more complicated than the BaConLaws model because it allows *oblique* collisions of the bat and ball. This is configuration 3 of Fig. 2.5.

9.4 Launch Velocity, Launch Angle and Spin Rate

The ball's launch variables are calculated by decomposing the initial velocities of the bat and ball into their normal and tangential components at the collision point as suggested in Fig. 9.3. These velocities are used with the principles of conservation of momentum and conservation of energy to yield the resultant normal and tangential velocities for the ball, which are then used to calculate the launch velocity of the ball and the angles φ and λ. The batted-ball spin rate is calculated from the normal and tangential linear velocities of the bat and ball and the ball's initial angular velocity.

The collision of two elastic bodies with friction has been described by numerous authors (e.g., Goldsmith 1960; Brach 2007). The first step in building the model is to calculate θ and from this, the normal and tangential components of the pre collision velocity vectors. The vertical angle of the line of centers is $\phi = Arc\sin\frac{D}{r_{\text{bat}} + r_{\text{ball}}}$. The initial velocity components of the ball are $\mathbf{v}_{\text{ball-before-normal}} = \mathbf{v}_{\text{ball-before}}\cos\theta$ and $\mathbf{v}_{\text{ball-before-tangent}} = \mathbf{v}_{\text{ball-before}}\sin\theta$. The initial velocity components of the bat are $\mathbf{v}_{\text{bat-before-normal}} = \mathbf{v}_{\text{bat-before}}\cos\theta$ and $\mathbf{v}_{\text{bat-before-tangent}} = \mathbf{v}_{\text{bat-before}}\sin\theta$. The resultant normal velocity of the ball is

$$\mathbf{v}_{\text{ball-after-normal}} = \mathbf{v}_{\text{ball-before-normal}} - \frac{(\mathbf{v}_{\text{ball-before}} - \mathbf{v}_{\text{bat-cm-before}})(1 + CoR_{2\text{b}})m_{\text{bat}}}{m_{\text{ball}} + m_{\text{bat}}}$$

Calculation of the resultant tangential velocity of the ball, resultant angular velocity of the ball and the launch angle, λ, was described by Watts and Baroni (1989) and Sawicki et al. (2003). In these models, friction acted in the direction opposite to the slip of the ball, as we discussed in Sect. 5.4, Collisions with Friction. If friction was large enough, it halted the relative tangential velocity (the combined velocities of bat and ball surfaces relative to the collision point). When this occurred, slippage ceased, the ball stuck to the bat and the ball began to roll, contributing to the launch angular velocity. These models accounted for bat recoil and assumed conservation of linear and angular momentum for tangential bat and ball motions. Both models ignored deformation of the ball during collisions. They assumed that it remained a perfect sphere, however, see Fig. 5.7.

Table 9.1 shows the magnitude of the launch velocity, launch angle and the initial backspin rate as functions of the bat–ball collision offset for a ball traveling at 83-mph with 2000 rpm of backspin colliding at the sweet spot of the bat that is traveling at 62 mph.

9.5 Range, Hang Time and Ground Time

The launch speed, launch angle and spin rate were inputs for the Ball in Flight model of Chap. 7. It was used to calculate the batted ball's range and hang time. The rotation of the ball creates a Magnus force that acts perpendicular to the ball's trajectory. This force tends to lift the ball (if backspin) or depress the ball (if topspin). It is calculated as $F_{\text{Magnus}} = 0.5\pi\rho r_{\text{ball}}^3 \omega_{\text{ball}} v_{\text{ball}} C_{\text{M}}$, where ρ is the air density. Friction and turbulence of the air creates a drag force acting directly opposite to the ball's trajectory. This force is calculated as $F_{\text{drag}} = 0.5\pi\rho r_{\text{ball}}^2 v_{\text{ball}}^2 C_{\text{D}}$. Table 9.2 shows the ranges and hang times that result from various collision offsets.

Table 9.1 Launch speed (from the BaConLaws model) and launch angle and backspin (from the Bat–Ball Oblique Collision model)

Collision offset, D (in)	Launch speed (mph)	Launch angle (deg)	Backspin rate (rpm)
0.75	92	32	2132
0.70	92	30	1940
0.65	92	28	1748
0.60	92	27	1557
0.55	92	25	1365
0.50	92	23	1173
0.45	92	22	981
0.40	92	20	790
0.35	92	18	598
0.30	92	17	406
0.25	92	15	215
0.20	92	14	23
0.15	92	12	−169
0.10	92	10	−360
0.05	92	9	−552
0	92	7	−744
−0.05	92	6	−936

Ground time is also included in the Bat–Ball Oblique Collision model, but we will not discuss its details in this chapter. It was modeled using the ball's launch speed, launch angle and spin to find the angle of incidence on the first bounce. The incident horizontal and vertical velocity components and launch spin rate were then used to generate the bounce velocity, angle and spin rate. The Ball in Flight model was used to find the flight characteristics between bounces, including the incident angle on the subsequent bounce. Note that, for these collisions, the CoR and μ have values different from those for the bat–ball collision. Each bounce reduces the horizontal velocity and the spin rate. If μ is large enough to overcome, the combined angular and horizontal velocities, slippage stops and rolling begins

9.6 Probability of Success Model

The characteristics of a batted ball can be associated with the probability of batter success based on the potential of defensive players to prevent a base hit. The model contains four components that deal with four types of batted-ball behavior:

(1) The outfield component handles fly balls (range >130 ft (40 m) and hang time >1.0 s).
(2) The pop-up component handles pop-ups (range $\leq$ 130 ft (40 m) and hang time >1.0 s).

Table 9.2 Range and hang time outputs from the Ball in Flight model

Collision offset, D (in)	Launch speed (mph)	Launch angle (deg)	Backspin rate (rpm)	Range (feet)	Hang time (sec)
0.75	92	32	2132	381	5.3
0.70	92	30	1940	377	5.0
0.65	92	28	1748	370	4.7
0.60	92	27	1557	361	4.4
0.55	92	25	1365	349	4.1
0.50	92	23	1173	329	3.6
0.45	92	22	981	318	3.4
0.40	92	20	790	300	3.1
0.35	92	18	598	280	2.8
0.30	92	17	406	259	2.5
0.25	92	15	215	237	2.2
0.20	92	14	23	214	2.0
0.15	92	12	−169	192	1.7
0.10	92	10	−360	169	1.5
0.05	92	9	−552	147	1.2
0	92	7	−744	125	1.0
−0.05	92	6	−936	105	0.8

(3) The line drive component handles line drives (range ≥ 115 ft (35 m) and hang time ≤ 1.0 s).
(4) The infield component handles ground balls (range <115 ft (35 m) and hang time ≤ 1.0 s).

A more extensive, but simpler, repertoire of possible batting outcomes is shown in Fig. 9.6.

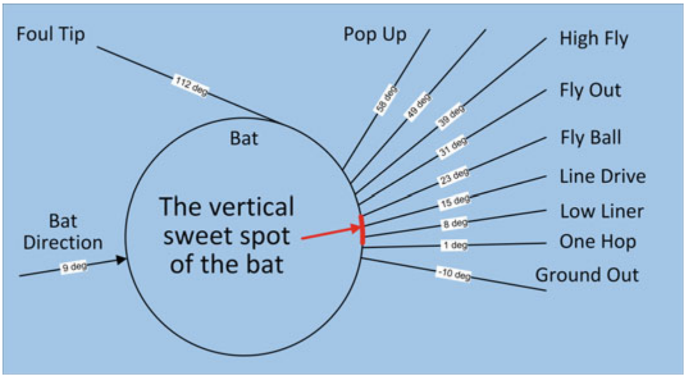

Fig. 9.6 The batting outcome depends on the vertical point of the bat–ball collision

Fig. 9.7 The sweet spot of the bat (red area)

An aside. You can change potential pop-ups (sure outs) into harmless foul tips. Before the game, smooth the pop-up to foul-tip area of the bat (Fig. 9.7) with fine steel wool. Be careful to not take off the paint or varnish. Before each plate appearance, lightly rub the pop-up to foul-tip area with sweat or saliva. Oil would not evaporate as quickly as sweat or saliva: but oil is not as slick and it would be easier for the umpire to detect oil. Now, a ball hitting this area will slide off for a foul tip rather than be a pop-up.

Our model uses several simplifying assumptions, such as either an infielder or outfielder might catch a fly ball depending on its range and hang time. All pop-ups are caught by an infielder, a pitcher or a catcher so the probability of success is zero. Only infielders catch line drives and grounders. Batters do not "beat-out" grounders caught by infielders. Furthermore, any batted ball that hits the ground two or more times before the infielders is an out. As an aside, we note that Statcast data show that of the 47,000 ground balls hit by major league batters in 2017, only 1.3% of them were fielded cleanly but "beat-out" for base hits (this does not include grounders that snuck through the infield untouched).

Each batted ball is associated with defensive coverage formulated as a function of time. A defensive player prevents a base hit if he or she can reach the ball during the hang time or ground time. To determine coverage, we positioned MLB outfielders on the *outfield arc* with a radius of 300 feet. See Fig. 9.8. The outfield arc is divided into thirds, with a player positioned at the center of each arc segment. For example, the outfield arc has a length of 471 feet ($300 \times \pi/2$) so it is divided into three segments each of which is 157 feet long. The right fielder, then, is positioned 300 feet from home plate, 78.5 feet from the right field foul line and 157 feet from the center fielder. The batted-ball's range yields a *range arc* with length equal to $\pi/2$ times the range.

On fly balls, each player's initial position is the center of an ellipse representing defensive coverage by the player (a fly ball is illustrated in Fig. 9.8). Hang time determines the likelihood that an ellipse will encompass the ball's end point. Probability of a base hit is the proportion of the range arc that is not overlapped by outfielder ellipses.

In Fig. 9.8, the outfielders are positioned on the outfield arc. The dashed line shows the range arc for a fly ball that is in the air for three seconds and travels 250 feet. Three-fourth of this range arc is overlapped by the three-second fielder ellipses. Therefore, the probability of success is 0.25.

For the infield component of the Probability of Success model, infielders were positioned on an *infield arc* with a radius of 115 feet. The infield arc was divided

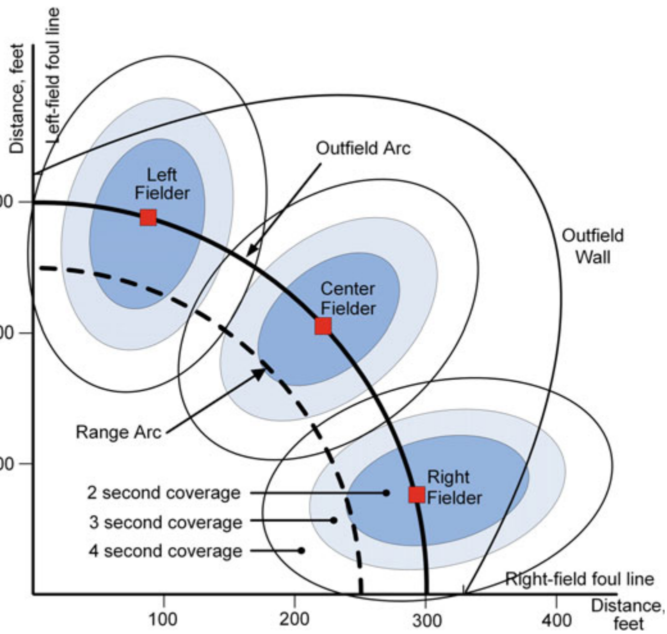

Fig. 9.8 Outfield component of the Probability of Success model containing the range arc, outfield arc and defensive coverage of the outfielders. The range arc is for a ball that hits the grass 250 feet from home plate

into quarters with a player positioned at the center of each arc segment. If a line drive or grounder passed the infield arc without encountering an infielder, it was a base hit. Therefore, only the infielders' lateral movements provided coverage. Success was the proportion of the range arc not covered by infielders. In addition, any line drive that crossed the infield arc more than eight feet off the ground was a base hit. The minus 0.05 collision offset one-hopper of Table 9.2 and the 0 and +0.05 collision offset line drives were evaluated with the infield component of the model.

The Probability of Success model assumes that the speed of outfielders and infielders is 23 ft/sec. Fielder reaction time loses are 8 ft (0.35 s) forward, 12 ft (0.52 s) sideways and 15 ft (0.65 s) backwards. These values were selected as reasonable numbers and are not based on empirical data. However, such data might now be available from Statcast in examples like this: https://www.mlb.com/video/statcast-looks-at-play-at-home/c-31459495.

These are the steps in executing the Probability of Success model: (1) determine the ball's range from Table 9.2, (2) draw the range arc, (3) determine ball's hang time from Table 9.2, (4) draw fielder coverage ellipses and finally, (5) compute the probability of success with this formula.

$$\text{Probability of success} = 1 - \frac{\text{Portion of range arc covered by ellipses}}{\text{Range arc}}$$

This is done for both infielders and outfielders, although only the outfielders coverage is shown in Fig. 9.8.

9.7 Outputs of the Probability of Success Model

We ran our models at collision offset increments of 0.05 inches. Results are given in Table 9.3. Pitch speed was 92 mph yielding a ball speed of 83 mph at the bat–ball collision point: pitch backspin was 2000 rpm. Contact occurred at the bat's point of maximum horizontal sweetness and the speed of the bat's collision point was 62 mph (Bahill and Karnavas 1989). The coefficient of friction, μ, was measured to be 0.5. The angles γ and ψ of bat and ball were both ten degrees. The radius of the bat, $r_{\text{bat}} = 1.3$ in; the radius of the ball, $r_{\text{ball}} = 1.452$ in; the weight of the bat, $wt_{\text{bat}} = 32$ oz; and the weight of the ball $wt_{\text{ball}} = 5.125$ oz. Ranges and hang times were found using the Ball in Flight model.

For collision offsets greater than 0.25 inches, as hang time increased, the probability of success decreased. Collision offsets greater than 1.5 inches produced pop-ups that were assigned a success probability of zero. The model assumed no outfield walls. In most major league stadiums, batted-balls hit farther than 325 feet have a chance of clearing a wall, because the average distances are 325 feet down the foul lines and 400 feet in center field. Thus, the model underestimates success for any batted ball with a chance to be a home run.

In Table 9.3, the 0.10–0.75 collision offset rows were evaluated with the outfield component of the Probability of Success model. The minus 0.05, 0.0 and plus 0.05 collision offset rows were evaluated with the infield component. Column 2, launch velocity, came from the BaConLaws model. Columns 3 and 4, launch angle and launch backspin, came from the Bat–Ball Oblique Collision model. Columns 5, 6 and 7, the range, hang time and height at the infield arc came from the Ball in Flight model. Finally, column 8, the probability of success came from the Probability of Success model.

As an aside, batters wanting to hit home runs would want launch angles around 27°–32°. Whereas, batters wanting to hit singles would want launch angles around 10°–15°.

Figure 9.8 shows the probability of success as a function of the collision offset. In it, we subjectively defined the prime collision offset range to be between −0.05 and 0.35 inches. Batted balls in this range have probabilities of success greater than 0.300, which we are sure would please any MLB batter. However, this prime *collision* offset range is not what we ultimately want. We want to transform this into the best *contact* offset range (the abbreviation co in Fig. 9.4), because this determines the vertical size of the sweet spot of the bat.

Table 9.3 Nominal inputs and outputs for the Probability of success model

Collision Offset, D (in)	Launch Speed (mph)	Launch Angle (deg)	Backspin Rate (rpm)	Range (feet)	Hang time (sec)	Height at the infield arc (ft)	Probability of Success
0.75	92	32	2132	381	5.3		0.000
0.70	92	30	1940	377	5.0		0.007
0.65	92	28	1748	370	4.7		0.051
0.60	92	27	1557	361	4.4		0.072
0.55	92	25	1365	349	4.1		0.078
0.50	92	23	1173	329	3.6		0.087
0.45	92	22	981	318	3.4		0.093
0.40	92	20	790	300	3.1		0.138
0.35	92	18	598	280	2.8		0.250
0.30	92	17	406	259	2.5		0.525
0.25	92	15	215	237	2.2		1.000
0.20	92	14	23	214	2.0		1.000
0.15	92	12	−169	192	1.7	13	1.000
0.10	92	10	−360	169	1.5	9.2	1.000
0.05	92	9	−552	147	1.2	5.5	0.483
0	92	7	−744	125	1.0	1.8	0.490
−0.05	92	6	−936	105	0.8	–	0.320

9.8 Height of the Sweet Spot

The vertical size (height) of the sweet spot of the bat is important because it determines the required accuracy of the swing that the batter must attain in order to get a base hit.

We will now describe our first technique for determining the vertical size of the sweet spot of the bat: it uses the Probably of Success model. First, we use Fig. 9.4 to find the distance between the bat–ball point of contact and the center axis of the bat. This is called the *contact offset* (*co*). The angle between the line of centers (connecting the centers of the bat and ball) and the vector $\mathbf{v}_{\text{bat-before}}$ is $\phi = Arc\sin\frac{D}{r_{\text{bat}} + r_{\text{ball}}}$. Therefore, the contact offset $co = r_{\text{bat}}\sin\phi = \frac{Dr_{\text{bat}}}{r_{\text{bat}} + r_{\text{ball}}}$. This contact offset distance is inserted as an additional column in Table 9.4.

According to the data in Table 9.4 and Fig. 9.9, balls hit with collision offsets between ±0.05 might be caught by infielders, hence the probability of success varies from around 0.3 up to 1.0 and are handled with the infield component of the Probably of Success model. Balls hit with collision offsets between 0.1 and 0.25 are sure hits because they go over the infielders and hit the grass in front of the outfielders. Balls hit with collision offsets between 0.25 and 0.75 might be caught by an outfielder. So, they are handled with the outfield component of the Probably

Table 9.4 Nominal data with the addition of the contact offset column

Collision Offset, D (in)	Contact offset (in)	Launch Speed(mph)	Launch Angle (deg)	Backspin Rate (rpm)	Range (feet)	Hang time (sec)	Height at the infield arc (ft)	Probability of Success
0.75	0.355	92	32	2132	381	5.3		0.000
0.70	0.332	92	30	1940	377	5.0		0.007
0.65	0.308	92	28	1748	370	4.7		0.051
0.60	0.284	92	27	1557	361	4.4		0.072
0.55	0.261	92	25	1365	349	4.1		0.078
0.50	0.237	92	23	1173	329	3.6		0.087
0.45	0.213	92	22	981	318	3.4		0.093
0.40	0.189	92	20	790	300	3.1		0.138
0.35	0.166	92	18	598	280	2.8		0.250
0.3365	0.159	92	18	546	274	2.7		0.300
0.30	0.142	92	17	406	259	2.5		0.525
0.25	0.118	92	15	215	237	2.2		1.000
0.20	0.095	92	14	23	214	2.0		1.000
0.15	0.071	92	12	-169	192	1.7	13	1.000
0.10	0.047	92	10	-360	169	1.5	9.2	1.000
0.05	0.024	92	9	-552	147	1.2	5.5	0.483
0	0.000	92	7	-744	125	1.0	1.8	0.490
-0.05	-0.024	92	6	-936	105	0.8	-	0.320

Height of sweet spot = 0.159 + 0.024 = 0.183

of Success model. Balls hit with collision offsets between 0.4 and 0.75 have low probabilities of success.

In Fig. 9.9, we defined the prime collision offset range to be collision offset values that gave a probability of success of exactly 0.3. But there is no such value in Table 9.3. So, to find such a value, we tried linear interpolation, but that did not work because the data are nonlinear. Therefore, we ran additional simulations until we found that exact value. It is the extra row in Table 9.4 for a collision offset of 0.3365 inches. Now, we need to relate these *collision offsets* to *contact offsets*. The corresponding contact offsets from Table 9.4 are −0.024 and 0.159 (highlighted in blue). The height of the sweet spot of the bat is the difference between these numbers. Therefore, the sweet spot of the bat is 0.183 inches high (4.6 mm), about one-fifth of an inch. Perhaps, this 0.183 number should be about 0.01 larger, because a few collision offsets between −0.05 and −0.06 might be base hits. Statements like this one are made to help assess the accuracy of our sweet spot size estimates.

The contact offsets in Table 9.4 are functions only of r_{bat}, r_{ball} and D. However, the shape of the data in Fig. 9.9 depend on the batter's probability of success, which depends on the range and the hang time, and therefore on a multitude of other parameters. Specifically, the batter's probability of success depends on the dimensions of the ball field, the speed and reaction times of the fielders, the placement of the fielders, the size and mass of the bat and ball, the velocities of the

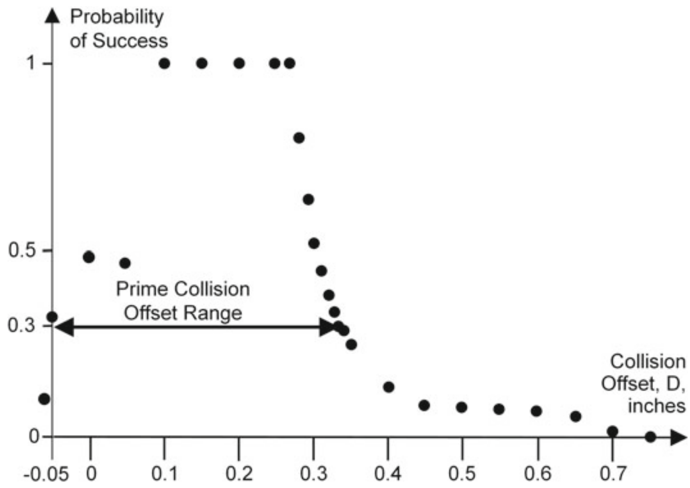

Fig. 9.9 Probability of success as a function of the collision offset, derived primarily from the data in Table 9.3

bat and ball and the spin of the ball, although Nathan et al. (2012) stated that the pitch spin has no effect.

We put our simulation results into Tables like 9.4 and 9.5 for most of the parameters of our model. We found that, for normal variations in MLB, the most important parameter was the speed of the bat. The second most important parameter was the diameter of the bat: results for the bat diameter are given in Table 9.5. As the least significant effect, the contact offset is a cord of the arc on the bat's surface. If instead of the cord, we wanted the distance along the surface of the bat we would increase the distance by an insignificant 0.06%. Considering all of these approximations, uncertainties and variabilities, we conclude that the sweet spot of an MLB bat is one-fifth of an inch high (5 mm) (Fig. 9.10).

Table 9.6 summarizes the results of many simulations. In order to compare the effects of changing important properties of the model, we used the relative sensitivity function (Smith et al. 2008), which is defined as

$$\text{relative sensitivity} = \frac{\text{percent change in } F}{\text{percent change in } \alpha} = \frac{\Delta F}{F}\frac{\alpha}{\Delta\alpha}$$

where F is the function being evaluated, the vertical size of the sweet spot and α is the parameter being changed, for example, the bat diameter.

This sensitivity analysis summarized in Table 9.6 shows that, for normal variation of parameters, the speed of the bat is the most important variable in the model. If the bat speed is increased, then the height of the sweet spot decreases. If the bat speed is decreased, then the height of the sweet spot increases. The reason for this is that a higher bat speed gives a higher launch velocity and a longer range. Meaning

Table 9.5 Data for determining the vertical size of the sweet spot of the bat with the bat diameter reduced from 2.61 to 2.5 inches

Collision Offset, D (in)	Contact offset (in)	Launch Speed (mph)	Launch Angle (deg)	Backspin Rate (rpm)	Range (feet)	Hang time (sec)	Ball height at the infield arc (ft)	Probability of Success
0.75	0.347	92	32	2190	382	5.4		0.00
0.70	0.324	92	30	1995	379	5.1		0.00
0.65	0.301	92	29	1799	372	4.8		0.04
0.6	0.278	92	27	1603	363	4.5		0.07
0.55	0.255	92	25	1408	352	4.1		0.08
0.5	0.231	92	24	1212	338	3.8		0.08
0.45	0.208	92	22	1017	321	3.5		0.09
0.4	0.185	92	20	821	303	3.1		0.13
0.35	0.162	92	19	625	283	2.8		0.23
0.33	0.149	92	18	547	274	2.7		0.30
0.3	0.139	92	17	430	261	2.5		0.48
0.25	0.116	92	15	234	239	2.2		1.00
0.2	0.093	92	14	39	217	2.0		1.00
0.15	0.069	92	12	-157	193	1.7	13	1.00
0.1	0.046	92	10	-353	170	1.5	9.3	1.00
0.05	0.023	92	9	-548	148	1.2	5.6	0.48
0	0.000	92	7	-744	125	1.0	1.7	0.49
-0.05	-0.023	92	5	-939	104	0.8	-	0.32

Height of sweet spot = 0.149 + 0.023 = 0.172

Fig. 9.10 The red area is the sweet spot of the baseball bat. It is one-fifth of an inch high. The center of mass is indicated with cm and the center of percussion is indicated with cop

it will be easier for the ball to get into the outfielder ellipses of Fig. 9.8. To be successful, the batter, therefore, must compensate by reducing the launch angle. In summary, increasing bat speed decreases the vertical size of the sweet spot.

This system is nonlinear. In a linear system, the relative sensitivities would have the same value for bat speed changes of 1, −3 and 5 mph.

This sensitivity analysis shows that the diameter of the bat is the second most important parameter in the model. Changing from an ash bat to a maple wood bat would probably reduce the diameter from 2.61 inches (66 mm) to 2.5 inches (64 mm). (Manufacturing does this to keep the weight down: maple wood is denser than ash.) This would reduce the height of the sweet spot from 0.183 to 0.172 inches. This reduction has a large relative sensitivity coefficient. Therefore, not surprisingly, reducing the diameter of the bat reduces the vertical size of the sweet spot.

Table 9.6 Summary of sweet-spot-height variability with the Probability of Success model, arranged in order of decreasing importance (sensitivity)

Conditions	Vertical size (height) of the sweet spot, inches	Relative sensitivity (importance)
Nominal values	0.183	
Bat speed decreased by 3 mph from 62 to 59 mph	0.196	$\frac{13}{183} \times \frac{62.1}{-3} = -1.47$
Bat diameter decreased from 2.61 to 2.5 inches	0.172	$\frac{-11}{183} \times \frac{2.61}{-0.11} = +1.43$
Bat swing angle decreased from 10° to 9°	0.205	$\frac{22}{183} \times \frac{10}{-1} = -1.20$
CoR decreased by 3.6% from 0.465 to 0.448, Table 8.4	0.191	$\frac{8}{183} \times \frac{0.465}{-0.017} = -1.20$
Bat swing angle increased from 10° to 11°	0.162	$\frac{-21}{183} \times \frac{10}{1} = -1.15$
Bat speed increased by 1 mph from 62 to 63 mph	0.180	$\frac{-3}{183} \times \frac{62.1}{1} = -1.02$
CoR increased by 6.9% from 0.465 to 0.497, Table 8.4	0.171	$\frac{-12}{183} \times \frac{0.465}{0.032} = -0.95$
Bat speed increased by 5 mph from 62 to 67 mph	0.170	$\frac{-13}{183} \times \frac{62.1}{5} = -0.88$
Ball's collision speed increased from 83 to 90 mph	0.173	$\frac{-10}{183} \times \frac{83}{7} = -0.65$
Bat weight decreased from 32 to 31 oz	0.186	$\frac{3}{183} \times \frac{32}{-1} = -0.52$

We will now investigate a second, easier but less accurate, model for determining the vertical size of the sweet spot of the bat. From the ball's trajectory, derived with the Ball in Flight model, we compute where the ball will first hit the ground. We assume that an MLB batter wants the ball to go over the infielders and hit the grass in front of the outfielders. Therefore, we suppose that an MLB batter wants the ball to hit the ground between 140 and 270 feet (43–82 m) from home plate. This is the basis of the Desired Range model. From interpolation in Table 9.4, the contact offsets corresponding to 140 and 270 feet are 0.016 and 0.154 inches. Therefore, the estimated vertical size of the sweet spot of the bat, which is the difference between these two numbers, is 0.138 inches (3.5 mm). This is about one-seventh of an inch. This number is smaller than the one-fifth of an inch derived with our Probably of Success model, because this Desired Range model does not utilize the gaps between the fielders and it ignores line drive and ground ball base hits.

An NCAA (college) softball player wants to hit a line drive/fly ball. She also wants the ball to go over the infielders and hit the grass in front of the outfielders. Thus, an NCAA softball batter wants the ball to hit the ground between 115 and 180 ft (35–55 m) from home plate. For NCAA softball, we assumed

$r_{\text{bat}} = 1.31,\ wt_{\text{bat}} = 26,\ r_{\text{ball}} = 1.92,\ wt_{\text{ball}} = 6.75,$
$v_{\text{ball-before}} = 65,$ pitch spin rate $= -1300,\ CoR = 0.47,$
bat speed $= 55$ and ball angle $(\gamma) =$ bat angle $(\psi) = 10.$

Desired range model for NCAA softball		
Desired range of the batted ball	Resulting contact offsets	Vertical size (height) of the sweet spot
115–180 feet	0.121 and 0.320	0.199 inches (5.1 mm, one-fifth of an inch

With these parameters, the vertical size of the sweet spot of the softball bat is 0.199, one-fifth of an inch (5.1 mm). Even though the softball is bigger than the baseball, the height of the sweet spot is about the same, because the dimensions of the ball field are different and therefore, the desired range for the softball (115–180 feet) is smaller than the MLB desired range of 140–270 feet. This conclusion does not apply to left-handed slap-hitters in NCAA softball.

9.9 Discussion

In general, if changing a parameter increases the launch speed of the batted ball (like increasing the bat speed or the CoR) and everything else is held constant, then the ball's range will be bigger and the height of the sweet spot will be smaller. For example, assume a ball is launched at 92 mph, at an 18-degree angle with 780 rpm of backspin. It will travel 250 feet with a hang time of 2.8 seconds. According to Fig. 9.8, this is on the borderline of being caught by an outfielder (probability of success = 0.502). Now let us launch a ball slightly faster at 94 mph, with the same launch angle and backspin. It will travel 257 feet with a hang time of 2.9 seconds and it most probably will be caught by an outfielder (probability of success = 0.355). What does this mean in terms of the sweet spot? It means that if the batter increases the launch velocity, then he or she must also reduce the contact offset (and therefore the launch angle) in order to make the ball drop in front of the outfielders. Therefore, increasing the launch speed decreases the vertical size of the sweet spot of the bat.

We can now see a difference produced by the different performance criteria. The old criterion of maximizing batted-ball speed was designed for home runs. It recommended increasing batted-ball launch speed for all situations. Our new performance criteria of maximizing the probability of a base hit were designed for singles. It recommends controlling batted-ball speed and launch angle. The sweet spot is smaller for higher bat speeds, so a trade-off must be made. Our experience with MLB batters, is that those who had very high bat swing speeds also had large variabilities and therefore less accuracy. They also had less success in MLB. When we presented Fig. 4.10 in Chap. 4, we commented that swing speed data for the

MLB batter had small variability for physiological data (Bahill and Karnavas 1991). We now see why. It is very important for batters to have all swings be alike. So, batters train to reduce the variability of bat swing speeds. This keeps the size of the sweet spot constant. In a different vein, on a changeup, the batter must delay the onset of the swing but keep the swing speed constant.

In this chapter, we gave the results of many simulations conducted to determine the vertical size (height) of the sweet spot of the bat. We believe that the most accurate estimate is that the sweet spot of the bat is one-fifth of an inch high. The Desired Range model gives smaller estimates, because it does not utilize the gaps between the fielders and it ignores the possible success of line drives and grounders. On the other hand, the Desired Range model shows that, even though the softball is bigger than the baseball, the height of the sweet spot is about the same, because the desired range for NCAA softball is smaller than it is for MLB.

We showed that the height of the sweet spot is about one-fifth of an inch. Then we showed that the vertical size of the sweet spot would depend on the dimensions of the ball field, the speed and reaction times of the fielders, the placement of the fielders, the size and mass of the bat and ball, the velocities of the bat and ball, the coefficient of restitution and the spin of the ball. The reason for presenting all of this variability was to help understand the *reliability* of the magnitude of our sweet spot estimates. Applying this variability to the Probability of Success model and considering all approximations and uncertainties, we conclude that the sweet spot of a bat is one-fifth of an inch high with a range of one-sixth to one-fourth of an inch.

In our problem statement for Sect. 9.2, we wrote that we wanted to understand how the vertical size of the sweet spot of the bat depended on the bat weight, bat shape, coefficient of friction, bat swing speed, bat swing angle (usually an uppercut) and bat–ball collision offset at impact: these are all under the batter's control. The bat weight has little effect on the vertical size of the sweet spot as shown in Table 9.6, but it has a big effect on batter success as discussed in Sect. 4.12.2. The bat shape is important because, as shown in this chapter, to maximize the vertical size of the sweet spot, the bat diameter in the region of the sweet spot should be as large as allowed by the rules. In this respect, manufacturers of maple wood bats are punishing batters: manufacturers should enlarge the bat diameter in the region of the sweet spot, and then they can reduce the diameter in other less important regions of the barrel. One possibility is shown in Fig. 9.11.

The coefficient of friction does not have an effect on the size of the sweet spot, because the ball is gripping the bat in the prime collision offset range (Cross 2011). However, above the sweet spot, lower friction could change a pop-up into a foul tip, as mentioned with Fig. 9.7. As bat swing speed goes up, the height of the sweet spot goes down. Therefore, batters should not sacrifice accuracy for increased swing speed.

The bat swing angle is important as shown in Table 9.6. In Sect. 9.3 and Fig. 9.5, we showed that making that the bat's swing angle equal to the ball's angle of descent (γ) was an advantage. In keeping with our philosophy of trying to find a second technique to verify our results and conclusions, we ran simulations as in Table 9.4 and Fig. 9.9 for a bat being swung level instead of at a ten-degree upward

Fig. 9.11 Maple bat with a tapered end. The tapered end allows the diameter at the sweet spot to be its maximum while keeping the weight down

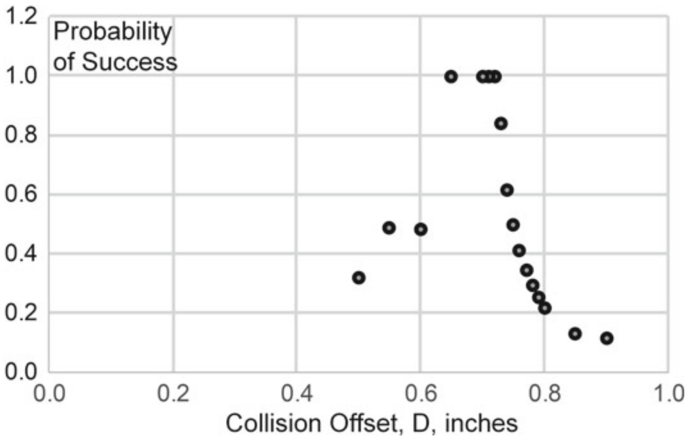

Fig. 9.12 Probability of success as a function of collision offset for a *level swing*

angle. The result is shown in Fig. 9.12. The width of the prime collision offset range is narrower than in Fig. 9.9. The height of the sweet spot is now 0.132 inches, less than the 0.183 of the normal upward swing. The data are also shifted to the right, which means that the position of the sweet spot will be higher on the bat, where the collision plane is at a higher angle.

In this chapter, we have shown examples of the following four modeling themes. Use at least two techniques to derive results. Numbers should have at least two components, such as magnitude and a reliability. Enough details should be given to allow other researchers to replicate the results. State your assumptions.

9.10 Summary

This chapter presented many performance criteria that have been used in previous baseball studies. Then it presented the probability of success performance criterion. It incorporated this performance criterion into our bat–ball collision model. Simulating this model showed that the most important parameter in determining the vertical size of the sweet spot of the bat was the bat swing speed. The second most important parameter was the diameter of the bat. The results of simulating our models produced the conclusion that the sweet spot of the bat is about one-fifth of an inch high (5 mm).

References

Adair, R. K. (2002). *The physics of baseball* (3rd ed.). New York: Harper Collins.

Bahill, A. T., & Baldwin, D. G. (2004). The vertical illusions of batters. *Baseball Research Journal, 32,* 26–30.

Bahill, A. T., & Karnavas, W. J. (1989). Determining ideal baseball bat weights using muscle force-velocity relationships. *Biological Cybernetics, 62,* 89–97.

Bahill, A. T., & Karnavas, W. J. (1991). The ideal baseball bat. *New Scientist, 130*(1763), 26–31.

Baldwin, D. G. & Bahill, A. T. (2004). A model of the bat's vertical sweetness gradient. In M. Hubbard, R. D. Mehta & J. M. Pallis (Eds.), *The engineering of sport 5* (vol. 2, pp. 305–311). *Proceedings of the 5th International Engineering of Sport Conference*, September 13–16, 2004 Davis, CA: International Sports Engineering Association (ISEA), Sheffield, England.

Brach, R.M. (2007). Mechanical impact dynamics: rigid body collisions. Wiley.

Cross, R. (2011). Physics of baseball and softball. Springer.

Goldsmith, W. (1960). *Impact: the theory and physical behavior of colliding solids*. London: Edward Arnold Publ. Ltd.

Nathan, A. M., Cantakos, J., Kesman, R., Mathew, B., & Lukash, W. (2012). Spin of a batted baseball, 9th conference of the international sports engineering association (ISEA). *Procedia Engineering, 34,* 182–187. https://doi.org/10.1016/j.proeng.2012.04.032.

Sawicki, G. S., Hubbard, M., & Stronge, W. J. (2003). How to hit home runs: Optimum baseball bat swing parameters for maximum range trajectories. *American Journal of Physics, 71,* 1152–1162.

Smith, E. D., Szidarovszky, F., Karnavas, W. J., & Bahill, A. T. (2008). Sensitivity analysis, a powerful system validation technique. *The Open Cybernetics and Systemics Journal, 2,* 39–56. https://doi.org/10.2174/1874110X00802010039.

Watts, R. G., & Baroni, S. (1989). Baseball-bat collisions and the resulting trajectories of spinning balls. *American Journal of Physics, 57,* 40–45.

Wymore, A. W. (1993). *Model-based systems engineering*. Boca Raton: CRC Press.

Chapter 10
The Advantage of Eye–Hand Cross-Dominance for Baseball Batters

10.1 Modus Operandi

Purpose: People who are right-handed but left-eye dominant or left-handed but right-eye dominant are said to be eye–hand cross-dominant. The purpose of this chapter is to explain why, in certain circumstances, it is an advantage for a batter to be cross-dominant.

To understand new baseball puzzles, we use physics first, then physiology and finally psychology. As an example, let us apply this process to a recent anomaly in baseball statistics. In Major League Baseball (MLB), there was a striking increase in the home run production rate starting in 2014, as shown in Fig. 10.1, using data from https://baseballsavant.mlb.com/statcast_search and https://www.baseball-reference.com/.

When pondering a new puzzle, we first try to explain it using physics. Physicists have investigated the ball's contribution to the coefficient of restitution (bounciness), but it seems to have remained constant throughout recent decades. Next, they suggested that the flatter seams on the major league baseball, compared to the National Collegiate Athletic Association (NCAA) baseball, would reduce the drag coefficient and thereby increase the range of the batted ball. However, the flatter seams would also decrease the Magnus lift force and thereby *decrease* the range. Evidentially, the effect of drag reduction is greater than the effect of the Magnus lift force reduction, because physics experiments and simulations have shown that MLB's flatter seams increased the range of a home run ball by 30 feet (Kensrud et al. 2015).

Lindbergh and Lichtman (2017) wrote that "The current barrage [of home runs] began in earnest immediately after the 2015 All-Star break." They sent several dozen game-used balls to Lloyd Smith's laboratory at Washington State University. This lab found that in comparing 2014 baseballs to 2016 baseballs, the newer balls had measurable differences (that were not visually apparent) that would increase the batted ball's range: they had lower seam heights, smaller circumferences and the

A. T. Bahill, *The Science of Baseball*,
https://doi.org/10.1007/978-3-030-03032-2_10

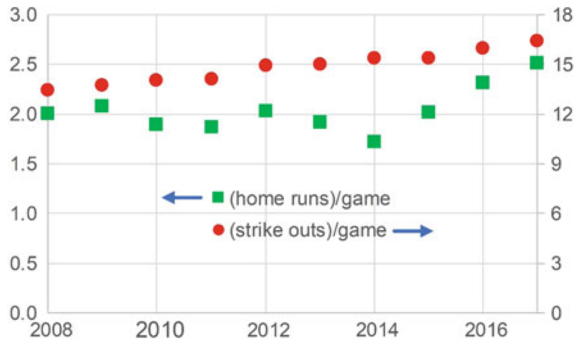

Fig. 10.1 Home runs and strikeouts per game. Seasonal average home runs per game and strikeouts per game for major league baseball in the last decade. There is a striking increase in the home run production rate starting in 2014. These data do not include playoff games

ball's contribution to the coefficient of restitution was slightly higher. Unfortunately, no variances were given for these data. Since then, many baseball blogs have jumped on this *juiced ball* bandwagon. However, there are two problems with this story. First, it would have produced a jump in the home run production rate at the All-Star break of 2015, not a linear increase between 2014 and 2017 as shown in Fig. 10.1. Second, MLB was using flat-seam baseballs years before the All-Star break of 2015.

For example, in 2010 and earlier, Kensrud compared the drag coefficient of the MLB flat-seam baseball to that of the NCAA high-seam baseball (Kensrud 2010). Later, in 2013, after studying the effects of the flat-seam baseball in MLB, the NCAA made a change reducing their regulation seam height from 0.048 to 0.031 inches (1.2–0.8 mm) effective in 2015. However, after this change, the mean number of home runs per game in college baseball actually *decreased* from 1.40 with a standard deviation of 0.34 to 1.28 with a standard deviation of 0.20, but this result was not statistically significant (Fs.ncaa.org/DOCS/stats/baseball_RB/reports/trendsYBY.pdf).

The low seams of the MLB were not created by design or rules. They are merely an artifact of the hand-stitching process used in the one factory in Costa Rica that has produced all MLB baseballs since 1990 (see https://www.youtube.com/watch?v=sXS9dfzUbxw). MLB has not published a rule for the height of the seams. Their rules for baseballs are very loose. Therefore, almost any seam height qualifies.

The conclusion of this section is that MLB probably used a flat-seam baseball from 1990, not by rule but by serendipity. Therefore, this is not the reason for the increase in the home run production rate starting in 2014.

It has been suggested that global warming and associated weather variations might be the cause for the increase in the home run production rate, because the range of the batted ball is inversely proportional to air density. And air density is inversely related to altitude, temperature and humidity, and is directly related to barometric pressure, see Chap. 7. Table 10.1 shows the effects of weather changes in one major league city.

Table 10.1 San Diego weather in July

	Historical multiyear average	2017 average	Change in air density	Change in batted-ball range for a perfectly hit ball
Average daily temperature high/low	75/65 °F	77/69 °F	−0.005 (kg/m^3)	+0.56 ft
Average daily barometric pressure	29.94 in Hg	29.96 in Hg	+0.002 (kg/m^3)	−0.22 ft
Average daily relative humidity	75%	80%	−0.001 (kg/m^3)	+0.11

How will global warming affect the game of baseball? Table 10.1 shows that, so far, it has had no effect. Typical annual changes in the weather might have increased the range of a home run ball, but only by one half of a foot. If global warming were to cause a two degree Celsius increase in temperature, this would be like comparing statistics between June and July in San Diego, Saint Louis or Los Angeles. In Boston, comparing May to June would be equivalent to global warming of 5 °C. Obviously, global warming is not the cause of the increase in home run production. Therefore, physics does not provide an answer for the increased home run production rate that started in 2014.

Therefore, let us try physiology for an explanation. Today's players are more athletic due to conditioning, nutrition, supplements and training. So, they have higher bat swing speeds. But this did not happen suddenly in 2014. So, physiology does not provide an answer.

Okay, so let us try psychology. MLB created game-changing metrics for performance. For example, pitchers are no longer evaluated solely on won–loss record and earned run average. Instead, everyone is talking about pitch speed. Pitchers seem to be throwing faster with many of them throwing at 100 mph. This would produce more home runs, because the faster the ball comes in, the faster the ball goes out, see Eq. (5.8). At the same time, MLB and television announcers are glamorizing the home run. Ball trajectories are continually being displayed on television and on the internet. This might have caused batters to *decide* to try hitting more home runs by consciously swinging faster and launching the ball at higher angles. Therefore, psychology may be the reason for the increase in home runs. Both the pitcher and the batter gain more publicity because of higher pitch speeds and more home runs. Finally, after pursuing physics, physiology and psychology, we should *follow the money*. High-speed pitchers and prolific home run hitters draw in the crowds (and their money), and hence might be paid more. This probably caused pitchers to *decide* to throw harder and batters to *decide* to swing faster and with higher launch angles.

10.2 Myth 1, Left-Handed Batters Are Better Than Right-Handed Batters

The following statistics are from the BaseballSavant (Willman 2017) for the regular 2017 Major League Baseball (MLB) season, https://baseballsavant.mlb.com/statcast_search

What is of interest in the present discussion is the reasons that have been given for left-handed batters being "better" than right-handed batters. It has been suggested that left-handed batters have an advantage because they are two feet closer to first base. This reason implies that their advantage is "beating out" more ground balls for base hits. However, of the 28,000 ground balls hit by major league right-handed batters in 2017, 1.30% of them were fielded cleanly, but were beat out for base hits (this does not include grounders that snuck through the infield untouched), whereas of the 19,000 ground balls hit by left-handed batters and fielded cleanly by infielders, only 1.29% resulted in base hits. Therefore, being two feet closer to first base does not enable left-handed batters to beat out more grounders. Caution, this conclusion does not apply to slap hitters in NCAA softball.

Some authors have written that the left-handed batter's head will be facing first base at the end of the swing. We do not think that this is an advantage. Because after the swing, the batter does not want to look at first base rather, he wants to get his eye on the ball and see where it goes.

Perhaps the only advantage of batting left-handed results from the baseball tradition of preferring left-handed batters facing right-handed pitchers. Since most pitchers are right-handed, the practice of platooning means that left-handed batters will get more plate appearances and experience. In the next section, we will discuss whether platooning is justified.

Figure 10.2 shows the batting averages for right-handed and left-handed batters. Sometimes the RHBs were better and sometimes the LHBs were better. But given that the standard deviations of these averages are 0.50, the differences are not statistically different.

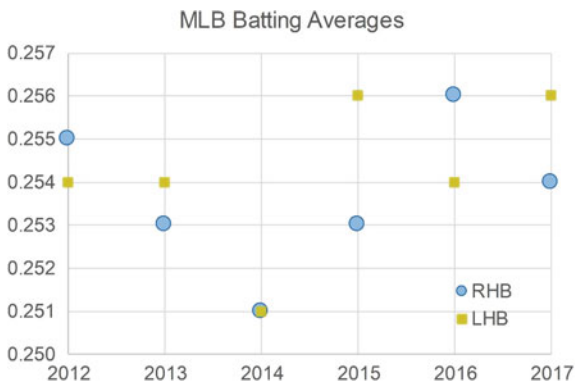

Fig. 10.2 Seasonal batting averages. For major league baseball in recent years, the batting averages for Left-Handed Batters (LHB, yellow squares) are about the same as for Right-Handed Batters (RHB, blue disks). These differences are not significant given that typical annual batting average standard deviations are around 0.050

Weighted averages. When computing an average of averages, it is necessary to weight the data. For example, if there were ten batters with Batting Averages (BAs) of 0.300 and one batter with a BA of 0.100, then you would *not* want to say that the average BA wa 0.200. Instead, you would compute the weighted average of the BAs which would be $wBA = \frac{10\times0.300+1\times0.100}{11} = 0.282$. This certainly makes more sense. This is why we use weighted batting averages.

The following table shows how we computed the weighted batting average for MLB players. For each player we took his number of Hits and divided it by his number of at bats (AB), this gives his batting average (BA). Then we weighted his BA by multiplying it by his number of at bats (AB) divided by the total number of at bats by all players. In this example, if we average the BAs we get 0.200, which is too low. Whereas, if we average the weighted BAs, we get 0.260 which is just right, because 130/500 = 0.260.

Player's name	Hits	AB	BA	Weighted BA
A	100	300	0.333	0.600
B	25	150	0.167	0.150
C	5	50	0.100	0.030
Sum	130	500		
Average			0.200	0.260

Now, on an interesting tangent, if a 6-year-old child writes right-handed and throws right-handed, would it be more natural for him or her to start batting right- or left-handed? Should the dominant arm push or pull the bat? Do most right-handers bat from the third-base side of the plate because it is physiologically natural, or because that is the way they were taught? What if batting from the left side of home plate (as viewed by the catcher and the umpire) was called batting left-handed, would right-handed children then be taught to stand on the right side of the plate?

10.3 Myth 2, Batting Opposite Handed to the Pitcher Is an Advantage

In MLB in 2017, against Right-Handed Pitchers (RHP), Right-Handed Batters (RHB) had an average batting average of 0.253, whereas Left-Handed Batters (LHB) had an average of 0.261. However, given the large variances, these differences are not significant: they might be due to chance. What is of interest in the present discussion is the bogus reasons that have been given for left-handed batters being better than right-handed batters against right-handed pitchers. Humans love to propose causes.

Some people have written that hitters can handle pitches on the inside portion of the plate better than the outside. Also, hitters can track and see a ball that is moving toward them better than away. Others have written that the biggest advantage has to do with the angle of the ball. A right-handed batter must look over his left shoulder and the ball is "coming at quite an angle." Our trajectory simulations show that the pitchers' release points for right-handed pitchers and left-handed pitchers only differ by four degrees (Fig. 10.3). This would not make a difference in the ability to track the pitch. Continuing their argument, they have said that the offset of your eyes gives you depth perception. So, when you're looking over your shoulder, you have lost the distance between your two eyes perpendicular to the pitch "quite a bit," so you have lost that tenth of a second to see the ball! Still others have written that there are more right-handed pitchers in major league baseball. So, all batters get more practice hitting against right-handed pitchers. Therefore, they do better. These reasons are all fallacious.

Table 10.2 shows the batting averages for different handedness for the MLB 2017 regular season. The Batting Average (BA) were weighted by the number of At Bats (AB). If you use Statcast Search you might get different numbers than these because, at the time of this writing, the Min ABs filter does not work when data were grouped by "League." It only worked when the data were grouped by Player.

Fig. 10.3 Terry Bahill tracking a simulated pitch. Our subjects tracked a plastic ball that was pulled along a fishing line by an aerospace velocity servo system. The infrared emitters and photodetectors that measured the eye movements were mounted on the special eyeglass frames shown here worn by Professor Bahill. Head movements were measured using the two light-emitting diodes mounted directly on top of his head and the third positioned at the end of the brass tube

Table 10.2 Batting averages for different handedness for the MLB 2017 regular season

Batter	Pitcher	Average weighted BA	Standard deviation	Number of batters, n
RHB	RHP	0.253	0.045	349
RHB	LHP	0.266	0.057	336
LHB	LHP	0.246	0.053	122
LHB	RHP	0.261	0.043	259

The numbers in Table 10.2 show that RHBs do slightly better against LHPs, $BA = 0.266 \pm 0.057$, than against RHPs, $BA = 0.253 \pm 0.045$. However, even with a large number of batters, the standard deviations show that the differences are not statistically significant. They could easily be due to chance. In summary, opposite handedness gives the batter a slight but not significant advantage, as shown here.

BA	RHP	LHP
RHB	0.253	**0.266**
LHB	**0.261**	0.246

To further explore this opposite handedness myth, let us look at one of the modern designer metrics for batter performance, On-base Plus Slugging (OPS). In Table 10.3 we give the OPS, which is the sum of the weighted safe on-base average plus the slugging average.

Opposite handedness (printed in boldface) does not give the batter an advantage, as shown here. The opposite-handed conditions have the largest and smallest OPS. The same-handed conditions give the two OPS in the middle.

OPS	RHP	LHP
RHB	0.733	**0.765**
LHB	**0.670**	0.771

There is a lot of variability in individual performance against right-handed and left-handed pitchers. Some batters have as much as a 0.100-point difference in their batting averages against right-handed and left-handed pitchers. However, other batters have no difference. This implies that the difference in performance is not due to physics or physiology. Maybe it is due to psychology. Specifically, it might be due to the fear factor. The advantage of the opposite-handed batter might be nothing more than *fear*: When a right-handed batter sees a ball thrown by a right-handed

Table 10.3 OPS for different handedness for the MLB 2017 regular season

Batter	Pitcher	wOBA	SLG	OPS = wOBA + SLG
RHB	RHP	0.314	0.419	0.733
RHB	LHP	0.328	0.437	**0.765**
LHB	LHP	0.331	0.440	0.771
LHB	RHP	0.298	0.372	**0.670**

pitcher coming straight at his head, he doesn't know if it is a curveball that will cross the plate for a strike, or a wild fastball that will hit his head. On the other hand, the left-handed pitcher would have to be wild as a March hare to raise as much adrenaline in the batter.

10.4 Myth 3, Eye–Hand Cross-Dominance Is an Advantage for the Batter

People who are right-handed but left-eye dominant or left-handed but right-eye dominant are said to be eye–hand cross-dominant. This might be an advantage for batters.

To determine your dominant eye, choose an object across the room. Stretch your arms straight out in front of you with your palms facing away. Place one hand over the other, leaving a one-inch-diameter triangular hole above your thumbs. Look through this hole at the selected object. Close one eye and then the other. The eye that sees the object through the hole is your dominant eye. You can also do this experiment by looking into a mirror and putting the hole in your hands over the reflection of your dominant eye.

Cross-dominant rifle shooters have problems sighting their weapons. They have the highest failure rates qualifying on the shooting ranges in the Armed Forces. A right-handed but left-eye dominate person will put the rifle butt on his right shoulder. He will want to sight with his dominate left eye, but it is his right eye that is behind the gun sight.

The data in Table 10.4 are not consistent. However, what is of interest in the present discussion is the bogus reasons that were given for cross-dominant batters being better. Some people believe that cross-dominant batters can "see" the ball better because their dominant eye has a bigger field of view, unblocked by the nose.

Table 10.4 Published studies of cross-dominant batters, listed in chronological order

Do eye–hand cross-dominant batters have higher batting averages?		
Answers	Subjects	References
No, the batting averages were 0.246 versus 0.284 for crossed and uncrossed batters, respectively	28 collegiate batters	Adams (1965)
Yes	400 professional baseball batters	Teig (1980)
Yes, the batting averages were 0.302 versus 0.298	234 collegiate batters	Milne et al. (1995)
Yes, the batting averages were 0.242 versus 0.239	92 collegiate batters	Classe et al. (1996)
No, the batting averages were 0.264 versus 0.273	113 Los Angeles Dodgers	Laby et al. (1998)
Yes, the batting averages were 0.310 versus 0.250	23 collegiate batters	Portal and Romano (1998)

However, peripheral vision is not used by batters. Batters are only interested in seeing the pitcher's release point and the first half of the pitch. During these periods, the ball is near the fovea of both eyes. Other students of baseball have written that eye–hand cross-dominance is an advantage for the batter because the batter's dominant eye is an inch closer to the pitcher who is 60 feet away: this is insignificant. Another bogus reason is that information from the dominant eye is processed by the brain 15 ms faster than information from the non-dominant eye: this is irrelevant. These fallacious explanations were not satisfying to us, so we strove to develop our own explanation. Our explanation is complicated, and it will take up the rest of this chapter. If this problem were simple, it would not have baffled so many people for such a long time.

10.5 Time to Contact

To hit the ball the batter must predict where and when the ball will contact his bat. Let us first see how the batter can judge *when* the ball will be at the collision point. In his novel, *The Black Cloud*, Hoyle (1957) showed that the time until contact, τ, with an object moving along the line of sight can be approximated with the equation

$$\tau \approx \frac{\gamma}{d\gamma/dt}$$

where γ and $d\gamma/dt$ are, respectively, the object's angular size and rate of change of angular size, both of which are readily available in brain circuitry. The following paragraphs are based on Bahill and Karnavas (1993). References to the original literature can be found there. Estimations of time until contact that are used to control physiological motor actions are based on this variable. For example, it has been shown that birds use τ when diving into the water to catch prey, and athletes use τ when jumping to hit a dropped ball, adjusting strides when running hurdles and timing their swings in table tennis; for these tasks, time until contact is judged with an accuracy around 2–10 ms. Cricket players time their swings with an accuracy of ± 5 ms. Top sports players estimate the time until contact of the bat and ball with an accuracy of better than three milliseconds. The batter's calculation of time until contact has three sources of error. First, they use the approximation $\tan\theta = \theta$. Second, the ball is not headed directly at the batter's eye. In our simulations, these two sources produced errors of about one millisecond at the start of the swing. The third source of error, which results from the batter hitting the ball 1.5 feet in front of his eyes, produces a constant (and therefore easily compensated for) 11 ms of error in underestimating the time of arrival at impact.

The human visual system can implement this equation for τ. First, there is psychophysical evidence that the human brain contains units tuned to size (γ), and size-tuned neurons have been found in monkey visual cortex. Second, psychological studies have shown that the human visual system has specialized “looming detectors" that compute $d\gamma/dt$ independent of the object's trajectory. Specific monkey brain neurons are sensitive to changing size, $d\gamma/dt$. Using these two pools of neurons, the brain could compute τ.

In this section, we proposed a model for estimating time until contact (Bahill and Karnavas 1993; Bahill and Baldwin 2004). We stated that the human brain has neuronal circuits that could do the needed computations. We explained that the parameters of a pitch are within physiological thresholds for these neuronal circuits. Next, we asserted that people can accurately estimate time until contact. From the instant the ball leaves the pitcher's hand, the batter's retinal image contains accurate cues for estimating time until contact. The human visual system can utilize these cues producing errors less than ±5 ms. This is the needed accuracy, because inaccuracy of ±9 ms would cause the ball to be hit foul.

10.6 Physiology of Tracking the Ball

There are four types of eye movements: saccadic (să•käd′•ik) eye movements, which are used in reading text or scanning a roomful of people; smooth pursuit eye movements, used when tracking a moving object; vergence eye movements, where the eyes move in opposite direction are used when looking between near and far objects and vestibulo-ocular eye movements, used to maintain fixation during head movements. These four types of eye movements have four independent control systems, involving different areas of the brain. Their dynamic properties, such as latency, speed and bandwidth, are different, and they are affected differently by fatigue, drugs and disease.

The specific actions of these four eye movement systems can be visualized by considering a duck hunter sitting in a rowboat on a lake. He scans the sky using saccadic eye movements, jerking his eyes quickly from one fixation point to the next. When he sees a duck flying in the sky, he tracks it using smooth pursuit eye movements. If the duck lands in the water near his boat, he moves his eyes toward each other with vergence eye movements. Throughout all this, he uses vestibulo-ocular eye movements to compensate for the movement of his head caused by the rocking of the boat. Thus, all four eye movement systems are continually used to control gaze position.

To track the pitch, the batter can use the head-movement system in addition to each of these eye movement systems. Does he? Early studies by Bahill and LaRitz (1984) suggested several strategies for tracking a baseball: track the ball with head movements and smooth pursuit eye movements and fall behind in the last 5 feet of flight; track with eyes only, or with head only, and fall behind in the last 8 feet; track the ball over the first part of its trajectory with smooth pursuit eye movements, make a saccadic eye movement to a predicted point ahead of the ball, continue to follow it with peripheral vision, and finally, at the end of the ball's flight, resume smooth pursuit tracking with the ball's image on the fovea. The fovea is the small area in the center of the retina that has fine acuity. It is about one degree in diameter and subtends an angle about twice the size of the sun or the moon. For a man with his arm extended in front of him, the clinical fovea is the width of the fingernail on his little finger. This is the only part of the retina that has sharp color vision.

10.7 The Simulated Pitch

This section is based on Bahill and LaRitz (1984). To discover how well a batter tracked the ball, we had to be able to determine the precise position of the ball at all times, and thus we could not use a real pitcher or a pitching machine. Instead, we simulated the trajectory of a pitched baseball, as shown in Fig. 10.3. We threaded a fishing line through a white plastic ball and stretched the line between two supports, which were set 80 feet apart in order to easily accommodate the 60.5 feet between the pitcher's rubber and home plate; a string was attached to the ball and wrapped around a pulley attached to an aerospace velocity servo system, so that when the motor was turned on, the string pulled the ball down the line at speeds between 60 and 80 mph. The ball crossed the plate 2.5 feet away from the subject's shoulders, simulating a high-and-outside pitch thrown by a left-handed pitcher to a right-handed batter. This, like all our constraints, was designed to give our subjects the best possible chance of keeping their eyes on the ball. A low curveball thrown by a right-handed pitcher would have been much harder to track.

By controlling the speed of the motor and counting the rotations of the shaft, we could compute the position of the ball at every instant of time, and thus compare the position of the ball to the position of the batter's gaze. We defined both positions in terms of the horizontal angle of the ball: the angle between the line of sight from the batter's eye pointing straight out toward center field and the line of sight pointing at the ball (labeled θ in Fig. 10.4). This angle is about 5° when the left-handed pitcher releases the ball, it increases to 60° at the bat–ball collision point and to 90° when the ball crosses the plate.

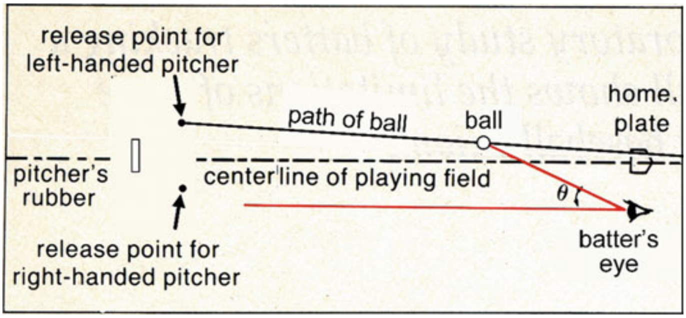

Fig. 10.4 The horizontal angle of the ball. The horizontal angle of the ball, θ, as defined in this study, starts at 5° when the left-handed pitcher releases the ball, it increases to 60° at the bat–ball collision point and to 90° when the ball crosses the plate. The horizontal and vertical scales are different. All of the figures in this chapter are for right-handed batters

We measured horizontal eye movements with a photoelectric system using infrared emitters and photodetectors aimed at the iris–sclera borders of both eyes as shown in Fig. 10.3. As the eye moved horizontally, the amount of reflected infrared light changed, causing a variation in the current of the photodetectors. Amplifying the difference in the currents of the two detectors produced a voltage proportional to horizontal eye position. (Although we sampled each millisecond, our data were filtered and compressed, producing 30-Hz bandwidth position traces and 7-Hz bandwidth velocity traces.) Since we deliberately configured the simulation to minimize vertical target movements, vertical eye movements, which were measured by electrooculography, were negligibly small.

Head movements were measured with a video camera mounted on the ceiling, looking down on the subject's head. Two Light-Emitting Diodes (LEDs) were placed on top of the subject's head, and a third LED was mounted on a brass tube 7.8 inches above his head (see Fig. 10.3). The video signal was digitized, and the coordinates of the centers of the three LEDs were computed; from these coordinates, we computed the yaw, pitch and roll angles as well as the lateral and forward–backward position of the head.

We ran many subjects through our simulation, including graduate students, students on the university baseball team and a member of the Pittsburg Pirates baseball team. All had 20/20 uncorrected vision. Figure 10.5 shows the results of one experiment, which were typical of the results obtained with students. This subject tracked the ball well (less than 2° error) until the ball reached 16°, corresponding to 9 feet in front of the plate, at which point he started to fall behind. When the ball reached the 50° point, 2 feet in front of the plate, the image of the ball was 34° off of his fovea. The ball covered the angle between 16° and 50° in 67 ms, for an average angular velocity of 507°/s—much too fast for any human to track. The maximum smooth pursuit velocity occurred just before the ball crossed the plate: the eye was going 50°/s, and the head was going 20°/s, giving a gaze velocity of 70°/s. This subject used both head and eye movements to track the ball; in contrast, some of our other subjects used only eye movements to track the ball, and others used primarily head movements.

Figure 10.6 shows an example of the results produced by a major league baseball player, Brian Harper. He tracked the ball using head and eye movements, keeping his eye on the ball longer than our other subjects did. He was able to keep his position error below 2° until the ball reached 24°, 5.5 feet from the plate. When the ball reached the 50° point, the image of the ball, which was traveling at 1100°/s, was 16° off his fovea, better than our other subjects, but too far off to track the ball. The peak velocity of his smooth pursuit tracking was 120°/s; at this point, his head velocity was 30°/s, thus producing a gaze velocity of 150°/s. In three simulated pitches to this major league batter, at speeds of 60, 67 and 70 mph, the overall tracking patterns were the same; his maximum smooth pursuit eye velocities were 120, 130 and 120°/s, respectively. This was surprising because the literature states that the fastest human smooth pursuit eye movements are about 70°/s. The small saccade at 0.3 s in Fig. 10.6 is analogous to the larger saccade shown in Fig. 10.7.

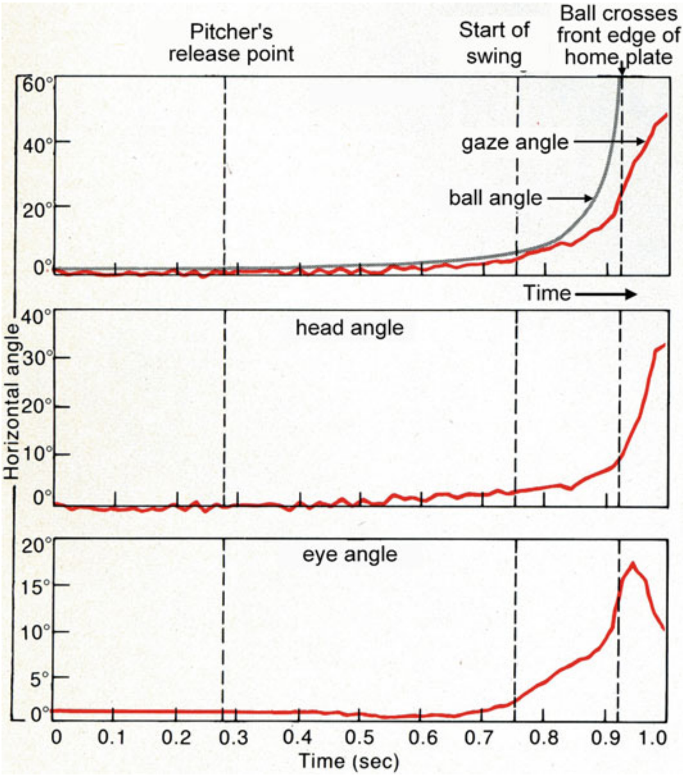

Fig. 10.5 Head, eye and gaze position during a simulated pitch. The gray line in the top graph represents the horizontal angle of the ball, the angle θ in Fig. 10.4, as it would be seen by a right-handed batter facing a left-handed pitcher. The red line represents the horizontal angle of gaze of the subject trying to track this ball; this curve was generated by adding the horizontal head angle (middle graph) and the horizontal eye angle (bottom graph), two of the parameters measured in our experiments. Movements to the right appear as upward deflections

The gaze graph of Fig. 10.6 differs from the gaze graph in Fig. 10.3 because, in addition to combining eye and head angles, it also takes into account the side-to-side and front-to-back movements of the head; such translations of the head produce changes in the gaze angle. The data show that the contribution of the translation angle was slight until the ball was almost over the plate.

Obviously, the major league batter had faster smooth pursuit eye movements than our other subjects. In fact, his smooth pursuit eye movements were faster than any ever reported in the literature. He also had better head–eye coordination, tracking the ball with equal-sized head and eye movements, whereas our other subjects usually used mostly head or mostly eye movements. However, despite these superiorities, he was not able to keep his eye on the ball all the way from the pitcher's release point to the point of bat–ball collision. No one can do that.

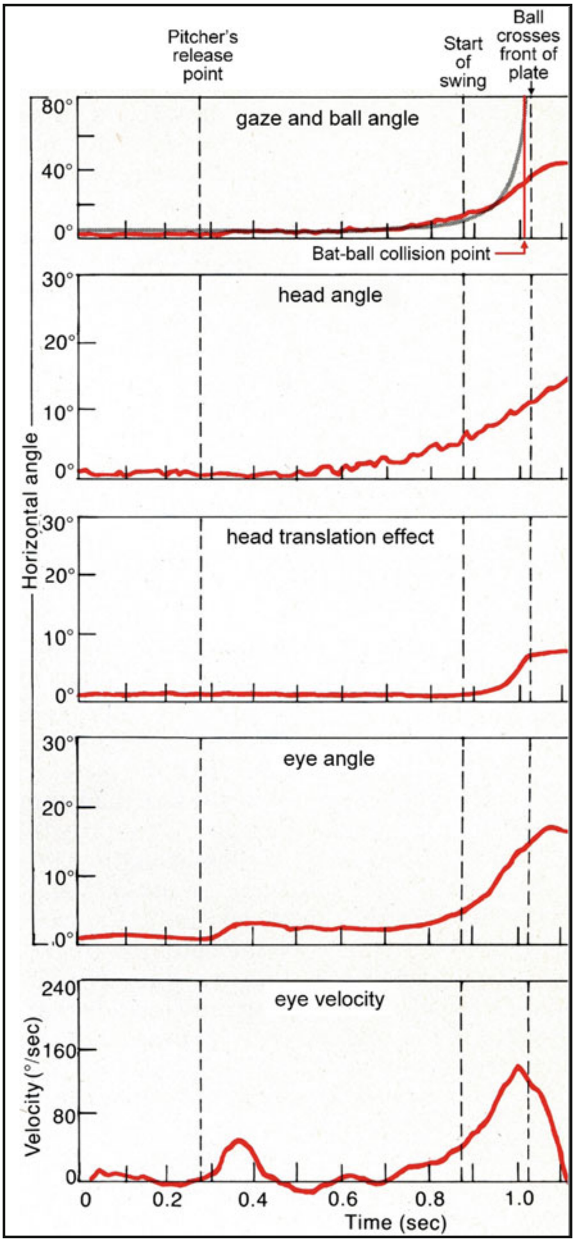

Fig. 10.6 Head, eye and gaze positions while tracking a simulated pitch. The success of a major league batter in tracking a simulated pitch is shown in these graphs, which have the same format as in Fig. 10.5, except that the horizontal gaze angle also uses the head-translation angle shown in the middle graph. This was a slow pitch, 67 mph, which should have given the batter the best chance to keep up with the ball

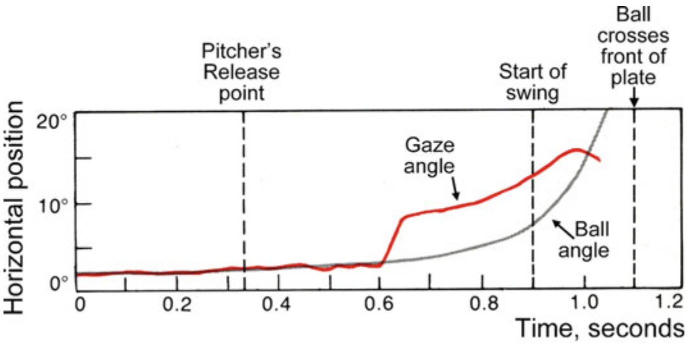

Fig. 10.7 Anticipatory saccade. An anticipatory saccade put the eye (red line) ahead of the ball (gray line)

10.8 Seeing the Ball During the Collision

Therefore, we now have another conundrum. It is impossible for a human to keep his eye on the ball continuously from the pitcher's release point to the bat–ball collision point. However, many people have claimed that they have seen the ball hit their bat. Their descriptions of the collision are very vivid. So many people can't just be fooling themselves. How can this be explained? Figure 10.7 offers a suggestion.

The subject of Fig. 10.7 was able to see the ball hit his bat by making an anticipatory saccade, indicated by the jump in the gaze angle (red line) at 0.6 s. This saccade put his eye ahead of the ball (gray line), which he continued to track with peripheral vision as evidenced by the gaze and ball curves running parallel, until the ball was on the fovea near the point of contact. The subject did not move his head until after the ball crossed the plate.

We caution that our study, although it does warrant some useful generalizations, has limitations. First, our subjects never actually swung their bats at the ball; head–eye coordination might be different if the subjects did swing the bat. Second, we simulated the easiest pitch for a batter to track: a slow high-and-outside changeup thrown by an opposite-handed pitcher; in this case, a left-handed pitcher to a right-handed batter. Nevertheless, even with these limitations, we can reasonably make the following generalizations.

Although the major league batter was better than our students at tracking the simulated pitch, it is clear from our studies that batters, even major league batters, cannot keep their eyes on the ball. Our major league batter was able to track the ball until it was 5.5 feet in front of the plate. This could hardly be improved on; we hypothesize that the best imaginable athlete could not track the ball closer than 5 feet from the plate, at which point the ball is moving three times faster than the fastest human could track. This finding runs contrary to one of the most often-repeated axioms of batting instructors—"Keep your eye on the ball"—and makes it difficult to account for the widely reported claim that Ted Williams could see the ball hit his bat.

10.9 Seeing the Bat During the Collision

When a baseball bat moving at 62 mph hits a baseball traveling in the opposite direction at 83 mph there is a violent collision (remember Fig. 5.7). During the collision, the kinetic energy in the motion of the bat drops by 218 Joules (J): a loss of 193 J in linear translational kinetic energy and a loss of 25 J in angular rotational kinetic energy (see Table 4.3 and Fig. 10.8). Notably, 218 J is equivalent to dropping a 50-pound weight from your waist onto your toe or having a one-pound rock hit your windshield while you are driving down a highway at 70 mph.

These numbers were derived using the BaConLaws model of Chap. 4 and Fig. 1.4. It gives equations and values. Now, we want to switch to a different model. We want to switch to a model representing the spectator's viewpoint: that would be the Sliding Pin model of Fig. 1.7 and Sect. 5.3.

In a frame-by-frame analysis of a high-speed video of a major league batter we measured the linear position of the bat, x_{ss}, and the angle of rotation of the bat about the knob, ψ. These are printed in red in Fig. 10.9. From these, we computed the total linear velocity of the sweet spot of the bat, $v_{ss\text{-}total}$, and the time rate of change of

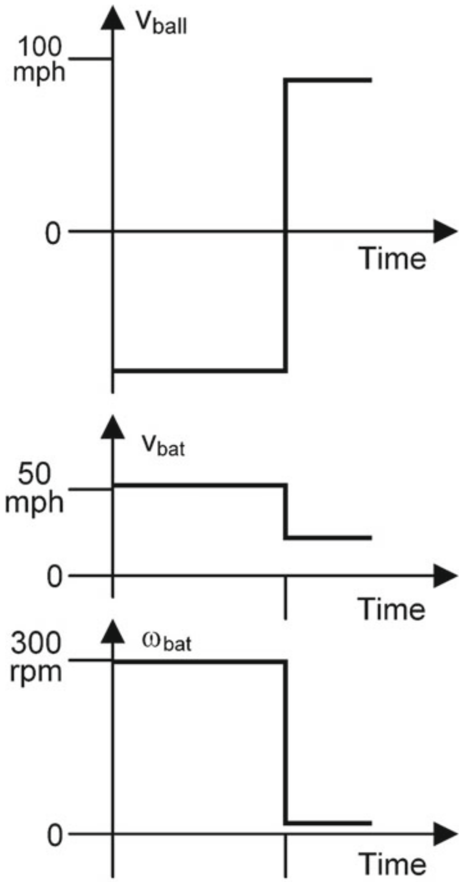

Fig. 10.8 Bat and ball velocities from the BaConLaws model. The bat and ball velocities change abruptly during the bat–ball collision

the angle of rotation, $\beta = \frac{d\psi}{dt}$. These are printed in blue in Fig. 10.9. $v_{ss-total} = v_{ss} + d_{knob-ss}\beta$. Graphs of these data showed that during the collision there was (1) a big abrupt change in the ball velocity as it changed from negative to positive, (2) a sudden drop in the total linear velocity of the sweet spot of the bat, $v_{ss\text{-}total}$, and (3) a sharp drop in the angular velocity of the bat, β.

Now, imagine a film of Ted Williams hitting a baseball (or any present-day batter in a slow motion video like these https://www.youtube.com/watch?v=lX_dm39fkfw or https://www.youtube.com/watch?v=t_vEJu3jmpw). His swing is smooth and graceful, although the kinetic energy of his bat changes by around 218 J during the collision. The reason his swing seems so smooth is that we visualize the integrated movement of his body, arms, hands and bat, which seem fluid and continuous. We do not notice the short jerk in the bat's motion at the time of the collision. What we see is the position and the angle of the bat (see Fig. 10.9). Their changes are not visually obvious because it is just a short small jerk in the middle of the entire swinging motion. Hence, what we see does not change much.

However, the velocities of linear translation and angular rotation *do* change a lot during the 1 ms collision. The translational speed of the sweet spot of the bat drops to one-fourth of its precollision speed. The angular rotation rate of the bat drops to one-third of its precollision rate. However, changes in velocity are accelerations and humans do not use acceleration information when tracking targets.

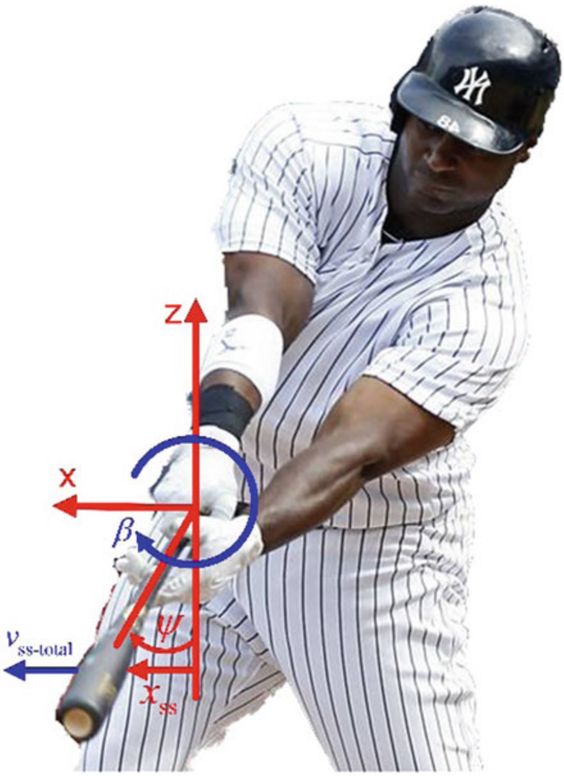

Fig. 10.9 The sliding pin model represents the spectator's viewpoint. The spectators primarily see the position of the sweet spot of the bat, x_{ss}, and the angle of rotation of the bat about the knob, ψ

As a result, the movement of the bat that we visualize well (linear position and rotational angle) does not change much, whereas, the velocities that change a lot are not visualized well. This explains why people do not perceive an abrupt jerk of the bat when the bat and ball collide.

What about the batter? Would he be able to see the effects on the bat of this violent collision? Probably not. Figures 10.5 and 10.6 show typical tracking of our simulated pitch. The batters fell behind the ball when it was 5 to 10 feet in front of the plate. No batter could keep his eye on the ball from the pitcher's release point to the bat–ball collision point. This finding runs contrary to baseball's hoary urban legend that Ted Williams could see the ball hit his bat. However, in reality, Ted Williams could not see the ball hit his bat. In a letter that he sent to Bahill dated January 23, 1984 he wrote

> Received your letter and have also had a chance to read your research, and I fully agree with your findings.
>
> I always said I couldn't see a ball hit the bat except on very, very rare occasions and that was a slow pitch that I swung on at shoulder height. I cam[e] very close to seeing the ball hit the bat on those occasions.

P. O. BOX 481
ISLAMORADA, FLORIDA KEYS
33036

January 23, 1984

Prof. A. Terry Bahill
Electrical & Computer Engineering
Carnegie-Mellon University
Schenley Park
Pittsburgh, PA 15213

Dear Mr. Bahill:

Received your letter and have also had a chance to read your research, and I fully agree with your findings.

I always said I couldn't see a ball hit the bat except on very, very rare occasions and that was a slow pitch that I swung on at shoulder height. I cam very close to seeing the ball hit the bat on those occasions.

As to participating in your other experiments; at this time, I can't tell you that I can comply with your request.

Regarding the current theories of some of the present batting coaches (with which I absolutely disagree) to watch the ball go into the catcher's mitt - by doing that, you don't give yourself a chance to swing and open up properly. Try it yourself - look down at the plate and try to make a full swing. I hope you don't throw your back out of joint!

In any event, good luck with your projects.

Sincerely,

Ted Williams

Ted Williams

TW/shg

In summary, the bat–ball collision is violent. Everyone can see its effect on the ball: the ball is squashed (remember Fig. 5.7) and its velocity changes by around 175 mph. However, no one sees the collision's effect on the bat. Because, first of all, the bat–ball collision only lasts 1 ms, which is too short for visual pattern recognition. Second, even in slow motion, the spectator only sees the smooth movement of the batter's body, arms, hands and bat, which glide continuously. The spectator cannot see abrupt changes in the bat's translational velocity or angular rotational velocity. This explains why nobody sees an abrupt jerk of the bat when the bat hits the ball, not even Ted Williams.

On the "very, very rare occasions" when Ted Williams saw the ball hit his bat he must have made an anticipatory saccade (as in Fig. 10.7) that put his eye ahead of the ball and then he let the ball catch up to his eye. This was the strategy employed by the subject of Fig. 10.7: this batter observed the ball over the first half of its trajectory, predicted where it would be when it crossed the plate, and then made an anticipatory saccade that put his eye ahead of the ball. Using this strategy, the batter could see the ball hit the bat. However, because of the short duration of the collision, this image would seem like a still photograph and would not allow him to visualize the jerk of the bat.

In conclusion, you can't keep your eye on the bat.

10.10 Tracking Eye Movements

But why would a batter *want* to see the bat–ball collision? He cannot use the information gained in the last portion of the ball's flight to alter the course of his bat. We suggest that he uses the information to discover the ball's actual trajectory, that is, he uses it to *learn* how to predict the ball's location when it crosses the plate —how to be a better hitter in the future. The anticipatory saccade, shown in Fig. 10.7, must be made before the end of the trajectory, because saccadic suppression prevents us from seeing during saccades. This suppression of vision extends about 20 ms after the saccade. So, if you want to see the ball hit your bat, you must make your anticipatory saccade near beginning of the swing.

Batters do not use vergence eye movements while tracking the pitch. This is reasonable, since vergence eye movements are not needed to track the ball between the pitcher's release point at 55.5 feet and 20 feet from the plate, and there is not enough time to make such movements between 20 feet and the collision point.

This paragraph is an aside strictly for eye movement aficionados. Please refer to Fig. 10.10 bottom. Suppose our batter made a 60-degree conjugate saccade (a five-to-ten-degree 30-ms saccade would be more likely) when the ball was about 250 ms out, just over 20 feet from the plate. If there were an object at this predicted collision point one meter from the eyes (which there is not), it would produce a four-degree binocular disparity. This could trigger, after a 160 ms latency, a two-degree (by each eye) convergent eye movement. This vergence eye movement would have a duration of 250–500 ms (Schor 2011). This vergence eye movement would end long after the pitch. Furthermore, the eyes would be moving when the ball hit the bat, which is the time when the batter wants his eyes to be stationary. In summary, there is no time or desire for the batter to use vergence eye movements. So, any claim that a batter saw the ball hit his bat must be based on monocular vision; only the dominant eye can see the bat–ball collision.

The vestibulo-ocular eye movement system is also used when tracking a pitch. In the measurements of the eye movements of the major league batter, we detected vestibulo-ocular eye movements to the left during the early part of the ball's trajectory, as the head was moving to the right; this appears as the slight dip between 0.5 and 0.7 in the eye trace in Fig. 10.6. (He did this in all his recorded tracking efforts.) At this point, his head position was changing faster than the angular position of the ball, and the vestibulo-ocular eye movement compensated for the premature head movement. Why would the batter want to give his head a head start? The answer is that the head is heavier than the eye and consequently takes longer to get moving; therefore, in the beginning of the movement, as the head starts turning to the right, ahead of the ball, the vestibular system in the inner ear signals the eye movement system to make a compensating eye movement to the left.

However, this vestibulo-ocular compensation must soon stop. In the end, the eye and the head must both be moving to the right, and now the batter must, therefore, suppress his vestibulo-ocular reflex so that the tracking head movement does not produce compensating eye movements that would take his eye off the ball. This major league batter was very good at suppressing his vestibulo-ocular reflex. Our subjects, who were not as good at suppression, either moved their heads very little or they did not make head movements until after the ball crossed the plate.

Most people can suppress their vestibulo-ocular reflex. To see this effect, hold your thumb at arm's length in front of your face. From either a standing position or while seated in a rotatable chair, rotate your body, head, arms and thumb as one unit to the right and then to the left. Keep your eyes focused on your thumb. You should see the world swirl past behind your thumb. It should seem strange to you because you are doing something unusual: you are suppressing your vestibulo-ocular reflex. Our major league batter was very good at suppressing his vestibulo-ocular reflex.

The fact that our major league batter used his head to help track the ball seems to violate another often-repeated batting axiom, "Don't move your head." He made head tracking movements in the range of 10–20 degrees, which were probably small enough to go unnoticed by a coach. He was able to suppress his vestibulo-ocular reflex for these head movements. However, body movements could produce head movements of 40° or 50°, which, along with correlated poor performance, would be noticed by a coach. Therefore, we think the axiom should be expanded: "Don't let your body move your head, but it's okay to make small head movements to help track the ball."

In comparison, golf is an easy game, because the ball is stationary. There is no need to track the ball in golf. Accordingly, golfers are told to keep their heads stationary. Therefore, there is no need for suppression of the vestibulo-ocular reflex, thus making the task even easier.

Tracking eye movements might depend on the instructions given to the subjects (Fogt and Persson 2017). If the batter plans to swing the bat at the ball, then he might be interested in seeing the bat–ball collision. However, if the coach, or the experimenter, has told the batter to "take," that is not swing at the pitch, then the tracking eye movements might be different, because the batter would know that there would be no bat–ball collision to see.

10.11 Two Tracking Strategies

Sometimes our subjects used the strategy of tracking with head and eyes and falling behind in the last 5 feet (Fig. 10.10, top), and sometimes they used the strategy of tracking with head and eyes but also using an anticipatory saccade (Fig. 10.10, bottom). We think that batters might use the latter strategy when they are learning the trajectory of the pitch and the former strategy when getting base hits.

The optimal hitting strategy is to track the ball with head movements and smooth pursuit eye movements and fall behind in the last five feet. The optimal learning strategy is to track the ball over the first part of its trajectory with head movements and smooth pursuit eye movements, make a fast saccadic eye movement to the predicted point of bat–ball collision, and then let the ball catch up to the eye. The batter observes the ball, makes a prediction of where it will hit his bat, sees the actual position of the ball when it hits the bat, and uses this feedback to learn to predict better next time.

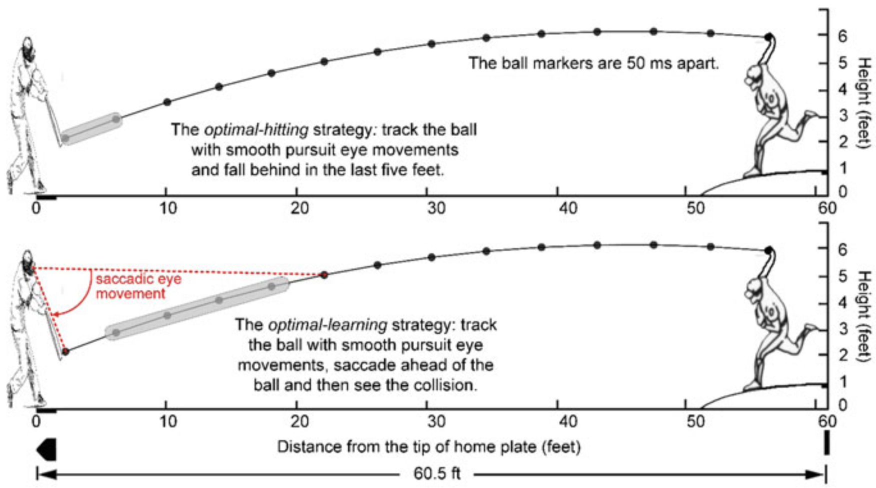

Fig. 10.10 Two tracking strategies. The batter's eye is not on the ball when the ball is in the gray ovals. The swing begins about 150 ms before bat–ball contact. About 15 feet in front of the plate for this slow 60 mph changeup

Ted Williams' statement "I couldn't see a ball hit the bat except on very, very rare occasions," implies that he did not need to use the optimal learning strategy because he had already learned to hit the ball.

Batters are not consciously aware of using these strategies. Just as you, the reader of this book, are not aware of the eye movements that you are making right now. While reading, you typically make a three-degree saccade to the right, then another and another. Your return to the beginning of the next line is accomplished with a saccade that is about ten degrees to the left and one half of a degree down. However, the saccade speeds and saccadic suppression prevents you from being aware of these eye movements. During a saccade, you do not see the world sweep across your retina: likewise, in a mirror, look at one eye, then the other; you do not see your eyes moving. Similarly, the batter is not aware of using these strategies or of switching between them.

10.12 The Advantage of Eye–Hand Cross-Dominance

The blind spot of the retina can mask the image of the bat–ball collision. The optic disk is an area in the human retina where the optic nerve passes out of the eyeball and up to the brain. There are no photoreceptors in the optic disk, so we do not see images projected onto it. Therefore, it is a *blind spot*. It is important to note that humans are not aware of the blind spots in their fields of vision, because their brains just "fill in" the holes. On the retina, the optic disk is about 6° wide. The center of the optic disk is 15.5° nasal and 1.5° superior to the center of the fovea. Figure 10.11 gives a simple test to demonstrate your blind spot.

We have now come to the crux of this chapter. We want to answer the question, "Why might eye–hand cross-dominance be an advantage for the batter?" Everything in this chapter has led up to answering this question.

In Fig. 10.12, the batter tracked the ball with head movements and smooth pursuit eye movements until it was about 5.5 feet in front of the front edge of the plate, which is marked with a black dashed line in Fig. 10.12. Then he fell behind. The bat–ball collision typically takes place 1.5 feet in front of the plate, which is marked with a thin straight red line. So, in this figure, at that point, the blind spot of his dominant right eye would have obscured the image of the collision. However,

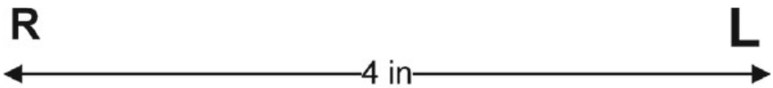

Fig. 10.11 Test illustrating the blind spot. Hold this book (or position your computer display screen) at arm's length (roughly two feet). Close or cover your left eye. Look at the letter R with your right eye. Be aware of the L in your peripheral vision, but do not look it. Keep focused on the R. Now slowly bring the page closer to your face. When it is around 18 inches away, the L will disappear. Keep bringing it closer. At around 12 inches, the L will reappear. The left eye test is analogous; just interchange R with L and right eye with left eye

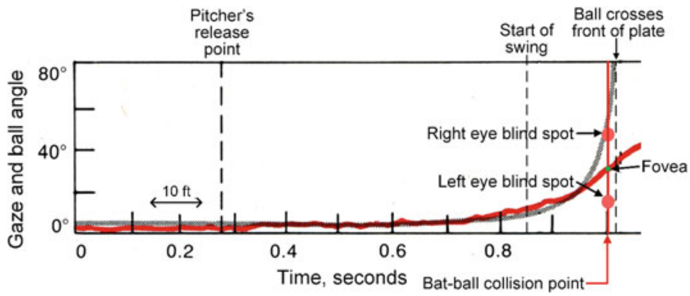

Fig. 10.12 The blind spot obscures the collision. For this pitch, the batter could not see the bat–ball collision because the blind spot of his dominate right eye masked its image. He was using the optimal hitting strategy. This figure contains the same ball and gaze position traces as in Fig. 10.6

the blind spot of his left eye would have been far away from the collision. Therefore, if he were left-eye dominant, then he *would* have been able to see the collision. *This* is the advantage of the cross-dominant batter.

The studies listed in Table 10.4 showed a lot of variability in their answers to the question, "Is eye–hand cross-dominance an advantage for the batter?" Our model gives a reason for this variability.

First, it would only be an advantage on the swings where the batter was using the optimal hitting strategy. Second, it would depend on just how far his eye was behind the ball. The blind spot would prevent feedback for pitches where the eye was 10°–20° behind the ball at the time of the bat–ball collision. These two effects produce variability in the data. People who were hoping for an unequivocal answer were wanting an explanation that would be the same for every pitch. Our explanation only comes into play for certain tracking behaviors of the batter, namely, when he is using the optimal hitting strategy, and when his eye is 10°–20° behind the ball at the time of the collision.

10.13 Summary

- Left-handed batters per se have no advantage over right-handed batters.
- Some right-handed batters have lower batting averages against right-handed pitchers than against left-handed pitchers. However, this is not due to physics or physiology: it might be due to psychology, to fear.
- The vergence eye movement system is too slow to keep both foveae on the ball, so only the dominant eye can see the bat–ball collision.
- Our major league batter was very good at suppressing his vestibulo-ocular reflex.
- To track the pitch, batters coordinate head movements, saccadic eye movements, smooth pursuit eye movements and vestibulo-ocular eye movements.

- Batters use one of the following two tracking strategies:
  - The optimal hitting strategy is to track the ball with head movements and smooth pursuit eye movements and fall behind in the last five feet.
  - The optimal learning strategy is to track the ball over the first part of its trajectory with head movements and smooth pursuit eye movements, make a fast saccadic eye movement to the predicted point of the bat–ball collision, and then let the ball catch up to the eye. Thus, the batter observes the ball, makes a prediction of where it will hit his bat, sees the actual position of the ball when it hits his bat, and uses this feedback to learn to predict the ball's trajectory better the next time.
- Finally, cross-dominant batters *do* have an advantage on some pitches. Because for non-cross-dominant batters, the blind spot of their dominate eye can obscure the bat–ball collision.

References

Adams, G. L. (1965). Effect of eye dominance on baseball batting. *Research Quarterly. American Association for Health, Physical Education and Recreation, 36*(1), 3–9. https://doi.org/10.1080/10671188.1965.10614650. Published online: 17 Mar 2013.

Bahill A. T., & LaRitz, T. (1984). Why can't batters keep their eyes on the ball. *American Scientist, 72*, 249–253.

Bahill, A. T., & Karnavas, W. J. (1993). The perceptual illusion of baseball's rising fastball and breaking curve ball. *Journal of Experimental Psychology: Human Perception and Performance, 19*(1), 3–14 (This paper was described in Science News, February 20, p. 116).

Bahill, A. T., & Baldwin, D. G. (2004). The rising fastball and other perceptual illusions of batters. In G. Hung & J. Pallis (Eds.), *Biomedical engineering principles in sports* (pp. 257–287). Kluwer Academic.

Classe, J. G., Daum, K., Semes, L., Wisniewski, J., Rutstein, R., Alexander, L., et al. (1996). Association between eye and hand dominance and hitting, fielding and pitching skill among players of the southern baseball league. *Journal of the American Optometric Association, 67* (2), 81–86.

DI Committee Changes to Flat-seamed Baseballs for 2015 Championship, http://www.ncaa.com/news/baseball/article/2013-11-05/di-committee-changes-flat-seamed-baseballs-2015-championship. Last Accessed August, 2018.

Fogt, N., & Persson, T. (2017). A pilot study of horizontal head and eye rotations in baseball batting. *Optometry and Vision Science, 94*(8), 789–796. https://doi.org/10.1097/opx.0000000000001100.

Hoyle, F. (1957). *The black cloud*. Middlesex England: Penguin Books.

Kensrud, J. R. (2010). *Determining aerodynamic properties of sports balls in situ, Master of Science thesis in mechanical engineering*. Washington State University.

Kensrud, J. R., Smith, L. V., Nathan, A., & Nevins, D. (2015). Relating baseball seam height to carry distance. *Procedia Engineering, 112,* 406–411.

Laby, D. M., Kirschen, D. G., Rosenbaum, A. L., & Mellman, M. F. (1998). The effect of ocular dominance on the performance of professional baseball players. *Ophthalmology, 105*(5), 864–866. https://doi.org/10.1016/s0161-6420(98)95027-8.

Lindbergh, B., & Lichtman, M. (2017, June 17). The Juiced Ball Is Back, *The Ringer*.

Milne, C., Buckolz, E., & Cardenas, M. (1995). Relationship of eye dominance and batting performance in baseball players. *International Journal of Sports Vision, 2*(1), 17–21.

Portal, J. M., & Romano, P. E. (1998). Major review: Ocular sighting dominance: A review and a study of athletic proficiency and eye-hand dominance in a collegiate baseball team. *Binocular Vision & Strabismus Quarterly, 13*(2), 125–132.

Schor, C. M. (2011). Neural control of eye movements, Chapter 9. *Adler's Physiology of the Eye*, 220–242.

Tieg, D. (1980). *Major league baseball research project* (pp. 1–9), Ridgefield: CT, Institute for Sports Vision.

Willman, D. (2017). *The BaseballSavant*, https://baseballsavant.mlb.com/statcast_search. Last Accessed November 2018.

Chapter 11
Dénouement

11.1 Introduction

Purpose: This chapter consolidates the insights and wisdom in this book.

11.2 What We Were Thinking

This book is about engineering the sport of baseball. It may have seemed to be about physics, but we were always on the lookout for instances where physiology or psychology should have come into play. For example, in Chaps. 4 and 7 it was essential to use physiology's force–velocity relationship of muscle. We also continually looked for fatigue and warm-up effects in data. Some of our studies, like the rising fastball that was not included so far in this book, dealt with issues that could only be explained using physiological psychology (Bahill and Karnavas 1993; Bahill and Baldwin 2003, 2004).

We made sure that we studied papers that had models different from ours. We did not want confirmation bias to restrict the papers that we chose to incorporate. Trying to hit a baseball with a bat is a task that is very attention demanding. Therefore, we looked for effects of cognitive overload. We were also on the alert for outliers that might challenge principles of physics that we used. For example, when we stated that energy cannot be created or destroyed, we were aware that in nuclear reactions mass can be converted into energy and vice versa. So we contemplated possible effects in our baseball environment and decided that there were none. The point of this paragraph is that while it might have seemed that we were merely modeling the physics of baseball, we were, and you the reader should have been, continually looking for other factors that could have affected our conclusions.

What does a person need to be a successful batter? Obviously, he or she must have good coordination, excellent vision, athleticism, desire and a strong work

A. T. Bahill, *The Science of Baseball*,
https://doi.org/10.1007/978-3-030-03032-2_11

ethic. When concentrating on the pitch, he or she must be able to ignore peripheral vision, the auditory system, the olfactory system and pain sensors. In addition, tracking the ball from the pitcher's release point to where it crosses the plate requires suppression of the vestibulo-ocular reflex (Bahill and LaRitz 1984), above average smooth pursuit eye tracking capability (Bahill and LaRitz 1984), an exemplary ability to learn to track unique smooth pursuit visual targets (McHugh and Bahill 1985) and a tremendous amount of cognitive effort (Kahneman 2011).

In a classic psychology experiment summarized by (Kahneman 2011), 4-year-old children were exposed to a cruel experiment. They were given a choice of one Oreo cookie, which they could eat at any time, or two Oreo cookies if they could wait fifteen minutes for the reward. About half the children managed the task of waiting fifteen minutes. A dozen years later, a large gap had opened between those who had resisted temptation and those who had not. The resisters had higher measures of executive functions in cognitive tasks, especially the ability to allocate their attention efficiently (Mischel et al. 1989). My conjecture is that children who can control their impulses and concentrate on the task at hand will have the potential to become more successful baseball and softball players because they have and will develop their executive functions more fully. This will allow them to be good at deciding *when* to do what. The following poem, which is explained in the appendix, is analogous to the third chapter of the book of *Ecclesiastes*, with apologies to Pete Seeger.

There is a season for everything,
a time for every action under heaven:
a time for thinking, and a time for reacting;
a time for planning, and a time for executing plans;
a time for exercising, and a time for relaxing;
a time for dreaming, and a time for studying;
a time for chitchat, and a time for negotiation;
a time for playing, and a time for practice;
a time for cheers, and a time for tears.

In writing this book, we were aware of differences in human cognitive processing. When we evaluated data published in peer-reviewed journals, we strove to discern the authors' recognition of how these human differences affected the authors' evaluation of their own data. For example, we expected less variability in the data of major league baseball players compared to collegiate players. If this was not apparent in the data, then the data were suspect.

We investigated the backgrounds of the authors of the papers that we relied on. We used this knowledge to help understand how they might have analyzed their data and created their models. For, example, the physicist's Effective Mass model does not use the force-velocity relationship of muscle to help understand how the batted-ball speed depends on bat weight. Whereas, the bioengineer's BaConLaws model connects directly with the force-velocity relationship of muscle.

In creating a model, we were always cognizant of the reader. We continually worried about whether or not a reader could replicate our experiments and equations.

Now, let us stop discussing what we were thinking while writing this book and return to what we actually wrote.

11.3 What We Wrote

Collisions between baseballs, softballs and bats are complex, and therefore their models are complex. One purpose of this book was to show how complex these collisions could be, while still being modeled using only Newton's axioms and the conservation laws of physics. Accordingly, this book presented the BaConLaws model for the speed and spin of balls and bats after the bat–ball collision in terms of these same four variables before the collision.

Chapter 1 presented Newton's axioms and laid the groundwork for analyzing bat–ball collisions. It also presented ten alternative models for the swing of a bat. Using text and figures, Chap. 2 explained nine common configurations of bat–ball collisions. Chapter 3 started the development of the sets of equations for these configurations.

The workhorse of this book, Chap. 4, contains our most comprehensive model, the BaConLaws model. It models a collision at the sweet spot of the bat with spin on the pitch. It has five equations and five unknowns. The equations are complete and comprehensive. This chapter contains a sensitivity analysis of the model, which shows that the most important variable in the model, in terms of maximizing batted-ball speed, is the bat speed before the collision. This chapter starts the fulfillment of the first purpose of this book by showing what may be the most complex model that is compatible with our simple technique and Newtonian physics. It also fulfills another purpose of this book, namely, to help batters select or create baseball or softball bats that would be the best for them. Cupping the barrel end of the bat does not help. This chapter is unique in the science of baseball literature.

The BaConLaws model also describes the motion of the *bat* after the collision. This is a big deal. Many models describe the motion of the ball after the collision, but few (if any) describe the motion of the bat. When you see a batter hit the ball, do you see the jerk of the bat? Can you describe it? Well these equations do. The jerk of the bat is readdressed in Chap. 9.

Chapter 5 contains four alternative models for bat–ball collisions. Their purposes are different and they are based on different fundamental principles. The Effective Mass model was created by physicists independent of the author of this book. Therefore, comparisons to it are important for validating the BaConLaws model. The Spiral Center of Mass model and the Sliding Pin model are data based, not theory based. They use a different approach and they use a different *type* of data. Finally, the Collision with Friction model considers friction during the collision. It is shown that this type of collision cannot be modeled using only the conservation laws. Therefore, this model completes the fulfillment of the first purpose of this book, by showing a configuration that is too complex for our simple technique.

Chapter 6 recapitulated Chaps. 1–5. These chapters are at a higher level of abstraction than typical physics of baseball papers, because they ignored details of the collision, such as (1) during the collision the ball can slip, slide, roll or grip the bat, and the ball switches between these modes, (2) the coefficient of friction changes from dynamic to static and back, (3) the bat and ball deform during the collision, (4) some collisions have normal and tangential velocity components and (5) the bat has a twist or a rotation about its long axis. This book also ignored the difference between the kinetic, energetic and kinematic coefficients of restitution, the energy loss due to tangential forces and losses in angular momentum: it grouped all of these energy losses into one parameter, the kinematic coefficient of restitution. We modeled the parameters of the bat and ball only at times just before and just after the collision. Because the equations are at a high level, it was possible to verify each major equation by at least two techniques. This book used simple terms that were presented in Table 1.1 that should be understandable by all students of the science of baseball. This book did not obfuscate with jargon, rules of thumb or esoteric terms. Using only fundamental principles, it is hoped that the reader gained intuition about the behavior of the bat and ball before and after collisions.

One purpose of the Ball in Flight model of Chap. 7 was to show how altitude, temperature, barometric pressure and relative humidity affect air density and consequently how air density affects the flight of the ball. To do this, we needed equations for the flight of the ball that included air density. Therefore, the first challenge of this chapter was to derive equations for the flight of the ball that included the dependence on air density. These equations were not restricted to Newton's axioms and they relied heavily on experimental data. Next, this chapter showed that air density is inversely related to altitude, temperature and humidity, and is directly related to barometric pressure. Air density affects how far a batted ball travels. As shown by this model, on a typical July afternoon in a major league baseball stadium, altitude is the most important factor, explaining 80% of the variability. This is followed by temperature (13%), barometric pressure (4%) and relative humidity (3%). A simple linear algebraic equation was presented that predicts air density in terms of these four variables. A different model showed how the batted ball's range depends on both the drag force and the Magnus force and considered the relative importance of each. As an aside, this chapter answered the question of whether a person could throw a heavy ball or a light ball farther. If all other parameters are held constant, a heavier ball might be thrown *slightly* farther than a lighter ball.

The purpose of Chap. 8 was to investigate the accuracy of simulations of the flight of the baseball. When the television announcer says, for example, "That home run went 431.1 feet." Our readers will know that he should have said, "The *true* range of that home run was 430 feet plus or minus 30 feet." The most important properties in these simulations are, in decreasing order of importance, CoR, Wind velocity, Air density, Initial spin of the batted ball, Launch speed and the Drag coefficient. These properties affect the range of the batted ball. The values stated on television broadcasts and internet sites for the range of home run balls probably have an estimated margin of error of around ±10% because they do not state values for these parameters. The easiest way to add accuracy would be to give the wind velocity during the ball's flight.

Chapter 9 presented the probability of success performance criterion. It incorporated this performance criterion into our bat–ball collision model. Simulating this model showed that the most important parameter in determining the vertical size of the sweet spot of the bat was the bat swing speed. The second most important parameter was the diameter of the bat. The results of simulating our models produced the conclusion that the sweet spot of the bat is about one-fifth of an inch high (5 mm).

Chapter 10 started with an explanation of our modus operandi for explaining baseball puzzles, namely, we use physics first, then physiology and finally psychology. This process led us to the following conclusions.

- Left-handed batters per se have no advantage over right-handed batters.
- Some right-handed batters have lower batting averages against right-handed pitchers than against left-handed pitchers. However, this is not due to physics or physiology: it might be due to psychology, to fear.
- The vergence eye movement system is too slow to keep both foveae on the ball, so only the dominant eye could possibly see the bat–ball collision.
- To track the pitch, batters coordinate head movements, saccadic eye movements, smooth pursuit eye movements and vestibulo-ocular eye movements.
- Batters use one of the following two tracking strategies:
  - The optimal hitting strategy is to track the ball with head movements and smooth pursuit eye movements and fall behind in the last five feet.
  - The optimal learning strategy is to track the ball over the first part of its trajectory with head movements and smooth pursuit eye movements, make a fast saccadic eye movement to the predicted point of the bat–ball collision, and then let the ball catch up to the eye. Thus, the batter observes the ball, makes a prediction of where it will hit his bat, sees the actual position of the ball when it hits his bat and uses this feedback to learn to predict the ball's trajectory better the next time.
- Finally, cross-dominant batters *do* have an advantage on some pitches. Because for non-cross-dominant batters, the blind spot of their dominate eye can obscure the bat–ball collision.

The effects of most properties in a model depend on the performance criteria being used. For the BaConLaws model of Chap. 4, the most important model variables and parameters, in terms of <u>maximizing batted-ball speed</u>, were the bat speed at the start of the collision and the Coefficient of Restitution (CoR). For the Ball in Flight model of Chap. 7, the most important model variables and parameters, in terms of <u>maximizing the range</u> of the batted ball, were the batted-ball speed and the diameter of the ball. For the Probability of Success model of Chap. 9, the most important model variables and parameters, in terms of <u>maximizing the vertical size of the sweet spot</u> of the bat, were the bat speed at the start of the collision and the diameter of the bat. These three models used different performance criteria, and therefore had different conclusions.

11.4 The Rising Fastball

For over 100 years, before the development of high-speed tracking cameras, batters complained about the rising fastball. They said it started normally, but right in front of home plate the ball suddenly jumped up three inches, making it hop over their bat. Well, such behavior is impossible according to the laws of physics. Furthermore, the manager and the first base coach never saw a ball jump over a bat. But the batters insisted that it did (Bahill and Karnavas 1993; Bahill and Baldwin 2004). In order to explain this phenomenon, we will use material from many previous chapters in this book.

The rising fastball is the pitcher's fault, or perhaps we should say it is due to his sneakiness. The pitcher induces the perceptual illusion of the rising fastball. He grooves the batter with a succession of pitches (or maybe just one) with the same speed. This causes the batter to create a mental model of the pitch, particularly of its speed. If the pitcher now throws a faster pitch and the batter uses his now outdated mental model. Then, the batter will underestimate the height of the ball at the collision point and will hence swing under the ball.

Let us use Fig. 10.10 (repeated here as Fig. 11.1) to explain the rising fastball in more detail. The batter observes the ball over the first third of its flight. Using his mental model that he created from the previous pitch, he underestimates the pitch speed, and therefore miscomputes the height of the bat–ball collision point. Then, at the start of his swing, he takes his eye off the ball to look at the predicted bat–ball collision point. When the ball comes back onto his fovea, it is higher than he thought it would be. Thus, he complains that the ball just hopped over his bat.

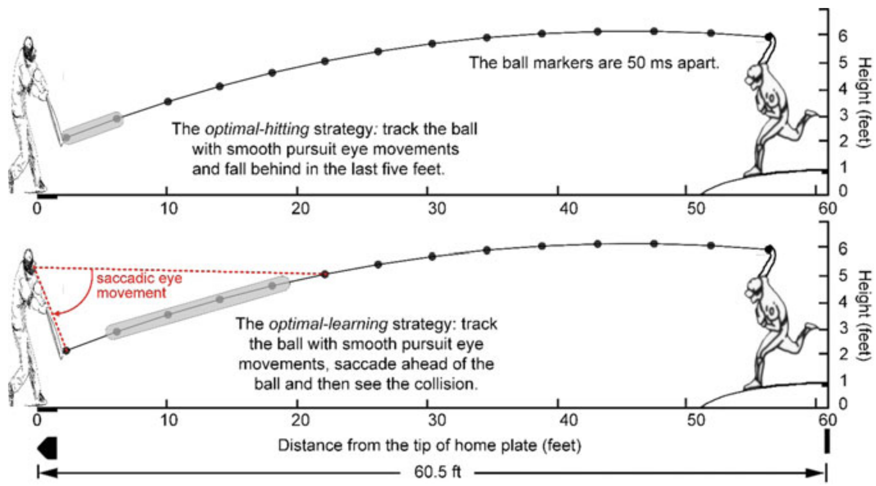

Fig. 11.1 Two tracking strategies

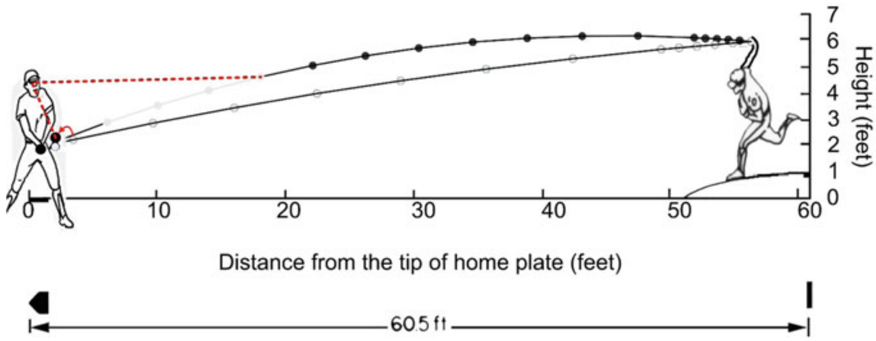

Fig. 11.2 The ball hopping over the bat

In Fig. 11.2, the batter last sees the ball (indicated with the dashed red line) when it is about 18 feet in front of the tip of the plate. The next time he sees the ball it is above his bat.

The rising fastball is a perceptual illusion that the pitcher produces by making the batter create an inappropriately slow mental model of the pitch. Then, when he throws a faster pitch, the batter thinks that it hopped over his bat. With the advent of computer tracking systems that show the true trajectory of the ball, batter doesn't complain about it anymore, although they may still perceive it.

11.5 Memoryless Versus Dynamic Systems

This section is not about baseball: it is intended for equation aficionados. The BaConLaws model of Chap. 4 comprises equations that give values for variables after the bat–ball collision in terms of values for those same variables before the collision. It is a memoryless model. The present values of the outputs depend only on the present values of the inputs. The variables are not functions of time. It uses algebraic not differential equations. The model is implemented with a spreadsheet. The following equations describe the BaConLaws model:

$$A = \frac{\left(v_{\text{ball-before}} - v_{\text{bat-cm-before}} - d_{\text{cm-ip}}\omega_{\text{bat-before}}\right)(1 + CoR_{2b})}{m_{\text{ball}}I_{\text{bat}} + m_{\text{bat}}I_{\text{bat}} + m_{\text{ball}}m_{\text{bat}}d_{\text{cm-ip}}^2}$$
$$v_{\text{ball-after}} = v_{\text{ball-before}} - Am_{\text{bat}}I_{\text{bat}}$$
$$v_{\text{bat-after}} = v_{\text{bat-before}} + Am_{\text{ball}}I_{\text{bat}}$$
$$\omega_{\text{bat-after}} = \omega_{\text{bat-before}} + Am_{\text{ball}}m_{\text{bat}}d_{\text{cm-ip}}$$
$$\omega_{\text{ball-after}} = \omega_{\text{ball-before}}$$

In contrast, the Ball in Flight model of Chap. 7 describes the movement of the ball as a function of time. Its inputs, outputs and state are functions of time. It is a dynamic system. Its future state depends on its present state and its present and

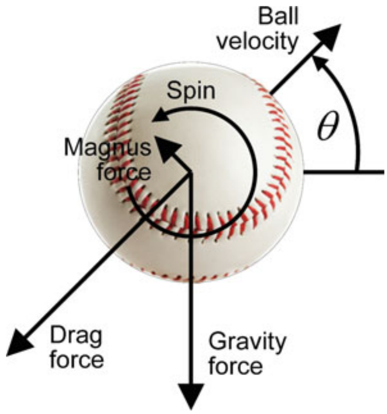

Fig. 11.3 Forces acting on the ball in flight

future inputs. The state of a dynamic system is the smallest set of variables (called state variables) such that knowledge of these variables at $t = t_0$, together with the knowledge of the input for $t \geq t_0$, completely determines the behavior of the system for any time $t \geq t_0$. The Ball in Flight model uses differential not algebraic equations. It is implemented with a computer simulation.

$$F_{\text{gravity}} = m_{\text{ball}} g$$

$$F_{\text{drag}} = 0.5\pi \rho r_{\text{ball}}^2 v_{\text{ball}}^2 C_{\text{D}}$$

$$F_{\text{Magnus}} = 0.5\pi \rho r_{\text{ball}}^3 \omega_{\text{ball}} v_{\text{ball}} C_{\text{M}}$$

Figure 11.3 and the above equations explain the forces acting on the ball in flight. The Ball in Flight model can be described with the standard equations of linear dynamic systems, aka state-space notation. In Fig. 11.3, let the direction of ball motion be the y-direction. We can write the sum of the forces in the y-direction as

$$F_{\text{y}} = -F_{\text{D}} - F_{\text{g}} \cos(90 - \theta)$$
$$F_{\text{y}} = -0.5\pi \rho r_{\text{ball}}^2 C_{\text{D}} v_{\text{ball}}^2 - m_{\text{ball}} g \sin\theta$$

For a ball flying through the air, our system equation is

$$m\ddot{y} = u$$

This means that the total force on the ball, u, is equal to the mass times the second derivative with respect to time of the position, y. In our dot notation, y double dot, $\ddot{y}$, is the second derivative with respect to time, which, in this case, is the acceleration and y dot, $\dot{y}$, is the first derivative, which is velocity. This is a second-order system so we will need two state variables represented by x_1 and x_2. Let them be the position and velocity of the ball in the y-direction.

$$x_1 = y$$
$$x_2 = \dot{y}$$

Then, we obtain

$$\dot{x}_1 = x_2$$
$$\dot{x}_2 = \ddot{y} = \frac{1}{m}u$$

Or substituting the total force in the y-direction

$$\dot{x}_1 = x_2$$
$$\dot{x}_2 = -\frac{\pi \rho r_{\text{ball}}^2 C_{\text{D}}}{2m_{\text{ball}}} x_2^2 - g \sin\theta$$

We were trying to get these equations into the vector-matrix form of

$$\dot{\mathbf{x}} = \mathbf{Ax} + \mathbf{Bu}$$

But we did not succeed because of the nonlinear x_2^2 term. We can write similar state equations for the perpendicular direction, but they will have similar squared terms.

This section explained the fundamental difference between the memoryless models of Chaps. 1–5 and 9, and the dynamic state-based model of Chap. 7.

In modeling a system, the first and most important question that needs to be answered is whether the system is memoryless or dynamic. To elaborate on this concept, let us consider a few physical systems. An ideal spring is a memoryless system, because the output position depends only on the input force applied, whereas an ideal mass is a dynamic system, because the output position depends on the applied input force as well as the initial position and velocity of the mass. An ideal resistor is a memoryless system, because the output voltage depends only on the input current, whereas a resistor–capacitor system is dynamic, because the output voltage depends on the input current as well as the initial capacitor voltage.

Let us now consider a totally different type of state-based system, one that is not described by differential equations. Let us look at the state-based game of baseball. If a baseball game were called due to rain, "What state information would you need to store to restart the game at a later date?" You would need to store the batting order, the runs scored by each team, the current inning, whether it is the top or the bottom of the inning, the last batter for each team, the number of outs in this half of the current inning, the balls and strikes on current batter, the names of the runners on first, second and third base and a list of players who have been removed from the game (this is important in baseball, because a removed player cannot return). You would need all this state information to restart a rain-delayed or postponed game. If you want to go into detail, you can also consider the number of times each catcher, manager and coach has gone out to talk to the pitcher. For Little League games you could list how many innings each pitcher pitched (pitchers are limited to six innings per week) and the children who were in attendance (players who were not there for the original game cannot play in the resumed game).

When creating models, we must be aware that there are two fundamentally different types of systems: memoryless and dynamic. In a memoryless system, the present values of the outputs depend only on the present values of the inputs. The models of Chaps. 1–5 and 9 were memoryless. In contrast, the Ball in Flight model of Chap. 7 was dynamic. Its future state depends on its present state and its present and future inputs. In Chap. 7 we hid these differential state equations from the reader.

Appendix

We concluded our paragraph about the 4-year-old children resisting their urge to eat the Oreo cookies with, “The resisters had higher measures of executive functions in cognitive tasks and especially the ability to allocate their attention efficiently.” Let us now analyze that sentence.

The field of cognitive neuroscience proposes that executive functions reside in a particular area of the brain named the prefrontal cortex. The basic executive functions include cognitive processes such as impulse control, use of working memory, attention control, resistance to interference and cognitive flexibility.

The first two of these functions develop in early childhood. *Impulse control*, also known as response inhibition, is an executive function that permits people to inhibit their impulses in order to select behaviors that are more likely to satisfy their goals. The resistors in the Oreo cookie experiment had good impulse control. *Use of working memory* is an executive function that holds and processes information for a short time.

The last three of these basic executive functions develop later in life. *Attention control* is an executive function that allows people to allocate their attention, to choose what they pay attention to and what they ignore. Attention control can be described as a person’s ability to concentrate or focus. *Resistance to interference* is an executive function that allows people to shutout stimuli that are irrelevant to the task at hand or to the mind’s current state. *Cognitive flexibility* is an executive function that allows people to efficiently switch between thinking about two different concepts and perhaps to control multiple tasks concurrently.

Multiple basic executive functions create high-order executive functions, which include planning, scheduling, negotiating, performing trade-off studies and problem-solving.

The executive functions that are most important for baseball players are arguably impulse control, use of working memory, attention control, resistance to interference and planning.

My conjecture is that children who can control their impulses and concentrate on the task at hand will probably become better baseball and softball players because they have and will develop their executive functions more fully. This will allow them to be good at deciding *when* to do what. The following poem is analogous to the third chapter of the book of *Ecclesiastes*, with apologies to Pete Seeger.

There is a season for everything,
a time for every action under heaven:
a time for thinking, and a time for reacting;
a time for planning, and a time for executing plans;
a time for exercising, and a time for relaxing;
a time for dreaming, and a time for studying;
a time for chitchat, and a time for negotiation;
a time for playing, and a time for practice;
a time for cheers, and a time for tears.

A time for thinking, and a time for reacting.

It takes exceptional attention control for a batter to track a pitch and predict the ball's position at the time of the collision. The batter must resist interfering distractions. On the other hand, the swing of the bat is merely a reaction. It is an over-practiced reaction with little variability.

Meanwhile, the pitcher is trying to confuse the batter's thinking. The pitcher will use the batter's working memory against him. The pitcher produces the perceptual illusion of the rising fastball by fooling the batter into creating an inappropriately slow mental model of the pitch in his working memory. Then, when he throws a faster pitch, the batter underestimates its speed, and therefore its height when it crosses the plate: consequently he complains that the ball hopped over his bat.

The batter must also practice impulse control. He must wait for his pitch and when it arrives he cannot try to kill it.

A time for planning, and a time for executing plans.

Before each pitch, every fielder plans what he or she will do for every contingency. For instance, assume that the game is tied in the bottom of the sixth inning. There are no balls, no strikes and no outs. There are runners on first and third. Each fielder must formulate a plan. For example, on a deep fly ball, an outfielder will throw the ball to the cutoff man (the second baseman or the shortstop depending on where the ball was hit). On a lazy fly ball, if the runner on third is tagging, the outfielder will throw to home plate through the cutoff man. On a shallow hit, if the runner on third is advancing, then the outfielder will throw to the catcher; if not, then the fielder must throw to second base. All of these plans must be in the fielder's working memory before the pitch. Because, when the ball is hit, there is no time for planning: there is only time for executing the plan. After the planning and right before the pitch, each fielder must focus on picking up a sign of the type of pitch to come. Then, using cognitive flexibility, he or she must switch attention to the batter picking up any clues he might divulge, and finally the fielder must switch attention to the predicted bat–ball collision point.

A time for exercising, and a time for relaxing.
Athletes must be in good physical shape. Regularly scheduled exercise can help achieve this. However, all work and no play makes Jack a dull boy.

A time for dreaming, and a time for studying.
There is no time for daydreaming during a game. Attention control is paramount, whereas, between games, there is plenty of time for study; to study the opposition, to read books like this one and to learn about the world around us.

A time for chitchat, and a time for negotiation.
Talking about personal lives helps players understand how their teammates will react during a game. It is important that outfielders, for example, know each other well. On a line drive between them, a trade-off decision must be made quickly so that one of them runs in and the other runs out: this prevents collisions and broken bones. In contrast, most players will not negotiate with their agents during the season because they do not want the distraction.

A time for playing, and a time for practice.
When you are playing a game, attention control must keep your brain totally engaged in the game. In Chap. 4, we quoted Dave Baldwin as saying that if you lose a game, don't blame the umpire or your teammates; just go home and practice harder.

A time for cheers, and a time for tears.
After every win, all players cheer, whereas when a team is eliminated from the championship tournament, many players cry.

References

Bahill, A. T., & Baldwin, D. G. (2003). The vertical illusions of batters. *The Baseball Research Journal, 32,* 26–30.

Bahill, A. T., & Baldwin, D. G. (2004). The rising fastball and other perceptual illusions of batters. In G. Hung & J. Pallis (Eds.), *Biomedical engineering principles in sports* (pp. 257–287). Kluwer Academic.

Bahill, A. T., & Karnavas, W. J. (1993). The perceptual illusion of baseball's rising fastball and breaking curve ball. *Journal of Experimental Psychology: Human Perception and Performance, 19*(1), 3–14.

Bahill, A. T., & LaRitz T. (1984). Why can't batters keep their eyes on the ball. *American Scientist, 72*, 249–253.

Kahneman, D. (2011). *Thinking, fast and slow*. NY: Farrar, Straus and Giroux.

McHugh, D. E., & Bahill, A. T. (1985). Learning to track predictable target waveforms without a time delay. *Investigative Ophthalmology & Visual Science, 26,* 932–937.

Mischel, W., Shoda, Y., & Rodriguez, M. L. (1989). Delay of gratification in children. *Science, 244*(4907), 933–938. https://doi.org/10.1126/science.2658056.

Chapter 12
General Modeling Principles

12.1 Introduction

The following statement was on Richard Feynman's whiteboard when he died. By *create* he meant derive equations mathematically, on a whiteboard, in real-time, in front of an audience and without notes.

What I cannot create,
I do not understand.
Richard Feynman

What I cannot model,
I do not understand.
Terry Bahill

Purpose: This chapter extracts the modeling lessons learned throughout this book into one cohesive whole. It is based on Bahill (2016).

12.2 Why Model?

This book is about modeling and simulation of bat–ball collisions and the flight of the ball. A *model* is a simplified representation of some aspect of a real system. A *simulation* is an implementation of a model, often on a digital computer. Models are ephemeral: they are created, they explain a phenomenon, they stimulate discussion, they foment alternatives and then they are replaced by new models. Everyone knows how to make a model, but most modelers miss a few tasks. Therefore, we wrote this chapter that presents a succinct description of the modeling process shown in Fig. 12.1.

A. T. Bahill, *The Science of Baseball*,
https://doi.org/10.1007/978-3-030-03032-2_12

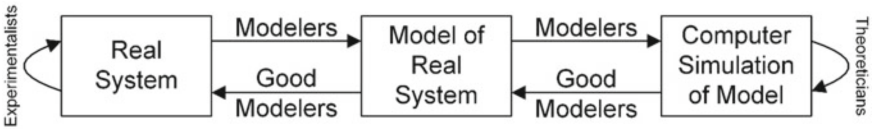

Fig. 12.1 The modeling process

Most systems are impossible to study in their entirety, but they are made up of hierarchies of smaller subsystems that can be studied. Nobel Laureate Herb Simon (1962) explained the necessity for such hierarchies in complex systems. He wrote that complex systems are decomposable, enabling subsystems to be studied without the entire hierarchy. For example, when modeling the movement of a pitched baseball, it is sufficient to apply Newtonian mechanics considering only gravity, the ball's velocity and the ball's spin. One need not be concerned about electron orbits of atoms in the cowhide cover or the motions of the sun and the moon. Forces that are important when studying objects at one level seldom affect objects at another level. When modeling baseball systems, we are fortunate that we do not have to consider how astronomical black holes form or the entanglement of subatomic particles, which Einstein mocked as "spooky action at a distance."

Table 12.1 shows a sampling of the levels of two of the hierarchies that were used in this book. Items at the bottom of each section of this table are at the lowest level considered in this book. Items that are higher up in the table are at a higher level of abstraction. The point is, in Chap. 7, for example, we studied altitude, temperature, humidity and barometric pressure and derived equations for them. Later, we studied the equations for F_{gravity}, F_{drag} and F_{Magnus}. Later still, we studied the range of the batted ball. We studied them independently. Models should only exchange inputs and outputs with other models at the same level or those one level higher or lower.

12.2.1 Purpose of Models

Models can be used for many reasons such as guiding decisions, understanding an existing system (done in this book), improving a system, creating a new design or system, controlling a system, improving operator performance, suggesting new experiments, guiding data collection activities (done in this book), allocating resources, identifying cost drivers, increasing return on investment, helping to sell the product and reducing risk. Running business process models clarifies requirements, reveals bottlenecks, reduces cost, identifies fragmented activities and exposes duplication of efforts.

Table 12.1 Levels in the bat–ball modeling hierarchy

Chapter 7 the Ball in Flight model
What effects air density and what does air density effect?
Sensitivity analysis
Range of the batted ball
The order of determining numerical values for the parameters (Table 7.15)
The right-hand rules
$F_{\text{gravity}} = m_{\text{ball}} g$ $F_{\text{drag}} = 0.5\pi\rho r_{\text{ball}}^2 v_{\text{ball}}^2 C_{\text{D}}$ $F_{\text{Magnus}} = 0.5\pi\rho r_{\text{ball}}^3 \omega_{\text{ball}} v_{\text{ball}} C_{\text{M}}$
Air density
Altitude, temperature, humidity and barometric pressure
Chapter 4 the BaConLaws model
Advice for choosing and modifying a bat
Sensitivity analysis
KE_{lost}, Eq. (4.11)
Output equations, Eqs. (4.8), (4.9), (4.10) and (4.12)
Conservation laws, Eqs. (4.3), (4.4) and (4.7)
Newton's axioms, *CoR*, Eqs. (4.5) and (4.6)
$v_{\text{ball-before}}$, $\omega_{\text{ball-before}}$, $v_{\text{bat-cm-before}}$, $\omega_{\text{bat-before}}$, $v_{\text{ball-after}}$, $\omega_{\text{ball-after}}$, $v_{\text{bat-cm-after}}$ and $\omega_{\text{bat-after}}$

12.2.2 *Kinds of Models*

There are different kinds of models: there are models of behavior, of structure, of performance and for analysis. *Models of behavior* describe how the system responds to external excitation: that is, how the system functions transform the inputs into outputs. The BaConLaws model is a model of behavior. It describes the linear and angular velocity of the bat and the ball after the collision in terms of these same parameters before the collision. *Models of structure* describe the components and their interactions. Three-dimensional CAD/CAM images check the buildability of structures. *Models of performance* describe units, values and tolerances for properties such as weight, speed of response, power required, etc. These might be captured in requirements. Typical baseball performance measures include batting average, slugging average and On-Base Plus Slugging (OPS). *Models for analysis* are used to calculate the properties of the whole system from the properties of its parts. For example, the time for a car to accelerate from 0 to 60 mph can be calculated from the mass of the car, the power of the drive train, the aerodynamic drag coefficient and the friction of the tires on the pavement.

12.2.3 Types of Models

There are many types of models. Most people use only a few and think that is all there are. Here is a partial list of some of the most commonly used types of models: physiological and physical laws and principles, differential equations, difference equations, algebraic equations, geometric representations of physical structure, computer simulations and animations, Laplace transforms, transfer functions, linear systems theory, state-space models, e.g., $\dot{x} = \mathbf{A}x + \mathbf{B}u$, state machine diagrams, charts, graphs, drawings, pictures, functional flow block diagrams, object-oriented models, UML and SysML diagrams, Markov processes, time-series models, physical analogs, Monte Carlo simulations, optimization equations, statistical distributions, mathematical programming, financial models, Pert charts, Gantt charts, risk analyses, trade-off studies, mental models, stories, scenarios and use cases. The best type of model depends on the particular system being studied and the background of the modeler.

To understand how people make decisions, we would use at least the following three models: confirmation bias, attribute substitution and representativeness. For biological domains, we must first choose a virus, a bacterium, a plant or an animal. Once we have chosen our subject, we could then derive its genome. For social domains, we might use a novel, an encyclical, a song, a poem or perhaps even a joke.

Most models require a combination of these types. For example, in this book we used Newton's axioms, the conservation laws of physics, algebraic equations, spreadsheets, figures, tables, simulations, an optimization package, design of experiments and statistics. Hence, our BaConLaws model and our Ball in Flight model comprise many types of models.

12.2.4 Tasks in the Modeling Process

The following checklist contains the principle tasks that should be performed in a modeling study. The modelers should look at each item on the list and ask if they have done that task. If not, they should state why they did not do it. In this checklist, we describe {in squiggly braces} the parts of the BaConLaws model that implement the individual tasks.

- Describe the system to be modeled. {The BaConLaws model describes head-on collisions between bats and balls. It gives the velocity and spin of the bat and ball before and after collisions. It does not describe the dynamics during the collision nor the swing of the bat.}
- State the purpose of the model. {To explain bat–ball collisions with precise, correct equations, without jargon.} This includes defining the performance criterion function.

- Determine the level of the model. {The level for the BaConLaws model encompasses the ball velocity, the bat velocity and the bat angular velocity after the collision in terms of those same parameters before the collision. The time scale is in milliseconds.}
- State the assumptions and at every review reassess the assumptions. {Our assumptions were stated in Sects. 3.1.2 and 3.2.1.4.}
- Investigate alternative models. {Many bat swing models were presented in Chap. 1. Alternative collision configurations were explained in Chaps. 2 and 3. Chapter 3 also presented nine alternative definitions for the sweet spot of the bat. The BaConLaws model was given in Chap. 4 and alternative models were given in Chaps. 5 and 9. Having alternative models helps ensure that you understand the physical system. No model is more correct than another. Alternative models just emphasize different aspects of the physical system. They are not competing models; they are synergetic.}
- Select a tool or language for the model and simulation. {We used the What'sBest! Optimizer, Pascal, Excel spreadsheets, the Math Type equation editor and MS Word.} This should not be a casual decision. You should not merely accept the default. You should use a trade-off study to help you select the best tool.
- Make the model. {Creating the BaConLaws model was described in Chap. 4.}
- Integrate with models for other systems. {The outputs of the BaConLaws model became inputs to the Ball in Flight model of Chap. 7 and the Probability of Success model in Chap. 9.}
- Gather data describing system behavior. {We used data from our internal databases, from peer-reviewed journal papers and from the following databases.}
  http://mlb.com/statcast/
  https://baseballsavant.mlb.com/statcast_search
  https://www.baseball-reference.com/
- Show that the model behaves like the real system. {The outputs of the simulations were compared to the data listed in the above paragraph.}
- Verify and validate the model. {Verification means, Did you build the system right? For the BaConLaws model, the outputs of the simulations agree with data listed in the above paragraph. The double checks in the simulation ensure correctness of the spreadsheets. For example, the kinetic energy lost is computed with Eq. (4.11) and also by summing individual kinetic energy components as shown in Tables 4.3 and 5.3. The conservation laws were used in the derivations and the final outputs of the simulation were inserted into the conservation law equations to ensure consistency of the spreadsheet. The main output of the BaConLaws model was compared to the output of the Effective Mass model of Sect. 5.2. The physics was peer-reviewed by two anonymous physics professors. Each of the main BaConLaws equations was derived using at least two techniques. Finally, the equations were checked by an independent mathematician. Validation means, did you build the right system? Our customer

wanted a system that described head-on collisions between bats and balls. They wanted a system that would give ball velocity, bat velocity and the bat angular velocity after the collision in terms of those same parameters before the collision. This is what our system does. Finally, we performed a sensitivity analysis, which is a powerful validation tool (Smith et al. 2008). It warns if something is wrong with the model.} Enough details should be given to allow other researchers to replicate your results. If other people cannot replicate your experiments and analysis, then your model fails validation.

- Explain a discovery that was not planned in the model's design. {(1) We were surprised when the equation for the kinetic energy lost in the collision, Eq. (4.11), fell right out of BaConLaws set of equations. (2) Before writing this book, we did not expect to prove that cupping the barrel end of the bat does little good. (3) Although it seems intuitive, we were surprised when the mathematics showed that the baseball could be thrown farther than a tennis ball.}
- Perform a sensitivity analysis of the model. {The most important parameters, in terms of maximizing batted-ball speed, are the velocity of the center of mass of the bat before the collision and the coefficient of restitution, *CoR*. The least important parameters are the angular velocity of the pitched ball and the distance between the center of mass and the impact point. The second-order interaction terms are small, which is good.}
- Perform a risk analysis. {*Risk to our publisher*. The biggest risk is that people might be reluctant to buy a book with equations in it. Also, Springer would be disappointed if sales were low. Therefore, by writing with the reader in mind, we tried to ensure that sales would not be below expectations. We anticipate no copyright problems, because most of the material is original and we have permissions for the two figures that are not. *Risk to our reader*. Someone could modify their bat and hurt himself or herself working with tools or they could be thrown out of a game. *Risk to the author*. If our equations were wrong, we would confuse our readers and tarnish our reputations. *Risk to quality*. The book is produced in India. Typographical and editing mistakes that occur are hard to correct because of poor communication channels. *Risk to baseball managers, general managers and umpires*. It will put a burden on these people to understand the results of mathematical modeling. *Risk to MLB*. It could embarrass MLB into disclosing their algorithms. Some of these risks may seem unlikely. But a risk analysis is supposed to explore unlikely risks.}
- Analyze the performance of the model. {This was described above in the verification paragraph.}
- Re-evaluate and improve the model. {In the future, we will derive equations for configurations 3 and 4. We will explain why the curveball curves. We will also investigate the cognitive processing and decision-making of the batter (Bahill and Baldwin 2004; Bahill et al. 2005; McBeath et al. 2008; Bahill and Madni 2017). We will describe the thrust and parry of the pitcher and the batter.}
- Suggest new experiments and measurements for the real system that might challenge existing models. {Major League Baseball (MLB) is providing copious amounts of new data. Next, scientists need MLBs actual algorithms and

measurements for the spin on the batted ball, particularly for the home run trajectories that are so popular. Another proposed area of measurement and display involves the erratic meandering of fielders trying to catch pop-ups. This behavior and the paper by McBeath et al. (2008) show that the ball's trajectory must contain bizarre loops and cusps. MLB should show these trajectories on the television screen to help laypeople understand the fielders' wanderings. In the third edition of this book, once we build a gold-standard input data set for swings of the bat, we will directly compare the BaConLaws and the Sliding Pin models.}

12.2.5 Choose a Cute Name for Your Model

You want people to relate to the name of your model. This will enhance financial support. In the following couplets, we give the original model name and then an alternative name. Which do you think is best?

- Would you rather have had your taxpayer dollars

  support research on the Big Bang or on a theory of the origin of the universe?
  support research on dark energy or on the existence of transparent matter?
  support the Superconducting Super Collider or the search for the God particle?
  get rid of weapons of mass destruction or a tyrannical despot?

- Would you rather

  go to the opera *The Marriage of Figaro* or to Mozart's opera in D major Köchel No 492?
  listen to Beethoven's *Ode to Joy* or his Symphony Number 9 in D minor, Opus 125?
  listen to Mussorgsky's *Night on Bald Mountain* or his musical picture in D minor?
  listen to Wagner's Overture to Act III of *Lohengrin* or see the Chinese downhill snow skiing scene in the Beatles' movie *Help?*

- Would you rather

  read an article about $E = mc^2$ or a paper about mass–energy equivalence?
  study the DNA double helix or chromosomal structure?
  see a grand slam or a bases-loaded home run in baseball?
  see a Hail Mary or a fourth-quarter fourth-down 40-yard pass in football?

- Are you more likely to

  have wished for the fall of the Iron Curtain or of communism in eastern Europe?
  order Baked Alaska or ice cream covered with roasted merengue?
  watch the World Series or the MLB championship games?
  watch the Super Bowl or the NFL championship game?

- In Kahneman's model for human thinking, which do you relate to

  System 1 or the fast, instinctive and emotional system?
  System 2 or the slow, deliberative and logical system?

- Are you more likely to say

  Navy SEALs or navy sea air land forces?
  SWAT team or special weapons and tactics team?

The point of this page is to convince you that a distinctive descriptive name for your model will help people remember it and relate to it. This will be aided if your name is iconic. Examples of iconic images include the flag of the United States of America, the Statue of Liberty, a crucifix, a Star of David, the Nazi swastika, the Apple Computer Company logo and the Mona Lisa. Examples of iconic smells include Hydrogen Sulfide (rotten eggs) and Methyl Mercaptan (the odor in natural gas). Our favorite perfume fragrances are eau de Wet Dog and Impending Desert Rain. You want your name to be as memorable as the eight notes at the beginning of Beethoven's fifth symphony, the three dramatic notes in Neil Diamond's *Sweet Caroline* and the opening measures of Stanley Kubrick's 1968 film *2001: A Space Odyssey* (aka Strauss' *Also sprach Zarathustra*, opus 30, 1896).

12.2.6 Model-Based Design

There are two common techniques for designing a system or making a model: the first is model-based or theory-based (Bahill and Szidarovszky 2009) and the second is data-based (Bahill 2016). Here are some steps for model-based system design. Find appropriate physical, physiological and psychological principles, then using the tasks listed in the above section, design, build and test a model, then design and conduct experiments to collect data. Use these data to verify and validate the model. Use the model to make predictions and guide future data collection activities.

Example 1

Chapter 4 started with the following fundamental principles of physics: Conservation of Energy, Conservation of Linear Momentum, the Definition of *CoR*, Newton's Second axiom and the Conservation of Angular Momentum. These conservation laws are the models (or theories) that the BaConLaws model and the Effective Mass model were based on.

Example 2

Chapter 7 started with the right-hand rules and the three forces that affect the ball in flight: gravity pulls the ball downward, air resistance or drag operates in the opposite direction of the ball's motion and if the ball is spinning, there is a Magnus force perpendicular to the direction of motion. Watts and Bahill (1990) wrote these equations for those forces:

$$F_{\text{gravity}} = m_{\text{ball}} g$$

$$F_{\text{drag}} = 0.5\pi\rho r_{\text{ball}}^2 v_{\text{ball}}^2 C_{\text{D}}$$

$$F_{\text{Magnus}} = 0.5\pi\rho r_{\text{ball}}^3 \omega_{\text{ball}} v_{\text{ball}} C_{\text{M}}$$

These equations are the models (or theories) that the Ball in Flight model of Chap. 7 was based on.

12.2.7 Data-Based Design

The second technique for designing a system or making a model is data-based. With this technique, the modeler starts with measuring and organizing the data and then he or she makes a model that fits that measured data. The Spiral Center of Mass and the Sliding Pin models of Chap. 5 were data-based. We found the experimental data first and then we created the model to match that data.

The BaConLaws and the Effective Mass models started with the model of a free-end collision involving the velocity of the center of mass of the bat and the bat's angular rotation about the center of mass. In contrast, for the Sliding Pin model, we first found experimental studies that gave the linear velocity of the knob and the angular velocity of the bat about the knob right before the collision. We then used that data to make our model.

12.2.8 Second Sourcing

It is good practice to make sure that anything you regularly buy has a second source. That way if your first source disappears, you can continue to function.

Modelers should entice other scientists to create different models for the same physical system. This will help validate their models.

Many fields of science are demanding replication of important experiments and results. Failures to replicate previous findings are common in science, particularly in the psychological literature, where half of the important findings cannot be replicated (https://en.wikipedia.org/wiki/Replication_crisis).

If you are going to remodel your house, which faucet manufacturer are you likely to specify, Moen or LightInTheBox? Think about repair and maintenance of the system in ten years.

Would you buy a chandelier with incandescent light bulbs and a dimmer control? Keep in mind that they do not make incandescent replacement light bulbs anymore.

Missile manufacturers will not specify a part if there is not a second source. They want to ensure that they can continue manufacturing even if their first source goes bankrupt.

The atomic bombs dropped in WWII, Little Boy and Fat Man, were of different designs and used different fissionable elements (U_{235} and Plutonium, respectively). If one design did not work, then there was still a second source.

The Apollo 13 mission was not a disaster, because they had a second source of power: the lunar lander.

The county directors of elections would like to have a second source for their hardware and software. Because on Election Day, they have only one chance to get it right. A second source would also ameliorate cyberattacks.

Suppose your new primary care physician tells you that some test has just revealed cancer and she recommends that you start radiation treatment immediately. Would you ask for a second opinion before proceeding?

When asking for driving directions to a destination, it makes sense to ask for alternative routes (perhaps the quickest, the shortest and also the cheapest, i.e., no tolls), so that you have alternatives, in case of a massive traffic jam.

It is a good idea to have two e-mail accounts. That way if Comcast decides to block one of your correspondents because he or she fits their profile of a “bad person” or if Microsoft is “upgrading” their e-mail system, you can still communicate with the world.

I am sure that all readers of this book can access it from more than one place: you have multiple sources for this book. I am also confident that you back up your hard disk everyday. So now, dear reader, please put down this book and go back up your hard disk.

12.2.9 The SIMILAR Process

This section presents a process that we use for doing everything. We used this process when writing this book. Processes are used by individuals, teams and organizations to increase predictability of outcomes and ultimately probability of success. Over the years, these processes have been described in both technical and nontechnical terms. Although they used different vocabularies and levels of detail, it turns out that most process descriptions were surprisingly similar. Bahill and Gissing (1998) compared the descriptions of a hundred processes and extracted the similarities. They discovered that these seven key activities are common to most processes: **S**tate the problem, **I**nvestigate alternatives, **M**odel the system, **I**ntegrate components, **L**aunch the system, **A**ssess performance and **R**e-evaluate. These seven activities are conveniently summarized using the acronym, SIMILAR: **S**tate, **I**nvestigate, **M**odel, **I**ntegrate, **L**aunch, **A**ssess and **R**e-evaluate. They are

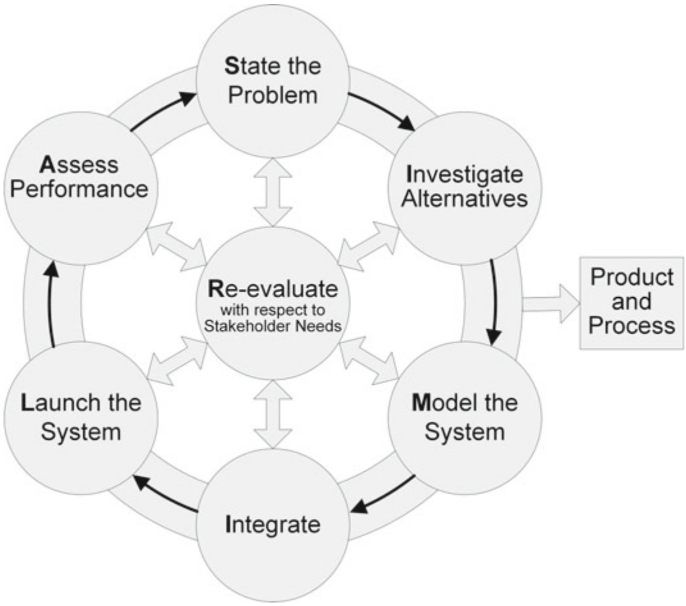

Fig. 12.2 The SIMILAR process

incorporated into the SIMILAR process of Fig. 12.2. We use this process to provide the overall context for problem-solving. At the outset, we note that the functions in the SIMILAR process are performed iteratively and in parallel. Each activity in this process is described next.

12.2.9.1 State the Problem

The problem statement begins either with a description of the purpose of the system, the top-level functions that it is expected to perform or a deficiency that needs to be corrected. The problem should be stated in terms of *what* needs to be done, not *how* it must be done. The problem may be described using stories and use case models. Inputs are provided by end users, operators, maintainers, suppliers, acquirers, owners, customers, bill payers, regulatory agencies, affected individuals or organizations, sponsors, manufacturers and other stakeholders. The Re-evaluate activity will help refine the problem statement.

12.2.9.2 Investigate Alternatives

Alternatives are evaluated using criteria such as performance, cost, schedule and risk. Since no one particular alternative is likely to be best on all evaluation criteria, multi-criteria decision-making techniques are used to identify the preferred alternatives. This type of analysis is typically repeated when additional data become available. For example, evaluation criteria should be computed initially based on estimates made by design engineers. Then, models are constructed and evaluated. Next, simulation data are generated. Thereafter, prototype performance is measured, and ultimately tests are performed on the real system. When designing complex systems, alternative designs are generated to explore design sensitivities to specific parameters of interest and to reduce project risks. Alternative designs range from analysis of alternatives at the system level down to alternative subsystem designs. As importantly, investigating alternatives helps to clarify and occasionally reformulate the statement of the problem.

12.2.9.3 Model the System

Abstract models are typically created for most alternatives. After a design has been selected, the model for the preferred alternative is consistently elaborated (that is, expanded) and then used to manage system development and use throughout the system's lifecycle. A variety of system models can be used to create system designs. These include physical analogs, analytic equations, state machines, block diagrams, functional flow diagrams, object-oriented models, computer simulations and mental models. The engineering function is typically responsible for creating both the product and the process for producing it. Therefore, models are invariably constructed for both the product and the process, and capture the relationships between them. For example, *process* models can be used to study schedule changes, create dynamic PERT charts and perform sensitivity analyses to determine the effects of delaying or accelerating certain subprojects. Executing process models can reveal bottlenecks and fragmented activities, identify opportunities to reduce cost and expose duplication of effort. *Produc*t models help in understanding and explaining the system, conducting trade-off studies and identifying and managing risks.

12.2.9.4 Integrate

Integration means bringing elements together so they work as a whole to accomplish their intended purpose and deliver value. Specifically, systems, enterprises and people need to be integrated to achieve desired outcomes. To this end, interfaces need to be designed between subsystems. Subsystems are typically defined along natural boundaries in a manner that minimizes the amount of information exchanged between the subsystems. Well-designed subsystems send finished products to other subsystems. Feedback loops around individual subsystems are easier to manage than feedback loops involving densely interconnected subsystems.

12.2.9.5 Launch the System

Launching the System means either deploying and running the actual system in the operational environment, or exercising the model in a simulated environment to produce outputs necessary for evaluation. In a manufacturing environment, this might mean modifying and using commercial-off-the-shelf hardware and software, writing prototype code and/or bending metal. In the business environment, launching the system means that the business plan is decomposed into tasks and actions and is deployed throughout the company. The purpose of the system launch is to provide an environment that allows the system or its model to do what it is being designed to do.

12.2.9.6 Assess Performance

Evaluation criteria, technical performance measures and metrics are used to assess performance. For example, evaluation criteria are used to quantify requirements in trade-off studies. Technical performance measures are used to mitigate risk during both design and manufacturing. Metrics are used to manage a company's processes. Ultimately, it comes down to measurements. If you cannot measure it, you cannot control it. If you cannot control it, you cannot improve it.

12.2.9.7 Re-evaluate

Re-evaluation is arguably one of the most important activities of the SIMILAR process. For over a century, engineers have used feedback to control systems and improve performance. It is one of the most fundamental engineering concepts. Re-evaluation is a continual process with multiple parallel loops. Re-evaluation means observing outputs and using this information to modify the inputs, the product and/or the process. The SIMILAR process of Fig. 12.2 clearly shows the distributed nature of the Re-evaluate function in the feedback loops. However, it is important to realize that all the loops will not always come into play. The loops that are used depend on the problem to be solved, the time in the system lifecycle and the problem context.

12.2.9.8 The SIMILAR Process Applied to This Book

Let us now show how the SIMILAR process was used in the developing this book.

State the problem: In the big inning, there were no books that derived (1) equations for the speed and spin of the bat and the baseball after the collision in terms of these same variables before the collision and (2) equations governing the flight of the ball. And, we needed such equations in order to understand baseball.

Investigate alternatives: We considered publishing a book, multiple papers, a monograph and a website containing such equations and their models. We considered hardback books, paperback books and electronic delivery. We negotiated with four alternative book publishers.

Model the system: The first draft and subsequent revisions done with MS Word and Visio was the first model of the book. The final book used professional XML publication software.

Integrate: The list of references at the end of each chapter suggests how the knowledge in this book was integrated with the scientific literature. This was the most arduous of the seven SIMILAR process activities. We also integrated the author in Arizona, the editors in New York City and the producers in India. However, feedback to India was flawed.

Launch the system: The first edition of this book was published in January 2018.

Assess performance: The publisher and I tracked sales of the book. We sought critical comments from students in my class and other readers of the book.

Re-evaluate: We realized that we needed a chapter assessing the accuracy of our simulations. So we wrote one for the second edition. We resurrected our Probability of Success model and incorporated it into the second edition. Then, we discovered in our data an explanation for the advantage of the cross-dominant batter. This was such a surprise that we exuberantly included it in the second edition.

We are now ready to repeat this process for the third edition.

References

Bahill, A. T. (2016). Model for absorption of perfluoropropane intraocular gas after retinal surgeries. *International Journal of Medical and Health Sciences Research (PAK Publishing Group), 3*(5), 50–76. https://doi.org/10.18488/journal.9/2016.3.5/9.5.50.76.

Bahill, A. T., & Baldwin, D. G. (2004). The rising fastball and other perceptual illusions of batters. In G. Hung & J. Pallis (Eds.), *Biomedical engineering principles in sports* (pp. 257–287). Dordrecht: Kluwer Academic.

Bahill, A. T., Baldwin, D. G., & Venkateswaran, J. (2005). Predicting a baseball's path. *American Scientist, 93*(3), 218–225.

Bahill, A. T., & Gissing, B. (1998). Re-evaluating systems engineering concepts using systems thinking. *IEEE Transactions on Systems, Man, and Cybernetics, Part C (Applications and Reviews), 28*(4), 516–527.

Bahill, A. T., & Madni, A. M. (2017). *Tradeoff decisions in system design*. New York: Springer Publishing Company. ISBN 978-3-319-43710-1.

Bahill, A. T., & Szidarovszky, F. (2009). Comparison of dynamic system modeling methods. *Systems Engineering*, *12*, 183–200.

McBeath, M. K., Nathan, A. M., Bahill, A. T., & Baldwin, D. G. (2008). Paradoxical pop-ups: Why are they difficult to catch? *American Journal of Physics, 76*(8), 723–729.

Simon, H. A. (1962). The architecture of complexity. *Proceedings of the American Philosophical Society, 106,* 467–482.

Smith, E. D., Szidarovszky, F., Karnavas, W. J., & Bahill, A. T. (2008). Sensitivity analysis, a powerful system validation technique. *The Open Cybernetics and Systemics Journal, 2,* 39–56. https://doi.org/10.2174/1874110X00802010039.

Watts, R. G., & Bahill, A. T. *Keep your eye on the ball: Curveballs, knuckleballs, and fallacies of baseball* (1st edn 1990). New York: W. H. Freeman and Co.

Index

A. T. Bahill, *The Science of Baseball*,
https://doi.org/10.1007/978-3-030-03032-2